Localisation and function of Phosphoinositide-specific Phospholipase C in *Sacchromyces cerevisiae*

by

Ding Luo

A thesis submitted to the University of Birmingham

for the degree of

DOCTOR OF PHILOSOPHY

School of Biosciences

College of life and environmental sciences

University of Birmingham

B15 2TT

Jan. 2010

Supervisors: Dr. Stephen K. Dove and Professor Robert H. Michell

ABSTRACT

Phosphoinositide-specific phospholipase C enzymes (PLCs) cleave the plasma membrane phospholipid PtdIns(4,5)P_2 to generate two messengers, inositol (1,4,5) trisphosphate [Ins(1,4,5)P_3] and diacylglycerol (DAG) (Kirk 1990). Ins(1,4,5)P_3 is an important second messenger in animal cells. It releases calcium from intracellular stores by opening Ins(1,4,5)P_3 receptors (InsP_3Rs) and is formed in response to activation of cell surface hormone and growth factor receptors. It is also important for its immediate phosphorylation to form higher phosphorylated inositol phosphates (Ins*P*s) (Auesukaree *et al*., 2005; Perera *et al.*, 2004; York *et al*., 1999), which are critical for various cell signaling functions.

Sub-families of PLC enzymes exist in cells and the regulation of the β and γ type PLCs via G-protein coupled receptors and receptor tyrosine kinases respectively, is well understood. In contrast, the regulation of PLC-δs is still a mystery. This is particularly frustrating because these enzymes are the only isoforms of PLC found in fungi and plants, as well as animals, and thus are likely to perform an ancient and important function.

Plc1p is the single PLC of the δ family in the budding yeast *Sacchromyces cerevisiae*. It plays a key role in generating Ins(1,4,5)P_3 in this fungi in response to stress and yet the yeast genome encodes no Ins(1,4,5)P_3 receptor. This suggests that the functions of PLC-δs are mediated in a novel fashion, probably occurs via the higher inositol phosphates that derived upon rapid phosphorylation of Ins(1,4,5)P_3 by a series of kinases (Arg82p, Ipk1p, Kcs1p and Vip1p).

This study focuses on the localisation of GFP-Plc1p in order to gain insight into its function. Plc1p is present in both cytoplasm and nucleus. Plc1p is too large to diffuse through the nuclear pore complex, and thus relies on nuclear export signals (NES) and nuclear localisation signals (NLS) to facilitate its passage through the nuclear envelope. By creating mutants of Plc1p that are restricted to one of these compartments: GFP-Plc1p^{CAAX} for plasma membrane localisation, GFP-Plc1p^{NES} for nucleus and GFP-Plc1p^{PKI} for cytoplasm, I investigated which defects persist in yeast expressing these mutants as their sole Plc1p.

My data suggest that these mutants do appear to display distinct subsets of phenotypes consistent with the idea of separate pools of inositol phosphates. I showed that both cytoplasmic and nuclear pools of Plc1p are important for function as neither *PLC1*^{NES} nor *PLC1*^{PKI} rescue the stress sensitivity of *plc1*Δ mutants. Therefore, Plc1p are likely to shuttle in between different compartments to exert its diverse functions. It will be instructive to characterise inositol phosphate metabolism in these mutants to determine in which compartments basal and stimulated rises in inositol phosphates occur in yeast cells.

In addition, I report the novel finding that Plc1p interacts with one (or more than one) of its metabolites. Plc1p appears to associate tightly with the plasma membrane in the absence of the inositol phosphate kinase Arg82p, most likely due to the absence of Arg82p-derived inositol polyphosphates, and such association is required for intact PH, X-Y and C2 domain – disruption in any of these domains would result in failure of such association.

Hence, higher phosphorylated inositol phosphates seem to influence Plc1p's localisation, and a physiological feedback cycle of regulation probably exists where Plc1p may be regulated by the products of its own catalytic activity. Future studies will seek to understand the role of this feedback cycle in stress signalling and physiology in yeast cells.

ACKNOWLEDGEMENTS

There are many people who have helped substantially and provided their support during the years that this project has taken to complete.

First and foremost, I would like to thank my Ph.D supervisor Dr. Stephen K. Dove for his enthusiasm, patience and the invaluable advice that I have received during my study and for this report. I would like to express my sincere appreciation to him for the precious time, support and kindness that he has been offering me.

I would also like to express my deep gratitude to Professor Bob Michell. It was a great pleasure to have him around to provide me with immeasurably insightful thoughts, and to review my thesis drafts and to guide me in completing this work.

To all previous and current members of Dr Dove's lab, thanks for your help and every fantastic moment that we have shared. It's been so great to have known and spent time with you all over the past a few years.

Also, I greatly appreciate the financial support of the Darwin Trust Edinburgh that has funded my studies and my life over the last three years in the U.K.

Last, but most importantly, I must acknowledge my beloved parents who bore me, raised me, supported me, taught me and loved me. To my mother, whose unconditional love, emotional support, continual encouragement, particularly in my moments of despair, has been the strength and motivation that support me throughout

my life. To my adorable dog, for his spiritual contribution to the family, it has been noticed and appreciated.

Dedication

I am dedicating this thesis to my father, who has passed away. Dad, I am sorry you are not here to enjoy the moment but you are in my thoughts now and forever.

It is times like these that remind us all of how great the loss is.

I love you, Dad!

CONTENTS

Chapter 1: Introduction

Chapter 2: Materials and methods

Chapter 3: Plc1p localisation and function

Chapter 4: Regulation of the plasma membrane association of Plc1p

Chapter 5: Concluding remarks and future work

ABBREVIATIONS

S. cerevisiae	*Saccharomyces cerevisiae*
E. coli	*Escherichia coli*
WT	*Wild-Type*
ORF	Open reading frame
DIC	Differential interference contrast
GFP	Green fluorescence protein
GST	Glutathione-S-transferase
HA	Hemagglutinin
PLC	Phosphoinositide-specific Phospholipase C
DAG	*sn-1,2-diacylglycerol*
PKC	Protein kinase C
PPIn	Phosphoinositides
PtdIns	Phosphatidylinositol
PtdIns(4,5)P_2 /PIP_2	Phosphatidylinositol 4,5-bisphosphate
*Ins*P*s/I*P*s*	*Inositol polyphosphates*
PP-Ins*P*s	Inositol pyrophosphates
InsP_3/IP_3	Inositol (1,4,5) trisphosphate
InsP_4/IP_4	Inositol (1,4,5,6) tetrakisphosphate
InsP_5/IP_5	Inositol (1,3,4,5,6) pentakisphosphate
InsP_6/IP_6	Inositol (1,2,3,4,5,6) hexakisphosphate
InsP_7/IP_7	Diphosphoinositol pentakisphosphate (" *PP*-InsP_5 ")
InsP_8/IP_8	Bis-diphosphoinositol tetrakisphosphate ("$(PP)_2$-InsP_4")
$PLC1^{NES}$	$PLC1^{L190A/L193A}$
$PLC1^{4R}$	$PLC1^{R111L/R117S/R120S/R123E}$
$PLC1^{KRLR}$	$PLC1^{K170A/R171A/R173A}$
$PLC1^{KKLRK}$	$PLC1^{K94A/K95A/R97A}$
$PLC1^{R2/3}$	$PLC1^{R117S/R120S}$
$PLC1^{R2/4}$	$PLC1^{R117S/R123E}$
$PLC1^{R3/4}$	$PLC1^{R120S/R123E}$
$PLC1^{R1}$	$PLC1^{R111L}$
$PLC1^{4R/E425G}$	$PLC1^{R111L/R117S/R120S/R123E/E425G}$

ARG82$^{\Delta asp}$	*ARG82*$^{\Delta 283\text{-}308aa}$
DTT	Dithiothreitol
PMSF	Phenylmethanesulfonyl fluoride
IPTG	Isopropyl β-D-1-thiogalactopyranoside
DSP	Dithiobis (succinimidyl propionate)
MES	2-(*N*-morpholino)ethanesulfonic acid
NES	Nuclear export signals
NLS	Nuclear localization signals
NPC	Nuclear pore complex
RT	Room temperature

Chapter 1 Introduction

1.1 Discovery of Phosphoinositides and recognition of their importance

Signaling systems translate extracellular information into chemical messages to which the intracellular machinery can respond (Downes and Currie, 1998). Receptor proteins first detect alterations in the external physical or chemical environment of the cell and then trigger changes in the activity of enzyme(s) or ion channels that transform and amplify this information. A group of molecules referred as 'second messengers' are important components of most signal transduction cascades. They are responsible for relaying the external signals received by receptors to intracellular target molecules, usually through binding to and activating effector molecules such as protein kinases, ion channels, and a variety of other proteins.

Three major second messenger groups have been defined: hydrophilic molecules, including cAMP, cGMP, Ins(1,4,5)P_3 and Ca^{2+}; gases, such as nitric oxide (NO) and carbon monoxide (CO); and hydrophobic molecules, such as diacylglycerol and other lipids.

Phosphoinositides (PPIn), the various inositol lipids, function as second messengers or the precursors to second messengers, and also fulfil a number of other regulatory functions (Clarke, 2003). PPIn regulatory pathways are ubiquitous in eukaryotic cells. They are responsible for regulating multiple responses to a wide range of external stimuli in diverse cells, including stress responses, mitogenesis, apoptosis, cell motility and membrane trafficking (Clarke, 2003).

Studies on phosphoinositides began around eighty years ago when *myo*-inositol, the hexahydroxycyclohexane that is the head-group of phosphatidylinositol, was identified as a component of the lipids of mycobacteria (Anderson, 1930). An understanding of the structures of inositol lipids and their metabolic turnover only started developing after Jordi Folch discovered an 'inositol phospholipid fraction' in a bovine brain extract in the 1940s. Folch's compound contained phosphate and inositol in an approximate molar ratio of 2:1 and was named 'diphosphoinositide' (Folch, 1949).

During the 1950s and 1960s three major classes of inositol phospholipids were isolated: mono-, di-, and tri-phosphoinositide, which are now more correctly referred as phosphatidylinositol (PtdIns or PI), phosphatidylinositol 4-phosphate (PtdIns4*P* or PI4*P*), and phosphatidylinositol 4,5-bisphosphate (PtdIns(4,5)P_2 or PI(4,5)P_2), respectively (Michell, 1986). Despite being quantitatively minor lipids, these phosphoinositides are widely distributed in many types of cells and tissues (Downes, 1982; Folch, 1959; Wagner *et al*., 1961). Structural characterization showed that they all have an *sn*-1,2-diacylglycerol 'backbone', and an inositol phosphate 'headgroup' (Figure 1.1).

These lipids first came to attention in 1953 when Mabel and Lowell Hokin observed that cell surface receptors could induce rapid turnover of "PtdIns" (Hokin and Hokin, 1955a, b; Hokin and Hokin, 1953). In the same year, hydrolysis of phosphoinositides at the diester phosphate bond was described when Sloan-Stanley found that brain homogenates hydrolysed Folch's 'diphosphoinositide' fraction more quickly than any other phospholipid, with inositol phosphate(s) as direct product(s) (Sloane-Stanley,

1953). A phospholipase C (PLC) activity was detected by several groups and a "PtdIns-specific PLC" was partially purified and characterized by Dawson and his colleagues in 1959, and then, later, by Hawthorne's lab (Atherton and Hawthorne, 1968; Dawson, 1959; Kemp *et al*., 1961).

A major change occurred when a large body of evidence was interpreted by Robert Michell's group as showing a direct link between cell surface receptor signaling and

Fig 1.1: Structures of phosphatidylinositol, phosphatidylinositol 4-phosphate and phosphatidylinositol 4,5-bisphosphate

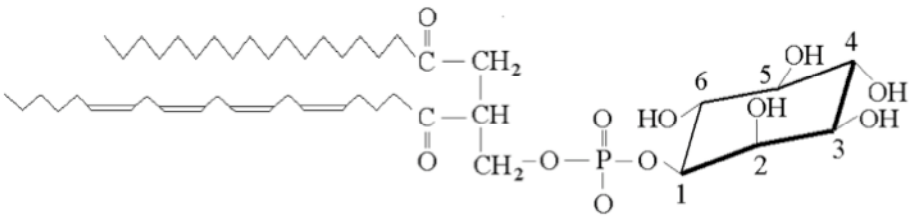

PtdIns (Monophosphoinositide)

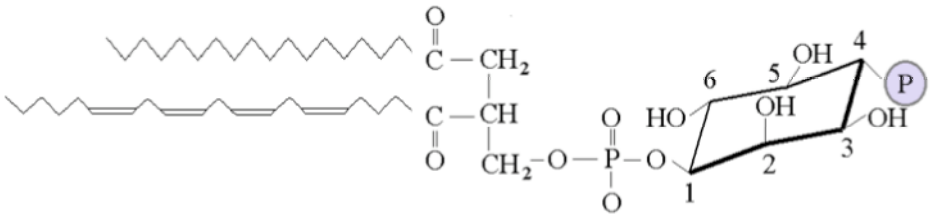

PtdIns4*P* (Diphosphoinositide)

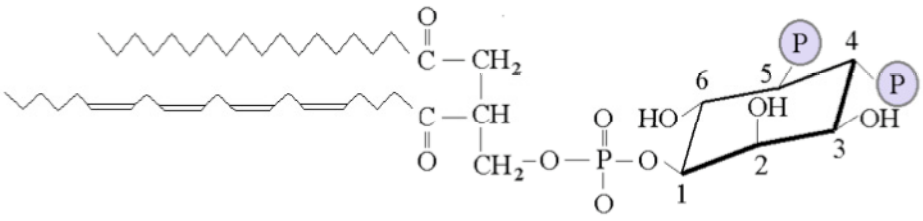

PtdIns(4,5)P_2 (Triphosphoinositide)

phospholipase C-catalyzed PtdIns hydrolysis. Michell also put forward the idea that PtdIns turnover might be associated with an increase of cytoplasmic [Ca^{2+}] in stimulated cells (Michell, 1975). However, the fact that PLC enzymes are highly sensitive to Ca^{2+} themselves muddled the issue of whether PLC activation was a downstream event in response to increased intracellular Ca^{2+} or an initiator of this increase (Michell, 1982). Then, in 1981, Judith Creba and Peter Downes in Michell's lab identified PtdIns(4,5)P_2 and PtdIns4P as the likely *in vivo* substrates of receptor-activated PLCs (Creba *et al*., 1983; Michell *et al*., 1981). These observations indicated that Ins(1,4,5)P_3 might be an intracellular second messenger. This was soon settled when Ins(1,4,5)P_3 stimulated release of Ca^{2+} from the ER membrane was discovered (Streb *et al*., 1983).

These reports opened up the study of phospholinositide-specific PLC (which will from now on be referred to simply as PLC) as a key enzyme in agonist-stimulated phosphoinositide metabolism (Downes, 1985).

In the late 1980s and 1990s, a new focus for inositide research emerged with the discovery of the novel inositol lipids PtdIns3P and PtdIns(3,4,5)P_3 in 1988 (Traynor-Kaplan *et al*., 1988; Whitman *et al*., 1988), and of PtdIns5P and PtdIns(3,5)P_2 in 1997 (Dove *et al*., 1997; Rameh *et al*., 1997). By 1996, the crystal structure of PLC-δ_1 made it clear that no PPIn with a D3-phosphate could serve as a substrate for PLC, and this was later confirmed by experimental work (Essen *et al*., 1996).

There are now 7 PPIn known and their structures are shown below (Figure 1.2).

Fig 1.2: Structures of phosphatidylinositol and its phosphorylated derivatives

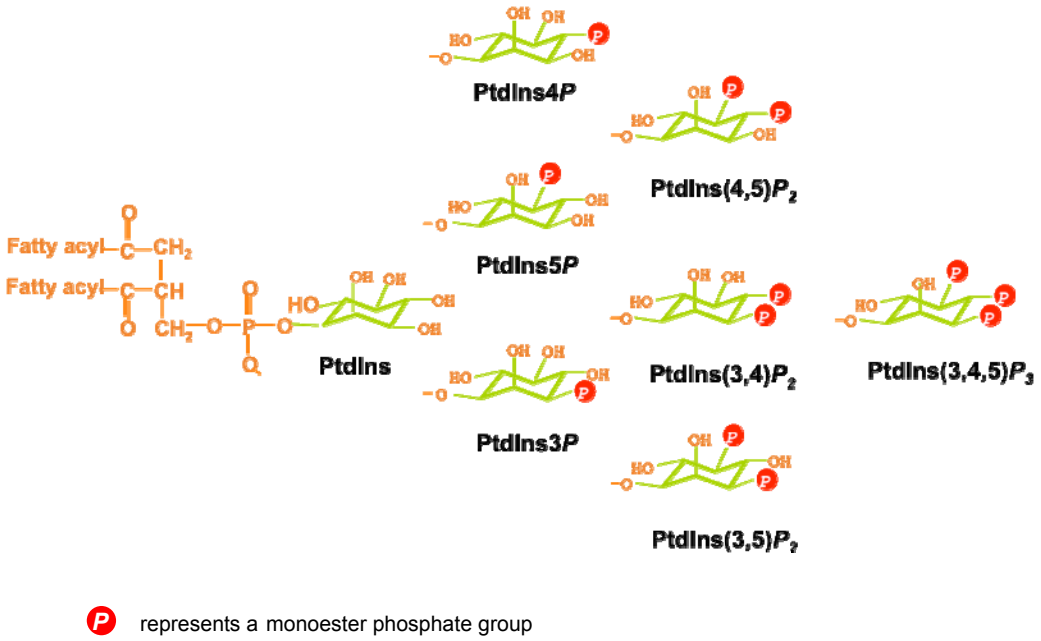

1.2 The synthesis of phosphoinositides in eukaryotic cells

All phosphoinositide synthesis starts with formation of *myo*-inositol. *Myo*-inositol is one of nine possible regio-isomers of hexahydroxycyclohexane: a group of molecules collectively known as the inositols. *Myo*-inositol (hereafter referred to as inositol) is of the most common naturally occuring inositol. Once its D1 hydroxyl is linked to a lipid, then all of the other 5 hydroxyls become stereochemically unique (Overduin *et al*., 2001). It is the only isomer used by most cells in phospholipid synthesis and has also been adapted to many other roles (Michell, 1997).

The synthesis of inositol is catalyzed by two enzymes: an NAD^+-dependent *myo*-inositol-3-phosphate synthase (MIPS, called Ino1p in yeast) that converts glucose-6-phosphate to D-*myo* inositol-3-phosphate (Ins3*P*). Ins3*P* then serves as the substrate for an inositol monophosphatase (Ins*P*ase) that releases free inositol (Michell, 2008).

Phosphatidylinositol (*sn*-1,2-diacylglycero-3-phospho-D-1-*myo*inositol; PtdIns) is an acidic diacylglycerolipid, and is generally the most abundant inositol glycerophospholipid, constituting ~5-20% of the total lipid in eukaryotic cells (Rameh and Cantley, 1999). It is synthesized from CDP-diacylglycerol (also termed CMP-PtdOH) by PtdIns synthase at the endoplasmic reticulum, by transferring a phosphatidyl residue to the D1-hydroxyl of inositol (Shen and Dowhan, 1996) (Fig 1.3).

Figure 1.3: Route of synthesis of phosphatidylinositol

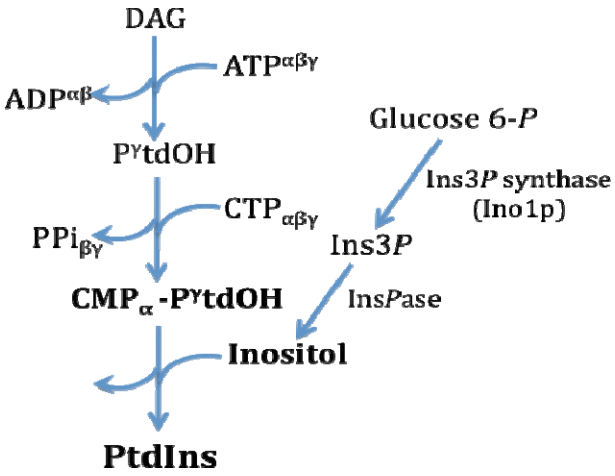

DAG, diacylglycerol; PtdOH, phosphatidic acid or phosphatidate; CTP, cytidine trisphosphate; CMP, cytidine monophosphate; PtdIns, phosphatidylinositol

Synthesis of PtdIns takes place in the ER and PtdIns turnover has a half-time in weeks. In contrast, the synthesis of PPIn from PtdIns is very rapid and phosphate group turnover occurs in seconds or minutes. All of the PPIn are derived from the parent lipid phosphatidylinositol by combinatorial phosphorylation that is catalysed by families of lipid kinases and lipid phosphatases (Overduin *et al*., 2001) (Fig 1.4). The ATP-dependent kinase/phosphatase enzyme pairs that interconvert PtdIns, PtdIns4*P*, and PtdIns(4,5)P_2 were first detected in erythrocyte ghosts, liver plasma membranes and brain cytosol (Hokin and Hokin, 1964; Michell and Hawthorne, 1965;

Kai *et al.*, 1966). Both kinases and phosphatases tend to display specificity for a particular hydroxyl or phosphomonoester at the D-3-, 4-, or 5- position of the inositol ring and also require that certain other hydroxyls are either free or are phosphorylated. For example, PtdIns 4-kinases will only phosphorylate the 4-position of the inositol ring of PtdIns when all other hydroxyls are free and unphosphorylated (Kirk, 1990), and phosphatases of the myotubularin family attack the D3-posphates of PtdIns3*P* and PtdIns(3,5)P_2, but not those in PtdIns(3,4,5)P_3 or PtdIns(3,4)P_2 (Robinson and Dixon, 2006).

Figure 1.4: The network of interconversion between PPIn (Balla, 2006)

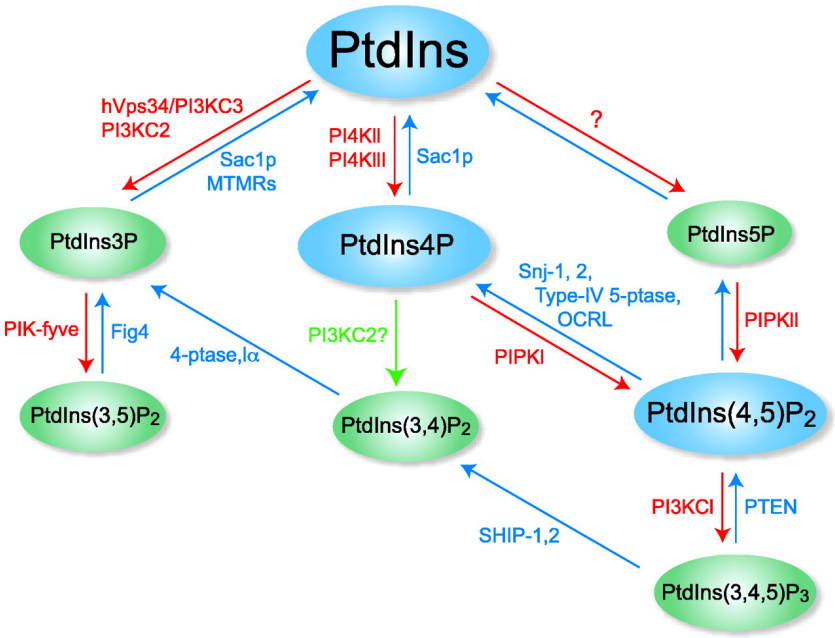

PPIns are phosphorylated (red arrows) by PPIn kinases and dephosphorylated (blue arrows) by PPIn phosphatases. Most PtdIns(4,5)P_2 are formed through PtdIns4*P* by PtdIns 4-kinases, which remains as the canonical route for PtdIns(4,5)P_2 synthesis (enlarged blue circles).

1.3 General characteristics of acutely regulated and house-keeping PPIn

Phosphoinositides can be grouped into two types: acutely regulated and housekeeping or constitutive lipids. The 'acutely regulated phosphoinositides' such as PtdIns(3,4,5)P_3 tend to be second-messengers, and changes in their concentrations are

rapid and transient upon receptor stimulation. They initiate their effects by binding and allosterically regulating target proteins known as effectors. The housekeeping lipids are always present in cells and are generally involved in membrane trafficking or other constitutive functions (Overduin *et al*., 2001). These lipids are employed by cells use to mark particular compartments (Toker, 2002). For example, some PtdIns4*P* is associated with the Golgi and a number of proteins, such as the lipid-transfer proteins OSBP and FAPP, seem to require its presence in order to localize and function at this compartment (Toker, 2002).

PtdIns3*P* is a key component in endosomal membrane trafficking and depletion of this lipid results in an aberrant morphology of these organelles (Corvera, 2001; Lemmon, 2003). PtdIns(3,5)P_2 also functions in the endo-lysosomal system and regulates the fission/fragmentation of lysosome/vacuoles both constitutively and in stressed cells (Dove *et al*., 1997; Rudge *et al*., 2004).

PtdIns(3,4,5)P_3 has a major plasma membrane signaling role. It exists in very low concentrations in quiescent cells but its levels can be transiently and dramatically enhanced upon activation of type I PPIn 3-kinases, and PtdIns(3,4,5)P_3 activates multiple pathways that control cell survival and growth (Di Paolo and De Camilli, 2006).

PtdIns5*P* has been suggested to be a regulator in some cellular processes, including PtdIns(3,4,5)P_3 signalling and exocytosis (Morris *et al*., 2000; Sbrissa *et al*., 2004), but its role in these activities, if any, requires further clarification.

1.4 PtdIns(4,5)P_2

PtdIns(4,5)P_2 is mainly concentrated at the plasma membrane (Di Paolo and De Camilli, 2006), but is also present in the Golgi and the nucleus (Halstead *et al*., 2005). Two consecutive phosphorylations of PtdIns by Type III PtdIns 4-kinase and Type I PtdIns4*P* 5-kinase form the main path of PtdIns(4,5)P_2 synthesis (Hinchliffe *et al*., 1998). However, a small fraction of PtdIns(4,5)P_2 might also be made by Type II PtdIns5*P* 4-kinase from PtdIns5*P* (Santarius *et al*., 2006).

PtdIns(4,5)P_2 serves as the substrate for two second messenger systems: for generation of the survival signal PtdIns(3,4,5)P_3 and as a substrate of PLCs, leading to production of the two second messengers InsP_3 and DAG (Toker, 2002). Both of these systems are activated by cell surface receptors in response to a wide variety of physical and chemical stimuli, probably in all animals, and maybe in some other eukaryotes (Toker, 2002).

A large body of evidence also points to regulatory roles for PtdIns(4,5)P_2 itself (Insall and Weiner, 2001). These include the regulation of actin cytoskeletal dynamics, chromatin remodeling, ion channel gating, clathrin-mediated endocytosis, exocytosis, vesicle trafficking and focal adhesion formation (Di Paolo and De Camilli, 2006; Downes *et al*., 2005; Heilmann, 2008; Santarius *et al*., 2006; van Rheenen *et al*., 2005).

PtdIns(4,5)P_2 can influence cytoskeletal organisation through regulating the concentration of free actin monomers in the cell as a result of its association with actin-binding proteins such as profilin (Lassing and Lindberg, 1985). Actin uncapping

can also be regulated by PtdIns(4,5)P_2 through its interaction with gelsolin or CapZ-related proteins. This allows elongation of pre-existing actin filaments (Schafer *et al*., 1996). PtdIns(4,5)P_2 also interacts with many cytoskeletal anchoring proteins such as talin, vinculin, and proteins of the ERM (Ezrin, Radixin, and Moesin) family (Barret *et al*., 2000; Hirao *et al*., 1996)**.**

There is evidence that the vacuolar/lysosomal fission/fusion equilibrium depends on proper maintenance of the traffic of plasma membrane-synthesised PtdIns(4,5)P_2 between vacuolar and plasma membranes (Mayer *et al*., 2000; Wiradjaja *et al*., 2007). The metabolites of PtdIns(4,5)P_2 – DAG, inositol polyphosphates or both – might regulate vacuole fusion (Seeley *et al.*, 2002), as evidence has recently shown that vacuole fusion *in vitro* is blocked by sequestration of DAG or by PLC inhibitors (Jun *et al*., 2004).

PtdIns(4,5)P_2 accumulates at the cleavage furrow of dividing cells (Emoto *et al*., 2005; Field *et al*., 2005; Wong *et al.*, 2005). The presence there of high concentrations of PtdIns(4,5)P_2 and of actin binding proteins that bind PtdIns(4,5)P_2 suggests a role for this lipid in cytokinesis (Field *et al*., 2005). Treatment with a PLC inhibitor (U73122) or sequestration of PtdIns(4,5)P_2 causes an impairment in cleavage furrow function and a defect in cytokinesis, suggesting that hydrolysis of PtdIns(4,5)P_2 is essential for this process, maybe because they require Ins(1,4,5)P_3 stimulated release of intracellular Ca^{2+} (Wong *et al*., 2005).

1.5 Phosphoinositide-specific Phospholipase C mediated hydrolysis of PtdIns(4,5)P_2 and the Ins(1,4,5)P_3/ DAG pathway

The cell-surface receptor mediated activation of phosphoinositide-specific phospholipase C (PLC) to hydrolyze PtdIns(4,5)P_2, forms the two second messengers inositol 1,4,5-trisphosphate (Ins(1,4,5)P_3 or InsP_3) and *sn*-1,2-diacylglycerol (DAG) (Berridge, 1983). Most of the DAG derived from PPIn in animal cells has a distinctive fatty-acid profile: 1-stearoyl 2-arachidonyl DAG. This DAG remains in the plasma membrane and activates the classical isoforms of protein kinase C (cPKCs) via binding to their C1 domains (Rhee, 2001) (Fig 1.5). Activation of cPKCs can lead to diverse intracellular events in a variety of different tissues. These include regulation of cellular growth and proliferation, cardiac hypertrophy, smooth muscle contraction, mitogenesis and/or differentiation, stimulation of Na^+/H^+ exchange, activation of MAP kinases, and increased transcription of the nuclear proto-oncogenes c-*myc* and c-*fos* (Berridge and Irvine, 1989; Grobler and Hurley, 1998).

Figure 1.5: Hydrolysis of phosphatidylinositol 4,5-bisphosphate by PLC

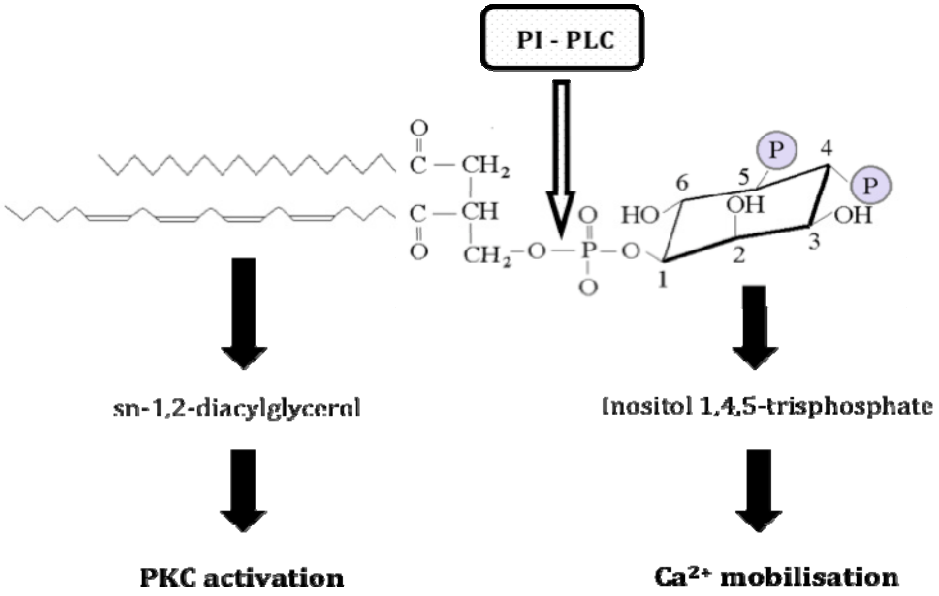

PLC derived DAG also occurs in nuclei: the levels of nuclear DAG changes during the cell cycle, at around the G1-S transition and the G2–M boundary (Sun *et al*., 1997). These two distinct pulses of DAG result in PKC activation in the nucleus, leading to specific cellular/nuclear activity at different cell stages. (D'Santos *et al*., 1999).

Budding yeast has a homolog of mammalian protein kinase C (*PKC1*), but its domain structure is different from any known mammalian PKC isotype. In addition, the protein kinase activity of Pkc1p does not respond to DAG, Ca^{2+} or the other activating cofactors normally required for stimulation of mammalian cPKCs *in vitro* (Watanabe *et al*., 1994).

The other product of the PLC pathway, InsP_3, is water soluble and diffuses away from the plasma membrane to associate with a specific InsP_3 receptor, a ligand-gated Ca^{2+} channel that releases Ca^{2+} from the cortical endoplasmic reticulum that is closely apposed to the plasma membrane (Fig 1.6). As mentioned earlier (Section 1.1), this was first demonstrated by Streb et al. (Streb *et al*., 1983).

Fig 1.6: The DAG/InsP$_3$ pathway in mammalian cells

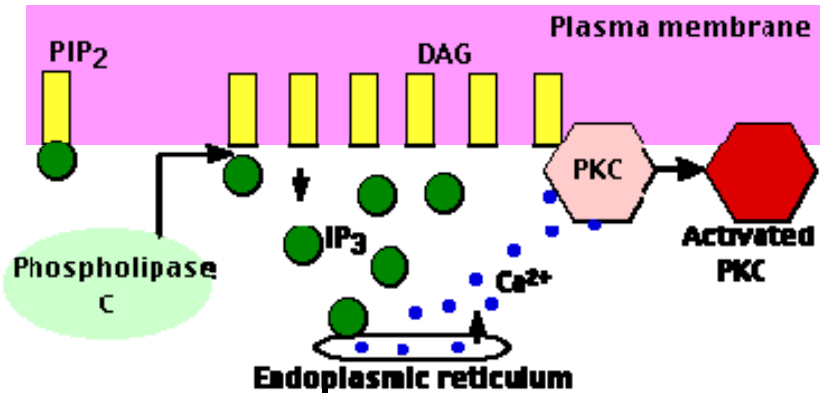

InsP_3 mediated elevation of cytosolic Ca^{2+} levels leads to the stimulation of a variety of calmodulin-dependent enzymes, including protein kinases and phosphoprotein phosphatases (Cockcroft and Stutchfield, 1988b; Kirk, 1990). Through its regulation of intracellular Ca^{2+}, InsP_3 regulates many cellular processes, including fertilization, cell growth, transformation, secretion and smooth muscle contraction (Kirk, 1990). This elevation of cytosolic Ca^{2+} also helps to activate cPKCs: the Ca^{2+} dependent phosphatidylserine-binding C2 domain of these enzymes requires low micromolar Ca^{2+} concentrations before it can associate with the plasma membrane and be activated by DAG (Kirk, 1990).

The other pivotal role of InsP_3 is as the substrate for a series of kinases that generate inositol polyphosphates or inositol pyrophosphates. These molecules have very diverse functions including regulating membrane trafficking, cytoskeletal organization, gene expression, and mRNA export. Highly phosphorylated inositol phosphates are especially important in lower organisms since only animal cells express classical InsP_3 receptor channels. Thus InsP_3 in lower organisms appears to be rapidly converted to form the higher inositol polyphosphates or inositol pyrophosphates (Tisi *et al*., 2004). The inositol polyphosphates and their kinases are important in this study and will be introduced in greater detail in a later section.

1.6 Phosphoinositide-specific Phospholipase Cs

1.6.1 PLC isoenzymes

There are PLCs that are not inositide-specific, but they are beyond the scope of this study. So, the term PLC(s) in this work will refer only to the PI-PLCs.

The eukaryotic PLC family is a diverse group of enzymes, that share considerable sequence similarity within shared domains and also display a common core domain organization (Rhee and Bae, 1997). PLC isoforms are classified according to sequence similarity into six types: PLC-β (β_1–β_4), PLC-γ (γ_1 and γ_2), PLC-δ (δ_1, δ_3 and δ_4), PLC-ε, PLC-ζ and PLC-η (η_1 and η_2) (Katan, 1998; Rebecchi and Pentyala, 2000; Rhee and Bae, 1997). Each isoform is encoded by a different gene, and further molecular diversity is generated by splice variants (Katan, 1998).

The PLC isoforms differ in domain organization, mechanisms of receptor-regulated activation and size: ~85 kilodaltons (kDa) for the PLC-δ subfamily, 120-155 kDa for PLC-β and PLC-γ subfamilies, up to 230-260 kDa for PLC-ε. The subcellular location of each isoform is often determined by the non-conserved domains (Cockcroft, 2006).

Among all the PLC subfamilies, PLC-δs are ubiquitously expressed in eukaryotes, appearing in yeasts, slime moulds, filamentous fungi, plants, and other organisms. DNA sequence comparisons indicate that an ancestral form of PLC-δ was likely present in the primordial eukaryotes that gave rise to multicellular organisms, and the other PLC subfamilies then evolved from this archetypal PLC-δ after the split between fungi, plants and animals about 940 million years ago (Koyanagi *et al.*, 1998; Rhee and Bae, 1997). PLC-ε, PLC-η, and the classical PLC–β and PLC-γ isoforms only exist in metazoans, and PLC-ζ is found only found in sperm (Cockcroft, 2006).

1.6.2 Structure of PLC isoenzymes

PLCs are multidomain proteins. The common core structure shared by most PLC family enzymes is comprised of four elements: a PH domain, 2-4 EF-hands, a

catalytic domain (consisting of a combination of the conserved X and Y regions) and the C2 domain (C2) (Katan, 1998)(Fig 1.7).

Figure 1.7: Domain organization of mammalian PLC isoforms (Katan,2005)

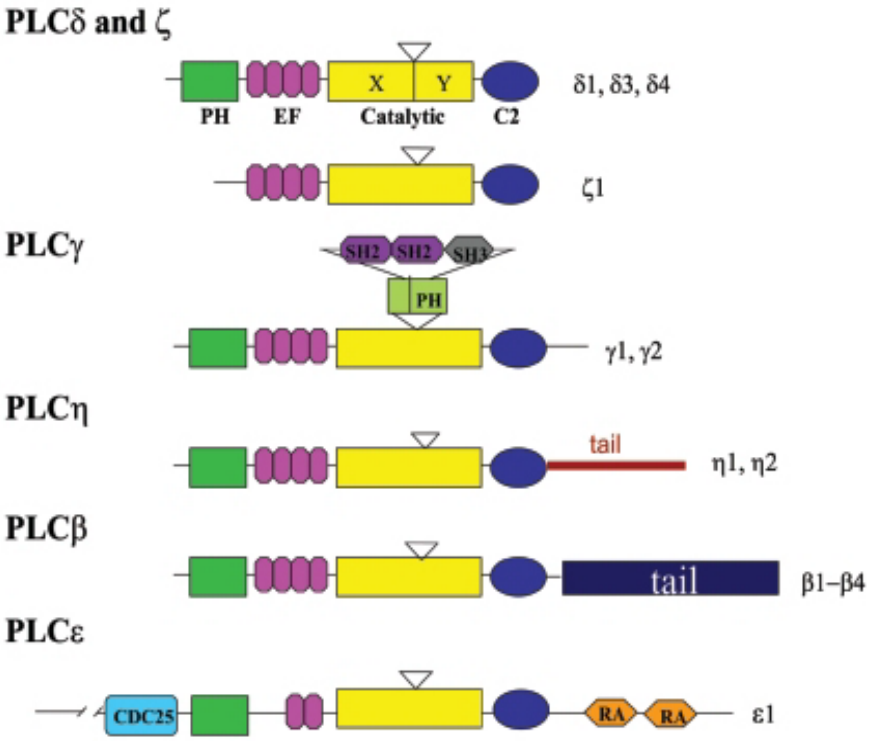

PLC-γ, is unique in having a second PH domain, two SH2 (Src homology 2) and one SH3 (Src homology 3) region formed as a flexible loop in its catalytic domain. PLCε contains a guanyl-nucleotide exchange factor activity (CDC25) at the N-terminus and two RA (Ras association) domains at the C-terminus. The sequences unique to PLC-η (tail) and to PLC-β, are also located at the C-terminus.

The PH domain

Both the localization and the function of PLCs are known to be regulated through membrane targeting motif(s), such as the PH (Pleckstrin Homolgy) domain. Most PLCs contain an amino-terminal PH domain, a ~130 residue module that is also found in many other signalling proteins. The lack of obvious catalytic properties means that PH domains are largely viewed as adaptors or binding sites that tether binding

partners to membranes (Yagisawa *et al*., 1998). The sequences of PH domains are not well conserved among PLCs suggesting that they might bind disparate ligands, most often phosphoinositides and Gβγ subunits (Rhee, 2001), but the three-dimensional structure of the "generalized PH domain" is highly conserved (Bottomley *et al.*, 1998; Lemmon and Ferguson, 2000).

The binding of PLC-δ_1 to PtdIns(4,5)P_2, via its PH domain, is important for the processive catalysis of the substrate by PLC-δ_1 (Cifuentes *et al*., 1993; Lomasney *et al*., 1996). Mutations of the PH domain yields PLC-δ_1 mutants that show low rates of hydrolysis *in vivo* or *in vitro* in the absence of detergents (Yagisawa *et al*., 1998). Equilibrium binding measurements infer a co-distribution between PLC-δ_1 and its substrate (Cifuentes *et al.*, 1994). Later, a study by Ferguson and Lemmon demonstrated that the PH domain residues form a strong non-covalent bond with the 4- and 5-phosphates of PtdIns(4,5)P_2 (Ferguson *et al*., 1995) and this tethers PLC-δ_1 to the polar head of substrate at the plasma membrane (Garcia *et al*., 1995).

PPIn 3-kinase activity is required for some PLC isoforms to be recruited to their lipid binding partners (Falasca *et al*., 1998). PLC-γ_1 can be recruited by PtdIns(3,4,5)P_3 through the affinity of the NH_2-terminal PH domain for this lipid (Rhee, 2001). Accordingly, targeting of PLC-γ_1 to the plasma membrane is dependent upon type I PPIn 3-kinase activity. The PH domain in PLC-β_1 binds to PtdIns3*P* and Gβγ in cells where PPIn 3-kinase is activated. These two components act synergistically to shift PLC-β_1 to the membrane surface, though PLC-β_1-PH was found to bind to other phosphoinositides as well but with lower affinity (Razzini *et al*., 2000).

The PH domain of PLC-δ_1 was also reported to have a higher affinity for inositol phosphates than for lipids, eg, InsP_3 interacts with PLC-δ_1 via its PH domain with high affinity and thus prevents it from binding with PtdIns(4,5)P_2 (Cifuentes *et al*., 1994; Lemmon *et al*., 1995). Indeed, there is a growing body of literature suggesting that inositol phosphates can inhibit the interaction between many PH domains and phosphoinositides (Hirata *et al.*, 1998). In this study, I present some evidence in support of this view.

The EF-hand

With the exception of PLC-ε, all PLC isozymes isolated to date have up to four helix-loop-helix structured EF-hand motifs located between the PH and X domains. The first two EF-hands present in mammalian, yeast and *Dictyostelium discoideum* isoforms are capable of binding divalent cations (Ca^{2+} and Mg^{2+}), whereas the remaining two EF-hands don't (Bennett *et al*., 1998; Drayer *et al*., 1994; Payne and Fitzgerald-Hayes, 1993). However, PLC-δ_1 crystals soaked in calcium or its analogs do not take up any cations (Essen *et al*., 1997).

The role of the EF–hand domains of PLC isozymes is not clear. They may function as regulatory motifs and/or as a link between the PH domain and the rest of the enzyme thus allowing the enzyme to exert its catalytic function after binding. More recent evidence indicates that the EF- hand domain of PLC-δ_1 might serve as a binding site for Ca^{2+} which is necessary for the efficient interaction between the PH domain and PtdIns(4,5)P_2 (Yamamoto *et al*., 1999). Also, a functional Nuclear Export Signal (NES) sequence was located in EF-hand of PLC-$\delta_{1\text{-}4}$, -β_1, -γ_1, -ε, and ζ_1, suggesting it may have a role in interaction with exportins to allow translocation of PLC from the

nucleus to the cytoplasm (Yamaga *et al*., 1999).

The catalytic domain: X-Y region

Among all the PLC subfamilies, the sequences of the X and Y domains are highly conserved (~150 and ~260 amino acids, respectively) (Williams, 1999). These two regions constitute the catalytic core of the enzyme. This domain is formed of α–helices and β-strands resembling an incomplete triose phosphate isomerase (TIM), α/β barrel (Rebecchi and Pentyala, 2000). The sequence homology in the X and Y domains is ~60% amongst all the isozymes, with even greater homology within individual PLC subfamilies (Rhee, 2001). The X domain is involved in both substrate and Ca^{2+} binding, while the Y domain primarily interacts with the substrate (Essen *et al*., 1996). Structural analyses have also demonstrated the importance of individual conserved residues within the catalytic core for substrate binding, catalysis, and membrane interactions. These include His-311, His-356, Glu-341, Asp-343, and Glu-390 (Essen *et al*., 1996).

There is also a ridge of hydrophobic residues, Leu-320, Tyr-358, Phe-360, Leu-529, and Trp-555, surrounding the active site known to be important for membrane interaction/insertion (Rebecchi and Pentyala, 2000).

The intervening sequence joining the X and Y domains is highly disordered and contains sequences that auto-inhibit all PLCs. Most of the activation mechanisms of PLCs involve removal of the X-Y linker from the active site. This linker has a variable length that is characteristic of each family: 40 to 110 residues in the -β and -δ subfamilies, and 190 residues in -ε (Rhee, 2001). This intervening sequence within

PLC-γ family is much larger (~400 residues) and includes multiple adaptor domains, and is designated as the Z region (X/Y spanning polypeptide). The Z-domain of PLC-γs contains two Src homology 2 (SH2) domains and one SH3 domain, which bind phosphotyrosine-containing sequences and proline-rich sequences, respectively. The SH2 and SH3, together with the PH domain, regulate the binding of the PLC-γ subfamily with their protein and lipid partners. These multiple adaptor domains are critical to extrinsic regulation of the -γ isoform as well as an intrinsic control of its catalytic activity (Rebecchi and Pentyala, 2000; Rhee, 2001).

The catalytic activities of eukaryotic PLCs have many properties shared in common (Rhee and Choi, 1992). The general mechanism of substrate hydrolysis for these eukaryotic enzymes could be briefly described as acid/base catalysis leading to the formation of inositol 1,2-cyclic phosphate in a phosphotransfer step, followed by phosphohydrolysis to convert it to an acyclic inositol phosphate (Heinz *et al*., 1998). Ca^{2+} is required by all PLCs as an essential component of the active site (Williams, 1999). The principle role of the metal is to facilitate the deprotonation of the attacking hydroxyl to greatly increase its nucleophilicity. The bound Ca^{2+} also functions as a stabilizer during the negatively charged transition state (Essen *et al*., 1997). PtdIns4*P* and PtdIns(4,5)P_2 are the preferred substrates, and steric constrains make the enzymes unable to hydrolyze 3-phosphorylated phosphoinositides (Bruzik and Tsai, 1994).

The C2 domain

The C2 domain is a region found in many proteins that bind phospholipids in either a calcium-dependent or -independent manner. Calcium binding to the C2 domain is known to function as an electrostatic switch that enhances phospholipid binding

(Sutton *et al*., 1995).

The C2 domains of PLC isozymes are about 120 residues long and in the δ subfamily, where we have structural information, consists of antiparallel β-strands arranged as a sandwich, with one end of the sandwich binding up to three calcium ions (Rhee, 2001). These calcium-binding regions (CBR) of δ-isoforms are homologous from yeasts to humans, suggesting conservation of some important function, but do not share as much similarity with the CBR of the other PLC subfamilies (Rhee, 2001).

A single C2 domain and short peptide cap the carboxy-terminal ends of PLCs of the -γ and -δ subfamilies, but PLC-βs (except for a splice variant of PLC-β_4) bear long carboxy-terminal extensions, which are assumed to enhance membrane binding, nuclear localization (Rhee, 2001), and activation by G protein subunits. This C-terminal extension and the PH domains, both interact with $G\alpha_q$ and $G\beta\gamma$, during the activation of PLC-βs (Wang *et al*., 2000). The C2 domain of PLC-ζ interacts with PtdIns3*P* or PtdIns5*P*, and this seems to inhibit the PLC (Kouchi *et al*., 2005).

1.7 Mode of regulation of PLC isoenzymes

1.7.1 Activation of PLC-β

A wide range of stimuli, from photons and odorant molecules to proteins, can activate PLC-β isozymes through transmembrane G protein-coupled receptors (GPCRs). Activated α subunits of the G_q subfamily or liberated Gβγ heterodimers or both, bind and activate various PLC-βs (Rebecchi and Pentyala, 2000; Rhee, 2001).

Fig 1.8 shows the standard model for G protein activation of PLC-βs. Agonist binding

with the receptor triggers exchange of GTP for GDP on the α subunit of the heterotrimeric G-protein associated with the GPCR. The active GTP-charged α subunit is released from the membrane, and either this α subunit or the βγ heterodimer or both bind to and stimulate the PLC-β (Rebecchi and Pentyala, 2000).

Fig 1.8: Regulation of PLC-β by G protein-coupled receptors (GPCRs) (Rebecchi and Pentyala, 2000)

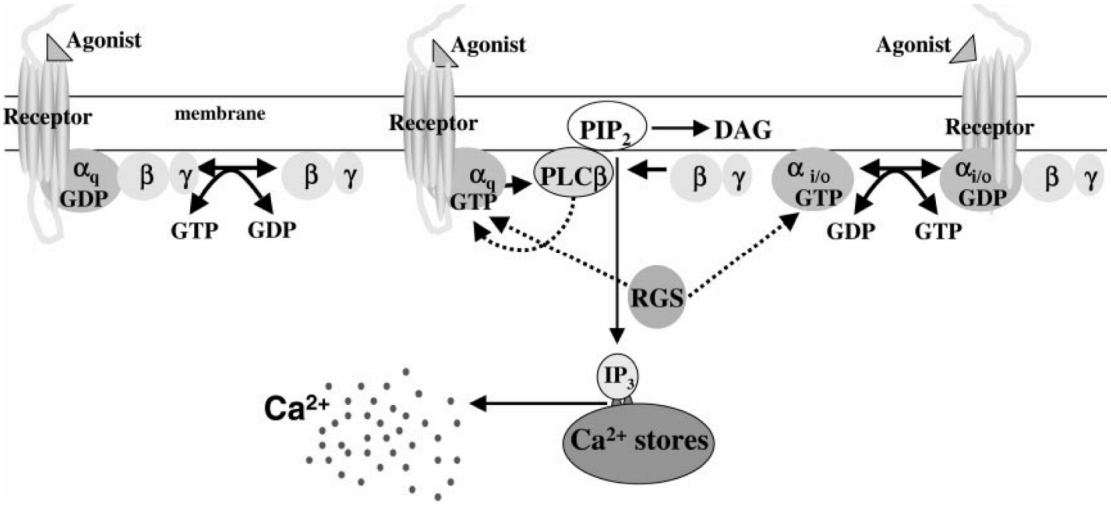

PLC-β can be regulated by the α_q subunit of Gα and βγ-subunits released from Gi/o. RGS (Regulator in G protein) proteins act as receptor-specific down-modulators of the Gα subunits. The continued receptor-catalyzed charging of α_q with GTP is required for PLC-β to remain active.

G proteins were implicated in phosphoinositide/calcium signaling even before PLC-β isoforms were identified (Boyer *et al*., 1989; Cockcroft and Gomperts, 1985; Cockcroft and Stutchfield, 1988a, b; Fain *et al*., 1988). The G_q subfamily of related pertussis toxin (PTX)-insensitive α–subunits (α_q, α_{11}, α_{14}, α_{15}, and α_{16}) were cloned at roughly the same time as the four PLC-β isoforms were first isolated (Strathmann and Simon, 1990). The G_o and G_i family of G-proteins are likely those that are sensitive to pertussis toxin (Cockcroft and Thomas, 1992). GPCRs that activate the

$G_q\alpha$-PLC-β signalling pathway include those for thromboxane A_2, bradykinin, bombesin, angiotensin II, histamine, vasopressin, acetylcholine (muscarinic m1 and m3), a_1-adrenergic agonists, C-C and C-X-C chemokines and endothelin-1 (Rhee, 2001). Different members of the G_q family activate PLC-β isoforms selectively: PLC-β_2 and PLC-β_3 appear more sensitive to βγ stimulation than PLC-β_1 (Camps *et al*., 1992; Lee *et al*., 1994; Park *et al*., 1993; Smrcka and Sternweis, 1993). $G\alpha_q$ purified using a βγ-affinity gel stimulates PLC-β_1 but not -β_2 (Park *et al*., 1992; Rhee and Choi, 1992a), and $G\alpha_{16}$ prefers PLC-β_2 (Lee *et al*., 1992; Rhee and Choi, 1992a). The mix and match relationships between initiator G-proteins and individual PLC isoforms provides a versatile system to suit the disparate needs of the panoply of cell types in which they are found (Cockcroft and Thomas, 1992). It is not yet clear exactly how the individual PLC-βs couple to particular receptors *in vivo*.

1.7.2 Activation of PLC-γ

Receptors for polypeptide growth factors, such as platelet-derived growth factor (PDGF), epidermal growth factor (EGF), fibroblast growth factor (FGF) and nerve growth factor (NGF) can activate PLC-γs both *in vivo* and *in vitro*. There are also receptors that lack intrinsic tyrosine kinase activity but which can nevertheless activate PLC-γs, such as the B and T-cell receptors, Fc receptor and receptors for a number of cytokines (Rebecchi and Pentyala, 2000).

Fig 1.9 represents the general mechanism of activation of PLC-γs. The binding of growth factors to receptor tyrosine kinases (RTKs) triggers the dimerisation of receptor subunits and the stimulation of their intrinsic tyrosine kinase activity. This results in transphosphorylation of multiple tyrosine residues on the cytoplasmic tails

of the receptors. PLC-γ and the Type IA PI 3-kinases are then recruited to these phosphorylated Tyr residues via their high-affinity SH2 domains, and both signaling enzymes are subsequently tyrosine phosphorylated at specific residues by the receptor or its associated accessory proteins (Rebecchi and Pentyala, 2000).

Fig 1.9: Regulation of PLC-γ by tyrosine protein kinases and PtdIns(3,4,5)P_3 (Rebecchi and Pentyala, 2000)

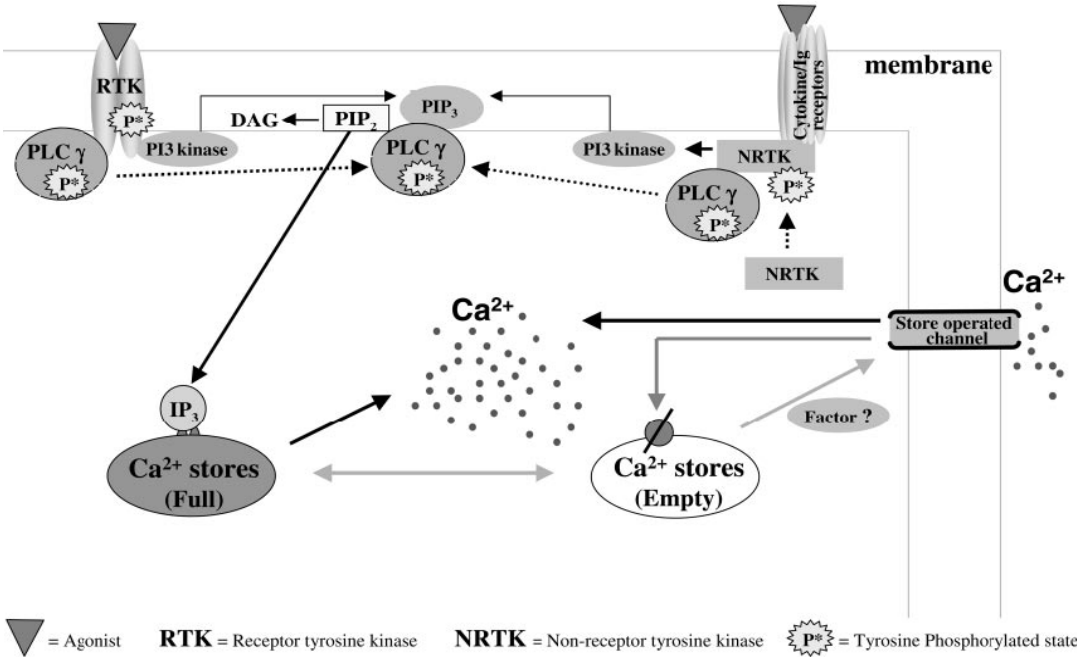

For PLC-γ_1 the sites of tyrosine phosphorylation are Tyr-783, Tyr-1254 and to a lesser extent, Tyr-472 (Kim *et al*., 1990; Wahl *et al*., 1990). A single mutation at Tyr-783 or Tyr-1254 affects PLC-γ activation *in vivo*, but only decreases its catalytic activity *in vitro* when the actin binding protein profilin is included in the assay: profilin-PtdIns(4,5)P_2 complexes are inhibitory to non-phosphorylated PLC-γs (Kim *et al.*, 1991). Over-expressing these mutants in fibroblasts results in different growth and cytoskeletal phenotypes, indicating each of these sites could have distinct functions (Pei and Williamson, 1998). These phosphorylations are necessary but not sufficient

to activate PLC-γs, and PtdIns(3,4,5)P_3 is essential as a positive factor during the process. PtdIns(3,4,5)P_3 binds the PH and SH2 domains of PLC-γs and helps to tether the enzyme to the membrane stably and enhances the rate of PtdIns(4,5)P_2 hydrolysis (Bae *et al*., 1998).

Regulation by non-receptor tyrosine kinases (nRTKs) occurs in a similar fashion. GPCRs can control PLC-γ function by activating nRTKs and PPIn 3-kinases. Upon stimulation, receptors recruit and activate nRTKs such as Src or Jak/Tyk, which become auto-phosphorylated and activated. The active nRTKs then recruit PLC-γs via their SH2 domain and tyrosine-phosphorylate and activate them (Fluckiger *et al*., 1998; Gusovsky *et al*., 1993; Park *et al*., 1992; Park *et al*., 1991).

1.7.3 Activation of PLC-ε

PLC-ε has an amino-terminal Ras guanine nucleotide exchange factor (RasGEF/ CDC25) motif and two carboxy-terminal Ras-associating (RA) domains (Lopez *et al.*, 2001), suggesting that it might be a GDP-GTP exchange factor for, and effector of, Ras (Shibatohge *et al*., 1998).

PLC-ε binds GTP-Ras with high affinity, and the association as well as co-expression of activated Ras with PLC-ε leads to PLC-ε activation and translocation from cytosol to the plasma membrane (Song *et al*., 2001). Once the reaction is terminated by the hydrolysis of Ras-bound GTP, Ras might be reloaded with GTP by the action of the RasGEF motif of PLC-ε, thereby prolonging the receptor-mediated activation of PLC-ε (Rhee, 2001). For example, EGF can stimulate PLC-ε by increasing GTP-Ras activity and causing membrane translocation and activation of PLC-ε (Rhee, 2001;

Song et al., 2001).

PLC-ε also appears to be activated by $G\alpha_{12}$, and the small GTPases of the Rho family (Rhee, 2001). Co-expression of a constitutively active mutant (GTPase-defective) of $G\alpha_{12}$ with PLC-ε specifically increased its PLC activity, whereas none of the other Gα subunits had such an effect (Lopez *et al.*, 2001). Therefore, thrombin and lysophosphatidic acid, whose receptors are coupled to $G\alpha_{12}$, might be able to activate PLC-ε (Rhee, 2001).

1.7.4 Activation of PLC-δ

PLC-δs are the only isoforms found in eukaryotic cells other than animals (Katan, 2005). However, despite the fact that much is known about the structure and catalytic mechanism of PLC-δs, their regulation is poorly understood.

PLC-δ isozymes are more sensitive to Ca^{2+} than the other isozymes and it has therefore been suggested that a rise in intracellular Ca^{2+} might trigger PLC-δ activation (Rhee, 2001). Fig 1.10 shows a possible route for PLC-δ stimulation in animal cells via a hierarchal arrangement of PLC subtypes that sustains calcium signaling in response to receptor activation. Various stimuli could activate multiple PLC subtypes: PLC-β by GPCRs and PLC-γ by nRTKs and PI 3-kinases. PLC-δs might then be activated by the resulting increase in cytosolic [Ca^{2+}], and could thus amplify and extend the Ca^{2+} signals initiated by PLC-β or PLC-γ (Rebecchi and Pentyala, 2000).

Plc1p, a PLC-δ type enzyme that is the sole PLC in yeast, can be activated by

Fig 1.10: Hierarchy of PLC subtypes in cell signaling (Rebecchi and Pentyala, 2000)

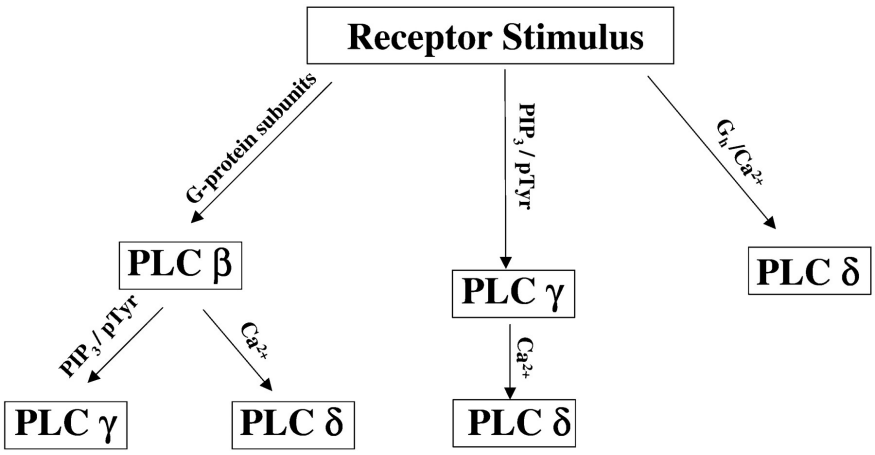

stresses, such as hypo-osmotic shock and heat (Perera *et al*., 2004). The molecular mechanism for this activation is obscure but does not involve Ca^{2+} influx because activation was not blocked by external BAPTA, a high-affinity Ca^{2+} chelator (Perera *et al.*, 2004).

Rat PLC-δ_1 can be regulated, at least *in vitro*, by G_h (75-80 kDa), a high-molecular-weight G protein (Rhee, 2001). G_h is a widely expressed, multidomain protein with tissue transglutaminase activity (Im *et al.*, 1997). It binds to PLC-δ_1 in α_1-adrenergically stimulated heart and liver cells (Chen *et al*., 1996; Das *et al*., 1993; Nakaoka *et al*., 1994) or oxytocin-stimulated myometrium (Park *et al*., 1998). Epinephrine was also found to potentiate G_h to from a complex with a 69 kDa active proteolytic fragment of PLC-δ_1 (Das *et al*., 1993; Feng *et al*., 1996; Park *et al*., 1998). This binding leads to an increased enzyme sensitivity to Ca^{2+}, causing its activation by 0.1-5 μM Ca^{2+} in the presence of GTP (Das *et al*., 1993). However, Murthy *et al*. demonstrated potential GTP inhibition of PLC-δ_1 activation by showing that free or GDP-bound G_h, but not GTP-bound G_h, associated with PLC-δ_1 in response to

receptor accupancy (Murthy *et al*., 1999).

A Rho GTPase-activating protein (p122 RhoGAP) has a strong affinity for PLC-δ_1 and enhance its catalytic activity up to 10-fold at low Ca^{2+}concentrations (~ 0.1 μM) and neither PLC-β_1 nor PLC-γ_1 responded to p122-RhoGAP (Homma and Emori, 1995; Yamaga *et al*., 2008).

A problem with all of these mechanisms is lack of universality. None can explain the activation of PLC-δs in all organisms: G_h and p122 are not present in many eukaryotes whose genomes encode a PLC-δ, and PLC cascade theory is also not relevant to organisms that lack any other PLCs.

More recently, the small Ral GTPases were reported to be involved in PLC-δ regulation: Ral binding to PLC-δ alone is sufficient to stimulate its activity *in vitro* (Sidhu *et al.*, 2005). Indeed, whilst this work was being prepared, a study by Ferguson's group demonstrated that angiotensin II type 1 receptor AT1R-stimulated Ins*P* formation was attenuated after PLC-δ_1 siRNA treatment in HEK 239 cells. This study also provided evidence of a RalGDS (Ral guanine nucleotide dissociation stimulator)/Ral-mediated AT1R stimulation of PLC-δ_1 (Godin *et al*., 2010). AT1R has traditionally been considered to be coupled to the activation of PLC-β via its association with Gαq/11 and also to induce tyrosine phosphorylation of PLC-γ_1 activation (Lea *et al*., 2002; Ochocka and Pawelczyk, 2003; Suh *et al*., 2008), and this further enhances the idea that GPCRs may be coupled to PLC-δ activation in some organisms.

1.8 Plc1p – The Phosphoinositide-specific Phospholipase C of *S. cerevisiae*

1.8.1 Plc1p belongs to the PLC-δ subfamily

The *S. cerevisiae* genome encodes a single PLC, Plc1p, of 100.6 kDa. The sequence of Plc1p is homologous to PLCs from other eukaryotes in the highly conserved X and Y domains, with 43-53% identity in the X domain and 18-20% identity in the Y domain (Yoko-o *et al*., 1993).

The following arguments suggest that yeast Plc1p is most closely related to the PLC-δ subfamily: The Plc1p domain organization and sequence are closest to the -δ isoforms than to the larger and more complex PLCs of the -β, -γ and -ε subfamilies (Flick and Thorner, 1993). The X and Y domains of Plc1p are situated near the carboxy-terminal end, as in PLC-δ isoforms, rather than internally as in the -β, -γ and -ε subfamilies (Yoko-o *et al*., 1993). As in the PLC-δs, ~75 amino acids separate the X and Y domains and this region includes a PEST motif (residues 521 to 568) (Rogers *et al*., 1986). A consensus Ca^{2+}-binding motif is present both in the EF-hand domain of Plc1p (residues 282 to 293) and in the corresponding region of the rat and bovine PLC-δs (Yoko-o *et al*., 1993).

However, Plc1p has a 100-residue extension at its amino-terminus that the mammalian -δ isotypes lack. Also, Plc1p is a basic protein whereas some of the animal PLC-δs (e.g. rat and bovine -δ enzymes) are acidic. The functional significance of these differences is currently unknown (Flick and Thorner, 1993).

1.8.2 Phenotypes of *plc1*Δ mutant

Deletion of *PLC1* has various phenotypic outcomes though the resulting *plc1*Δ cells

are viable in most strain backgrounds. Cells lacking *PLC1* can grow but are fragile and vulnerable to environmental stresses (Flick and Thorner, 1993; Yoko-o *et al*., 1993) (Figure 1.11). This reflects that fact that Plc1p and/or its products regulate the cytoskeleton, an important checkpoint function in the cell cycle, mRNA export, vacuole fusion, and presumably other regulatory pathways that control the responses of *S. cerevisiae* to changes in nutrient availability or environmental stresses (Ansari *et al*., 1999; DeLillo *et al*., 2003; Demczuk *et al*., 2008; Guha *et al*., 2007; Jun *et al*., 2004; Rebecchi and Pentyala, 2000; York, 2006).

Figure 1.11: plc1Δ phenotypes

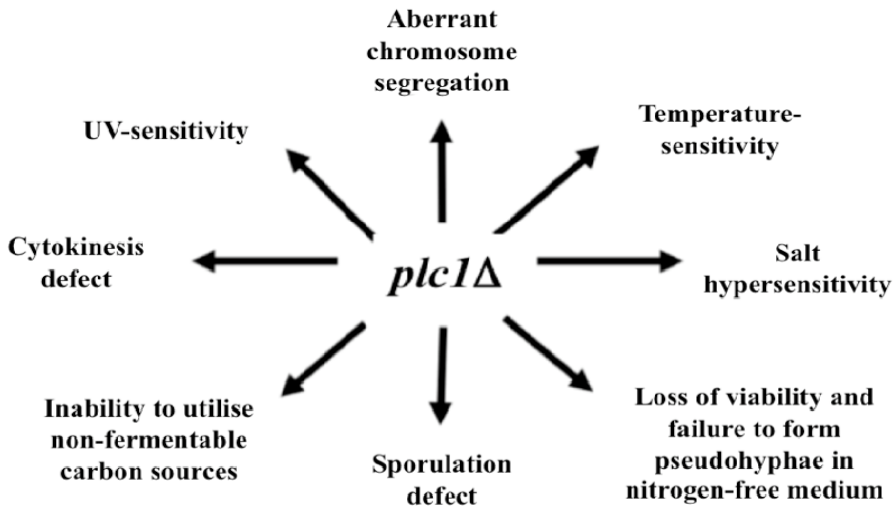

Cells depleted of *PLC1* are sensitive to various sources of stresses as shown in the figure.

The degree of the various stress phenotypes varies in different genetic strains and with different nutrients (Yoko-o *et al*., 1993). The growth of *plc1*Δ cells slows as the temperature increases and usually stops at around 37^{o}C (Flick and Thorner, 1993; Payne and Fitzgerald-Hayes, 1993; Yoko-o *et al*., 1993). *plc1Δ* cells grown at restrictive temperature become larger and multi-budded, do not complete cytokinesis

and show chromosome mis-segregation (Flick and Thorner, 1993).

Yeast lacking *PLC1* also have a deficiency in growth on media with limited nutrient sources, possibly because of mitochondrial abnormalities caused indirectly by the mRNA export defect. Yeast grow best with glucose as a carbon source, and *plc1Δ* mutants grow poorly on raffinose, galactose, and other non-fermentable carbon sources such as glycerol (Flick and Thorner, 1993).

Stationary phase cultures of wild-type and isogenic *plc1Δ* yeast display similar viability in complete medium, but viability of the *plc1Δ* strain drops to ~10% or less without a nitrogen source (Flick and Thorner, 1993).

plc1Δ are sensitive to hyper-osmotic stress and in some strain backgrounds they do not grow (Flick and Thorner, 1993). A previous student in our lab, Dr Nevin Perera, made progress in understanding the regulation and function of Plc1p, including the discovery that Plc1p is stimulated by hypo-osmotic stress to hydrolyse a 50% of cellular PtdIns(4,5)P_2 within two minutes (Perera *et al*., 2004).

Phosphorylation of Ins(1,4,5)P_3 to a series of 'higher' inositol polyphosphates (those with 4 or more phosphates) and inositol pyrophosphates is very rapid in yeast, so these accumulate fast when Plc1p is activated. This suggests that these molecules, rather than of accumulation of Ins(1,4,5)P_3, may be the physiologically important consequence of Plc1p activity.

Our understanding of the molecular information about the functions of Plc1p and

inositol phosphates and the phenotypes reported above are limited and thus there is much more to discover about these pathways.

1.9 The 'higher' inositol polyphosphates (Ins*P*s)

1.9.1 Synthesis of the 'higher' inositol polyphosphates (Ins*P*s)

Although the importance of InsP_3 has been known since 1983, roles for other inositol polyphosphates in cell regulation have only recently emerged. Our knowledge of the synthesis of the Ins*P*s has come mainly from studies of yeast and metazoan Ins*P*s kinases. Two major pathways of inositol polyphosphates synthesis are known. The first pathway, identified in *Dictyostelium*, proceeds directly from inositol via multiple phosphorylations (Stephens and Irvine, 1990). This pathway seems to be absent from many organisms, so I will not consider it further. The second pathway, begins with the action of Plc1p on PtdIns(4,5)P_2 followed by multiple phosphorylations of the liberated Ins(1,4,5)P_3. This latter pathway was discovered first in *S. pombe* and *S. cerevisiae* and completed by York *et al*. (York *et al*., 1999). InsP_3 is sequentially phosphorylated by four kinases (Arg82p, Ipk1p, Kcs1p and Vip1p) to InsP_6 and the pyrophosphorylated Ins*P*s (Fig 1.12).

Fig 1.12: Synthesis of 'higher' InsPs in S. cerevisiae (Demczuk et al., 2008)

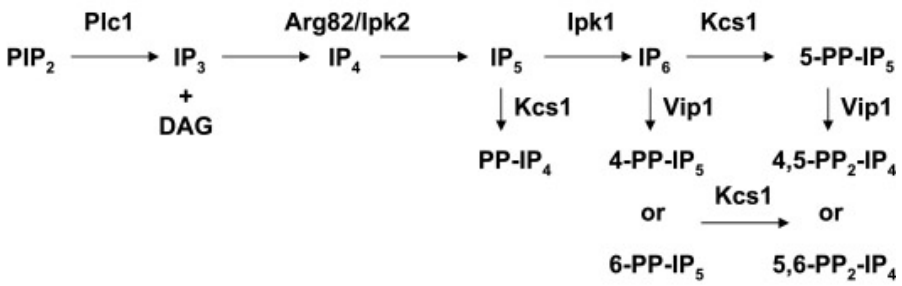

Arg82p (also called Ipk2p) is an inositol polyphosphate multikinase (IPMK). It phosphorylates InsP_3 to Ins(1,4,5,6)P_4 and then to Ins(1,3,4,5,6)P_5, while Ipk1p is primarily a 2-kinase and converts InsP_5 to InsP_6. Kcs1p, an inositol diphosphate synthase, phosphorylates InsP_6 to *PP*-InsP_5 and some InsP_5 to *PP*-InsP_4 (Seeds *et al.*, 2004). A revised and more complex pathway of Ins*P*s production in *S. cerevisiae* emerged after the discovery of a second inositol pyrophosphate synthase, Vip1p. Vip1p phosphorylates InsP_6 at P4 or P6 to generate 4/6-[*PP*]-InsP_5 or can phosphorylate InsP_7 (5-[*PP*]-InsP_5) produced by Kcs1p to form InsP_8 (4,5-[*PP*]$_2$-InsP_4 or 5,6-[*PP*]$_2$-InsP_4). Deletion of *VIP1* does not cause temperature sensitivity but its InsP_6 kinase activity is required for maintaining various cellular processes (Mulugu *et al*., 2007). A 3-kinase activity of Kcs1p and/or Arg82p/Ipk2p can compensate for loss of some, but not all, of the Ins*P*s/*PP*-Ins*P*s in *ARG82*(*IPK2*) deficient cells (Seeds *et al*., 2005).

Deletion of the inositol phosphate kinases, *ARG82*(*IPK2*), *IPK1* and *KCS1* inhibit inositol phosphate production at various steps but the deletions are not individually lethal (York, 2006). These mutants exhibit subsets of the phenotypes displayed by *plc1Δ* mutants, indicating that the resulting inositol polyphosphates are responsible for at least part of the functions of Plc1p. Oddly, deletion of *IPK1* produces very few phenotypes, indicating that *PP*-InsP_4 can probably fulfill many of the functions that normally require InsP_6, InsP_7 and InsP_8 (NM Perera and Sk Dove, 2002 pers. comm.).

In metazoans, the synthesis of higher Ins*P*s is similar to that in yeast except for an extra step: in mammals, InsP_3 is rapidly phosphorylated to Ins(1,3,4,5)P_4 by an InsP_3 3-kinase (Fig 1.13A). The function of Ins(1,3,4,5)P_4 is thought to contribute to

refilling of the ER Ca^{2+} store. Ins(1,3,4,5)P_4 is then phosphorylated by Arg82p(Ipk2p) (Seeds *et al*., 2004).

The synthesis of InsP_5 and InsP_6 in *Drosophila melanogaster* is fairly similar to the yeast pathway, despite the presence of active InsP_3 3-kinases and Ins(1,3,4,5)P_4 (Seeds *et al*., 2004) (Fig 1.13B).

Fig 1.13 (Seeds et al., 2004):

The Metazoan pathway of InsPs synthesis

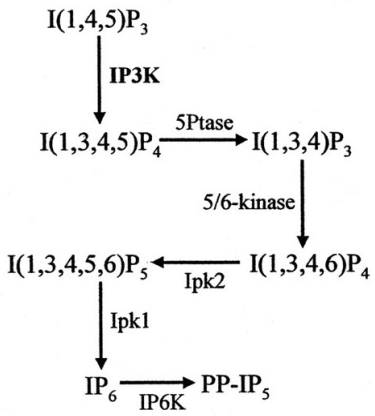

In metazoans, a five-step proposed pathway is initiated by Ins(1,4,5)*P*-3 kinase (IP3K), followed by 5-phosphatase attack, then turnover by the InsP_3 5-/6-kinases, Ipk2 and Ipk1.

B. Drosophila InsPs synthesis

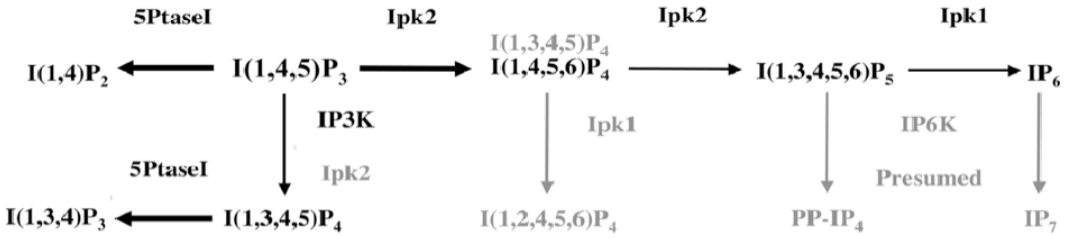

***Black font* highlights portions of the model that are directly supported by data obtained up to date. *Gray font* indicates portions that are presumed and not yet confirmed.**

The gene products of these Ins*P*s kinases and synthases are conserved throughout eukaryotes, from yeast to human. The *ARG82*(*IPK2*)*/IPMK* and *IPK1* routes are the essential major pathway in most eukaryotic species (York, 2006), but plants and mammals do possess alternative pathways that involve the Ins(1,4,5)P_3 3-kinase and Ins(1,3,4)P_3 5/6-kinase (York, 2006) and synthesis by lipid-independent routes (Brearley and Hanke, 1996; Shi *et al*., 2005; Stephens and Irvine, 1990).

1.9.2 Regulatory roles of inositol phosphates

Various Ins*P*s are associated with distinct aspects of cell regulation, and these will now be discussed in some detail. It is often not obvious how an individual Ins*P* can be regulated independently in view of the intrinsically interconnected metabolisms of many Ins*P*s. Many of the functions discussed below are constitutive, which would not require that some Ins*P*s to be acutely regulated.

1.9.2.1 Arg82p(Ipk2p) and InsP_4 /InsP_5

Arg82p (IPMK) catalyses the first enzyme step in the pathway leading from InsP_3 to the higher Ins*P*s. Arg82p was discovered because of its role in regulating arginine metabolism which is reported to be separate from its role in inositol phosphate signalling, though this is an area of some controversy. The InsP_3 kinase activity of Arg82p is involved in diverse processes including sporulation, mating, and the responses to stress in yeast (Dubois and Messenguy, 1994). In mice, Ipk2/IPMK is required for several development events: its deletion causes embryonic lethality at E8.5, and Ipk2/IPMK-deficient mice exhibit multiple morphological defects (Frederick *et al*., 2005).

Arg82p is an essential component of the ArgR-MCM1 transcription complex (Mcm1p, Arg80p, Arg81p and Arg82p) that binds to the ARG box in the promoters of arginine-regulated genes in the presence of arginine, leading to the activation or repression of multiple genes involved in homeostasis (Crabeel *et al*., 1995; El Bakkoury *et al*., 2000). Binding of Arg82p stabilizes Mcm1p/Arg80p (Cocco *et al*., 1998; Dubois and Messenguy, 1994). One group claims that inositol phosphate kinase activity is dispensible for control of arginine metabolism (Dubois *et al*., 2000), but another asserts that it is required: Ins(1,4,5,6)P_4 or Ins(1,3,4,5,6)P_5 is involved since *IPK1* deletion has no effect on arginine metabolism (Odom *et al.*, 2000).

Arg82p may facilitate the binding of Mcm1p/Arg80p to chromatin. The suggestion that PtdIns(4,5)P_2 and maybe also inositol polyphosphates may stimulate binding of the chromatin-remodeling BAF complex to chromatin in mammalian cells (Zhao *et al*., 1998b) and a similar actin-containing complex called ARI in yeast (Chi and Crabtree, 2000), raised the possibility that inositol polyphosphates might regulate chromatin remodeling with the assembly of the ArgR-MCM1 transcription complex *in vivo*. It was later claimed that Ins(1,4,5,6)P_4 or Ins(1,3,4,5,6)P_5 are required during chromatin remodeling, but this has been disputed (El Alami *et al*., 2003). Fig 1.14 illustrates the proposed mechanism of nuclear Ins*P*s in the transcriptional control.

Arg82p kinase activity might also be required for other transcriptional processes (Chi and Crabtree, 2000), for example the activation and repression of both nitrogen-responsive genes (El Alami *et al*., 2003) and for chromatin remodelling within the *PHO5* promotor (Steger *et al*., 2003).

Fig 1.14: Nuclear inositol phosphates control transcription and mRNA export (Chi and Crabtree, 2000)

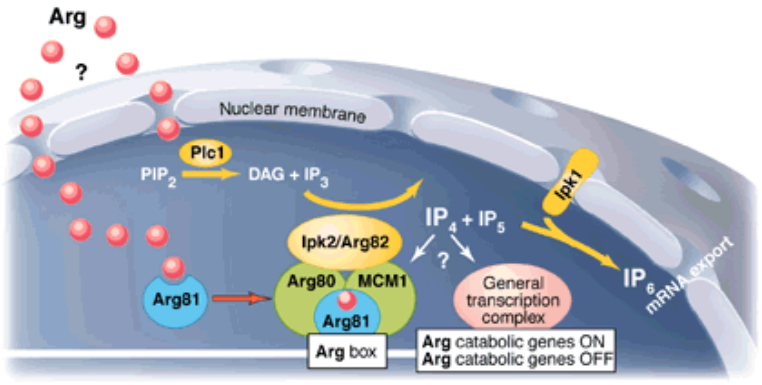

Arginine (Arg) either induces or represses genes involved in its metabolism. Inositol signaling is required for induction of genes whose proteins catabolise arginine. InsP_4 is likely to function in the binding of the ArgR-MCM1 transcription complex to gene promoters, or transcription initiation, or mRNA elongation. InsP_6 localized at the nuclear pore, contributes to the export of mRNA.

1.9.2.2 Ipk1p and InsP_6

The Arg82p(Ipk2p)/IPMK and Ipk1p route appears to be the major route to InsP_6 in all eukaryotes (York, 2006).

InsP_6 has been implicated in the regulation of diverse cellular events. It is found localised at the nuclear pore, where it is required for efficient export of mRNA in both yeast and mammalian cells (Feng *et al*., 2001; Saiardi *et al*., 2000a; York *et al*., 1999). However, where InsP_6 is produced does not seem that important: a plasma membrane-localised mutant of Ipk1p has no growth defect, showing that cytoplasmic production of InsP_6 can support mRNA export (Seeds *et al*., 2007) (see also section 1.10.3)

Other proposed roles for InsP_6 include directly interacting with synaptotagmin, a Ca^{2+}-sensitive vesicle protein that regulates endo- and exocytosis (Fleischer *et al*., 1994; Norris *et al*., 1995; Voglmaier *et al*., 1992), synaptic vesicle trafficking (Llinas *et al*., 1994; Niinobe *et al*., 1994; Schiavo *et al*., 1995), and receptor desensitization

(Palczewski *et al*., 1991). InsP_6 production is required for the asymmetric Ca^{2+} flux during left-right heart specification (Sarmah *et al*., 2005). It may also play a role as an antioxidant through binding of Fe^{3+}(Graf *et al.*, 1987) and as a phosphate store, especially in plants (Morton and Raison, 1963).

InsP_6 was found bound to the Ku70/80 subunits of DNA-PK, the DNA-dependent protein kinase involved in DNA repair, when this enzyme was crystallized, but the yeast homologue of Ku70/80, yKu70/80, does not bind InsP_6 (Hanakahi and West, 2002).

1.9.2.3 Kcs1p, Vip1p and inositol pyrophosphates

S. cerevisiae has two inositol pyrophosphate synthases, Kcs1p and Vip1p. Kcs1p, the predominant InsP_6 kinase capable of generating *PP*-InsP_5, was discovered as a second-site suppressor of protein kinase C mutants (Huang and Symington, 1995; Saiardi *et al*., 1999). Kcs1p can also phosphorylate other Ins*P*s to produce the pyrophosphates including *PP*-InsP_4, *PP*-InsP_5, $(PP)_2$-InsP_3 and $(PP)_2$-InsP_4 (Luo *et al*., 2002; Saiardi *et al*., 2000a; Saiardi *et al*., 2002; Seeds *et al*., 2005; York *et al*., 2005), and it also phosphorylates Ins(1,4,5)P_3 at the D3 position (Dubois *et al*., 2002; Seeds *et al*., 2005). Vip1p, the second inositol pyrophosphate synthase can synthesise several other pyrophosphorylated Ins*P*s (*PP*-InsP_4, *PP*-InsP_5 and $(PP)_2$-InsP_4) (Seeds *et al*., 2005; York *et al*., 2005).

Inositol pyrophosphates seem to be involved in diverse cellular processes, including endocytic trafficking (Saiardi *et al*., 2002), DNA recombination (Luo *et al*., 2002), vacuole morphogenesis (Saiardi et al., 2000), cell wall integrity and resistance to salt

stress (Dubois *et al.*, 2002). They also seem to be essential for the expression of genes regulated by the quality of the nitrogen source and of phosphate-responsive genes (El Alami *et al*., 2003). How they are involved in these processes remain ill-defined.

Recently, Kcs1p and its product *PP*-InsP_4 have been shown to be necessary for telomere maintenance and DNA repair: Mutants of *PLC1*, *ARG82* or *KCS1* lengthened telomere and increased levels of *PP*-InsP_4 result in shortened telomeres as compared with the wild-type cells, implicating *PP*-InsP_4 as a negative regulator of telomere length (York *et al*., 2005). How inositol pyrophosphatess regulate telomere length is not known, but, the PPIn 3-kinase-related protein kinase Tel1p may be involved (Saiardi *et al*., 2005).

Another important finding was that InsP_7 (5-*PP*-InsP_5) phosphorylates proteins non-enzymatically (Saiardi *et al*., 2004). InsP_7 only phosphorylates proteins that have been already phosphorylated on serine residues by ATP-dependant kinases, and this phosphorylation forms pyrophosphorylated serine residues (Bhandari *et al*., 2007).

1.10 Functional interactions of the Plc1p pathway with other systems

Recent studies have implicated Plc1p in a number of other yeast regulatory systems.

1.10.1 Involvement of Plc1p with nutrient modulation of growth

Nitrogen sensing

Plc1p was implicated in a nitrogen-sensing pathway that regulates the modulation of pseudohyphal differentiation (Ansari *et al.*, 1999; Toker, 2002). According to Schomerus and Kuntzel, re-addition of a nitrogen source (ammonium sulphate) to

nitrogen-depleted media provoked a rapid increase in InsP_3 and DAG generated from PtdIns(4,5)P_2 hydrolysis by activated Plc1p in wild-type *S. cerevisiae* (Schomerus and Kuntzel, 1992). In our lab, we found addition of NH_4 to nitrogen-starved yeast induced the formation of an unidentified InsP_4 suggesting that inositol phosphate outputs from Plc1p activation can be modulated depending upon cell state (Perera *et al*., 2004).

Another recent genetic study has provided a link between Plc1p and Gpa2p, one of the two heterotrimeric G protein α–subunit homologs in yeast and an element of the nitrogen sensing machinery that regulates pseudohyphal differentiation by modulating cAMP levels (Lorenz and Heitman, 1997). A putative heptahelical receptor, Gpr1p, coupled with Gpa2p, regulates cAMP synthesis and the protein kinase A (PKA) activity to control filamentation and growth (Lu and Hirsch, 2005; Trott *et al*., 2005).

In the absence of nitrogen, cells lacking Gpr1p, Plc1p, or Gpa2p fail to form pseudohyphae. This defect of filamentation in *plc1Δ* and *gpr1Δ* strains can be rescued by over-expression of Tpk2p, one of the three catalytic subunits of PKA in *S.cerevisiae*, via the cAMP pathway (by the catalytic subunit of cAMP-dependent protein kinase), or via the mitogen-activated protein kinase (MAPK) pathway (by introduction of *STE11-4*, a dominant-active allele of *STE11* that is a component of MAPK pathway). The cAMP and MAPK pathways converge to regulate transcriptional control of *FLO11,* which encodes a cell surface protein required for pseudohyphal formation (Rupp *et al.*, 1999).

Gpr1p acts mainly through the cAMP pathway involving Gpa2p. Physical association of Plc1p with Gpr1p was observed by two-hybrid and co-immunoprecipitation. This association is independent of Gpa2p, whereas Plc1p is required for Gpr1p/Gpa2p association (Ansari *et al*., 1999). It appears that the MAPK pathway is also dependent on Plc1p regardless of the presence of Gpr1p, based on analysis of transcriptional regulation of filamentation (Ansari *et al*., 1999).

The genetic and physical interactions between Plc1p, Gpr1p and Gpa2p suggest Gpr1p and Gpa2p act in concert with Plc1p, but in parallel to the small G-protein Ras2p, since Ras2p suppresses *gpr1Δ* and *gpa2Δ* phenotypes yet fails to rescue *PLC1* null mutants (Ansari *et al*., 1999). Also, *plc1*Δ*gpa2*Δ and *plc1*Δ*gpr1*Δ double mutants grow as well as the *plc1*Δ single mutant, while the *plc1*Δ*ras2*Δ mutant displays a strong synthetic growth defect (Demczuk *et al*., 2008). Therefore, Gpr1p interacts with Plc1p during the pseudohyphal formation through Gpa2p, in a Ras-independent, cAMP-dependent pathway (Demczuk *et al*., 2008).

The mechanism by which Plc1p regulates these interactions is unknown. As indicated above, Plc1p probably acts upstream of Gpa2p, possibly by hydrolysing PtdIns(4,5)P_2 locally and exposing a binding site for Gpa2p in the carboxy-terminal region of Gpr1p (Toker, 2002). However, since Arg82p and synthesis of Ins*P*s are required for normal PKA signalling, this simple explanation seems unlikely. Indeed *arg82*Δ cells display increased transcription of Msn2p-dependent stress-responsive genes which indicates a decreased activity of PKA in these mutants. Thus it is not clear whether it's the catalytic activity of Plc1p that is required in the regulation of cAMP synthesis and

PKA signalling or if Plc1p only serves as a scaffold protein that is essential for the Gpr1p-Gpa2p interaction (Demczuk *et al*., 2008).

Phosphate accumulation

In *S. cerevisiae*, the *PHO* pathway regulates several phosphate-responsive genes, including *PHO5,* which encodes repressible acid phosphatase. A cyclin-dependent kinase inhibitor (Pho81p) regulates the kinase activity of the cyclin-cyclin-dependent kinase complex Pho80p-Pho85p (Kaffman *et al*., 1994). Pho81p forms a stable complex with Pho80p-Pho85p regardless of the cellular phosphate level, but inhibits the kinase activity of Pho85p only under low phosphate conditions. The Pho80p-Pho85p complex regulates *PHO5* expression by controlling the activity and localisation of the transcription factor Pho4p through phosphorylation in response to intracellular phosphate levels (Kaffman *et al*., 1994; Kaffman *et al*., 1998; Ogawa *et al*., 1995; Schneider *et al*., 1994).

*plc1*Δ*, arg82*Δ and *kcs1*Δ cells have significantly reduced intracellular polyphosphate levels and *PHO5* is constitutively expressed in these mutants, suggesting that the inositol pyrophospate products of these enzymes are required for polyphosphate accumulation (Auesukaree *et al*., 2005).

Recently work by the York and O'Shea labs has highlighted the role of the InsP_6 kinase Vip1p in the regulation of phosphate homeostasis. Vip1p pyrophosphorylates InsP_6 at the 4- or 6- position and the resulting 4/6-[*PP*]-InsP_5 modifies the interactions between Pho81p and Pho80p-Pho85p: elevated levels of 4/6-[*PP*]-InsP_5 appear to

inhibit Pho85p kinase activity, but 5-[*PP*]-InsP_5 does not have this effect (Lee *et al*., 2008; Lee *et al*., 2007).

1.10.2 Role(s) of Plc1p in stress responses

Yeast cells lacking *PLC1* display defects in their responses to various stresses. Plc1p contributes to the regulation of approximately 2% of yeast genes in cells grown in rich medium. Most of these genes are required under limited nutrient or stressed environment and are derepressed in *plc1*Δ cells (Demczuk *et al*., 2008).

Plc1p participates in stress responses via regulating the transcription of Msn2p-dependent genes. Msn2p is a zinc finger transcription factor that plays an important role in transcriptional responses to starvation and other forms of environmental stress (Estruch, 2000; Estruch and Carlson, 1993; Martinez-Pastor *et al*., 1996). PKA, which is Plc1p-regulated (see earlier), negatively regulates transcription of Msn2p-dependent genes by phosphorylating Msn2p, preventing its nuclear translocation (Beck and Hall, 1999; Chi *et al*., 2001; Gorner *et al.*, 1998; Gorner *et al*., 2002) or its binding to the STRE elements in the promoters of stress-responsive genes (Hirata *et al*., 2003).

Osmotic stress

In *S. cerevisiae,* two protein kinase pathways are known to regulate the response to osmolarity changes in the media: the high osmolarity glycerol (HOG) response pathway (Hohmann, 2002) and the protein kinase C (Pkc1p) pathway (Gustin *et al*., 1998). There is no convincing evidence for a link between Plc1p and either of these pathways, despite the fact that Pkc1p is a homolog of mammalian protein kinase Cs. However, several sequence differences between the C1 domains of Pkc1p and of

classical PKCs make Pkc1p unresponsive to DAG and Pkc1p also fails to respond to Ca^{2+}(Watanabe et al., 1994).

However, *PLC1* mutants are osmosensitive, so Plc1p has some roles in maintaining osmotic homeostasis (Flick and Thorner, 1993). Plc1p is required for expression of the osmo-inducible *GPD1* gene and for intracellular accumulation of glycerol but its effect is much less important than the role played by Hog1p (Lin *et al*., 2002). A strain with both *PLC1* and *HOG1* deleted expressed lower levels of a *GPD1-lacZ* fusion and synthesized less glycerol than strains with either single deletion (Lin *et al*., 2002).

Plc1p has also been reported to interact physically with Sgd1p (Lin *et al*., 2002), a nuclear protein which is known as a suppressor of the osmo-sensitivity. *SGD1* is an essential gene which was initially isolated by complementation of the osmo-sensitive and glycerol-defective phenotype of the *S. cerevisiae hog1* mutant (Akhtar *et al*., 2000). *SGD1* displays genetic interactions with *HOG1* -- overexpression of Sgd1p suppresses the osmo-sensitivity of *hog1Δ* and *pbs2Δ* strains. Thus, Sgd1p probably operates downstream of Hog1p. It is still not clear how the association of Plc1p with Sgd1p could affect Sgd1p during stress responses, and it is speculated that it has something to do with Plc1p's function in kinetochore activity. Sgd1p could serve as the targeting component when Plc1p localises to specific chromosomal loci and modifies chromatin structure at these loci (Lin *et al*., 2000).

Another clue to the role of Plc1p in osmo-regulation comes from the fact that deleting *PHO81* or *SPL2*, another inhibitor of Pho85p activity, allows *plc1*Δ mutants to grow in high salt media (Flick and Thorner, 1998), suggesting that one of the roles of Plc1p

during growth in high salt conditions is to activate Pho85p, probably through Ins*P*s and *PP*-Ins*P*s (Lee *et al*., 2008; Steger *et al*., 2003).

Growth at high temperature

The *PLC1* promoter region contains a consensus element for binding of heat shock transcription factor and growth of *plc1Δ* cells ceases at elevated temperatures (37ºC or above)(Flick and Thorner, 1993). Hence, survival of yeast cells at higher temperatures may require increased expression of *PLC1* by heat shock induction (Flick and Thorner, 1993). Our lab has observed that yeast cells produce increased amounts of inositol phosphates, particularly InsP_6, in a Plc1p dependent manner when they are grown at elevated temperatures (NM Perera and SK Dove 2002, pers. comm.): The reason for this is unknown but levels of InsP_6 can increase almost 10-fold over basal when cells are grown at 37ºC.

Plc1p is also associated with regulation of Ume3p, a cyclin-type protein. When yeast cells are stressed in a variety of ways, they respond by inducing several highly conserved gene families that express cytoprotective heat shock proteins (Craig *et al*., 1993). Ume3p represses the transcription of the *HSP70* family member *SSA1*. Downregulation of this cyclin is part of the normal cellular response to stress: Ume3p is rapidly destroyed when cells are exposed to elevated temperatures to relieve repression of *SSA1* (Cooper *et al*., 1997; Cooper *et al.,* 1999). An *UME3* null allele also suppresses the hypersensitivity of *PLC1* mutant at elevated temperature (Cooper *et al.,* 1999). These results indicate that the growth defects observed in *PLC1* mutants under heat stress could be due to a failure to downregulate Ume3p.

1.10.3 Plc1p and the inositol phosphates it generates are needed for mRNA export from the nucleus

Eukaryotic mRNA undergoes a series of molecular events, including transcription, processing, export, translation and degradation. A key step is mRNA export from the nucleus, the outward translocation of mRNA-protein complex (mRNPs) complexes through nuclear pore complexes (NPCs). Functional connections between mRNA export and translation have been suggested (Culjkovic *et al*., 2006; Gross *et al*., 2007; Jin *et al*., 2003; Rosenwald *et al*., 1995), but these molecular mechanisms are less well defined.

GLE1 encodes Gle1p, a cytoplasmically-oriented nuclear-pore complex associated factor (York *et al.*, 1999). It is an essential mRNA export protein that is conserved from yeast to human cells (Murphy and Wente, 1996; Watkins *et al*., 1998). InsP_6 generated via sequential phosphorylation by the inositol phosphate kinases Arg82p and Ipk1p is required to support mRNA export: Plc1p was discovered to be involved in modulating the nuclear export of mRNA via the Gle1p-dependent β-exportin pathway when it was found that *plc1Δ*, *arg82Δ* and *ipk1Δ* but not *kcs1Δ* cells have a defect in mRNA export (York *et al*., 1999). Deletions of all these genes are synthetically lethal with a conditional allele of *GLE1* or various mRNA export factors (Weirich *et al*., 2006; York *et al*., 1999).

InsP_6 is directly required for mRNA export and the export function of Gle1p is dependent on InsP_6 (Bolger *et al*., 2008). InsP_6 directly binds to Gle1p (Weirich *et al.*, 2006) and they act together to stimulate the RNA-dependent ATPase activity of the DEAD-box protein Dbp5p (Alcazar-Roman *et al*., 2006). Dbp5p is essential for

mRNA export: It is recruited to the cytoplasmic fibrils of the NPC via interaction with the nucleoporins CAN/Nup159p and participates in the export of mRNAs out of the nucleus (Schmitt *et al.*, 1999).

Ins(1,3,4,5,6)P_5 can also activate Dbp5p and hence can partially compensate for loss of InsP_6 *in vitro* but is less efficient and requires a much higher concentrations of Ins(1,3,4,5,6)P_5 for this process to proceed at a normal rate (Weirich *et al*., 2006). Cells devoid of Plc1p or Arg82p normally display more severe phenotypes than those lacking the Ins(1,3,4,5,6)P_5-kinase Ipk1p, probably because *ipk1Δ* cells accumulate significantly increased levels of the direct InsP_6-precursor, Ins(1,3,4,5,6)P_5 and possibly also because Kcs1p can phosphorylate Ins(1,3,4,5,6)P_5 to produce *PP*-InsP_4 (Weirich *et al*., 2006).

There is also evidence that InsP_6-dependent mRNA export might be a feature of mammalian cells: when the InsP_6 levels in tissue culture cells were suppressed by expressing SopB, a *Salmonella Dublin* virulence factor that is relatively unspecific inositol polyphosphate phosphatase, mRNA accumulates in the nucleus (Feng *et al*., 2001).

Since mRNA export is a fundamental cellular process, a number of the *plc1*Δ phenotypes may be secondary consequences of this central defect.

One recent study has expanded the functions of InsP_6 to now include translation termination in *S. cerevisiae*, showing that Gle1p functions in termination via an InsP_6-

dependent activation of Dbp5 but InsP_6 is not involved in the initiation (Bolger *et al*., 2008).

1.11 Nuclear inositide signalling

Recent evidence has suggested the existence of nuclear specific pathways of inositide metabolism, though understanding of these processes remains incomplete (Irvine, 2003). One stumbling block to widespread acceptance of nuclear inositide signalling is the fact that most researchers cannot agree on whether the nucleus and the cytoplasm are insulated from one to another so that inositol phosphates generated in one compartment would not diffuse into the other compartment through nuclear pores. One important milestone in showing that inositol phosphates could be spatially restricted was a study that showed that many phosphorylated molecules, including higher inositol phosphates, are unable to pass through the pores of dialysis tubing, even when the molecular weight cutoff of the pores is 50 kD (Van der Kaay and Van Haastert, 1995). The explanation for this observation is still lacking but is thought to be a consequence of the high charge density and ordering of water into a hydration shell around these molecules. In any case, the 50 kD pore in these membranes is much larger than the 30 kD cutoff that characterises the nuclear pore complex (Van der Kaay and Van Haastert, 1995).

Whatever the details, much of the machinery for inositide signaling is present in the nucleus. Nuclear localisation has been observed for several PLCs, including PLC-β_1 and PLC-δ_4, in animal cells (D'Santos *et al*., 1998; Divecha *et al*., 1997; Liu *et al*., 1996; Martelli *et al*., 1992). In some cases, there are data that demonstrate that these enzymes are performing a real signaling function: insulin-like growth factor I (IGF-I)

activates nuclear PLC-β_1 and causes changes in nuclear phosphoinositides in Swiss 3T3 cells. IGF-1 activates only the nuclear pool of this enzyme and only nuclear PtdIns(4,5)P_2 is attacked during signaling. This process is both necessary and sufficient to drive IGF-1-induced cell division (Manzoli *et al*., 1997). Exactly how extracellular stimuli such as IGF-1 elicit selective nuclear inositide turnover is still obscure.

One surprising finding is that nuclear PtdIns(4,5)P_2 is present not only in the nuclear membrane, but also in ill-defined non-membranous complexes with protein that are completely resistant to extraction with detergents (Yagisawa *et al*., 2002). Some researchers have suggested that PtdIns(4,5)P_2 is bound to chromatin covalently, but how this could occur and why are not well understood (Yagisawa *et al*., 2002).

The outcomes of nuclear inositide signalling are equally ill-defined. InsP_3 receptors have been found localised to the inner nuclear membrane and could mediate nuclear calcium release (Gerasimenko and Gerasimenko, 2004). However, the above studies were all done at a time when the phosphorylation of InsP_3 was not well understood and hence it is possible that 'higher' inositol phosphates are involved. Indeed, since many of the known functions of InsP_6, InsP_7 and InsP_8 are nuclear, it is tempting to speculate that they mediate at least some of the effects of agonists, like IGF-1, on cell physiology.

1.12 Nucleo-cytoplasmic shuttling of PLCs

Most of the PLCs that have been observed in the nucleus, do not permanently reside there, at least in animal cells: they undergo some form of nucleo-cytoplasmic shuttling

(Faenza *et al*., 2005; Topham and Prescott, 2002; Yagisawa, 2006). Some enzymes that have traditionally been regarded as exclusively cytoplasmic have recently been found to maintain their steady-state localisation as a result of dynamic shuttling. PLC-δ_1 once thought of as a plasma membrane-localised enzyme in intact mammalian cells, is now known to be distributed between cytoplasm, nucleus and plasma membrane (Yagisawa *et al.*, 2002). PLC-δ_1 enters the nucleus upon stimulation and undergoes continuous nuclear/cytoplasmic shuttling even under unstimulated conditions (Diakonova *et al*., 1997; Yagisawa *et al*., 2002). Its translocation is also linked with cell cycle progression as it shifts localization to the nucleus at certain stages (Okada *et al*., 2002; Yagisawa *et al*., 2006).

1.12.1 Nuclear export and import of PLCs

Once we concede that PLCs can show dynamic localisation behaviour, it becomes important to know how nucleo-cytoplasmic shuttling of PLCs is regulated. It was originally suggested that nascent PLC enzymes, newly translated from RNA in the cytoplasm, depend on some extracellular stimuli or cell cycle-dependent signal to get imported into the nucleus (Yagisawa *et al*., 2006). In general, molecules as large as PLCs cannot freely diffuse through the nuclear pore complex, and so rely on nuclear localization signals (NLS) and nuclear export signals (NES) to enter and leave this compartment. The intracellular distribution of a given protein is the result of the balance of the strength of these two signals (Yagisawa *et al*., 2006).

Fig 1.15 illustrates a schematic representation for conventional nucleo-cytoplasmic shuttling. Briefly, binding of cargo protein to an adaptor called importin-α occurs via the NLS in the cargo, and this initiates the association with the carrier protein,

importin-β. This trimer can be recognized by the nuclear pore complex (NPC) and transported into the nucleus. Once in the nucleus, the complex dissociates, and the importins are transported back to the cytoplasm by a small G protein, Ran. For export, the cargo protein must bind to CRM1 (known as Crm1p or Xpo1p in *S. cerevisiae*), an exportin-1, through its NES and is then transported out of the nucleus. Leptomycin B, a specific inhibitor of Crm1p forms a covalent bond with CRM1 and blocks nuclear export, resulting in the accumulation of cargo proteins in the nucleus (Yoneda, 2000).

Fig1.15: Nuclear import and export machineries (Yoneda, 2000)

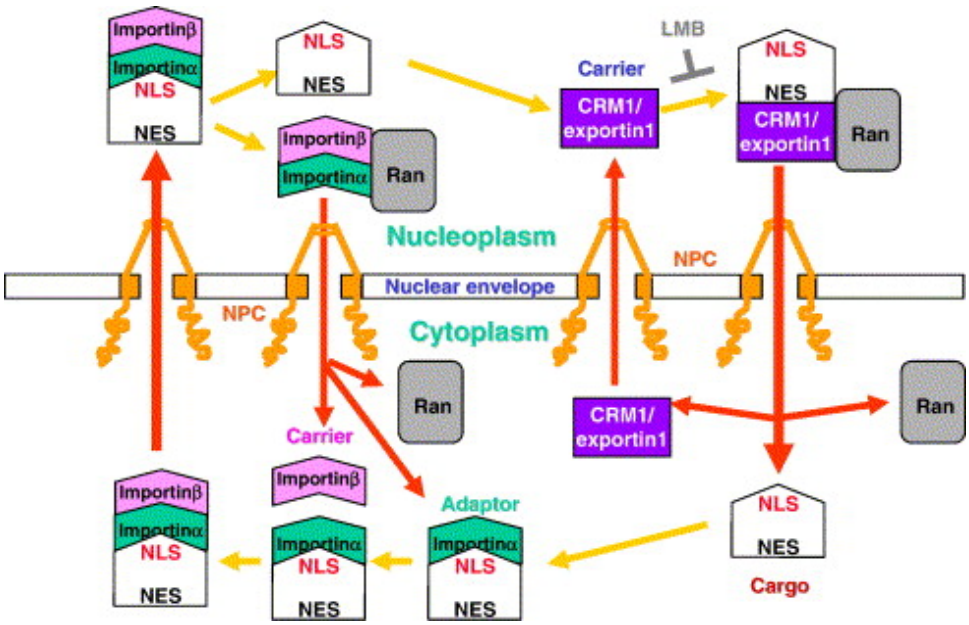

The first observation that suggested the presence of a functional NES in any PLC was an experiment in which Leptomycin B was used to treat MDCK cells expressing a GFP-tagged PLC-δ_1. The PLC accumulated in the nuclei of these cells, indicating nucleo-cytoplasmic shuttling of this enzyme and export via CRM1 (Kudo *et al*., 1998; Yoshida *et al*., 1990).

The canonical NES consensus sequence is a short leucine-rich motif. In mammalian PLC-δ_1, amino acid residues 164-177 of the EF-hand domain perform this function (Yamaga *et al*., 1999). There is an NES sequence in this region in the following enzymes: PLC-β_1, -δ_3, -γ_1, -ε, -ζ (Yamaga *et al*., 1999). The observed sequence variation probably reflects the differing strength of the NES in various isoforms (Fig 1.16).

Fig 1.16: The putative NES sequence of PLC-δ_1 and canonical NES sequences (Yamaga et al., 1999)

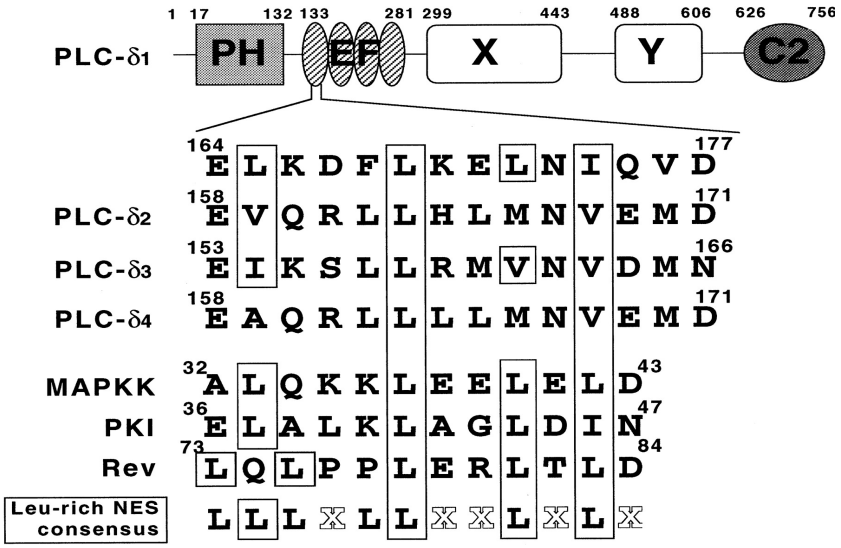

Schematic representation of PLC-δ type NES sequences in the EF-hand domain. The numbers above the structure refer to the amino-acids in rat PLC-δ_1. The NES sequences of mitogen-activated protein kinase kinase (MAPKK), protein kinase inhibitor (PKI) and Rev are also aligned as typical leucine-rich NES sequences. "X" denotes any amino acid, and important hydrophobic residues in the sequences are boxed. Note, the bovine PLC-δ_2 is actually a homolog of human and mouse PLC-δ_4.

Nuclear import is mediated by NLS sequences. They serve as the docking sites to bind to the carrier proteins for nuclear import. The necessary sequence elements for a functional NLS are less well defined than for the NES. They are usually short stretches of 5-10 basic amino acids, but some of the sequences that confer NLS function, particularly in viral proteins, have no obvious similarity to the suggested

canonical consensus.

For most animal PLCs, the functional NLS sequence is in the vicinity of the XY-linker (Yagisawa *et al*., 2006). Fig 1.17 shows NLS sequences from a number of PLC isoforms from different species - but note that the sequences from non-animal species have not been tested as being functional. *S. cerevisiae* Plc1p has such a NLS consensus sequence in its X-Y linker, but deletion of this motif has no effect on the localisation of this protein (SK Dove 2005, pers. comm.).

Fig 1.17: Sequence resembling classical NLS in the X domain and in the XY-linker region of the PLC isoforms (Okada et al., 2002)

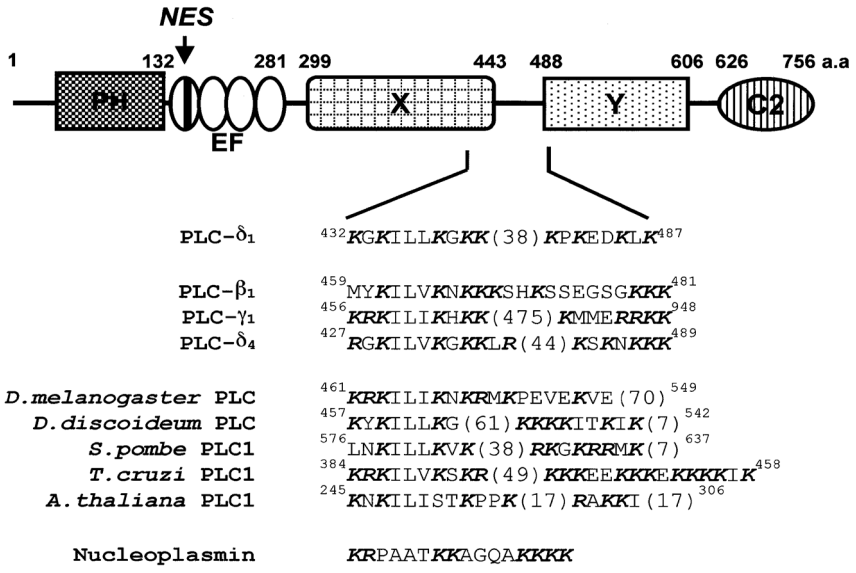

Sequence alignment of the C-terminus of the X domain and XY-linker in various PLCs. A schematic structure of PLC-δ_1 with the sequence resembling a classical NLS in this region is shown. The NLS sequence of nucleoplasmin is aligned as a typical bipartite NLS sequence.

In PLC-δ_1 two lysine residues (K432 and K434) are critical for the import signal but local secondary structure was also important for NLS function (Okada *et al*., 2002).

In addition, Corbett's group recently concluded that a 'classic' monopartite NLS was

formed by a loose consensus sequence of K(K/R)X(K/R) requiring a lysine in the position 1, followed by 2 basic residues at postion 2 and 4(Leung *et al*., 2003).

1.12.2 Signals that trigger PLCs to translocate

The steady-state localisation of a dynamically shuttling PLC depends upon the relative activities of the import and export machineries, so a shift in the equilibrium of the strengths of these two signals will cause a change in localisation. Many factors are now known to regulate this equilibrium, including receptor activation, stresses, and cell cycle progression (Yagisawa *et al*., 2006).

PLC-δ_1 accumulates in nuclei at the G1/S phase boundary in NIH-3T3 cells (Yagisawa *et al*., 2006), and nuclear translocation of PLC-ζ occurs during early embryonic development of mice (Larman *et al*., 2004; Sone *et al.*, 2005). Both growth factor receptor activation (Bertagnolo *et al*., 1995) and cell cycle progression (Faenza *et al*., 2000) can cause PLC-β_1 to relocate to the nucleus and this shift is critical for erythroid cell survival and differentiation (Faenza *et al*., 2002). Also, changes in a cell's PtdIns(4,5)P_2 complement can affect PLC-δ_1 localisation (Yagisawa *et al*., 2006). However, the mechanisms mediating these localisation shifts are poorly understood.

An increase in intracellular Ca^{2+} also seems to be important for nuclear localization: mechanisms that increase Ca^{2+} seem to facilitate PLC-δ_1 import and impede its export (Okada *et al*., 2005). Three possible explanations of how Ca^{2+} might regulate the localization of PLC-δ_1 are illustrated in Fig 1.18 (Okada *et al*., 2005).

Fig 1.18: Possible mechanisms for the Ca^{2+}-dependent regulation of nuclear transport of PLC-δ_1 (Yagisawa, 2006)

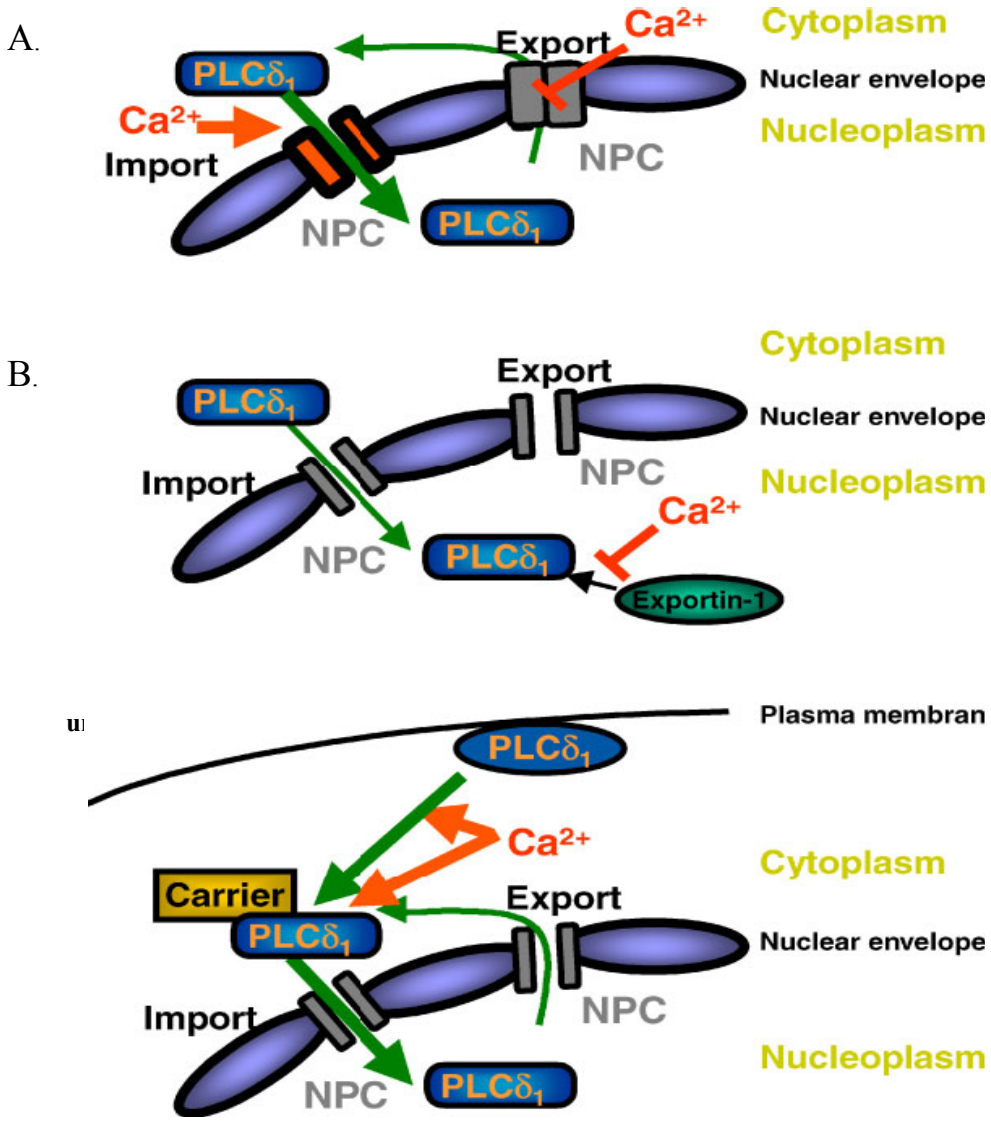

The proposed mechanisms by which Ca^{2+} might regulate PLC-δ_1 translocation: A. altering the structure of the NPC; B. down-regulating the formation of nuclear export complex; C. enhancing the formation of import carrier complex by changing the structure of PLC-δ_1 and/or increasing availability of PLC-δ_1 in the cytoplasm by dissociation of PLC-δ_1 from the plasma membrane.

1.13 Aim of this work

In contrast to PLC-β and PLC-γ, the regulation of PLC-δs is still largely a mystery. This is particularly frustrating because PLC-δs are the only PLCs in fungi, plants, and often non-animal eukaryotes, and are likely to perform an ancient and important function(s).

The budding yeast *S.* cerevisiae encodes a single PLC gene, Plc1p, which is an orthologue of mammalian PLC-δ. Plc1p generates InsP_3 in response to stress, but the yeast genome encodes no InsP_3 receptor. This suggests that the functions of PLC-δs are mediated in a novel fashion, probably involving 'higher' inositol phosphates (Ins*P*s) and pyrophosphorylated inositol phosphates (*PP*-Ins*P*s) that are generated from InsP_3 by inositol polyphosphate kinases.

Deleting or disrupting any of these genes in yeast results in defective Ins*P*s/*PP*-Ins*P*s synthesis. Accordingly, mutants in any of the genes encoding these proteins share a number of common defects. Yeast is therefore a powerful model in studying the Ins*P*s and *PP*-Ins*P*s derived from the PLC signalling pathway.

The aim of this work is to understand how yeast PLC-δ localisation is regulated, in order to gain insight into its function. Plc1p is present in both nucleus and cytoplasm in normal growing cells. I take advantage of its nuclear export signals (NES) and nuclear localization signals (NLS) to manipulate Plc1p's intracellular distribution by creating mutants that are restricted to nuclear or cytoplasmic compartments. The overall aim was to investigate which defects of *plc1*Δ cells would persist in yeast expressing Plc1p mutants restricted to only one compartment. I reasoned that this

would allow us to see if any of these mutants would only rescue subsets of the many stress-related phenotypes that are characteristic of cells lacking Plc1p, and so help us understand whether distinct pools of phosphoinositide signals might function independently in each of the two compartments.

I also focussed on the regulation of Plc1p by endogenous inositides and by possible interactions with other proteins. Mammalian PLC-δ_1 is known to interact with InsP_3 through its PH domain. I looked into the interaction of the yeast PLC-δ with the inositol phosphates it derives. This probably works as a feedback signal in PLC activation, and highlights the fact that PLCs can be regulated by the products of their own catalytic activity.

Chapter 2 Materials and Methods

2.1 Strains, Plasmids, Media and Reagents

Wild type *S. cerevisiae* FY833 was purchased from ATCC (Manassas, USA). BY4742 and some deletion strains bearing *KANMX4* deletion cassettes were purchased from EUROSCARF (Germany). The remaining deletion strains were either from the Dove lab yeast strain collection or else were made in this study. *S. cerevisiae* strains were grown in standard Yeast extract-Peptone-Dextrose (YPD) or Synthetic Complete (SC) minimal media supplemented with essential amino acids. The budding yeast strains used in this study are listed in Table 2.1.

E.coli TOP10 competent cells were used for all sub-cloning and were made competent as described below. BL21-star (DE3)-RIL cells were obtained from the Dove lab *E.coli* strain collection and were used to express GST (glutathione-S-transferase)-Plc1p fusion proteins. *E.coli* strains were propagated in LB broth or LB plates (containing appropriate antibiotics for plasmid retention) following routine manipulation.

Plasmid pUG36 and pUG34 were gifts from Dr. J. H. Hegemann (Institut für Mikrobiologie, Germany). Plasmid pGEX-6P-K-1 was obtained from Dr Dove who modified the commercially available vector pGEX-6P-1 (G.E Biotech) by inserting sequences that encode a protein kinase A phosphorylation consensus motif between the GST and the protein of interest. pUR34*NLS* was a gift from Dr. F. Rodrigues (Universidade do Minho, Portugal). pGEM-T Easy Vector System was purchased from Promega (Promega#A1360). pYcPlac111 was obtained from ATCC (#87587,

Table 2.1: S. cerevisiae strains used in this study

Strain	**Genotype**	**Source**
BY4742	*MATα his3Δ1 leu2Δ0 lys2Δ0 ura3Δ0*	Euroscarf
BY4742 *plc1Δ*	*MATα his3Δ1 leu2Δ0 lys2Δ0 ura3Δ0 plc1::kanMX4*	Euroscarf
BY4742 *arg82Δ*	*MATα his3Δ1 leu2Δ0 lys2Δ0 ura3Δ0 arg82::kanMX4*	Euroscarf
BY4742 *arg82Δplc1Δ*	*MATα his3Δ1 leu2Δ0 lys2Δ0 ura3Δ0 arg82::kanMX4 plc1::HIS3*	This study
BY4742 *ipk1Δ*	*MATα his3Δ1 leu2Δ0 lys2Δ0 ura3Δ0 ipk1::kanMX4*	Euroscarf
BY4742 *kcs1Δ*	*MATα his3Δ1 leu2Δ0 lys2Δ0 ura3Δ0 kcs1::kanMX4*	Euroscarf
BY4742 *vip1Δ*	*MATα his3Δ1 leu2Δ0 lys2Δ0 ura3Δ0 vip1::kanMX4*	Euroscarf
BY4742 *kcs1Δvip1Δ*	*MATα his3Δ1 leu2Δ0 lys2Δ0 ura3Δ0 kcs1::kanMX4 vip1::LEU2*	Dove lab
BY4742 *arg82Δvps41Δ*	*MATα his3Δ1 leu2Δ0 lys2Δ0 ura3Δ0 arg82::kanMX4 vps41::HIS3*	This study
FY833	*MATa ade2 his3 leu2 trp1 ura3*	Euroscarf
FY833 *(PLC1-3HA)*	*MATa ade2 his3 leu2 trp1 ura3 plc1::PLC1-3xHA-His3*	This study
FY833 *(PLC1-3HA; ARG82-9Myc)*	*MATa ade2 his3 leu2 trp1 ura3 plc1::PLC1-3xHA-His3 arg82::ARG82-9xMyc-Trp1*	This study
FY833 *(PLC1-GFP; ARG82-9Myc)*	*MATa ade2 his3 leu2 trp1 ura3 arg82::ARG82-9xMyc-Trp1 [pUG36-PLC1]*	This study
KWY120	*MATα xpo1::LEU2 ade2-1 ura3-1 his3-11,15 trp1-1 leu2-3,112 can1-100 [pKW440-XPO1-HIS3]*	Dove lab
KWY121	*MATα xpo1::LEU2 ade2-1 ura3-1 his3-11,15 trp1-1 leu2-3,112 can1-100 [pKW457-xpo1-1-HIS3]*	Dove lab
BY4742 *gpr1Δ*	*MATα his3Δ1 leu2Δ0 lys2Δ0 ura3Δ0 gpr1::LEU2*	This study
BY4742 *gpr1Δarg82Δ*	*MATα his3Δ1 leu2Δ0 lys2Δ0 ura3Δ0 arg82::kanMX4 gpr1::LEU2*	This study

Manassas, USA). pFA6a-His3MX6 was obtained from Dr Bill Parrish (UCSD, California).

Plasmid pUG34 used in this study is a low copy centromeric yeast expression vector and was modified by Dr. Hegemann so that GFP is expressed as a C-terminal fusion to any gene cloned into the multiple cloning site (Niedenthal *et al.*, 1996).

Plasmid pUG36 (YCp, *URA3*, P_{MET25}-*yEGFP3*-MCS-T_{CYC1} (Niedenthal *et al*., 1996) was used as the vector to express green fluorescent protein (GFP) fusion proteins (Fig 2.1). Proper cloning of an insert into the multiple cloning sites (MCS) of pUG36 allows the expression of yEGFP N-terminal fusion proteins under the control of methionine-regulated *MET25* promoter(Mumberg *et al*., 1994). Plasmids pUG36-*PLC1,* pUG36-*CAAX* and pUG36-*ARG82* were obtained from the Dove lab plasmid collection. PCR products encoding *PLC1* or *ARG82* were cloned into the *Bam*HI-*Hind*III sites of pUG36.

Media for growth of yeast strains: yeast extract, bacto-peptone, bacto-agar, bacto-tryptone, yeast nitrogen base without amino acids or ammonium sulphate were from Difco Laboratories (Detroit, MI).

2-O-Butyryl-Ins(1,3,4,5,6)P_5/PM, Membrane permeant Ins(1,3,4,5,6)P_5 was from Echelon (#Q-M1396).

All other biochemical reagents were from Sigma-Aldrich (St. Louis, MI) except as indicated, and were of Biotechnological grade or better. U73122 (#U6756) and its

Fig 2.1: pUG36 map

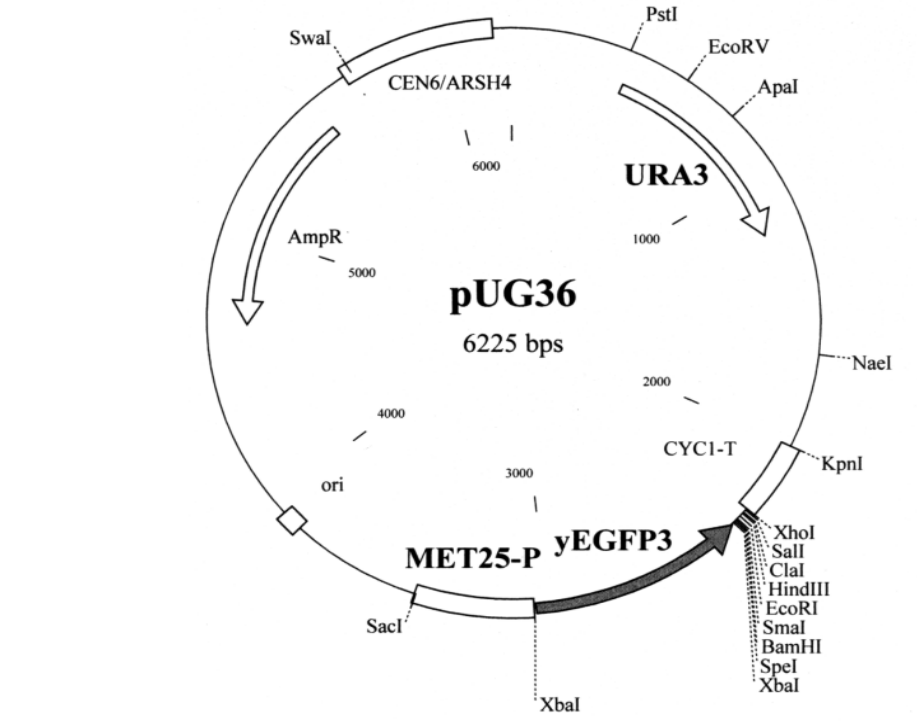

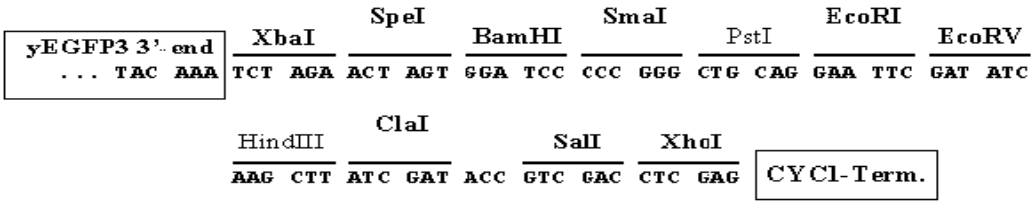

inactive analog U73433 (#U6881) were purchased from Sigma.

2.2 Media composition and solutions

All media were autoclaved for 15 mins at 121°C, cooled and glucose was then added to a final concentration of 2% (from a 40% w/v stock) prior to use.

Yeast extract Peptone Dextrose (YPD) (1L):

Glucose (2.0% w:v), Bactopeptone (2.0% w:v), Yeast extract (1.0% w:v), Adenine (100 mg), Uracil (100 mg)

Yeast extract Tryptone Dextrose (YTD) (1L):

Glucose (2.0% w:v), Bacto-tryptone (2.0% w:v), Yeast extract (1.0% w:v), Adenine (100 mg), Uracil (100 mg).

Luria Broth (LB) (1L):

Tryptone (1.0% w:v), Yeast Extract (0.5% w:v), NaCl (1.0% w:v)

LB + 100 μg/ml Ampicillin (1L):

LB, Ampicillin (100 μg/ml)

LB + 100 μg/ml Ampicillin + 50 μgml^{-1} Chloramphenicol (1L):

LB, Ampicillin (100 μg/ml), Chloramphenicol (50 μg/ml)

To prepare agar plates for YPD, YTD or LB media, Bacto agar (2.0% w:v) was added before autoclaving. Media was cooled to 50ºC and then glucose and/or antibiotics or salt were added.

Amino acid (AA) mix stock:

Adenine (2 g), Arginine (2 g), Tyrosine (30 mg), Isoleucine (2g), Phenylalanine (2.06 g), Glutamic acid (2 g), Aspartic acid (2 g), Valine (2 g), Threonine (2 g), Serine (2 g), Glycine (2 g), Proline (2 g), Alanine (2 g). Powder was milled in the IKA for 1 minute

and then stored at 4°C.

Synthetic Complete (SC) (1L):

Glucose (2.0% w:v), Yeast Nitrogen Base without Amino Acids & Ammonium Sulfate (1.7 g), Ammonium Sulfate (3 g), Glutamine (100 mg), AA mix stock (1g), 100 mg leucine, lysine, tryptophan, histidine, methionine, uracil; pH 5.7

For selective SC medium, the corresponding amino acid was omitted. For example, to make SC-Ura, 100mg Uracil was left out.

To prepare agar plates for SC media, the pH of SC was adjusted to 5.7 with 5M NaOH prior to the addition of Bacto agar (2.0% w:v). Media was then autoclaved, cooled and then glucose was added before use.

SC-Ura+Met (0.2g/L) agar (1L) :

SC-Ura, Methionine (100mg), Bacto agar (2.0% w:v)

SOC medium (1L):

Tryptone (2.0% w:v), Yeast Extract (0.5% w:v), NaCl (0.05% w:v), KCl (2.55 mM), adjust pH to 7 with NaOH. After autoclaving, sterile solution of $MgCl_2$ (10 μM) and Glucose (20 μM) were added.

× 50 Tris-Acetate-EDTA buffer (TAE):

Tris (2.0 M), Glacial acetic acid (0.94 M), 0.05 M EDTA (pH 8.0)

× 6 DNA gel electrophoresis sample buffer:

Tris.HCl (10 mM), Glycerol (50% v:v), Bromophenol blue (0.2% w:v)

× 5 SDS-PAGE sample buffer:

Tris.HCl (250 mM, pH 6.8), Glycerol (50% v:v), SDS (10% w:v), Bromophenol blue (0.5%, w:v). DTT (100 mM) was added fresh (from a 1M stock) before use.

× 10 SDS-PAGE running buffer:

Tris-Base(250 mM), Glycine (2.5 M), SDS (1% w:v)

× 10 transferring buffer for Western blotting:

Tris-Base(250 mM), Glycine (1.87 M)

PBST buffer (Phosphate buffered saline + Tween 20)

Sterile PBS (8.2 mM Na_2HPO_4, 1.5 mM KH_2PO_4, 139 mM NaCl, 3 mM KCl) was prepared using PBS tablets (Oxoid) and filter sterilised using a 0.22 μM filter or autoclaved. Tween 20 (0.1%) was added before use.

MES buffer

MES (10 mM), glucose (2.0% w:v)

TBST buffer (Tris-buffered saline + Tween 20).

Tris.HCl (50 mM, pH 7.5), NaCl (150 mM). Tween 20 (0.1%) was added before use.

2.3 Polymerase chain reaction (PCR)

All PCRs were performed with Expand High Fidelity PCR system (Roche) except as in indicated, in a TECHNE TC-3000 (Staffordshire, UK) thermal block cycler. Two reaction mixes were prepared according to manufacturers instructions as follows:

Master mix 1: Deoxyribonucleotide mix (200 µM of each dNTP, Bioline#39025), upstream primer (300 nM), downstream primer (300 nM), and target DNA were mixed in one "master mix" made up to 50 µl total volume with ice-cold ddH_2O.

Master mix 2: 10x buffer (5 µl) and Expand enzyme (0.75 ul) were made up to 50 µl total volume with ddH_2O and mixed.

The two master mixes were then thoroughly mixed again. All PCRs were then aliquoted into 50 µl reactions, since this was the volume that the thermal cycler temperature program was designed to control. The cycling profile was as follows:

94°C	94°C	T_{mi}-5°C	68°C	94°C	T_m-5°C	68°C	68°C	4°C
4 min	0.5min	1min	2min/1kb	0.5min	1min	2min/1kb	10min	12hrs
1 cyc	15 cycs			25 cycs			1 cyc	1 cyc

* Tmi is the Tm with only the initial matching region.

2.4 Site-specific mutagenesis: Splicing by Overlapping Extension PCR (SOE-PCR)

The following method was modified from *Molecular Cloning: A laboratory manual, third edition* (Sambrook J & Russell DW, eds), Cold Spring Harbour Laboratory Press, Cold Spring Harbour, New York, USA, 2001, Volume 2: 13.36.

Four primers were used to introduce a site-specific mutation by overlap extension. The first pair of primers (A & B) was used to amplify the DNA that contained the mutation site together with upstream sequences. Of which, Primer A harboured a wild-type sequence whereas primer B contained the mutation(s) to be introduced.

Similarly, the second pair of primers (C & D) was used to amplify the DNA that contained the mutation sites with downstream sequences. Of which, Primer D included a wild-type sequence whereas primer C harboured the mutation(s) to be introduced.

The two sets of primers were used in two separate amplification reactions to amplify over-lapping DNA fragments (fragment AB and CD). The mutation(s) of interest was located in the region of overlap and therefore in both sets of resulting amplified fragments. The overlapping fragments were mixed, denatured and annealed to generate heteroduplexes that could be extended via 'megapriming' and, in a third PCR, amplified into a full-length DNA using two primers that bound to the extremes of the two initial fragments (The overall strategy is sketched in Fig. 2.2).

Figure 2.2: Site-directed Mutagenesis by Overlap Extension
(Sambrook, 2001)

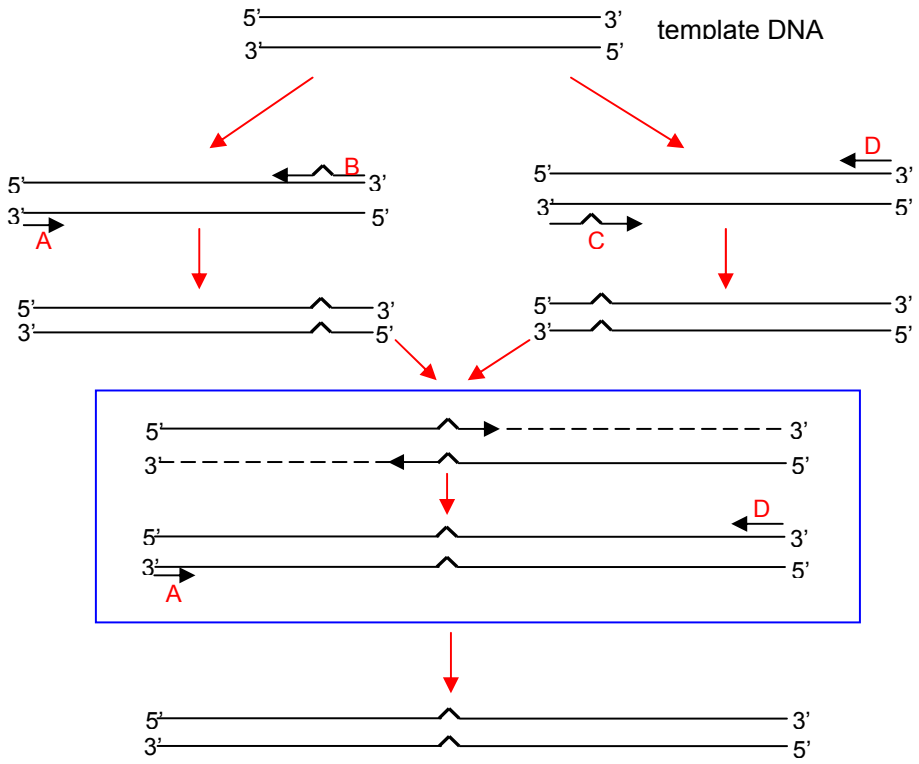

2.5 DNA sequencing

DNA sequencing was performed by the Functional Genomics and Proteomics Unit, University of Birmingham (Birmingham, UK). A reaction mix was prepared for each template to be sequenced, as follows: template (100 ~ 500 ng), primer (3.2 pmol), and ddH_2O were added to total volume of 10µl. The Genomics facility then added a Terminator Reaction Mix to each primer/DNA mix so supplied to give a final volume of 20µl. The reaction mixes were then amplified via PCR and the resulting chain-termination reaction resolved using an ABI sequencing device that separated the dye labelled fragments by capillary electrophoresis. The sequencing data were then analyzed in Chromas (version 1.45).

2.6 Plasmid construction

All DNA restriction enzymes and T4 DNA ligase were obtained from New England Biolabs, Inc (Beverly, MA). Standard molecular biology techniques were used for DNA manipulations. PCR products were purified by Qiagen II resin. Plasmids were purified by mini/midi/maxi prep kits obtained from Qiagen Ltd. All constructs were generated by transforming into *E. coli* TOP10 competent cells and confirmed by DNA sequencing. All oligos were synthesized by Alta Biosciences, University of Birmingham, UK and are listed in Table 2.2.

pUG36–*PLC1*$^{1\text{-}110}$

PLC1$^{1\text{-}110}$ was amplified from original pUG36-*PLC1* using oligonucleotides pUG36-SOEA1 and pUG36-SOED3 that incorporated unique *Bam*HI and *Hind*III restriction enzyme sites at the 5' and 3' ends respectively. The PCR product was digested with *Bam*HI and *Hind*III, then sub-cloned into *Bam*HI/*Hind*III-digested pUG36 vector.

Table 2.2: Oligos used in this study

Name	Sequence (5' to 3')
pUG36-SOEA1	GTGTGTGTGTCTTGTTACCAGACAACCATTACTTAT
pUG36-SOEA2	TTTTTTTT*GGATCC*ATGGAAAGCATACTTTTGCCTG
pUG36-SOED1	GTTTGTTTTTGTTTGATTAAGTTGGGTAACGCCAGG
pUG36-SOED2	TTTTGG*AAGCTT*TCATTGCTCATGCTGCTCTGTAAT
pUG36-SOED3	TTTTTG*AAGCTT*CTATTGCAATACGCGACATAGCGT
PLC1-330Top	TTT*GGATCC*AGAGGAATCAGGATGATTAGGATG
PLC1-1000Top	TTTTT*GGATCC*AGCAGCATGAGCAAGTGGATC
PLC1Trunc1	GTTTT*AAGCTT*TCACAGGCAAAAGTATGCTTTCCAT
PLC1_*NES*_f	AACAAA**GCT**AAAGCG**GCT**CACGTAGTTGCTTTGAAT
PLC1_*NES*_r	TACGTG**AGC**CGCTTT**AGC**TTTGTTGGAAACCTTATA
PLC1-ORF5	TGTGTG*AAGCTT*TAAAATTTGTGTATGAATAAATAAAGTGCAAAATAT
pUG36CAAX_f	*AGCTT*GGATCGGGTGGCTGTTGTATTATAAGTTAA*GAGCTCC*
pUG36CAAX_r	*TCGAGGAGCTC*TTAACTTATAATACAACAGCCA CCCGATCC*A*
PLC1NLS_KKLRK_f	TTAAC**GCTGCT**TTA**GCT**AAAGACTGTGATCTCAGCA
PLC1NLS_KKLRK_r	CAGTCTTT**AGC**TAA**AGCAGC**GTTAACAAGCTCATTTAT
PLC1NLS_KRLR_f	ATCCG**GCTGCT**TTG**GCT**TCGGACAGTAAACTTT
PLC1NLS_KRLR_r	A**AGC**CAA**AGCAGC**CGGATCTACTTCCTCTTGAT
PLC1NLS-C1	AA**TTG**GGAATCAGGATGATT**TCT**ATGACAAGAAGAAGAAGGAA
PLC1NLS-B1	AT**AGA**AATCATCCTGATTCC**CAA**TTGCAATACGCGACATA
PLC1NLS-C2	GACA**TCT**AGAAGA**GAA**AAGTTCTATGAATTTAAATTAATCAATAACAACG
PLC1NLS-B2	TT**TTC**TCTTCT**AGA**TGTCATCCTAATCATCCTGATTCC
PKI(2x)BamHI/SacI_f	*GATCC*TTGGCTTTGAAATTGGCTGGTTTGGATATT*GAGCTC*TTGGCTTTGAAATTGGCTGGTTTGG ATATT*G*
PKI(2x)BamHI/SacI_r	*GATCC*AATATCCAAACCAGCCAATTTCAAAGCCAA*GAGCTC*AATATCCAAACCAGCAATTTCAAA GCCAA*G*

PKI(2x)HindIII/XhoI_f	*AGCTT*TTGGCTTTGAAATTGGCTGGTTTGGATATT*CTCGAG*TTGGCTTTGAAATTGGCTGGTTTGGATATT*A*
PKI(2x)HindIII/XhoI_r	*AGCTT*AATATCCAAACCAGCCAATTTCAAAGCCAA*CTCGAG*AATATCCAAACCAGCCAATTTCAAAGCCAA*A*
PLC1_HindIII_f	TATATGAATG*AAGCTT*ACTGAAAGTGCTATAGATGAC
LEU2_KpnI_r	CTTT*GGTACC*CCATTTAGGACCACC
pGEasy_SacI_f	CTTT*GAGCTC*CCAACGCGTTGGAT
PLC1_HindIII_r	TTTCAGT*AAGCTT*CATTCATATACACTGCGTGAAT
PLC1_R117S/R120S_f	CAGGATGATT**TCT**ATGACA**TCT**AGAAGAAGGAAGTTCTA
PLC1_R117S/R120S_r	CTTCTTCT**AGA**TGTCAT**AGA**AATCATCCTGATTCCTCT
PLC1_R117S/R123E_f	CAGGATGATT**TCT**ATGACAAGAAGAAGA**GAA**AAGTTCTATG
PLC1_R117S/R123E_r	GAACTT**TTC**TCTTCTTCTTGTCAT**AGA**AATCATCCTGATTC
PLC1_R111L_f	CGTATTGCAA**TTG**GGAATCAGGATGATTAGGATGACAA
PLC1_R111L_r	ATCCTGATTCC**CAA**TTGCAATACGCGACATAGC
PLC1$^{1\text{-}999nt(no\ stop)}$_HindIII_r	GGG*AAGCTT*TTGCTCATGCTGCTCTGTAATTAAAA
PLC1^{end}_XhoI_r	TTT*CTCGAG*CTATAAAATTTGTGTATGAATAAATAAAGTGCAAAATATG
PLC1^{C2}_HindIII_f	AA*AAGCTT*ATGTTAGATCACCAACCTGATGGAAGT
D56677DL	GAGAAGGGCGTTTAGATAAAACCCCAACTT
D56678DL	TTTTTTGATGGTGATATCATCTTTCAGTGTCTC
ClaI_A	TCGAATTTTATCTACACAGTTATTGCCCAGATTG
XhoI_B	CGCCTA*CTCGAG*TAAAATTTGTGTATGAATAAATAAAGTGCAAAATATG
XhoI_C	CAAATTTTA*CTCGAG*TAGGCGATCTTTTTCCGGCCAAA
BamHI_D	AATACTCAAGCTATGCATCCAACGCGTT
LEU2TAG1	TTTTT*GGATCC*AGATGCAAGAGTTCGAATCTCTTA
LEU2TAG2	GTTTT*GGATCC*TTCCATTTTGTAATTTCGTGTCGT
PLC1_pFA6aHis3_f1	TAAACGTACAACGGTAAGGTCATTCACGCAGTGTATATGA_{CGGATCCCCGGGTTAATTAA}
PLC1_pFA6aHis3_r1	GTACGTATTTATGAATATGTGTATTTGGCCGGAAAAAGATCGC_{GAATTCGAGCTCGTTTAAAC}
VPS41_pFA6aHis3_f1	AGCATTTTAACGAAGAGTATATACCTACTATTAGACATTA_{CGGATCCCCGGGTTAATTAA}

VPS41_pFA6aHis3_r1	AAGTGTACACTTGCCTTGTGTATTAAATGATGATTCGATAGAATTCGAGCTCGTTTAAAC
PLC1-S3_f	GAACAATACATATTTTGCACTTTATTTATTCATACACAAATTTTACGTACGCTGCAGGTCGAC
PLC1-S2_r	ATGTACGTATTTATGAATATGTGTATTTGGCCGGAAAAAGATCGCATCGATGAATTCGAGCTCG
ARG82-S3_f	GTGATTGAAGGAGTTGAAACCTTGCTAGATATTTTTATGAAATTCCGTACGCTGCAGGTCGAC
ARG82-S2_r	TGTACCATATACCATAAACAAGGTAAACTTCACCTCTCAATATATATCGATGAATTCGAGCTCG
ARG82_XbaI_f	GAAAA*TCTAGA*ATGGATACGGTAAACAATTATAGGGT
ARG82_XhoI_r	TTT*CTCGAG*CTAGAATTTCATAAAAATATCTAGCAAGGT
ARG82_BamHI_f	TTTT*GGATCC*CCACAATAGCAATTGGTAAAATTGTTAAAATTGC
ARG82_PstI_f	AAAA*CTGCAG*CTTCAATTTGACAGAAGGATCTGTAGTCAT
BamHI-PLC1	GCGCGAGG*GGATCC*ATGACTGAAAGTGCTATAGATGAC
PLC1-HindIII	GGCGGCAGCGGCG*AAGCTT*CTATAAAATTTGTGTATGAATAAATAAAGTGC
PLC1_H439L_f	ATGGTGAAAATGGGCCAGTGGTATGC**CTA**GGATTTTTAACGTCAGCTATTCC
PLC1_H439L_r	GCTGACGTTAAAAATCC**TAG**GCATACCACTGGCCCATTTTCAC
PLC1_E425G_f	GTAGGTGCGTA**GGT**ATTGATATATGGGATGGTGAAAATGGGCC
PLC1_E425G_r	ACTGGCCCATTTTCACCATCCCATATATCAAT**ACC**TACGCACCTACAACCTTGTT
Gpr1_LEU2_f	AAGTGATCCGAAGTGTGACGAATAAAGCAAACTCTCCAACTCAAAAGATGCAAGAGTTCGAATCTCTTA
Gpr1_LEU2_r	GTATTACGTTCCTTACTTTCCATTTTCAAACATCGCGATACAAAAACTTTCCATTTTGTAATTTCGTGTCGT

[The italic font indicates the restriction sites incorporated; bold font indicates the mutation made; and the smaller-sized font indicates the beginning of the sequence homologous to the auxotrophic marker gene to be amplified.]

pUG36–*PLC1*$^{1\text{-}220}$

pUG36–*PLC1*$^{1\text{-}220}$ was constructed in the same way as pUG36–*PLC1*$^{1\text{-}110}$ but with PLC1Trunc1 as the 3' oligonucleotide.

pUG36–*PLC1*$^{1\text{-}333}$

pUG36–*PLC1*$^{1\text{-}333}$ was constructed in the same way as pUG36– pUG36–*PLC1*$^{1\text{-}110}$ but with pUG36-SOED2 as the 3' oligonucleotide.

pUG36–*PLC1*$^{110\text{-}220}$

PLC1$^{110\text{-}220}$ was amplified from original pUG36-*PLC1* using oligonucleotides PLC1-330Top and PLC1Trunc1 that incorporated unique *Bam*HI and *Hind*III restriction enzyme sites at the 5' and 3', respectively. The PCR product was digested with *Bam*HI and *Hind*III, then sub-cloned into *Bam*HI/*Hind*III-digested pUG36 vector.

pUG36–*PLC1*$^{220\text{-}333}$

PLC1$^{220\text{-}333}$ was amplified from original pUG36-*PLC1* using oligonucleotides pUG36-SOEA2 and pUG36-SOED2 that incorporated unique *Bam*HI and *Hind*III restriction enzyme sites at the 5' and 3', respectively. The PCR product was digested with *Bam*HI and *Hind*III, then sub-cloned into *Bam*HI/*Hind*III-digested pUG36 vector.

pUG36–*PLC1*$^{110\text{-}end}$

PLC1$^{110\text{-}end}$ was amplified from original pUG36-*PLC1* using oligonucleotides PLC1-330Top and pUG36-SOED1 that incorporated unique *Bam*HI and *Hind*III restriction enzyme sites at the 5' and 3' ends respectively. The PCR product was digested with

*Bam*HI and *Hind*III, then sub-cloned into *Bam*HI/*Hind*III-digested pUG36 vector.

pUG36–*PLC1*$^{220\text{-}end}$

pUG36–*PLC1*$^{220\text{-}end}$ was constructed in the same way as pUG36–*PLC1*$^{110\text{-}end}$ but with pUG36-SOEA2 as the 5' oligonucleotide.

pUG36–*PLC1*$^{333\text{-}end}$

pUG36–*PLC1*$^{333\text{-}end}$ was constructed in the same way as pUG36–*PLC1*$^{110\text{-}end}$ but with PLC1-1000Top as the 5' oligonucleotide.

pUG36–*PLC1*^{NES}

PLC1^{NES} (*PLC1*$^{L190A/L193A}$) was constructed by SOE-PCR amplification of pUG36–*PLC1* using oligonucleotides: PLC1_*NES*_f and PLC1_*NES*_r. The whole PLC1 gene with the NES being mutated was then amplified with pUG36SOEA1 and pUG36SOED1. The PCR product was digested with *Bam*HI and *Hind*III, then sub-cloned into *Bam*HI/*Hind*III-digested pUG36 vector.

pUG36–*PLC1*^{CAAX}

PLC1$^{no\ stop}$ (with stop codon removed) was amplified by PCR pUG36–*PLC1* using oligonucleotides: pUG36SOEA1 and *PLC1*ORF5 (this pair of oligos amplified the whole *PLC1* gene only without the last stop codon), and digested with *Bam*HI and *Hind*III, then sub-cloned into *Bam*HI/*Hind*III-digested pUG36 vector.

The CAAX motif sequence was synthesized as follows: pUG36CAAX_f and pUG36CAAX_r, 25 μl of each (20 pmol), were mixed and annealed using PCR block programmed as 94^{o}C for 5 min, 59^{o}C for 1 hour and quick cooled to 10^{o}C for 10 min.

Plasmid pUG36–*PLC1*^{CAAX} was created by cloning the annealed double stranded CAAX oligonucleotides into the *Hind*III/*Xho*I sites of pUG36– *PLC1*$^{no\ stop}$.

pUG36–*PLC1*^{PKI}

PKI(2x) motif sequence was synthesized as follows: PKI(2x)BamHI/SacI_f and PKI(2x)BamHI/SacI_r, 25 µl of each (20 pmol), were mixed and annealed using a PCR block programmed as follows: 94^{o}C for 5 min, 66^{o}C for 1 hour and quick cooled at 10^{o}C for 10 min.

pUG36–*PLC1*^{PKI} was created by cloning the *Bam*HI digested double strand PKI(2x) oligonucleotides into the *Bam*HI site of pUG36– *PLC1*.

pUG36–*PLC1*$^{NES/CAAX}$

PLC1$^{NES/no\ stop}$ (with stop codon removed) was amplified by PCR pUG36–*PLC1*^{NES} using oligonucleotides: pUG36SOEA1 and *PLC1*ORF5 (this pair of oligos amplified the whole *PLC1* gene save for the stop codon). *PLC1*$^{NES/no\ stop}$ was digested with *Bam*HI and *Hind*III, and exchanged with the *Bam*HI and *Hind*III digested *PLC1* fragment of pUG36–*PLC1*^{CAAX} construct to generate pUG36–*PLC1*$^{NES/CAAX}$.

pUG36–*PLC1*$^{NES/PKI}$

pUG36–*PLC1*$^{NES/PKI}$ was created by cloning the *Bam*HI digested double strand PKI(2x) oligosnucleotides into *Bam*HI site of pUG36– *PLC1*^{NES}.

pUG36-*PLC1*^{KKLRK}

pUG36-*PLC1*^{KKLRK} (*PLC1*$^{K94A/K95A/R97A}$) was constructed by SOE-PCR amplification of pUG36–*PLC1* using oligonucleotides: PLC1NLS_KKLRK_f and

PLC1NLS_KKLRK_r. The whole *PLC1* gene with the K94A/K95A/R97A mutations was then amplified with pUG36SOEA1 and pUG36SOED1. The PCR product was digested with *Bam*HI and *Hind*III, then sub-cloned into *Bam*HI/*Hind*III-digested pUG36 vector.

pUG36-*PLC1^{KRLR}*

pUG36-*PLC1^{KRLR}* (*PLC1$^{K170A/R171A/R173A}$*) was constructed in the same way as pUG36–*PLC1*$^{K94A/K95A/R97A}$ but using PLC1NLS_KRLR_f and PLC1NLS_KRLR_r oligonucleotides.

pUG36-*PLC1^{4R}*

pUG36-*PLC1^{4R}* (*PLC1$^{R111L/R117S/R120S/R123E}$*) was constructed in two steps:

PLC1$^{R111L/R117S}$ was amplified by SOE-PCR of pUG36–*PLC1* using oligonucleotides: PLC1NLS-C1 and PLC1NLS-B1. The whole *PLC1* gene with the R111L/R117S mutations was then amplified with pUG36SOEA1 and pUG36SOED1.

PLC1$^{R111L/R117S}$ was then further amplified by SOE-PCR using oligonucleotides: PLC1NLS-C2 and PLC1NLS-B2 to introduce two further mutations. The whole *PLC1* gene with the R111L/R117S/R120S/R123E mutations was then created by a second PCR step using oligos pUG36SOEA1 and pUG36SOED1. Finally, *PLC1^{4R}* was digested with *Bam*HI and *Hind*III, then sub-cloned into *Bam*HI/*Hind*III-digested pUG36 vector.

pUG36-*PLC1$^{R2/3}$*

pUG36-*PLC1$^{R2/3}$* (*PLC1$^{R117S/R120S}$*) was constructed by SOE-PCR amplification of pUG36–*PLC1* using oligonucleotides: PLC1_R117S/R120S_f and

PLC1_R117S/R120S_r. The whole *PLC1* gene with the R117S/R120S mutations was then created by a second round of PCR utilising oligos pUG36SOEA1 and pUG36SOED1. The PCR product was digested with *Bam*HI and *Hind*III, then sub-cloned into *Bam*HI/*Hind*III-digested pUG36 vector.

pUG36-*PLC1*$^{R2/4}$

pUG36-*PLC1*$^{R2/4}$ (*PLC1*$^{R117S/R123E}$) was constructed in the same way as pUG36–*PLC1*$^{R2/3}$ but using PLC1_R117S/R123E_f and PLC1_R117S/R123E _r oligonucleotides.

pUG36-*PLC1*$^{R3/4}$

pUG36-*PLC1*$^{R3/4}$ (*PLC1*$^{R120S/R123E}$) was constructed in the same way as pUG36–*PLC1*$^{R2/3}$ but using PLC1NLS-C2 and PLC1NLS-B2 oligonucleotides.

pUG36-*PLC1*^{R1}

pUG36-*PLC1*^{R1} (*PLC1*^{R111L}) was constructed in the same way as pUG36–*PLC1*$^{R2/3}$ but using PLC1_R111L_f and PLC1_R111L _r oligonucleotides.

pUG36-*PLC1*$^{(1\text{-}333)+C2}$

PLC1$^{1\text{-}333(no\ stop)}$ (with stop codon removed) was amplified by PCR pUG36–*PLC1*$^{1\text{-}333}$ using oligonucleotides: pUG36SOEA1 and PLC1$^{1\text{-}999nt(no\ stop)}$_HindIII_r (this pair of oligos amplified the whole *PLC1*$^{1\text{-}333}$ gene only without the last stop codon). pUG36-*PLC1*$^{1\text{-}333(no\ stop)}$ was created by digesting PCR of *PLC1*$^{1\text{-}333(no\ stop)}$ with *Bam*HI and *Hind*III, then sub-cloned into *Bam*HI/*Hind*III-digested pUG36 vector.

PLC1^{C2} was amplified by PCR using pUG36–*PLC1* as target DNA and

oligonucleotides: PLC1^{C2}_HindIII_f and PLC1^{end}_XhoI_r.

pUG36-*PLC1*$^{(1-333)+C2}$ was then created by cloning the *Hind*III/*Xho*I digested *PLC1*^{C2} into the *Hind*III/*Xho*I sites of pUG36-*PLC1*$^{1-333(no\ stop)}$.

pUG36-*PLC1*^{H439L}

PLC^{H439L} was constructed by SOE-PCR amplification of pUG36–*PLC1* using oligonucleotides: PLC1_H439L_f and PLC1_H439L_r. The whole *PLC1* gene with the H439L mutation was then amplified with BamHI-PLC1 and PLC1-HindIII. The PCR product was digested with *Bam*HI and *Hind*III, then sub-cloned into *Bam*HI/*Hind*III-digested pUG36 vector.

pUG36-*PLC1*^{E425G}

pUG36-*PLC1*^{E425G} was constructed in the same way as pUG36–*PLC1*^{H439L} but using PLC1_E425G_f and PLC1_E425G_r oligonucleotides

pUG36-*PLC1*$^{4R/E425G}$

pUG36-*PLC1*$^{4R/E425G}$ (*PLC1* $^{R111L/R117S/R120S/R123E/E425G}$) was constructed by SOE-PCR amplification of pUG36-*PLC1*^{4R} using oligonucleotides: PLC1_E425G_f and PLC1_E425G_r. The whole *PLC1* gene with the combined mutations was then created by PCR using oligos BamHI-PLC1 and PLC1-HindIII. The PCR product was digested with *Bam*HI and *Hind*III, then sub-cloned into *Bam*HI/*Hind*III-digested pUG36 vector.

pYcplac111-*ARG82*

pYcplac111-*ARG82* was constructed by PCR amplification of the *ARG82* ORF from

yeast genomic DNA using ARG82_BamHI_f and ARG82_PstI_f oligonucleotides. The PCR product was digested with *Bam*HI and *Pst*I, then sub-cloned into *Bam*HI/ *Pst*I -digested pYcplac111 vector.

pYcplac111-*ARG82^{D131A}*

pYcplac111-*ARG82^{D131A}* was constructed by inserting the *BamH*I digested *ARG82^{D131A}* fragment from pFV-*ARG82^{D131A}*(a gift from Dr. Evelyne Dubois, Brussels) to *BamH*I digested pYcplac111 vector.

pYcplac111-*Arg82$^{\Delta asp}$*

pYcplac111-*ARG82$^{\Delta asp}$* (*ARG82$^{\Delta(283\text{-}308)}$*) was constructed by inserting the *BamH*I digested *ARG82$^{\Delta asp}$* fragment from pFV-*ARG82$^{\Delta(283\text{-}308)}$* (a gift from Dr. Evelyne Dubois, Brussels) to *BamH*I digested pYcplac111 vector.

pUG34-*ARG82*

pUG34–*ARG82* was constructed by PCR amplification of the *ARG82* ORF from yeast genomic DNA using ARG82_XbaI_f and ARG82_XhoI_r oligonucleotides. The PCR product was digested with *Xba*I and *Xho*I, then sub-cloned into *Xba*I/*Xho*I -digested pUG34 vector.

pUG34-*ARG82^{G344R}*

ARG82^{G344R} was constructed by PCR amplification of pRS314-*ARG82^{G344R}* (a gift from Dr John York, Durham, USA) using ARG82_XbaI_f and ARG82_XhoI_r oligonucleotides. The PCR product was digested with *Xba*I and *Xho*I, then sub-cloned into *Xba*I/*Xho*I -digested pUG34 vector.

pUG36-*ARG82^{D131A}*

ARG82^{D131A} was constructed by PCR amplification of pYcPlac111-*ARG82^{D131A}* using oligonucleotides: Arg82_BamHI_f and Arg82_XhoI_r. The PCR product was digested with *Bam*HI and *Xho*I, then sub-cloned into *Bam*HI/*Xho*I -digested pUG36 vector.

pGEX6PK1–*PLC1* and pGEX6PK1–*PLC1^{E425G}*

PLC1 fragements of *BamH*I and *Xho*I digested pUG36-*PLC1* and pUG36-*PLC1^{E425G}*, were inserted into the *BamH*I/*Xho*I site of pGEX6PK1, respectively.

2.7 Yeast knock out & knock in

Deletion or knock in strain creation was accomplished via high efficiency transformation of the appropriate PCR construct into the correct competent *S. cerevisiae* strain.

2.7.1 Knock out

For deletion of certain (open reading frames) ORFs, an auxotrophic marker was amplified from a "knock-out plasmid" (all plasmids based on pRS416 or on pFA-KANMX4) by PCR using primers that contained sequences for annealing to the template plasmid, flanked by sequences that encode regions immediately before the start codon and after the stop codon of the corresponding ORFs. PCR products were used to transform yeast strains and putative knock-out strains were confirmed by sequencing the genomic DNA recovered from transformed cells.

BY4742 *plc1Δarg82Δ*

BY4742 *plc1Δarg82Δ* (*plc1*::*HIS3 arg82*::*KanMX4*) was created by PCR using the

knock-out plasmid pFA6a-HIS3MX6 (Longtine *et al*., 1998) using PLC1_pFA6aHis3_f1 and PLC1_pFA6aHis3_r1 oligonucleotides, followed by high efficiency yeast transformation to BY4742 *arg82*::*KanMX4* (EUROSCARF). Colonies were grown at 25 ^{o}C and selected on SC-His plates.

BY4742 *vps41Δarg82Δ*

BY4742 *vps41Δarg82Δ* (*vps41::HIS3 arg82*::*KanMX4*) was made in the same way as BY4742 *plc1Δarg82Δ* but using VPS41_pFA6aHis3_f1 and VPS41_pFA6aHis3_r1 oligonucleotides. Colonies were grown at 25 ^{o}C and selected on SC-His.

BY4742 *gpr1Δ*

BY4742 *gpr1Δ* (*gpr1::LEU2*) was created by PCR plasmid pYcPlac111(cen-ARS, LEU2, amp) (Gietz and Sugino, 1988) using Gpr1_LEU2_f and Gpr1_LEU2_r oligonucleotides, followed by high efficiency yeast transformation to wild-type BY4742 (Euroscarf). Colonies were grown at 25 ^{o}C and selected on SC-Leu.

BY4742 *gpr1Δarg82Δ*

BY4742 *gpr1Δarg82Δ* (*gpr1::LEU2 arg82::KanMX4*) was made in the same as BY4742 *gpr1Δ* but PCR product was transformed to BY4742 *arg82*::*KanMX4* (Euroscarf). Colonies were grown at 25 ^{o}C and selected on SC-Leu.

2.7.2 *PLC1* knock in mutant

To express *PLC1* mutants at endogenous levels, *PLC1* knock-in strains were constructed in pGEM -T -Easy with a *LEU2* gene inserted 3' to the *PLC1* gene to act as a selective marker (Fig 2.3).

***PLC1* (wild type) knock in**

A fragment encoding the whole *PLC1* ORF, including the promoter region and all intergenic sequences between *PLC1* and the adjacent two genes (*KAR9* and *ACM1*) was amplified by PCR. The template for this reaction was genomic DNA from wild type yeast BY4742 genomic DNA using D56677DL and D56678DL oligonucleotides. PCR product was TA coloned into the pGEM-T Easy (Promega#A1360) to create pGEM-T Easy-*PLC1*.

For construction of pGEM-T Easy-*PLC1-LEU2,* DNA encoding the selective marker *LEU2* was obtained by PCR from plasmid pYcPlac111 using LEU2TAG1 and

Fig 2.3: PLC1 mutant knock in

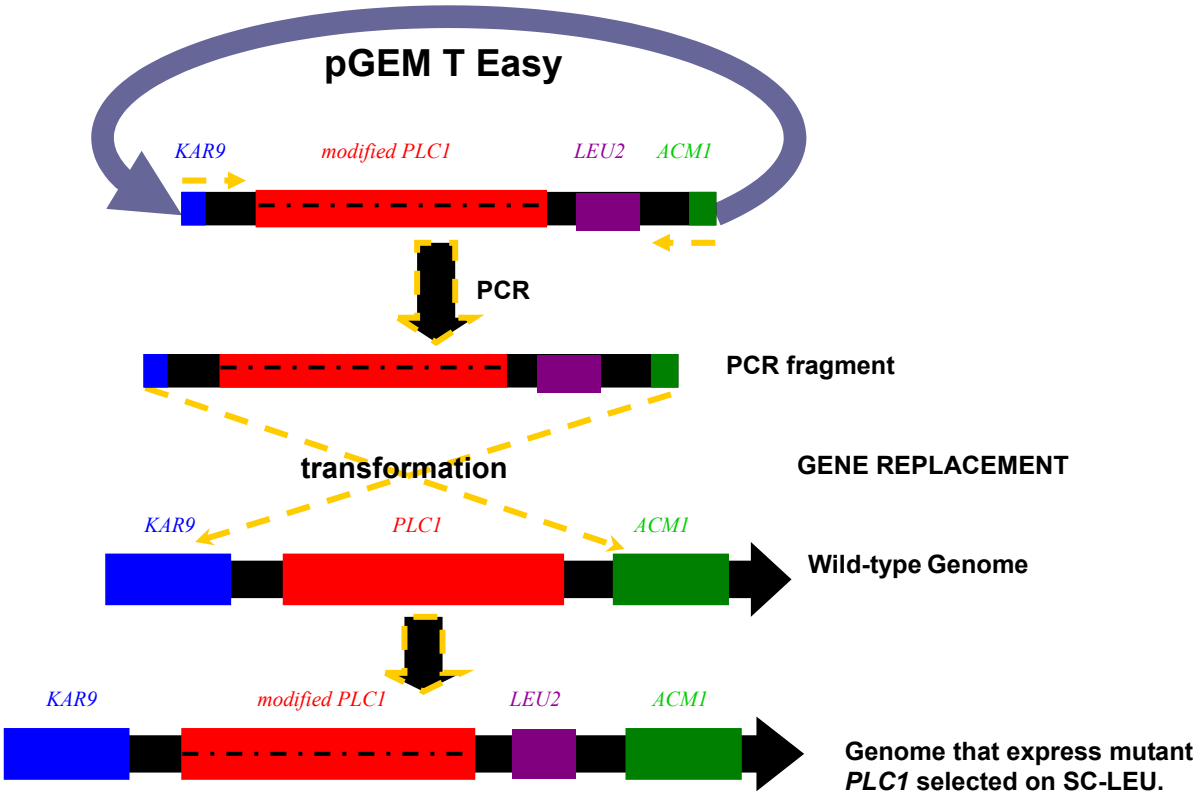

LEU2TAG2 oligos, followed by digestion with *BamH*I and insertion into the *BamH*I site of pGEM-T Easy-*PLC1*.

The resulting *PLC1-LEU2* fragment was amplified by PCR with D56677DL and D56678DL oligonucleotides. Reactions were conducted using Long Template Polymerase (Roche). The whole fragment was then transformed to competent wild-type BY4742. Colonies were recovered at 25 ^{o}C and selected on SC-Leu.

$PLC1^{NES}$ knock in

pUG36-$PLC1^{NES}$ was digested with *Hpa*I and *Cla*I, and exchanged with the *Hpa*I and *Cla*I digested *PLC1* fragment of pGEM-T Easy-*PLC1-LEU2* to create pGEM-T Easy-$PLC1^{NES}$-*LEU2*. $PLC1^{NES}$-*LEU2* was amplified and transformed to wild-type BY4742 as above. Colonies were grown at 25 ^{o}C and selected on SC-Leu.

$PLC1^{CAAX}$ knock in

A *Xho*I site was created in pGEM-T Easy-*PLC1-LEU2* right before the *PLC1* stop codon*, via* SOE-PCR using two pairs of oligonucleotides: (i) ClaI_A and XhoI_B, (ii) XhoI_C and BamHI_D, followed by PCR with ClaI_A and BamHI_D to produce a fragment with a unique *Xho*I. This fragment was then digested with *Cla*I and *BamH*I and exchanged with the *Cla*I/*BamH*I fragment of pGEM-T Easy-*PLC1-LEU2* to create a pGEM-T Easy-$PLC1^{XhoI}$-*LEU2*.

The CAAX sequence was then incorporated to pGEM-T Easy-$PLC1^{XhoI}$-*LEU2* by digesting pUG36-$PLC1^{CAAX}$ with *Cla*I and *Xho*I, and exchanging the resulting fragment with the *Cla*I/*Xho*I fragment of pGEM-T Easy-$PLC1^{XhoI}$-*LEU2*.

$PLC1^{CAAX}$-*LEU2* was amplified and transformed to wild-type BY4742. Colonies were grown at 25 ^{o}C and selected on SC-Leu.

PLC1^{PKI} knock in

A *Hind*III site was first inserted into pGEM-T Easy-*PLC1-LEU2* right before the *PLC1* start codon, by SOE-PCR conducted using two pairs of oligonucleotides: (i) PLC1_HindIII_f and LEU2_KpnI_r, (ii) pGEasy_SacI_f and PLC1_HindIII_r, then followed by PCR with pGEM-T-Easy_SacI_f and LEU2_KpnI_r to produce a fragment with the unique *Hind*III site. This fragment was then digested with *Sac*I and *Kpn*I and exchanged with the *Sac*I/*Kpn*I fragment of pGEM-T Easy-*PLC1-LEU2* to create a pGEM-T Easy-*PLC1*^{HindIII}*-LEU2*.

The PKI(2x) sequence was created as follows: PKI(2x)HindIII/XhoI_f and PKI(2x)HindIII/XhoI_r, 25 µl of each (20 pmol), were mixed and annealed using a PCR block programmed as follows: 94^{o}C for 5 min, 65^{o}C for 1 hour and quick cooled at 10^{o}C for 10 min. pGEM-T Easy-*PLC1*^{PKI}*-LEU2* was created by cloning the double-stranded, annealed PKI(2x) oligonucleotides into the *Hind*III site of pGEM-T Easy-*PLC1*^{HindIII}*-LEU2.* Orientation was determined by sequencing a number of correct plasmids, selected by creation of a new *Xho*I site.

PLC1^{PKI}*-LEU2* was amplified and transformed to wild-type BY4742. Colonies were grown at 25 ^{o}C and selected on SC-Leu.

2.8 High efficiency transformation of competent *E. coli* cells

Competent *E.coli* cells were prepared in the lab: Supercomp medium (60 ml: BIO101) was inoculated with an appropriate *E. coli* strain (200 µl of an overnight culture) and incubated at 37^{o}C until the A_{660} was ~0.3. 10 ml aliquots were then incubated on ice for 10 min and cells were collected through centrifugation at 3000 *g* for 5 min at 4^{o}C. Each cell pellet was resuspended in ice-cold 1 x Rubidium-$CaCl_2$ mixture (2.0 ml: BIO101). The cell suspensions were combined and incubated on ice for a further 20

min. Cells were collected as above, resuspended in ice-cold x 1 Rubidium-$CaCl_2$ mixture (4 ml: BIO101) containing 20% (w:v) glycerol, separated into 100 μl aliquots and stored at -80°C. On some occasions, E.coli were left over-night in the x 1 Rubidium-$CaCl_2$ mixture as this is reported to increase competency.

Transformation was carried out as follows: Plasmid DNA (0.1-10 μg) was added to an aliquot of competent *E. coli* cells (100 μl), incubated on ice for 30 min and heat shocked at 42°C for 90 seconds. SOC medium (1.0 ml) was immediately added to the cell suspension, mixed gently and incubated at 37°C for 60 min. Cells were collected through centrifugation at 6000 rpm for 10 seconds, resuspended in 100 μl of fresh SOC medium and plated onto a LB + 100 μg/ml Ampicillin agar plate. Plates were incubated at 37°C for 16-20 h.

2.9 High efficiency transformation of yeast

Polyethylene glycol (PEG), lithium acetate and single-stranded salmon testis DNA were obtained from Sigma Chemical Company.

The following method was adapted from *Methods in Yeast Genetics* (Adam, A., Goccschling, D.E., Kaiser, C.A., and Sterns T., eds), Cold Springs Harbour Laboratory Manual, 1997.

Cells were sub-cultured to 5 x 10^6 cells/ml in YPD+ 2.0% glucose medium (2 ml) and grown on at 30°C to 1~2 x 10^7 cells/ml. Cells were collected, resuspended in H_2O (1 ml), and centrifuged at 3000 x *g* for 1 min at 30°C. Cells were again collected, resuspended in 1ml of 100 mM lithium acetate (LiAc). The cell suspension was

centrifuged at 6000 x g for 15 seconds and the supernatant was removed. Single-stranded salmon testis DNA, ssDNA (carrier DNA; 2mg/ml in dH20) was boiled for 5 min and chilled on ice. The following solutions were then added to the cell pellet in the this order: 240 µl of 50% PEG, 36 µl of 1.0M LiAc, 50 µl of boiled ssDNA, 25 µl of ddH_2O containing the DNA (0.1~ 10 µg) to be transformed, and the resulting mixtures were mixed by vortexing vigorously until the cells were completely resuspended. Cells were then incubated at 30°C for 30 min followed by heat shock at 42°C for 25 min. Cells were collected by centrifugation at 6000 x *g* for 15 seconds, the supernatant was discarded and the cells were resuspended (very gently) in 200 µl of ddH_2O, plated out onto selective agar plates and incubated at 30°C.

2.10 Genomic DNA purification from budding yeast

The following method is from Gentra Puregene Handbook, second edition, Qiagen, p47~ 48, 09/2007.

2 ml of exponentially growing cells were collected and resuspended in 300 µl of Cell Suspension Solution (provided by the kit) with 1.5 µl of Lytic Enzyme Solution, the resulting mixture was incubated at 37°C for 30 min. Cells were pelleted by centrifugation at 16,000g for 1 min and resuspended in 300 µl of Cell Lysis Solution plus 100 µl of Protein Precipitation Solution, and vortexed vigorously for 20 s at high speed, then centrifuged at 16,000g for 3 min. The supernatant (approx. 400 µl) was decanted into a fresh tube containing 300 µl of isopropanol, mixed well and centrifuged at 16,000g for 1 min. The supernatant was carefully discarded and the tube drained by inverting it on a clean piece of absorbent paper. Then the DNA pellet was washed once with 300 µl of 70% ethanol and air dried for up to 10 min. The DNA

pellet was resuspended in 50 µl of DNA Hydration Solution plus 1.5 µl of RNase A Solution and incubated at 37°C for 30 min, then incubated at 65°C for 1 hour to dissolve the DNA.

2.11 SDS-PAGE (Sodium Dodecyl Sulphate-polyacrylamide Gel Electrophoresis)

5 x SDS sample buffer was added to protein samples to a final concentration of 1 x. Samples were then vortexed and incubated at 100°C for 5 min. Proteins were separated by a 10% (w:v) acrylamide resolving gel and separated in a Bio-Rad Mini-Protean II xi Cell at 100V for approximately 1.5 hour until the bromophenol blue dye-front reached the end of the gel or until the desired separation of the prestained molecular weight markers was achieved. Electrophoresis reagents and molecular weight markers were obtained from Bio-Rad.

2.12 Western blotting

Proteins separated by SDS-PAGE were transferred to a Hybond-ECL nitrocellulose membrane (Amersham Biosciences) for further analysis. The nitrocellulose membrane and two pieces of 3MM filter paper (Whatman) were cut to the size of the separating gel and pre-soaked in the blotting buffer. The gel was removed from the cassette and put into the blotting buffer. A blotting cassette was assembled according to the manufacturer's instructions, as follows: a sponge, two filter papers, gel (rinsed with blotting buffer), a nitrocellulose membrane, two filter papers and another sponge, from black (cathode) to the white (anode). The assembled blotting cassette and an ice block for cooling were inserted into the transfer tank with blotting buffer, and the transfer performed at 400 mA for 1 hour, followed by milk blocking (5% skimmed milk powder dissolved in PBST) for at least 1 hour. A specific antibody was added for

each experiment (in PBST) for an appropriate incubation time, then a 2nd antibody (in PBST) was incubated with the blot for at least 1 hour. Blots were then washed for 15 minutes (x 3) after each incubation with antibodies. The immunoreactive proteins were visualized by a chemi-luminescense detection system as follows: Solution A (100mM glycine, pH 10(with NaOH), 0.4mM luminol (Sigma#A-8511), 8mM 4-iodophenol (Aldrich#l1,020-1)) and Solution B (0.12% (w/w) hydrogen peroxide in water) were mixed in equal volumes just prior to use, and the resulting working solution incubated with the blot for 1 minute before exposure to film or CCD camera.

Chemiluminescence was detected by a Fluor-S™ Multimager (Bio-Rad) Gel Documentation System. Different exposure times were used depending on the intensity of the protein bands.

2.13 GFP-Plc1p mutant construct stability test

To analyze the stability of GFP Plc1p fusions, yeast whole-cell extracts were prepared as follows: 5 ml of exponentially growing cells were harvested by centrifugation at 3000 x g for 0.5 minutes, re-suspended in 200 µl of 0.1M NaOH, and incubated at room temperature (RT) for 5 minutes. The cells were again centrifuged and the supernatant was discarded. The cell pellet was then resuspended in 50 µl of 1x SDS-PAGE loading buffer and boiled for 3 minutes. Centrifugation was then carried out at maximum speed (13,000 x g) for 1 minute to remove the debris. The supernatant, containing the extracted total protein lysate, were loaded for Western analysis.

After SDS-PAGE, proteins were transferred to a nitrocellulose membrane and the immunoblots were probed with anti-GFP antibodies (anti-GFP mouse monoclonal

IgG_{2a}, Santa Cruz#SC-9996, B0507) (1:1000 dilution) and then secondary antibody (HRP-Goat anti-mouse IgG (H+L, Zymed Laboratory Ltd, #274061) at a 1:2000 dilution following the routine immunoblotting protocol described above. For each experiment, equal equivalents of cells were analysed.

2.14 Expression of GST-Plc1p and GST-Plc1p^{E425G}

pGEX6PK1-*PLC1* and pGEX6PK1-*PLC1*^{E425G} were transformed to BL21-star (DE3)-RIL competent *E. coli* cells. Transformants were selected on LB + 100 μg/ml Ampicillin + 50 μg/ml Chloramphenicol agar plates. Plc1p and Plc1p^{E425G} were expressed as a GST-tagged full-length fusion proteins.

The transformed *E. coli* strains were grown to an A_{600} of ~ 0.8 at 37^{o}C and induced by IPTG (0.1 mM) (Bio-Rad) with PMSF (0.4 mM) at 20^{o}C overnight (~ 12 hours). Cells were collected (8000 *g* for 5 min at 4^{o}C) and 'washed' in 40 ml ice-cold Breakage buffer (100mM Hepes-KOH, 150 mM NaCl, 5mM Benzamidine and 10mM EDTA, pH 7.5). All subsequent procedures were carried out at 4^{o}C. Cells were resuspended in 40 ml of Breakage buffer containing 1mg/ml lysozyme and 200 μl of bacterial protease inhibitor cocktail (Sigma, P8465 added immediately prior to use) and incubated, with stirring, on ice for 30 min. Inhibitor cocktail was included in all subsequent breakage buffers. The *E. coli* cells were disrupted using a sonicator by 10 x 5 s pulses at maximum intensity level. The final volume of lysis was adjusted to 45 ml with breakage buffer and 5 ml 10% (v:v) Triton X-100 was added, and incubated on ice with stirring for 30 min. Following homogenisation, the cells were centrifuged at 8000 rpm (Beckman J2-MC, rotor JA18) for 10 min at 4^{o}C and the supernatant was further centrifuged at 50,000g (Beckman L-70 ultracentrifuge, rotor Type 70 Ti) for

20 min at 4°C. This supernatant was filtered using 0.22 μm polyethylene sulphate (PES) filter discs (Millipore Ltd). Glutathione-Sepharose 4B resin (GE Healthcare) (1.33 ml of a 75% slurry) was equilibrated in breakage buffer containing 1% (v:v) Triton X-100 and 100 μl protease inhibitor cocktail for 30 min and washed 2 times in the same buffer. The filtered supernatant was added to the pre-swollen beads and rotated for 1 hour at 4°C to allow binding. Beads were recovered in a centrifuge at 200 g for 5 min at 4°C, followed by two washes with breakage buffer containing 0.1% (v:v) Triton X-100 and protease inhibitor cocktail, then another two washes with detergent-free breakage buffer, and a final wash in washing buffer (100mM Hepes-KOH, 150 mM NaCl, 5mM Benzamidine, pH 7.5) with protease inhibitor cocktail (all washing steps including recovery by centrifugation at 200 g for 5 min at 4°C). The beads were resuspended in 5 ml of washing buffer with protease inhibitor cocktail and poured into a poly-prep chromatography column (Bio-Rad,#731-1550) allowed to settle and the buffer drained out. GST-tagged proteins were then eluted in 3 ml (0.5 ml for each collected fraction) of detergent-free elution buffer (50 mM Tris, 150 mM NaCl, 5 mM Benzamidine, 20 mM Glutathione, pH 8.5).

Fractions containing protein were identified by protein assay (BioRad), made up to 50% (v:v) glycerol by adding pure, cooled, molecular biology grade glycerol to them on ice, whereupon they were gently mixed by pipetting up and down and stored at -80°C.

16 μl of purified GST-tagged protein from each fraction collected was loaded for SDS-PAGE analysis. Proteins were visualised with Coomassie brillant blue R250 (Sigma) in 50% (v:v) methanol and 7% (v:v) acetic acid (Fig 2.4).

Fig 2.4: SDS-PAGE of GST-tagged protein expression

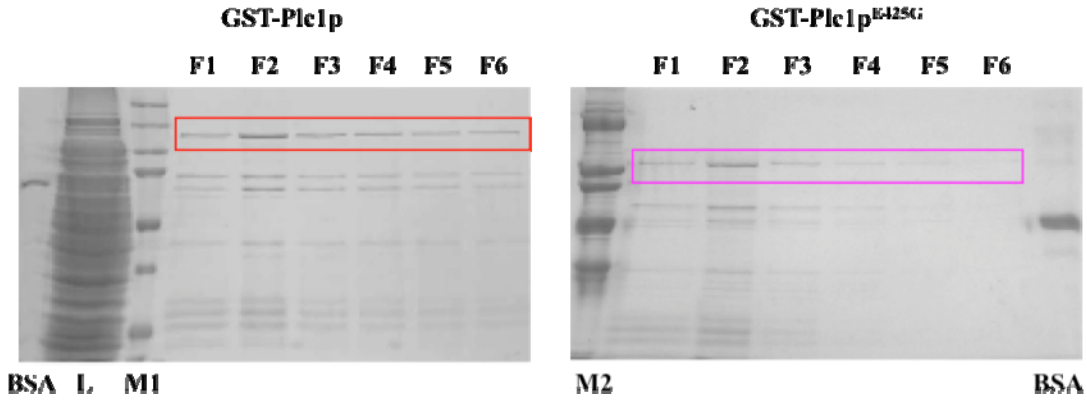

1L of BL21-star (DE3)-RIL cells expressing each GST-tagged protein as indicated was expressed as described above. The gel pictures shows resolution of 16µl from each 500µl fraction of eluted recombinant protein. 1µl of BSA (1mg/mg) was loaded as control. L indicates total lysate (after bead binding). M1 stands for Precision Plus Protein Standards (Bio-Rad,#161-0374) and M2 stands for SDS-PAGE high range standards (Bio-Rad,#161-0303).

2.15 Co-immunoprecipitation for putative binding of Arg82p and Plc1p

Epitope tagging of *PLC1* and *ARG82* in FY833 was conducted using Schiebel's S2/S3 genomic tagging primers (Knop *et al*., 1999).

ARG82::*ARG82-9Myc-TRP1* was constructed by PCR using the pYM6 plasmid as template (obtained from Dr Elmar Schiebel, University of Heidelberg) with oligonucleotides ARG82-S3_f and ARG82-S2_r, which included the sequences for annealing to the template plasmid, flanked by sequences complementary to the 40 nucleotides immediately before and after the stop codon of *ARG82*. A PCR fragment encoding this fragment was transformed into wild type FY833 cells, grown and selected on SC-Trp plates. Putative knock-in strains were confirmed by sequencing genomic DNA of *TRP1* clones.

plc1::*PLC1-3HA-HIS3* was constructed in the same way but using pYM2 as a

template (obtained from Dr Elmar Schiebel, University of Heidelberg) and oligonucleotides PLC1-S3_f and PLC1-S2_r. A PCR fragment obtained as above was transformed into wild type FY833 and FY833 *ARG82*::*ARG82*-9Myc cells. Correct colonies were selected on an SC-His plate and confirmed by sequencing the target fragment of genomic DNA.

Cells (100ml) were grown till OD A_{600} ~1.0. and collected (1000g, 4ºC, 5 min) and washed in 20 ml of ice-cold extraction buffer (200mM Tris-HCl pH8.0, 150mM Ammonium Sulfate, 10% Glycerol, 5mM EDTA, 150mM NaCl and 1mM PMSF, yeast protease inhibitor cocktail were added freshly before use.). Cells were then re-suspended in 600µl of the same extraction buffer and transferred to clean eppendorf tubes, containing 400 µl glass beads (Sigma). Cells were then broken in a Yeast Bead-beater by vigorous agitation for 1 min, followed by at least 1 min on ice: this was repeated 5 times. Centrifugation was then carried out (16,000g ~3 min, 4ºC) to remove all the beads and collect the total lysate.

Note, 5mM DSP (in DMSO) (Pierce, #22585) was added to each cell culture in 500µl extraction buffer before cell breakage. Meanwhile, 100 µl Protein G sepharose (GE Healthcare) (133 µl of a 75% slurry) was pre-washed in Breakage buffer (the same buffer as described in 2.14, protease inhibitor cocktail and 1mM PMSF were added before use) and collected at 500g for 5 min (x 3 times). anti-HA(BAbCO, # MMS-101R, 16B12)(1:2000), anti-cMyc(Santa Cruz,#SC-40, 9E10) (1:2000) and washed Protein G sepharose were together added to 500 µl breakage buffer, and incubated on a rotating wheel for 2 hours at 4^{o}C, then washed as above and the supernatant discarded. The total lysate was added to the beads, and incubated on a rotating wheel

for 2 hours/overnight at 4^{o}C. Supernatant and pellet were separated by centrifugation at 500g for 5 min and washed as above before adding SDS-PAGE loading buffer to the beads. Proteins bound to the beads were then resolved by SDS-PAGE and analyzed by western blotting.

2.16 Spot dilution assay

Exponentially growing cells (~ 1 x 10^{7}cells/ml) were harvested and the cell density were adjusted to exactly 1 x 10^{7}cells/ml first by counting the cells using a haemocytometer and then adjusting the cell suspensions by dilution. Then 5-fold serial dilutions of each cell suspension were made and 5 μl of each dilution spotted onto YTD or SC-Ura+Met (0.2g/L) (for various plasmid transformed constructs derived from pUG36) incubated at 37^{o}C for heat stress, or YTD/SC-Ura+Met (0.2g/L) plates containing 0.7 M NaCl at 23^{o}C for the salt sensitivity assay. Control plates were grown at 23^{o}C. Cells were grown under stress till colonies of wild-type cell were fully formed, normally 2 days for heat stress and 6 days for salt stress.

YTD plates were used in this assay because variations in batches of peptone caused variable and inconsistent results whereas tryptone proved to be a much more consistent product in our hands.

2.17 Hypo-osmotic shock and vacuole staining with the lipophilic dye FM4-64

The following method was adapted from Vida and Emr, 1995.

Strains were grown in YPD at 23°C to early exponential phase (no more than 1x10^{7} cells/ml). 5 ml cells for each strain were harvested and resuspended in 200 μl of YPD

media. FM 4-64 (Molecular Probes, #T13320) was added to 40 μM from a stock solution of 16 mM in DMSO. The cells were then incubated with shaking for 10-15 min at 23°C. After this preliminary labelling step, the cells were harvested at 200 g for 3 min at room temperature. Cells were then resuspended in 400μl of fresh YPD media, and incubated with shaking for 60 min to allow vacuole staining. After this "chase" period, Cells were again harvested at 200 g for 3 min, resuspended in a suitable volume of fresh YPD media and visualised by light/fluorescence microscopy. For salt stress experiments, NaCl was added to YPD media to a final concentration of 0.6 M for 10 min and visualised. For hypo-osmotic shock, cells in YPD + 0.6M NaCl were diluted with 9 volumes of YPD, and incubated with shaking for 60 min, before being visualised.

2.18 Fluorescence microscopy

Yeast strains were cultured to 0.6 ~ 1 x 10^7 cells/ml in appropriate media, washed with MES buffer (2-(*N*-morpholino) ethanesulfonic acid buffer) or MES with an appropriate concentration of NaCl for hyper- or hypo- osmotic treated cells.

Slides and cover-slips were prewashed with 70% ethanol and ddH_2O. Cover-slips were further processed by coating with poly-lysine (10mg/ml), followed by washing in ddH_2O. Slides and cover-slips were quick dried with streams of N_2.

Cells were dispersed thoroughly to achieve a ‘homogenous’ distribution, and were then visualized on a Nikon Eclipse E600 microscope with an XF100-3 filter cube (Omega Optical) and projector used was a Nikon Plan Apo (100×/1.40 oil DIC H). Images were acquired with an ORCA digital camera (Hamamatsu, Japan) and

processed in Adobe Photoshop. Figures showed representative fields from multiple experiments.

2.19 Statistical analysis

Plasma membrane, cytosolic and nuclear GFP fluorescence images were false-coloured in the programme Simple PCI and exported. The fluorescence intensity was then measured in Adobe Photoshop using the eyedropper tool. No cell was analysed where any part of the cell had the maximum fluorescence reading of 255, to avoid problems of saturation. All cells analysed were those that were representative of the population of cells from which they were derived. For each cell, 6 spots on each of the three localizations were randomly selected and measured (only cytosolic and nuclear readings were taken for chapter 3). Ten cells were examined for each genotype.

Sample mean and standard error of the mean (SEM) were calculated in Excel using the following formula: AVERAGE() and STDEV()/SQRT(COUNT()). Cells from different genotypes were compared by an unpaired Student's *t* test. Treated and untreated cells from same genotype were compared by paired *t* test.

2.20 Lipid Western/dot-blot assay

PtdIns3*P*, PtdIns(3,5)P_2 and PtdIns(4,5)P_2 were obtained from Prof. Andrew Holmes (The University of Melbourne) or Dr Gavin Painter (IRL, New Zealand). The lipid dot blot assay method was adapted from the work published by Lemmon group (Narayan and Lemmon 2006).

1 nmole (in chloroform:methanol:ddH_2O (400:56:4)) of each phosphoinositide was spotted onto a strip of Hybond C+ supported nitrocellulose membrane (Amersham Biosciences). All lipid manipulations were performed in clear glass vials (Supelco, #27134), and lipid solutions are stored at -80^oC under nitrogen. After spotting lipids onto nitrocellulose, the strips were dried for ~ 1 h at RT. Strips were then stored at -20ºC in a container with dry silica gel inside to provide a water free atmosphere until use.

Each strip was blocked for at least 1 h at 4^oC in TBST containing 3% (w/v) fatty-acid free bovine serum albumin (BSA). After blocking, the strip was incubated with purified GST-Plc1p or GST-Plc1p^{E425G} in TBST at a concentration of 2.5 μg/ml protein at RT for 2 hrs. The strip was then washed 5 times with TBST (5 min each), followed by routine immunoblotting protocol with mouse monoclonal anti-GST(sigma, #G-1160)(1;1000), and HRP-Goat anti-mouse IgG(H+L) (Zymed Laboratory Ltd, #274061)(1:2000).

2.21 Synchronizing yeast cells

To synchronize the yeast cell cultures, exponentially growing cells (0.6 ~ 1 x 10^7 cells/ml) were treated with: 200 ng/ml rapamycin (Alexix Biochemicals, #380-004-M001)(2.5mg/ml in DMSO) for ~ 6 hours to arrest cells at G1 phase, or 15μg/ml nocodazole (Sigma, #M1404) (10mg/ml in DMSO) for ~ 4 hours to arrest cells at M phase or 100 mM hydroxyurea (Sigma, #H8627)(2 M in ddH2O) for ~ 4 hours to arrest cells at S phase. Equal amounts of DMSO were added to control cells to test for vehicle effects.

The duration for drug treatment was based on those employed in previous studies (Heitman *et al*., 1991; Iwaki *et al*., 2007). Indeed, after each treatment, most cells appeared to show the typical characteristics for the cell stage they were arrested at. Cells then were subjected to microscopy.

Chapter 3 Plc1p localisation and function

3.1 Introduction

The function of PLC-δs in eukaryotes is not well understood, even though the δ-family is likely to be the closest in domain structure to the original, ancestral form of these enzymes (Koyanagi *et al.*, 1998; Rhee and Bae, 1997). PLC-δs are the only PLCs found in plants and fungi (Rhee, 2001), yet the regulation of these enzymes has never been resolved, as the proposed mechanisms require at least one protein component that is absent from some of the groups of organisms in which PLC-δs are found (Rebecchi and Pentyala, 2000). The fact that PLC-δs are present in lower organisms that lack InsP_3 receptors suggested that the functions of PLC-δs might be fundamentally different from the signalling processes that are initiated by the other, better characterized, families such as the PLC-βs and PLC-γs.

The discovery of yeast InsP_3 kinases was a first step in unravelling this mystery (York *et al*., 1999). This lead to the realisation that 'higher' inositol phosphates, such as InsP_6 and the inositol pyrophosphates, InsP_7 and InsP_8, might be derived from PLC-generated InsP_3 through the action of inositol phosphate kinases, at least in some organisms. This implied that PLC-δs might indirectly generate InsP_6, InsP_7 and InsP_8 in cells and that study of these might reveal major, and maybe ancestral, functions of PLC-δs.

Many of the most penetrative insights relating to PLC-δs and the higher inositol phosphates have come from studies of Plc1p, the δ-type PLC of *S. cerevisiae*.

Deletion of the *PLC1* gene gives rise to a pleiotrophic phenotype that includes sensitivity to heat and osmotic stresses, inability to grow on non-fermentable carbon sources and defects in vacuole and nuclear morphology (Flick and Thorner, 1993; Rebecchi and Pentyala, 2000; Yoko-o *et al*., 1993).

A number of proteins have been identified that bind 'higher' inositol phosphates. Unexpectedly, most of these proteins are nuclear and catalyze functions that are constitutive and would not be expected to be grossly regulated by the kind of signalling with which animal PLCs are usually associated (El Alami *et al*., 2003; Feng *et al*., 2001; Saiardi *et al*., 2000a; Seeds *et al*., 2007**;** Steger *et al*., 2003; Weirich *et al.*, 2006; York *et al*., 1999). Most animal PLC-δs are mainly cytoplasmic and seem to signal from the plasma membrane (Faenza *et al*., 2005; Topham and Prescott, 2002; Yagisawa, 2006). Many of the functions mediated by these inositol phosphate binding proteins do not seem to be obviously connected to processes that would explain the phenotypes of cells in which the *PLC1* gene has been deleted (*plc1*Δ).

The aim of this part of my work was to try and understand where Plc1p is inside yeast cells under a variety of conditions and to determine whether any treatment(s) would provoke movement of Plc1p between nucleus and cytoplasm. Underlying our initial thinking about Plc1p was the desire to investigate if there might exist separate pools of nuclear and cytoplasmic 'higher' inositol phosphates that might be regulated and function separately. Although the presence of nuclear pores would seem to preclude this, the inability of these highly charged molecules to pass through the pores of dialysis tubing with a 50 kD molecular cutoff suggests that higher inositol phosphates might not be as mobile as is commonly supposed (Van der Kaay and Van Haastert,

1995).

Some animals PLCs are constitutively nuclear: e.g. PLC-β_1 and PLC-δ_4 (Martelli *et al*. 1992; Liu *et al*. 1996; Divecha *et al*. 1997; D'Santos *et al*. 1998). Although the steady-state localisation of most mammalian PLC-δ_1 is at the plasma membrane and in the cytoplasm of normal growing cells, it constantly shuttles between the nucleus and cytoplasm (Yagisawa *et al*., 2002).

This and other evidence has lead to many suggestions of a nuclear inositol phosphate signalling system separate from the 'classical' plasma membrane signaling pathway (Divecha *et al*., 1991; Irvine, 2000; Martelli *et al*., 1992).

3.2 Plc1p abundance is very low in wild-type yeast

Plc1p is the sole PLC in yeast, and appears to play crucial roles in a number of ill-defined cellular events. Despite controlling several apparently disparate processes, Plc1p is reported to be expressed at very low levels from its native promoter in exponentially growing cells at 30ºC (Flick and Thorner, 1993; Fratti *et al*. 2004). To confirm this, I examined the expression of Plc1p by tagging it with three copies of the HA epitope at the C-terminus. Plc1p-3HA was not detected by western blot, which confirmed its low abundance *in vivo* (Fig 3.1 A).

I therefore decided to use the system developed by (Perera 2002, p.111) to detect Plc1p. The complete open reading frame of the *PLC1* gene was inserted into the yeast single-copy shuttle vector, pUG36 (YCp, *URA3*, P_{MET25}-*yEGFP3*-MCS-T_{CYC1}) (Niedenthal *et al*. 1996) such that Plc1p was expressed as an N-terminal GFP fusion.

Expression of GFP-Plc1p was under the control of the methionine-repressable *MET25* promoter. Maximal expression of GFP-Plc1p from this promoter, to about ten times the levels found in wild-type cells was possible in the absence of methionine whilst increasing concentrations of this amino acid could be used to progressively lower its expression (NM Perera and SK Dove 2002, unpublished). Although completely deregulated expression from p*MET25* results in substantial over-expression of Plc1p, our lab has previously shown that inositol phosphate metabolism is not significantly perturbed in cells under these conditions (NM Perera and SK Dove 2002, unpublished). Using this system, GFP-Plc1p (~130 kDa) could be detected by immunoblotting with an anti-GFP antibody and was found to be largely stable (Fig 3.1 B and APPX. Fig A).

Fig 3.1: Western blot for detecting the expression of Plc1p

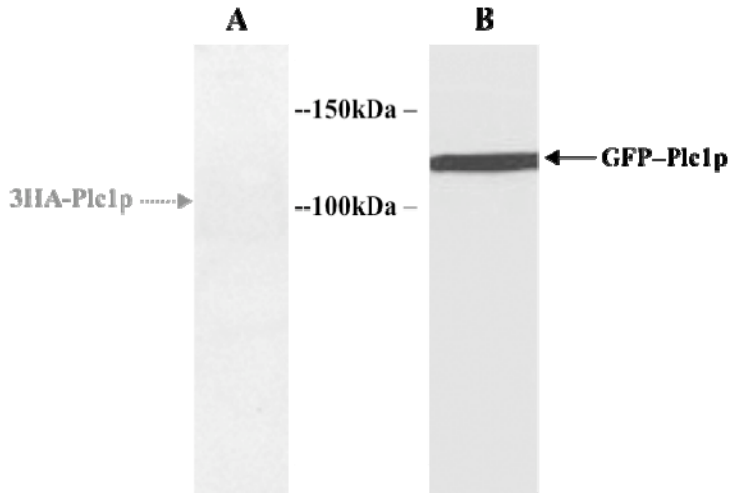

5ml of FY833 (*plc1::PLC1-3HA-HIS3*) cultured in YPD (2% glu), for A, or BY4742 + pUG36-*PLC1* cultured in SC-Ura-Met (2% glu) for B, were grown to OD600 ~0.7 (1x 10^7 cells/ml). After cell breakage, 32µl (~ 40%) total lysates were resolved by SDS-PAGE followed by western blotting. Samples were then electrophoretically transferred to nitrocellulose followed by incubation with anti-HA (1:2000) for A, or anti-GFP (1:1000) for B, respectively.

3.3 Intracellular localisation of GFP-Plc1p

To visualize the intracellular localization of Plc1p, I used the pUG36-*PLC1* construct to enhance the expression level of Plc1p. Plc1p tagged with green fluorescent protein (GFP-Plc1p) was over-expressed in both wild-type and *plc1Δ* cells, and observed by fluorescence microscopy (native expression of GFP-Plc1p produces insufficient signal, NM Perera 2002, pers. comm.).

Fluorescent proteins with different emission colours are valuable tools for *in vivo* multi-labelling experiments. DsRed is a 28 kDa red fluorescent protein (DsRed) cloned from coral of the *Discoma genus* (Baird *et al*. 2000). pUR34*NLS*, a construct that expresses DsRed as an amino-terminal fusion protein with an *NLS1* (nuclear localisation signal) fragment of the simian virus 40 large T antigen, specifically targets the DsRed construct to the nucleus (Rodrigues *et al*. 2001). Nuclei were revealed by fluorescence microscopy (under a different excitation wavelength) by co-transformation of the cells with a plasmid expressing a DsRed-NLS fusion protein (Fig 3.2).

GFP-Plc1p was a stable construct (APPX. Fig A) and distributed in both nucleus and cytoplasm, but more concentrated in the nucleus (Fig 3.2). The distribution of GFP-Plc1p was not significantly different in BY4742 wild-type and in a *PLC1* knockout mutant. As a control, the expression of transfected GFP was seen as even fluorescence throughout the cells, except within the vacuole (Fig 3.3). Significantly more fluorescent signal was detected in the nucleus of GFP-Plc1p than of GFP in wild-type ($P < 0.001$, Fig 3.3), indicating the existence of some mechanism for concentrating Plc1p in the nucleus. I also observed that BY4742 *plc1::KANMX4* cells grew more

Figure 3.2: Localisation of GFP-tagged Plc1p in wild-type and plc1Δ

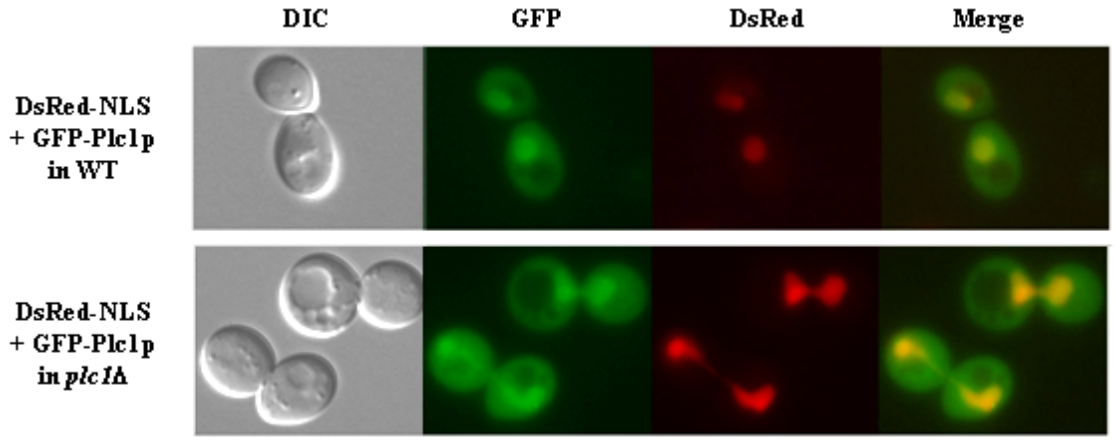

Genotype	Fluorescence Ratio (Nuclear/Cytosolic)
pUG36-*PLC1* in WT	1.71 ± 0.04
pUG36-*PLC1* in *plc1Δ*	1.65 ± 0.04

[There was no significant difference between the values in the two groups.]

Fluorescence images of logarithmic phase cultures (5 x 10^6 – 1 x 10^7 cells/ml) of wild type BY4742 (top) and *plc1Δ* (bottom) transformed with pUG36–*PLC1* and pUR34*NLS*, respectively. The left-hand columns show low light DIC images. The left-mid columns show the localisation of the indicated GFP constructs. The right-mid columns show the localisation of nuclei as obtained by transformation of cells with a NLS construct, and the merged images are shown in the right-hand columns. These images are representative of three replicate cultures. The table shows ratios of fluorescence intensity between the nucleus and cytosol. Each value represents the mean ± S.E.M. of ten determinations.

Figure 3.3: Localisation of GFP in wild-type cells

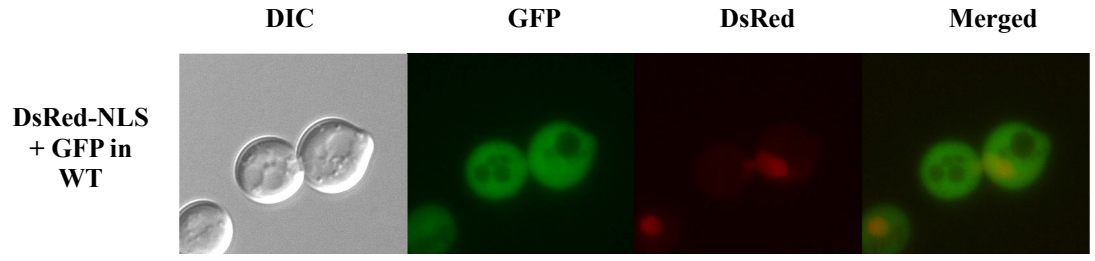

Genotype	Fluorescence Ratio (Nuclear/Cytosolic)
pUG36-*PLC1* in WT	1.71 ± 0.04
pUG36 in WT	$1.19 \pm 0.05^{***}$

[Significantly different from GFP-Plc1p in WT: $^{***}P<0.001$.]

Fluorescence images of logarithmic phase cultures (5 x 10^6 – 1 x 10^7 cells/ml) of wild type BY4742 transformed with pUG36, respectively. The left-hand columns show low light DIC images. The right columns show the localisation of the indicated GFP constructs. These images are representative of three replicate cultures. All strains were cultured in SC-Ura-Met + 2% glucose medium. The table shows ratios of fluorescence intensity between the nucleus and cytosol. Each value represents the mean ± S.E.M. of ten determinations.

slowly than wild-type even at the permissive temperature of 23 ^{o}C, indicating defects in *PLC1* depleted cells.

It is important to bear in mind that the readings of the fluorescence intensity collected in this study do not present the 'true' intensity. Each measurement in a set of fluorescence values will, in simple terms, represent the fluorescence emitted from the full depth of a chosen area of the imaged cell. Most of the fluorescence from the 'cytoplasm' areas will be from cytoplasmic constituents, with a little from overlying and underlying plasma membrane. Fluorescence that contributed to 'nuclear' measurements will have come both from the nucleus and from the cytoplasm and plasma membrane that overlie and underlie it, with the nucleus occupying maybe one-third of the depth of the cell. As a result, any change in the nucleus/cytoplasm fluorescence ratio provide a valid indication of the direction of any change in fluorescent protein distribution, but it will understate the relative changes in protein concentrations in the two compartments - and particularly in changes within the quite small nuclear volume.

3.4 Nucleo-cytoplasmic distribution of Plc1p and possible changes during cell cycle

So, is Plc1p constantly resident in the nucleus or does it, like the mammalian PLC-δ_1, undergo dynamic nucleo-cytoplasmic shuttling?

Since Plc1p appeares to include a potential nuclear export signal (NES) (see later section 3.6.1) I decided to look for evidence of nucleo-cytoplasmic shuttling. The nuclear export receptor Xpo1p mediates the nuclear export of proteins with a leucine-

rich NES, so I used a temperature-sensitive mutant *xpo1-1* to test for such shuttling (Maurer *et al*. 2001). At elevated temperature, *xpo1-1* is inactivated, allowing intranuclear proteins that contain a 'classic' NES to accumulate in the nucleus (e.g. Yrb1p) (Kunzler *et al.* 2000) (Figure 3.4). If Plc1p was undergoing this type of shuttling, then a larger proportion of GFP-Plc1p should be retained in the nucleus in the *xpo1-1* mutant at 37ºC.

Figure 3.4: Trafficking of NES-containing proteins through the temperature-sensitive xpo1-1 mutant of the XPO1 nuclear exporter

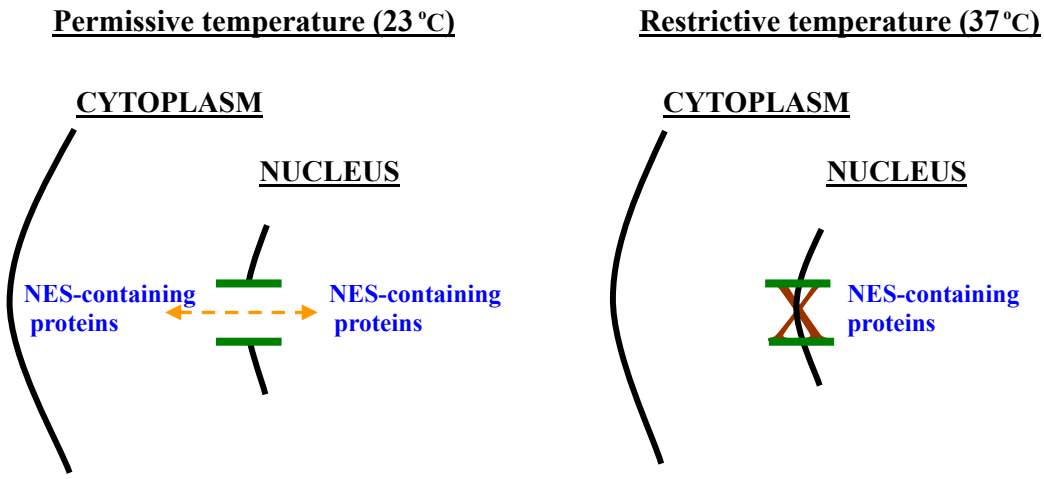

XPO1 and *xpo1-1* cells were transformed with a plasmid expressing GFP-Plc1p and grown at the permissive temperatures (23°C) before they were shifted to 37°C for 2 hours, followed by immediate microscopy. As the results in Fig 3.5 show, there was no obvious re-distribution of GFP-Plc1p observed in *XPO1* cells after shift from 23°C to 37°C. However, GFP-Plc1p did become significantly more concentrated in the nucleus of the *xpo1-1* strain after shift to 37°C (Fig 3.5).

Figure 3.5: Localization of GFP-Plc1p in XPO1 and xpo1-1

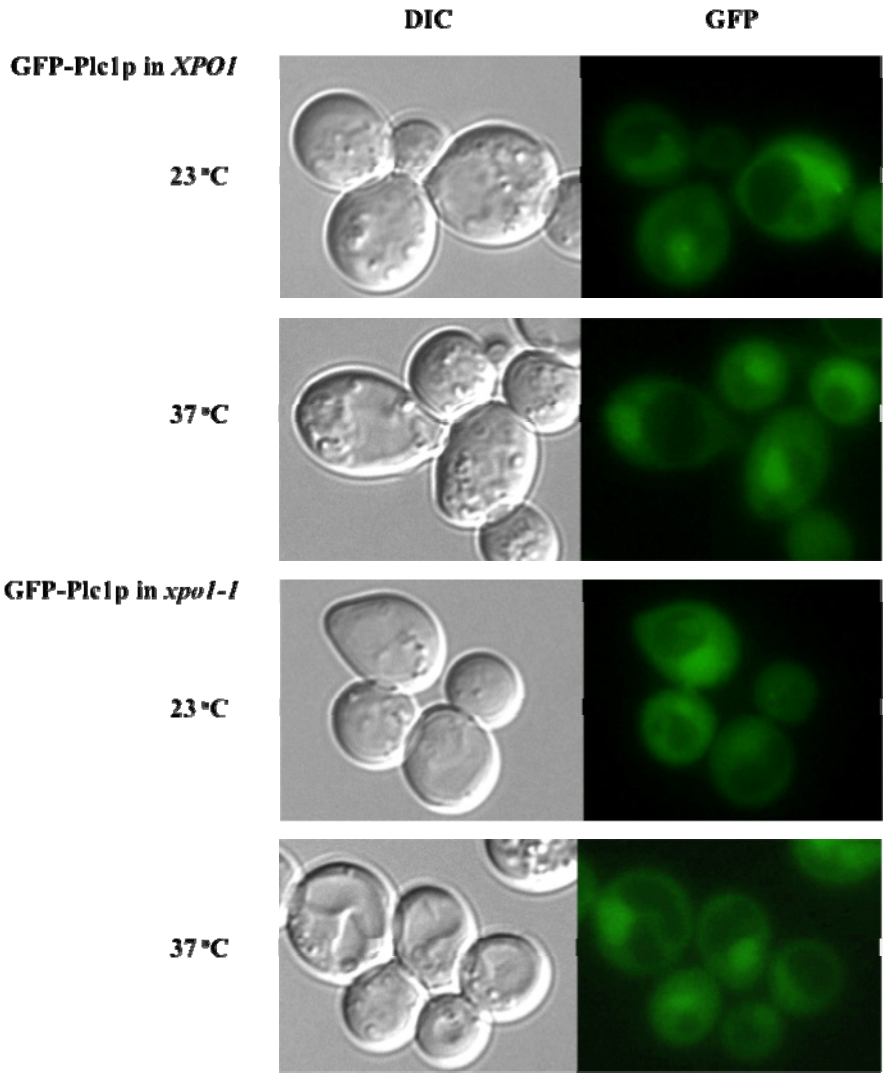

Genotype	Fluorescence Ratio (Nuclear/Cytosolic)	
	23 °C	37 °C
pUG36-*PLC1* in *XPO1*	1.62 ± 0.05	1.67 ± 0.06
pUG36-*PLC1* in *xpo1-1*	1.52 ± 0.03*	1.65 ± 0.05**

[Significantly different from GFP-Plc1p in *XPO1* at 23 °C: $0.01 <^{*} P < 0.05$.]

[Significantly different from GFP-Plc1p in *xpo1-1* at 23 °C: $0.001 <^{**} P < 0.01$.]

Logarithmic phase cultures (5 x 10^6 – 1 x 10^7 cells/ml) were grown at 23°C then either left at this temperature or shifted to 37°C for 2h. The left-hand columns show low light DIC images. The right columns show the localisation of the indicated GFP constructs. These images are representative of three replicate cultures. All strains were cultured in SC-Ura-Met-His+2% glu medium. The table shows ratios of fluorescence intensity between the nucleus and cytosol. Each value represents the mean ± S.E.M. of ten determinations.

Several experimental observations have suggested that Plc1p might be involved in cell cycle control (DeLillo *et al*., 2003; Lin *et al*., 2000). Plc1p is likely to regulate cell stress responses via the C-type cyclin Ume3p (Cooper *et al*. 1999). Growth control by the cyclin-dependent protein kinase complex Pho80p/Pho85p is dependent on Plc1p (Flick and Thorner 1998). Also, more recently, Plc1p was found to accumulate at the centromeres during G2/M stage of cell cycle and to affect kinetochore function (DeLillo *et al.* 2003).

I therefore examined Plc1p localisation at different stages of the cell cycle by arresting yeast cells at G1, M or S phase. Fig 3.6 shows the characteristic morphology of the budding yeast cell at different points in the cell cycle. Note, the nuclear envelope remains intact the whole time in *S. cerevisiae*. Rapamycin inhibits TOR kinase and arrests the cells at the G1 phase (Heitman *et al*. 1991). Nocodazole inhibits the polymerization of tubulin into microtubules and arrests cells at M phase, and hydroxyurea inhibits ribonucleotide reductase and arrests cells at S phase (Iwaki *et al*. 2007).

After these drug treatments, there was no marked change in the distribution of GFP-Plc1p between nucleus and cytoplasm (Fig 3.7). However, quantitation and statistical analysis of the imaging data revealed a significant drop in the ratio of nuclear GFP-Plc1p fluorescence intensity, relative to the cytoplasm in hydroxyurea treated cells compared with the distribution in untreated wild type cells ($P < 0.01$). No alterations in distribution were observed in any of the other drug-treated cells, even with longer treatments (data not shown). This indicates that cells tend to accumulate more cytosolic Plc1p during S phase, which is the preparation stage for mitosis, during

Figure 3.6: Shown below is a diagram illustrating the characteristic morphology of the budding yeast cell at various points in the cycle (Neumann FT A, 2005)

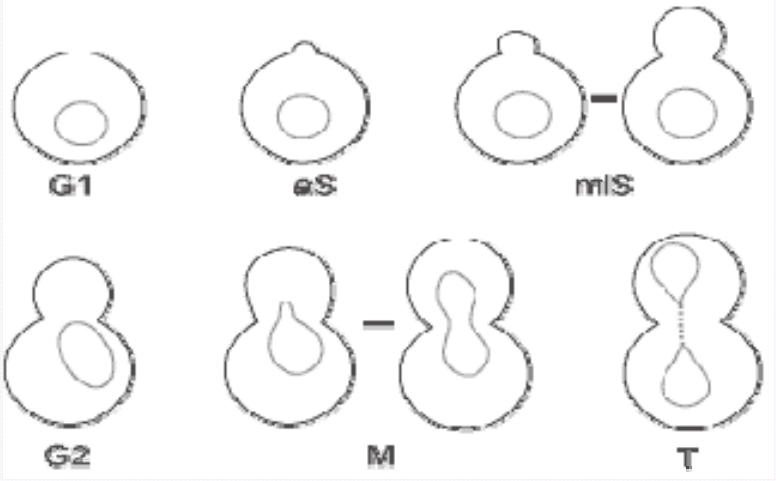

The following criteria are characteristic of indicated stage:
G1 phase: unbudded cells with round nuclei, or attached pairs of post-telophase cells that have two round, clearly separated nuclei; early S: with initial bud emergence, cells are in early S; mid-to-late S: cells with a bud big enough to form a ring at the bud neck, in which the nuclei are still round and centered in the mother cell; G2 phase: large budded cells (bud ≥ 2/3 size of mother cell) with the nucleus at the bud neck; mitosis (M): large budded cells in which the nucleus extends into the daughter cell due to spindle extension; telophase (T): two globular cells with two distinct nuclei that remain connected by residual nuclear structures.

which the bud emerges and DNA synthesis takes place. Plc1p then appears to accumulate in the nucleus during the G2/M phase when nuclear division occurs. This is consistent with the idea that Plc1p may contribute to essential activities in the nucleus during this time.

3.5 Plc1p localization during cell stresses

3.5.1 Heat stress

The Plc1p gene includes a presumptive binding site for heat shock transcription factor upstream of its TATA box (-156 to -169), and inactivation of Plc1p makes yeast more heat-sensitive (Flick and Thorner 1993). *PLC1* cells grow normally at 37°C, but *plc1Δ* cells grow very slowly and are prone to lysis (Fig 3.8). The *plc1Δ* cells are still viable for a time, but they become enlarged, multibudded and unable to complete cytokinesis

Figure 3.7: Localization of GFP-Plc1p at different stages of the cell cycle

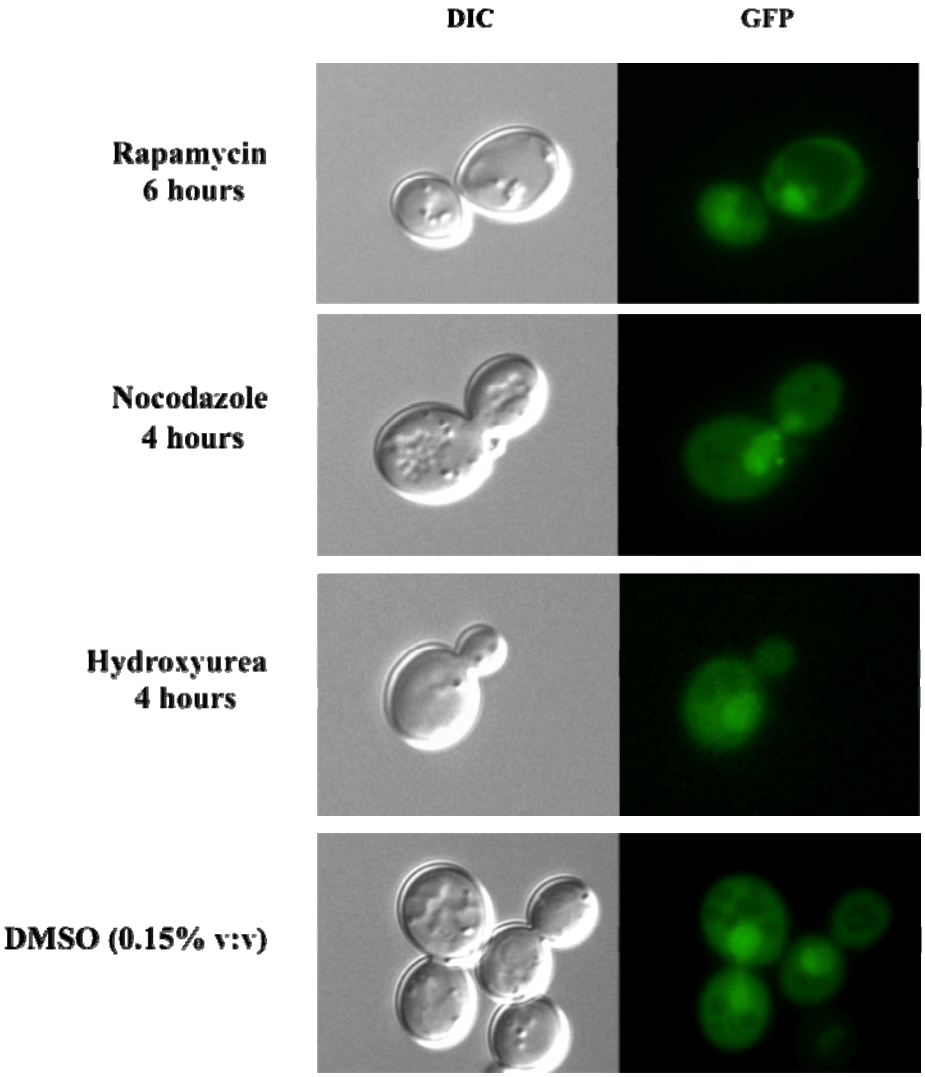

Genotype	Fluorescence Ratio (Nuclear/Cytosolic)				
	Untreated	Rapamycin (G1)	Nocodazole (M)	Hydroxyurea (S)	DMSO (control)
pUG36-*PLC1* in WT	1.71±0.04	1.79±0.06	1.62±0.07	1.54±0.01**	1.65±0.03

[Significantly different from GFP-Plc1p in WT: $0.001 <^{**} P < 0.01$.]

Low light DIC (left columns) and Fluorescence images (right columns) of logarithmic phase cultures (5 x 10^6 – 1 x 10^7 cells/ml) of *BY4742* + pUG36–*PLC1* at 23°C after 200 ng/ml Rapamycin treatment for 6 hours, 15µg/ml Nocodazole for 4 hours or 100mM Hydroxyurea for 4 hours. The bottom panel shows the untreated control cells in drug carrier DMSO (0.15% v:v). These images are representative of three replicate cultures. All strains were cultured in SC-Ura-Met +2% glu medium. The table shows ratios of fluorescence intensity between the nucleus and cytosol. Each value represents the mean ± S.E.M. of ten determinations.

(Flick and Thorner 1993). In mammalian cells, heat shock activates unidentified PLC isoenzymes, resulting in the synthesis of inositol polyphosphates (Calderwood and Stevenson 1993). Higher inositol phosphates also accumulate in *S. cerevisiae* cells incubated at 37ºC. After wild-type *S. cerevisiae* cultures were rapidly elevated from 23°C to 37°C, an activation of PtdIns(4,5)P_2 synthesis was detected, followed by PtdIns(4,5)P_2 depletion and a corresponding accumulation of InsP_6 that was sustained for at least ~1 hour. The increase in InsP_6 was not seen in *plc1Δ* cells, indicating a possible activation of Plc1p in response to heat stress (Perera *et al*., 2004).

Fig 3.8: Growth of wild-type and plc1Δ mutant at 37°C

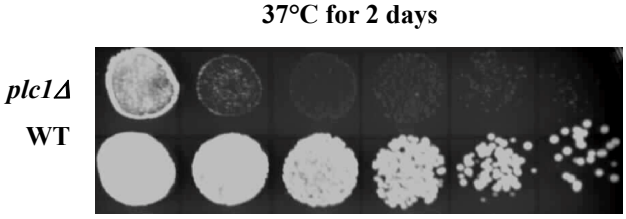

BY4742 wild-type and *plc1Δ* (*plc1*::*KANMX4*) cells were grown to exponential phase (~1 x 10^7 cells/ml) in YPD + 2% glu media. A dilution assay was then carried out as described section 2.16. Cells were serially diluted five-fold then grown on YTD agar plates (2% glu) at 37 °C for 2 days. Data are representative of three independent experiments.

I examined the distribution of GFP-Plc1p during heat stress. There was no detectable change in the localisation of Plc1p after growing at 37°C for 2 hours compared with the GFP distribution at the permissive temperature of 23°C, as in the data on *XPO1* cells grown at 23°C and 37°C that were discussed earlier. Also, no re-distribution was detected after a rapid shift from 23°C to 37°C (Fig 3.9). However, nearly half of the cells displayed punctate nuclear and cytoplasmic fluorescence, which may have influenced the intensity readings and might indicate an association of Plc1p with some kind of nuclear and membrane structures.

Fig 3.9: Localization of GFP-Plc1p in yeast growing at/after 37°C

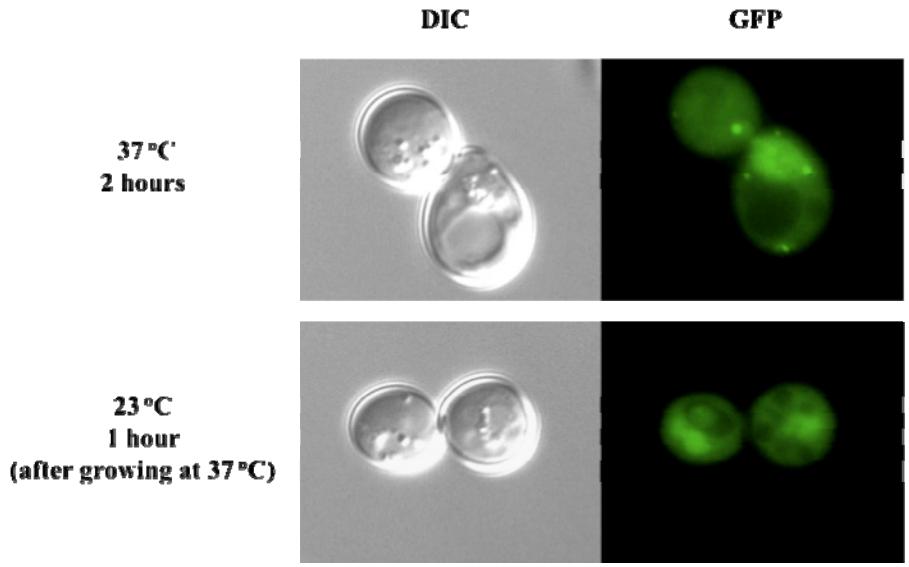

Genotype	Fluorescence Ratio (Nuclear/Cytosolic)		
	37'C 2 hours	23'C (shifted from 37'C)	23'C (untreated)
pUG36-PLC1 in WT	1.64 ± 0.07	1.74 ± 0.08	1.71 ± 0.04

[There was no significant difference between any of the above values.]

Low light DIC (left columns) and Fluorescence images (right columns) of logarithmic phase cultures (5 x 10^6 – 1 x 10^7 cells/ml) of BY4742 + pUG36–*PLC1,* growing at 37°C for 2 hours and at 23°C 1 hour after shifted from 37°C. These images are representative of three replicate cultures. All strains were cultured in SC-Ura-Met +2% glu medium. The table shows ratios of fluorescence intensity between the nucleus and cytosol. Each value represents the mean ± S.E.M. of ten determinations.

3.5.2 Osmotic stress

Osmotic stresses are amongst the most common environmental changes that yeast cells experience throughout their life cycle. Despite the variety of the responses they trigger, the signalling mechanisms that control these responses are incompletely understood (Hohmann 2002).

In yeast, the HOG (High Osmolarity Glycerol) pathway regulates many of the long-term cellular responses to an increased external osmolarity (Brewster *et al*. 1993; Schuller *et al*. 1994). This pathway is defined by the *PBS2* and *HOG1* genes, which encode members of the MAPKK (MAP kinase kinase) and MAPK (mitogen-activated

protein kinase) families respectively (Brewster *et al*. 1993). Activation of this pathway initiates a phosphorylation cascade that leads to nuclear translocation of phosphorylated Hog1p. Nuclear Hog1p regulates gene expression, involving both repression and activation (Proft and Serrano 1999), that leads to an accumulation of intracellular glycerol (Larsson *et al*. 1993). Homologs of Hog1p have been found in other eukaryotic cells, indicating that the HOG pathway is likely conserved, though its functions are not always the same (Han *et al*. 1994).

Flick and Thorner reported *plc1Δ* mutants were very sensitive to hypertonic stress (Flick and Thorner 1993). A double mutant of *plc1Δhog1Δ* was more osmosensitive and synthesized less glycerol than strains with single deletions. Plc1p and Hog1p therefore appear to function in independent pathways that regulate the response of yeast cells to increased extracellular osmolarity (Lin *et al*. 2002).

Responses to hypotonic shock are mediated through the *PKC1* signal transduction cascade (Davenport *et al*. 1995), *PKC1* encodes a protein kinase C-like protein in yeast (Levin *et al*. 1990). Genetic approaches have identified other protein kinases in the Pkc1p pathway, and these form a linear cascade from Pkc1p to the MAPKKK (Bck1p) (Costigan *et al*. 1992), to two MAPKKs (Mkk1p and Mkk2p) (Irie *et al*. 1993) and a MAPK (Mpk1p) (Lee *et al*. 1993). These enzymes are also conserved in mammalian cells (Lee *et al*. 1993).

It has long been suggested that an ill-defined PLC activity is regulated by hypotonic shock in animal cells. In several cell types, hypo-osmotic treatment leads to rapid hydrolysis of phosphoinositides and generation of inositol phosphates. This hydrolysis

was inhibited by the PLC inhibitor U73122 (Einspahr *et al*. 1988; Bender *et al*. 1993). Earlier experiments in our laboratory showed that hypo-osmotic stress induces Plc1p activation: After wild-type cells were hypo-osmotically shocked for 2 minutes, InsP_6 levels were raised about 3-fold (Perera *et al*., 2004).

In the terms of the localization of PLC during its activation, a previous study in MDCK cells found that PLC-δ_1 was both activated and translocated from the plasma membrane to the perinuclear region after hypo-osmotic stress (Yagisawa *et al*. 2002). I therefore examined the localization of Plc1p before and after osmotic stresses.

To visualize the localization of Plc1p during hyper-osmotic shock, exponential phase wild type cells expressing GFP-Plc1p were shifted to a synthetic complete medium (depleted of methionine and uracil) containing 0.6M NaCl. Images were taken at 2 min, 15 min and 2 hours. The cell suspensions were then quickly diluted ten-fold in the same medium but without the extra NaCl. The localization of GFP-Plc1p was again examined at 2 min, 15 min and 2 hours to record what occurs during the resulting hypo-osmotic stress.

Although there were no striking changes in the fluorescence distribution after either treatment (Fig 3.10), fluorescence quantitation and statistical analysis did detect a distinct decrease in the ratio of nuclear vs. cytosolic GFP-Plc1p resulting from the osmotic disturbances (Fig 3.10). A slight shift of Plc1p from the nucleus to the cytoplasm occurred within 2 minutes in response to the raised salt concentration and was gradually reversed ($P > 0.05$), and much the same happened when cells were diluted back into normal medium.

Figure 3.10: Localization of GFP-Plc1p in wild-type cells during hype- and hypo-osmotic shock

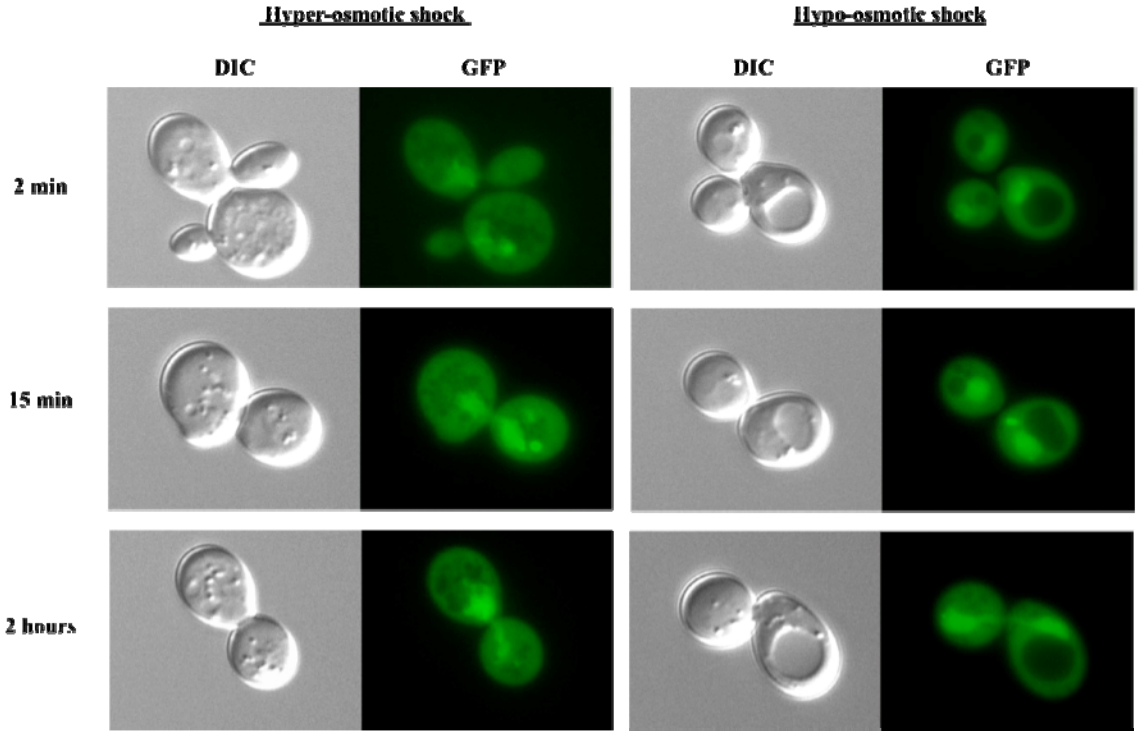

Hyper- & hypo-osmotic shock induced GFP-Plc1p localisation change

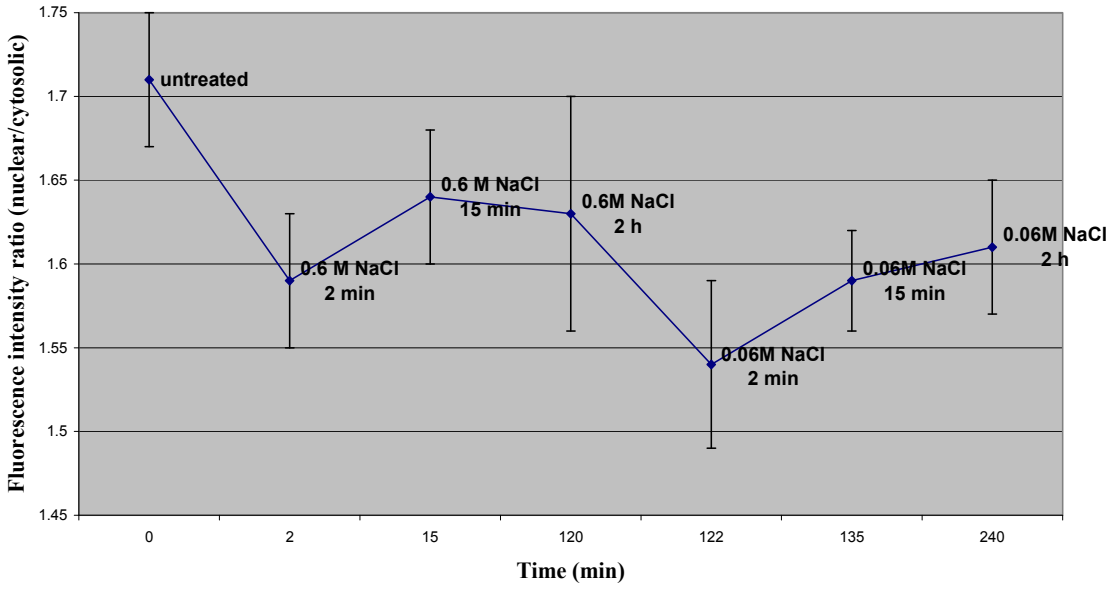

Treatment	Fluorescence Ratio (Nuclear/Cytosolic)		
time	2 min	15 min	2 Hrs
Hyper-osmotic shocked	$1.59 \pm 0.04^{*}$	1.64 ± 0.04	1.63 ± 0.07
Hypo-osmotic shocked	$1.54 \pm 0.05^{*}$	$1.59 \pm 0.03^{*}$	1.61 ± 0.04
untreated	1.71 ± 0.04		

[Significantly different from the untreated: $0.01 <^{*} P < 0.05$.]

Logarithmic phase cultures (5 x 10^6 – 1 x 10^7 cells/ml) of BY4742 + pUG36–*PLC1* at 25°C in SC-Ura-Met +2% glu + 0.6M NaCl medium (hyper-) for 2 min, 15 min, and 2 hours, followed by a shift to a 10 times diluted same media (hypo-) for another 2 min, 15 min, and 2 hours. These images are representative of three cultures. The table shows ratios of fluorescence intensity between the nucleus and cytosol. Each value represents the mean ± S.E.M. of ten determinations.

The latter result is consistent with the observation of Dr Perera that Plc1p was stimulated upon hypo-osmotic shock for 2 minutes and that the loss of cellular PtdIns(4,5)P_2 occurred at the plasma membrane (Perera *et al*., 2004). It seems that a sudden osmotic change to the growth environment in either direction results in a small proportion of the initially nuclear Plc1p moving to the cytoplasm. How this occurs remains to be determined.

Conclusively, I did not observe any change in Plc1p localisation after cells were subjected to raised temperature, but a small nuclear-to-cytoplasmic shift occurred after challenge in media of increased and decreased osmotic potential. Plc1p seems to undergo some rapid intracellular translocation in response to stresses. This then reverts to the 'normal' distribution fairly quickly.

3.6 How does Plc1p get into the nucleus: nucleo-cytoplasmic signalling of Plc1p

It has been suspected for a decade or so that some phosphoinositides reside in the nucleus, and that nuclear turnover might be regulated by mechanisms that are independent of the phosphoinositides in the plasma membrane and cytoplasmic membranes. Many of the key lipids and enzymes responsible for the metabolism of inositol lipids were also found in the nuclei (Irvine 2000). The yeast PLC distributes in both nucleus and cytoplasm throughout all stages of the cell cycle as well as during various stresses. Many of the postulated functions of Plc1p are nuclear functions, but

we wondered whether Plc1p might also have distinct functions in the cytoplasm, because much of the protein is present outside the nucleus. In order to address this question, I produced mutants of Plc1p that would be largely restricted to one compartment, so as to identify which phenotypes require nuclear or cytoplasmic Plc1p.

Unlike small molecules which pass through the NPC (nuclear pore complex) freely by diffusion, proteins as large as Plc1p are specifically selected to translocate through the nuclear pores, relying on their own NLS (nuclear localization signals) and NES (nuclear export signals). One of the goals of this study was to find two short amino-acid sequences, which were likely to be the NLS and NES that mediate the entry and exit of Plc1p from the nucleus.

3.6.1 Nuclear Export Signal in Plc1p

The canonical NES is a short leucine-rich sequence motif (Kunzler *et al*. 2000). Such NES sequences have been found in the EF-hand of rat PLC-δ_1, confering a predominantly cytosolic localisation upon this enzyme (Yamaga *et al*. 1999). Computer search of the amino-acid sequence of the open reading frame of *PLC1* revealed a putative NES-like motif in its PH domain, KLKALH (residues 189-194). Mutation of the leucines in the KLKALH motif proved critical for Plc1p nuclear export as a mutant Plc1p tagged with GFP in which these two leucines (Leu^{190} and Leu^{193}) were replaced by alanines showed aberrant localisation. This $Plc1p^{NES}$ mutant ($Plc1p^{L190A/L193A}$) was stable (APPX. Fig A) and displayed GFP fluorescence that was highly concentrated in the nucleus, suggesting an almost complete loss of NES function (Fig 3.11).

Figure 3.11: Localization of GFP-Plc1p^{NES}

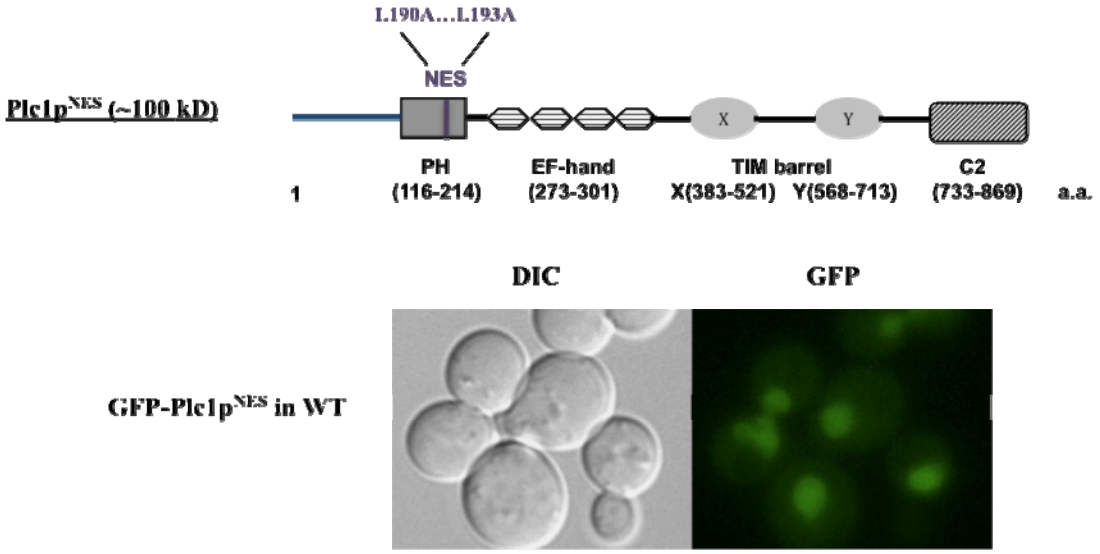

Genotype	Fluorescence Ratio (Nuclear/Cytosolic)
pUG36- *PLC1*^{NES} in WT	2.27 ± 0.05***
pUG36-*PLC1* in WT	1.71 ± 0.04

[Significantly different from GFP-Plc1p in WT: $^{***}P$<0.001.]

Low light DIC (left columns) and Fluorescence images (right columns) of logarithmic phase cultures (5 x 10^6 – 1 x 10^7 cells/ml) of BY4742 + pUG36– *PLC1*^{NES} (GFP-Plc1p$^{L190A/L193A}$). These images are representative of three replicate cultures. All strains were cultured in SC-Ura-Met +2% glu medium. The table shows ratios of fluorescence intensity in nucleus and cytosol. Each value represents the mean ± S.E.M. of ten determinations.

This Plc1p^{NES} is therefore a valuable reagent provided that the mutations I have introduced do not compromise the catalytic activity of Plc1p. This was tested by making an additional insertion mutation in addition to the NES which resulted in a mutant that no longer restricted in the nucleus though still bearing the L190A/L193A mutations, and the behavior of this mutant proved that these amino acid alterations in the NES mutant did not disrupt the catalytic function of Plc1p. This will be discussed in more detail in a later section (section 3.7).

3.6.2 Identification of the Nuclear Localization Signal (NLS) of Plc1p

3.6.2.1 Delimiting the location of the NLS in truncations of *PLC1*

The next step was to define the NLS of Plc1p. A typical NLS is generally a cluster or clusters of 5-10 basic amino acids in a distinct sequence pattern. For example, a basic amino acid cluster in the PH domain of PLC-δ_4 is responsible for its nuclear localization (Liu *et al*. 1996), two lysine's (K432 and K434) in the X-Y linker of PLC-δ_1 play a role in its nuclear entry (Yagisawa *et al*. 2002), and that the NLS of PLC-β_1 appears to be in its C-terminal region (Kim *et al*. 1996). It seems that PLC isozymes, even in the same family, can display a number of disparate ways of entering the nucleus using amino-acid motifs at a variety of positions in the protein.

Our search began with truncations of the *PLC1* gene. We expected that Plc1p might be similar to PLC-δ_1, with an NLS situated between the X and Y domains of the catalytic β-barrel because of a NLS sequence match existing in this linker. However, mutation of the putative NLS sequence in the X-Y linker of Plc1p did not alter nuclear localisation at all (data not shown). In addition, I observed that a truncation mutant encoding only the first 333 amino-acids of Plc1p was nuclear when expressed as an N-terminal GFP fusion (Fig 3.12).

This Plc1p$^{1-333}$ construct was stable (APPX. Fig A) and displayed the same subcellular localization as the full length Plc1p, as determined by fluorescence quantitation and statistical analysis, despite encoding only the Plc1p-unique N-terminal domain, the PH domain and the EF hand. This suggested that the NLS sequence must reside in the N-terminal ~333 amino-acids of Plc1p in a position different from that of the NLSs of mammalian PLCs.

Figure 3.12: Localization of GFP-Plc1p$^{1-333}$

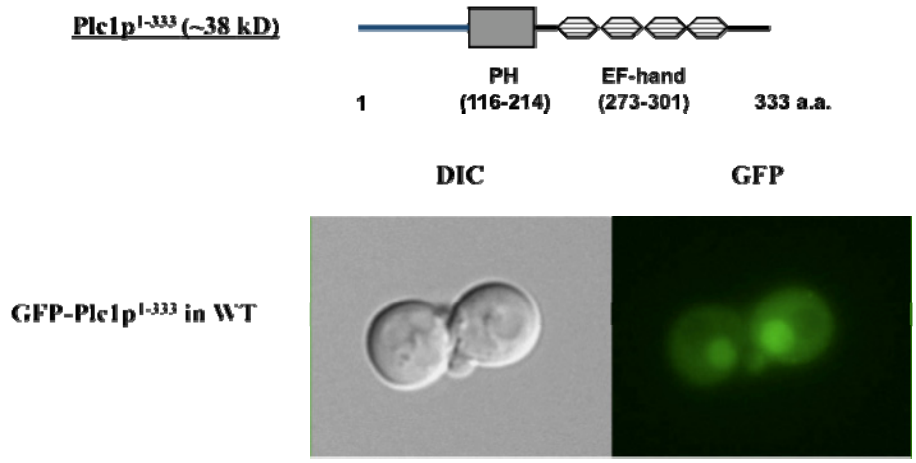

Genotype	Fluorescence Ratio (Nuclear/Cytosolic)
pUG36- *PLC1*$^{1-333}$ in WT	1.72 ± 0.06
pUG36-*PLC1* in WT	1.71 ± 0.04

[There was no significant difference between the above values.]

Low light DIC (left columns) and fluorescence images (right columns) of logarithmic phase cultures (5 x 10^6 – 1 x 10^7 cells/ml) of BY4742 + pUG36–*PLC1*$^{1-333}$. These images are representative of three replicate cultures. All strains were cultured in SC-Ura-Met +2% glu medium. The table shows ratios of fluorescence intensity in nucleus and cytosol. Each value represents the mean ± S.E.M. of ten determinations.

Further truncation mutants were constructed to define the region in which the Plc1p NLS resides more closely. All of these, including Plc1p$^{1-333}$, were transformed into wild-type cells (containing their own untagged, full-length Plc1p) and into *plc1*Δ mutants. No difference was observed in the localization of our Plc1p truncated mutants in wild type or *plc1Δ* cells, so only images of wild-type cells are shown.

None of the truncation mutants (GFP-Plc1p$^{220-333}$, GFP-Plc1p$^{1-220}$, GFP-Plc1p$^{1-110}$ or GFP-Plc1p$^{110-220}$) displayed marked nuclear fluorescence similar to that of full-length Plc1p, but there was a slight concentration of nuclear fluorescence in some cells. Statistical analysis revealed that the GFP-Plc1p-truncations did show some nuclear concentration but to a much lower degree than the full-length protein ($P < 0.001$) (Fig

3.13). That two of the non-overlapping constructs, Plc1p$^{1-220}$ and Plc1p$^{220-333}$, showed significant nuclear localisation. Since GFP itself cannot accumulate in the nucleus, the GFP-signal presumably derives from the Plc1p-truncations. This suggested that two weak NLSs might contribute to the nuclear localisation of Plc1p.

Figure 3.13: Localization of GFP-Plc1p$^{220-333}$, GFP-Plc1p$^{1-220}$, GFP-Plc1p$^{1-110}$, GFP-Plc1p$^{110-220}$

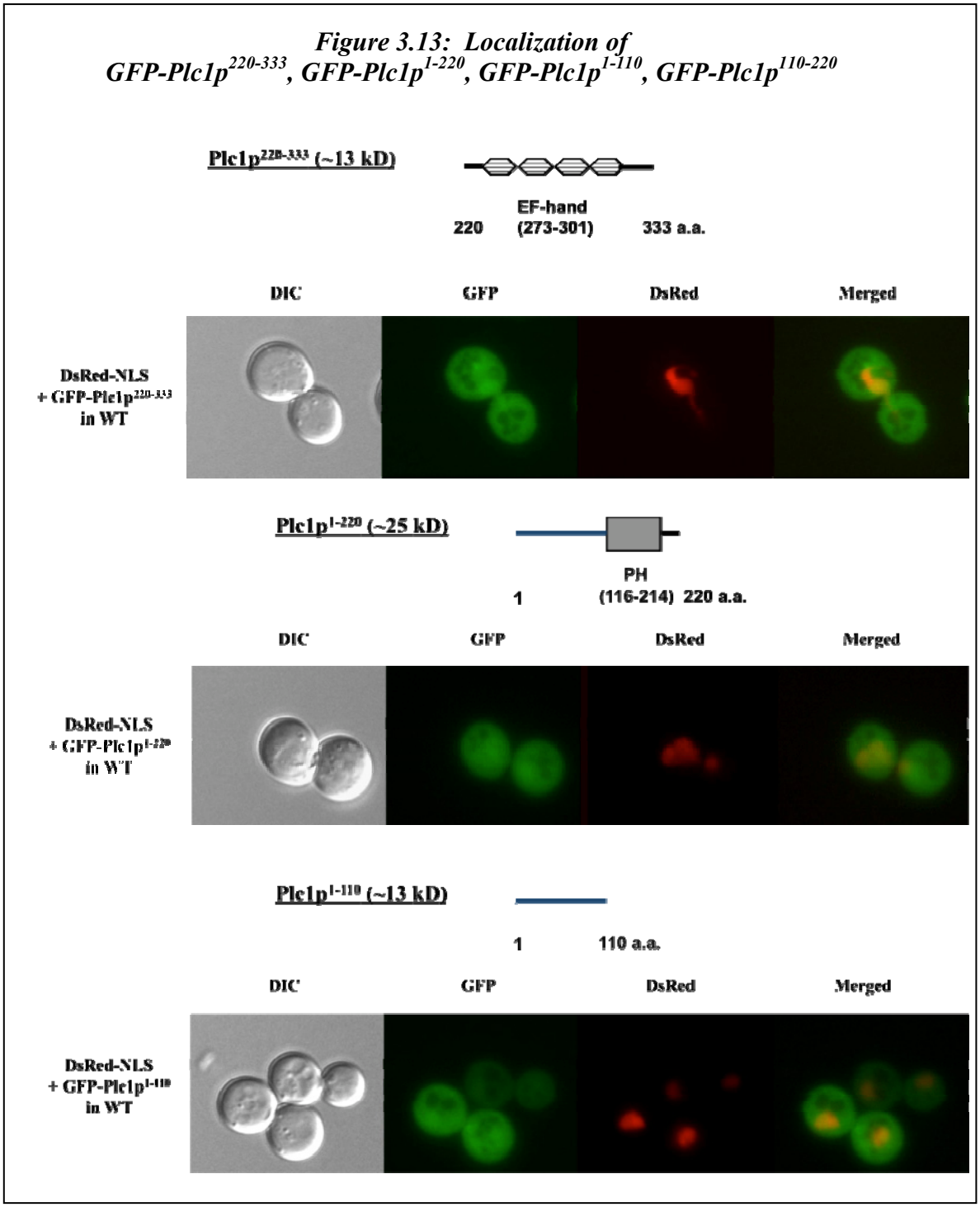

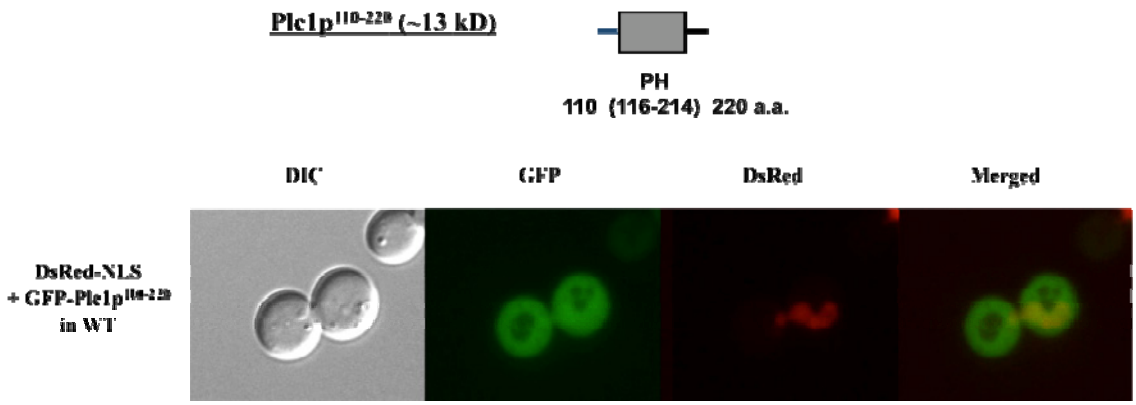

Genotype	Fluorescence Ratio (Nuclear/Cytosolic)
pUG36-*PLC1*$^{220\text{-}333}$ in WT	$1.32 \pm 0.02^{***/+}$
pUG36-*PLC1*$^{1\text{-}220}$ in WT	$1.38 \pm 0.03^{***/++}$
pUG36-*PLC1*$^{1\text{-}110}$ in WT	$1.19 \pm 0.02^{***}$
pUG36-*PLC1*$^{110\text{-}220}$ in WT	$1.19 \pm 0.02^{***}$
pUG36-*PLC1* in WT	1.71 ± 0.04

[Significantly different from GFP-Plc1p in WT: $^{***}P<0.001$.]

[Significantly different from GFP in WT: $0.01<^{+}P<0.05$, $0.001<^{++}P<0.01$]

Low light DIC (left columns) and Fluorescence images (right columns) of logarithmic phase cultures (5 x 10^6 – 1 x 10^7 cells/ml) of BY4742 transformed with indicated the truncation mutants, respectively. These images are representative of three replicate cultures. All strains were cultured in SC-Ura-Met +2% glu. The table shows the ratio of fluorescence intensity between nucleus and cytosol. Each value represents the mean ± S.E.M. of ten determinations.

However, these four truncation constructs were not very stable (APPX. Fig A), so source of the observed fluorescence may have come from liberated GFP. Attempts to express smaller truncation (less than 220 amino-acids) mutants of Plc1p were not successful.

In order to gain further insight into the nature of these sequences, I constructed N-terminal GFP-linked truncations that lacked increasingly large portions of the N-terminus of Plc1p: GFP-Plc1p$^{110\text{-end}}$, GFP-Plc1p$^{220\text{-end}}$ and GFP-Plc1p$^{333\text{-end}}$. I hoped that the N-terminal GFP fusions would protect the unnatural N-termini and so result in better stability. Two of these constructs, GFP-Plc1p$^{110\text{-end}}$ and GFP-Plc1p$^{220\text{-end}}$, were stable (APPX. Fig A) and concentrated in the nucleus (Fig 3.14). This was not

Figure 3.14: Localization of GFP-Plc1p$^{110\text{-}end}$, GFP-Plc1p$^{220\text{-}end}$, GFP-Plc1p$^{333\text{-}end}$

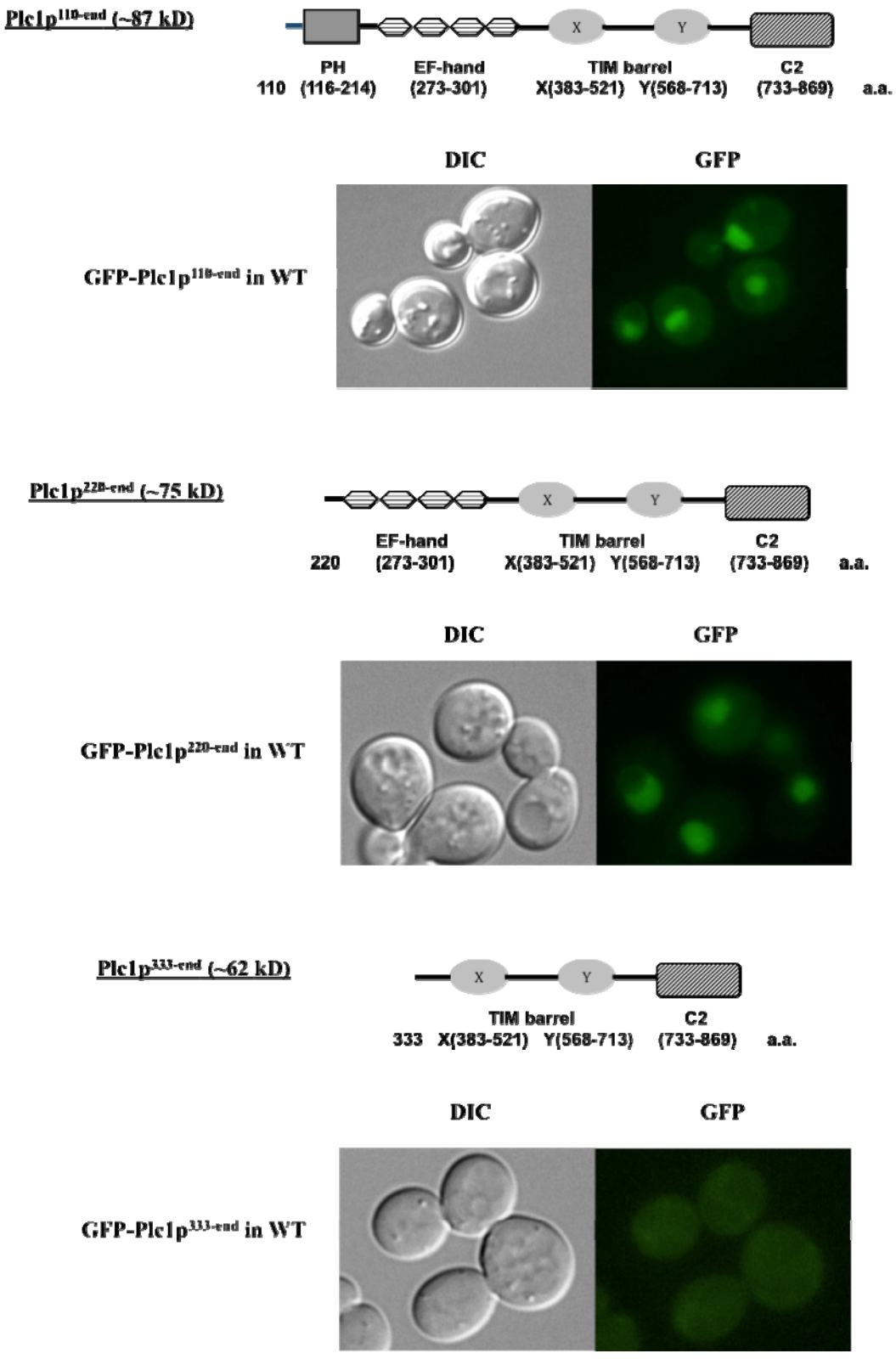

Genotype	Fluorescence Ratio (Nuclear/Cytosolic)
pUG36-*PLC1*$^{110\text{-}end}$ in WT	$2.06 \pm 0.04^{***/++}$
pUG36-*PLC1*$^{220\text{-}end}$ in WT	$2.10 \pm 0.04^{***/++}$
pUG36-*PLC1*$^{333\text{-}end}$ in WT	N/A
pUG36-*PLC1* in WT	1.71 ± 0.04
pUG36-*PLC1*^{NES} in WT	2.27 ± 0.05

[Significantly different from GFP-Plc1p in WT: $^{***}P<0.001$.]

[Significantly different from GFP-Plc1p^{NES} in WT: $0.001<^{++}P<0.01$.]

Low light DIC (left columns) and fluorescence images (right columns) of logarithmic phase cultures (5 x 10^6 – 1 x 10^7 cells/ml) of BY4742 transformed with the indicated truncation mutants, respectively. These images are representative of three replicate cultures. All strains were cultured in SC-Ura-Met +2% glu. The table shows ratio of fluorescence intensity in nucleus and cytosol. Each value represents the mean ± S.E.M. of ten determinations.

surprising, since the (220-end) construct is likely to lack a functional NES sequence and the (110-end) construct may have a disrupted NES, because the NES sequence is close to its end and may be obscured by the linker between GFP and the Plc1p sequence. The fluorescence of GFP-Plc1p$^{333\text{-}end}$, which encodes the X and Y domains and the C2 domain of Plc1p, was very poor (Fig 3.14), probably because of its instability (APPX. Fig A).

I had evidence from the C-terminal truncations that the first 333 amino-acids of Plc1p might include an NLS(s), and the N-terminal truncations suggested that there might be an NLS sequence between amino-acids 220 – 333 of Plc1p because the (220-end) construct is also nuclear. This lends weight to the idea that there is more than one means of achieving nuclear localisation in Plc1p with all the sequences required for both mechanisms residing in the first 333 amino-acids. Either or both of these sequences (1-220 and 220-333) may be a classical NLS sequences or may be protein-protein interaction domain(s) that allow Plc1p to interact with other protein(s) that containing their own NLS sequences and could thus “piggy-back” Plc1p into the nucleus.

3.6.2.2 Mutagenesis of putative NLS sequences in *PLC1*

Having located a possible NLS in the first 333 residues of Plc1p, I tried to define this NLS by site directed mutagenesis. I compared the N-terminal 333 amino-acids of *PLC1* with the corresponding regions of PLC-δ_1 and PLC-δ_3, which do not include NLSs (Cheng *et al*. 1995). This amino-acid alignment highlighted a cluster of basic amino-acid residues (R111, R117, R120, R123) immediately N-terminal to the PH domain of Plc1p, but not present in rat PLC1-δ_1. I therefore exchanged these four arginines in Plc1p with the corresponding amino acids in the rat PLC-δ_1 sequence: R111L/R117S/R120S/R123E. The resulting construct, GFP-Plc1p^{4R} (pUG36-*PLC1*$^{R111L/R117S/R120S/R123E}$), was stable (APPX. Fig A) and entered the nucleus less efficiently than wild-type GFP-Plc1p (Fig 3.15, $P < 0.01$).

A search for classical NLSs within the first 333 amino-acids was also mounted using the NLS consensus determined by Corbett's group (Leung *et al*. 2003). This comprises a loose consensus sequence of K(K/R)X(K/R), with a lysine in position 1, followed by basic residues in positions 2 and 4. This identified a KKLRK sequence (residues 94-98) and a KRLR sequence (residues 170-173).

I then performed site-directed mutagenesis on the *PLC1* possible NLSs, by converting the basic amino-acids in these two regions to neutral ones: K94A/K95A/R97A for KKLRK, and K170A/R171A/R173A for KRLR. These were ligated into pUG36 to create N-terminal GFP fusions, and transformed to BY4742 and BY4742 *plc1*Δ cells. Both mutants displayed decreased nuclear fluorescence, with GFP-Plc1p^{KKLRK} (K94A/K95A/R97A) having the more profound effect (Fig 3.15). GFP-Plc1p^{KRLR} (K170A/R171A/R173A) was stable but the K94A/K95A/R97A mutations yielded a

somewhat unstable construct (APPX. Fig A). Neither of these sequences on its own was sufficient to exclude Plc1p from the nucleus.

Conclusively, mutations of three putative NLSs in the first 180 amino-acids of Plc1p attenuated the nuclear localization of Plc1p. However, the nuclear localization of Plc1p was not abolished by loss of any single putative NLS, therefore they may act together. Attempts to combine these mutations failed because of the instability of these multiple mutant constructs (data not shown).

Figure 3.15: Localization of GFP-Plc1p^{4R}, GFP-Plc1p^{KKLRK} and GFP-Plc1p^{KRLR}

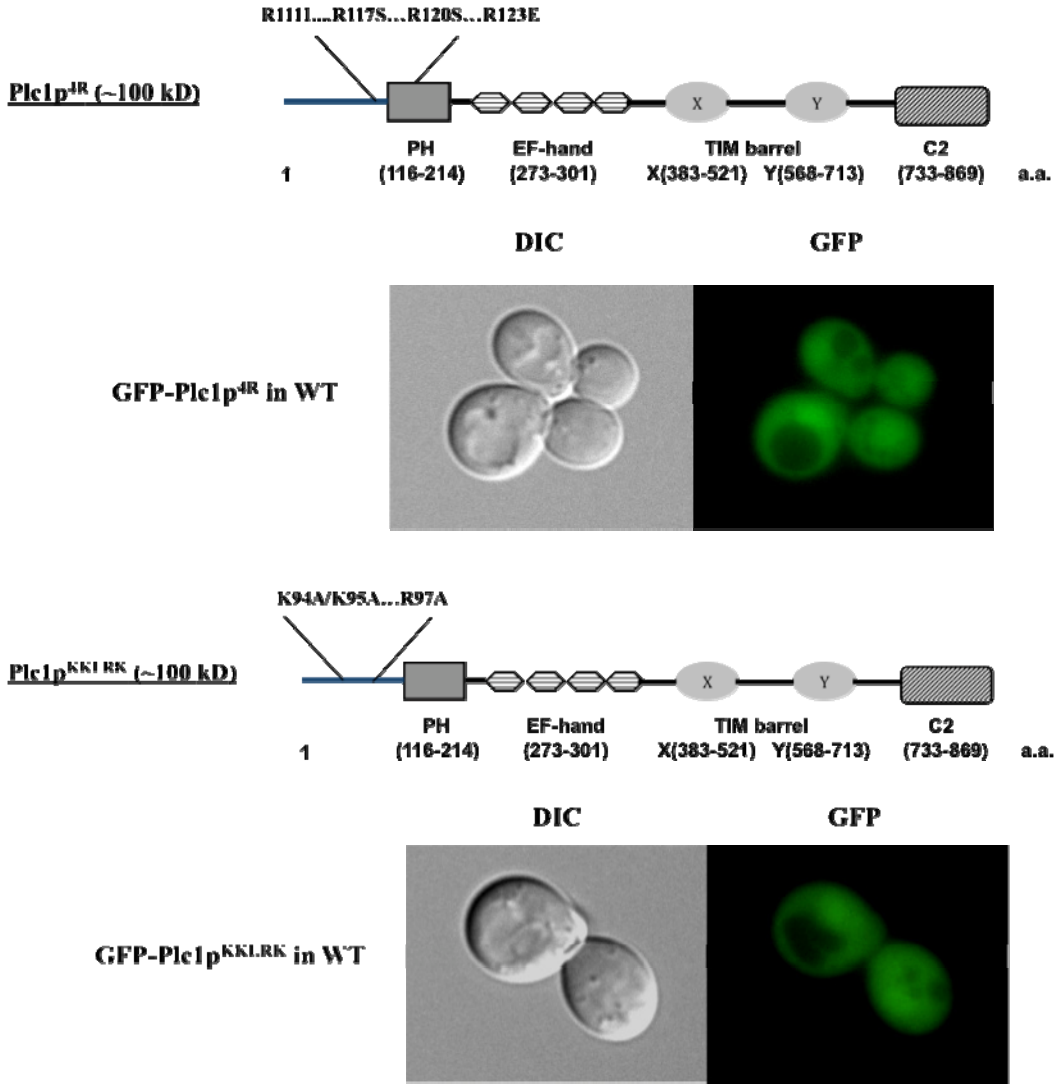

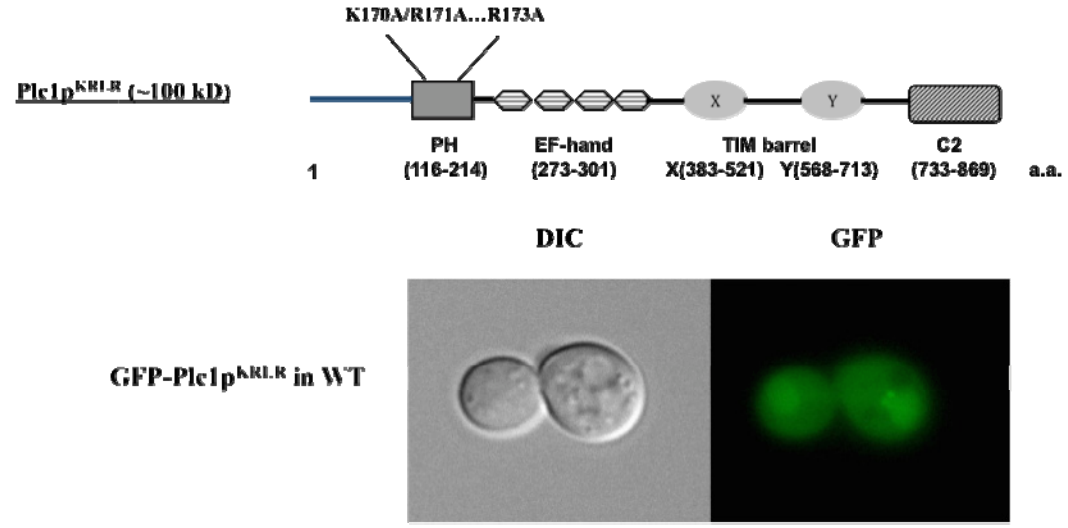

Genotype	Fluorescence Ratio (Nuclear/Cytosolic)
pUG36-*PLC1*^{4R} in WT	1.51 ± 0.04**
pUG36-*PLC1*^{KKLRK} in WT	1.47 ± 0.03***
pUG36-*PLC1*^{KRLR} in WT	1.57 ± 0.05**
pUG36-*PLC1* in WT	1.71 ± 0.04

[Significantly different from GFP-Plc1p in WT: $^{***}P<0.001$, $0.001<{}^{**}P<0.01$.]

Low light DIC (left columns) and Fluorescence images (right columns) of logarithmic phase cultures (5 x 10^6 – 1 x 10^7 cells/ml) of BY4742 transformed with the indicated PLC1 mutant constructs, respectively. These images are representative of three replicate cultures. All strains were cultured in SC-Ura-Met +2% glu medium. The table shows ratio of fluorescence intensity in nucleus and cytosol. Each value represents the mean ± S.E.M. of ten determinations.

3.6.3 A plasma membrane localised Plc1p mutant – *PLC1*^{CAAX}

Difficulty in defining the NLS sequence of Plc1p made it hard to determine the phenotypes of cells expressing exclusively cytoplasmic or nuclear Plc1p. I therefore tried to create a cytoplasmic version of Plc1p that would overcome the influence of NLSs.

The first strategy was to cause prenylation of Plc1p by adding a CAAX sequence to the C-terminus, in which C indicates a cysteine, A is an aliphatic amino acid (I used 2× isoleucines), and X is any amino acid (serine). A prenylated GFP was first made, and its intracellular localization in wild-type (BY4742) cells was examined. As

expected, GFP^{CAAX} was localised as a green fluorescent ring at the plasma membrane (Fig 3.16). Plc1p^{CAAX} was expected to be located at the plasma membrane.

Figure 3.16: Localization of GFP^{CAAX} and GFP-Plc1p^{CAAX}

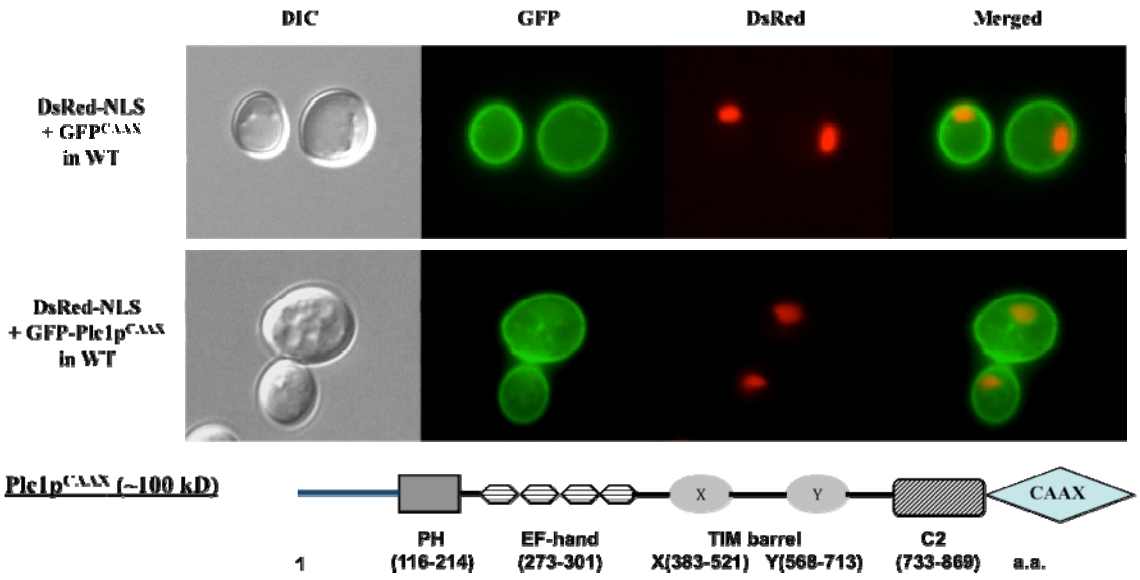

Genotype	Fluorescence Ratio (Plasma Membrane/Nuclear/Cytosolic)
pUG36-*CAAX* in WT	(1.40±0.02):(1.08±0.043):(1±0)
pUG36-*PLC1*^{CAAX} in WT	[(1.14±0.03)$^{+++}$:(1.14±0.04)$^{***/+++}$]$^{+}$:(1±0)
pUG36-*PLC1* in WT	(N/A): (1.71 ± 0.04): (1±0)

[Significantly different from GFP-Plc1p in WT: $^{***}P<0.001$.]

[Significantly different from GFP^{CAAX} in WT: $^{+++}P<0.001$, $0.01<^{+}P<0.05$.]

Fluorescence images of logarithmic phase cultures (5 x 10^6 – 1 x 10^7 cells/ml) of BY4742 transformed with the indicated constructs. The left-hand columns show low light DIC images. The left-mid columns show the localisation of the indicated GFP constructs. The right-mid columns show the localisation of nuclei as obtained by transformation of cells with a NLS construct, and the merged images are shown on the right-hand columns. These images are representative of three replicate cultures. All strains were cultured in SC-Ura-Met-His+2% glu medium. The table shows ratio of fluorescence intensity in PM (plasma membrane), nucleus and cytosol. Each value represents the mean ± S.E.M. of ten determinations.

GFP-Plc1p^{CAAX} was very stable construct (APPX. Fig A). A green fluorescent ring was detected on the yeast plasma membrane when Plc1p^{CAAX} was expressed in cells as a C-terminal GFP fusion of Plc1p, indicating that GFP-Plc1p^{CAAX} was indeed prenylated. However, there is still a small pool of Plc1p^{CAAX} in the nucleus (Fig 3.16):

probably as a result of immediate nuclear translocation of nascent Plc1p^{CAAX} after translation, before the prenyl transferases can get access to this mutant.

3.6.4 Cytoplasmic Plc1p mutant – *PLC1*^{PKI}

In addition to the plasma membrane localised *PLC1*^{CAAX} mutant, I decided to make a Plc1p that could be excluded from the nucleus by inserting into Plc1p two powerful NES from PKI.

The NES from the protein kinase A inhibitor PKI (LALKLAGLDI) can redirect a variety of proteins from the nucleus to the cytoplasm (Miller and Cross 2000). I first attempted to add a carboxyl-terminal PKI NES, but this did not generate a stable mutant (data not shown). I then put a tandem PKI NES sequence at the amino-terminus of Plc1p. This made a Plc1p^{PKI} mutant which was excluded from the nucleus and was stable (APPX. Fig A). In these cells, there was a "hole" in the GFP signal in the area of the nucleus, as indicated by co-localization with a nuclear marker, pUR34*NLS* (DsRed, see material section) (Fig 3.17).

3.7 The effects of the localisation of Plc1p on its functions

3.7.1 Stress responses of over-expressed *PLC1* mutants

Once we had the cytoplasmic- and nuclear-restricted Plc1p, I phenotypically characterized cells expressing these mutant alleles as their only Plc1p to determine how the cytoplasmic and nuclear pools of Plc1p and hence of the liberated inositol polyphosphates contributed to Plc1p function.

One concern was, the stress sensitivity of the Plc1p^{PKI} and Plc1p^{NES} mutants could

Figure 3.17: Localization of GFP-Plc1p^{PKI}

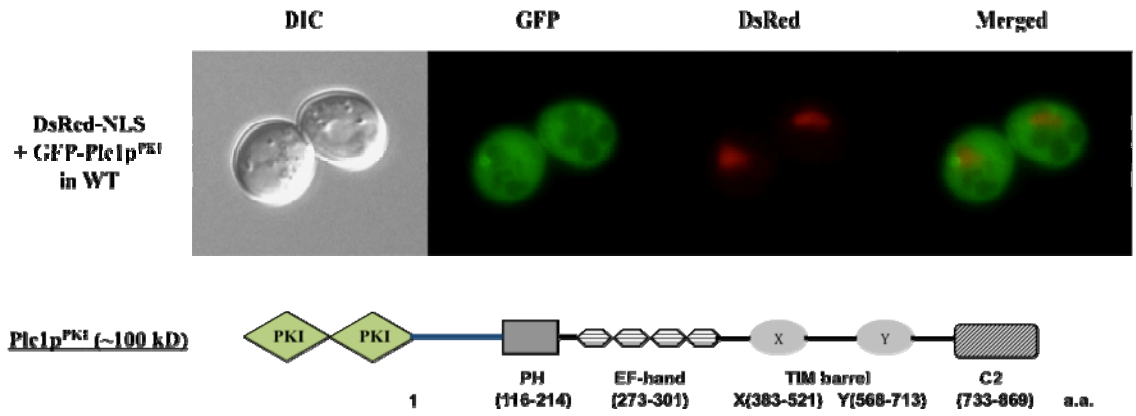

Genotype	Fluorescence Ratio (Nuclear/Cytosolic)
pUG36-*PLC1*^{PKI} in WT	0.71 ± 0.02***
pUG36-*PLC1* in WT	1.71 ± 0.04

[Significantly different from GFP-Plc1p in WT: $^{***}P$<0.001.]

Fluorescence images of logarithmic phase cultures (5 x 10^6 – 1 x 10^7 cells/ml) of BY4742 transformed with the indicated constructs. The left-hand columns show low light DIC images. The left-mid columns show the localisation of the indicated GFP constructs. The right-mid columns show the localisation of nuclei as obtained by transformation of cells with a NLS construct, and the merged images are shown on the right-hand columns. These images are representative of three replicate cultures. All strains were cultured in SC-Ura-Met-His+2% glu medium. The table shows ratio of fluorescence intensity in nucleus and cytosol. Each value represents the mean ± S.E.M. of ten determinations.

have been due to the restricted localization of Plc1p or to some a loss of catalytic activity. In particular, the mutations in Plc1p^{NES} map close to the PH domain of Plc1p, which is required for processive catalysis in animal cells (Cifuentes *et al*., 1993; Lomasney *et al*., 1996**)**. This must be addressed in some fashion via a control that puts back the Plc1p^{NES} mutant into the cytoplasm. If Plc1p^{NES} is normally catalytically active, then restoration of some cytoplasmic enzyme should also restore growth etc. If it does not, then the suspicion would be that the enzyme does not rescue growth, not because it is primarily nuclear, but because it is inactive.

I therefore additionally tagged Plc1p^{NES}, the mutant with a defective NES, with a CAAX prenylation signal to see whether the CAAX motif would prevent its accumulation in the nucleus. We had already observed the full growth of the Plc1p^{CAAX} mutant under stresses and CAAX is a strong signal that results in a protein become firmly attached to the plasma membrane. I reasoned that if Plc1p$^{NES/CAAX}$ possessed a localisation similar to Plc1p^{CAAX} and also appeared to be able to grow at 37ºC and in 0.7M NaCl, this would ensure us that the original mutations made in the Plc1p^{NES} didn't compromise its activity.

The construct including both the CAAX tag and the NES mutations was stable when expressed from pUG36 in yeast (APPX. Fig A). However, the CAAX tag did not localise Plc1p$^{NES/CAAX}$ mutant to the plasma membrane as we had hoped. Most of the GFP-Plc1p$^{NES/CAAX}$ was trapped in the nucleus, as confirmed by co-expression with the nuclear marker with some localized at the nuclear membrane (Fig 3.18).

Figure 3.18: Localization of GFP-Plc1p$^{NES/CAAX}$

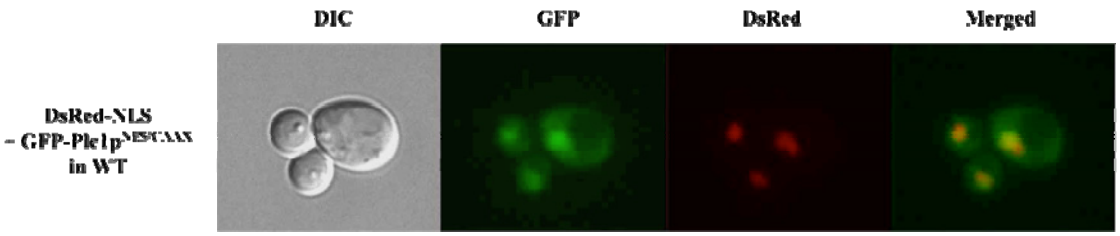

Genotype	Fluorescence Ratio (Nuclear/Cytosolic)
pUG36-*PLC1*$^{NES/CAAX}$ in WT	1.73 ± 0.10$^{***/+++}$
pUG36-*PLC1* in WT	1.71 ± 0.04
pUG36- *PLC1*^{NES} in WT	2.27 ± 0.05
pUG36-*PLC1*^{CAAX} in WT	1.14 ± 0.04

[Significantly different from GFP-Plc1p^{NES} in WT: $^{***}P<0.001$.]

[Significantly different from GFP-Plc1p^{CAAX} in WT: $^{+++}P<0.001$.]

Fluorescence image of logarithmic phase cultures (5 x 10^6 – 1 x 10^7 cells/ml) of BY4742 transformed with pUG36-*PLC1*$^{NES/CAAX}$. The left-hand columns show low light DIC images. The left-mid columns

show the localisation of the indicated GFP constructs. The right-mid columns show the localisation of nuclei as obtained by transformation of cells with a NLS construct, and the merged images are shown on the right-hand columns. These images are representative of three replicate cultures. All strains were cultured in SC-Ura-Met-His+2% glu medium. The table shows ratio of fluorescence intensity in nucleus and cytosol. Each value represents the mean ± S.E.M. of ten determinations.

I then created *PLC1* allele (Plc1p$^{NES/PKI}$) that included both the inactivated NES and two copies of the PKI NES at its N-terminus. The resulting Plc1p$^{NES/PKI}$ mutant was stable (APPX. Fig A). As shown in Fig 3.19, the PKI NESs doesn't direct all of the Plc1p$^{NES/PKI}$ out of the nucleus. Indeed, a nuclear marker of pUR34*NLS* co-localised with some GFP in the nucleus but nuclear localisation was no longer dominant -- cytoplasmic localisation is indeed restored in this mutant.

Figure 3.19: Localization of GFP-Plc1p$^{NES/PKI}$

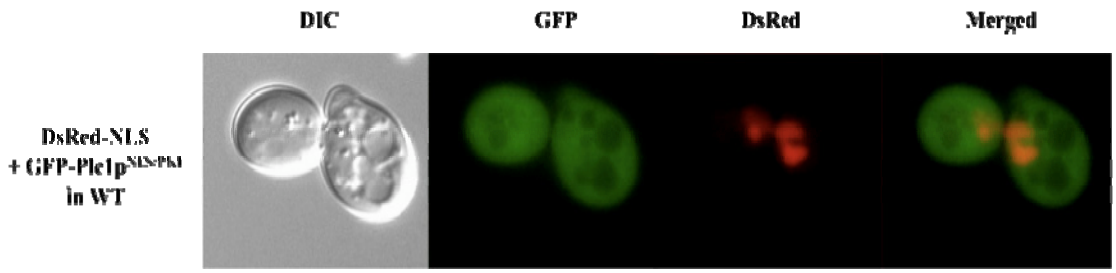

Genotype	Fluorescence Ratio (Nuclear/Cytosolic)
pUG36-*PLC1*$^{NES/PKI}$ in WT	0.81 ± 0.02$^{***/+++/###}$
pUG36-*PLC1* in WT	1.71 ± 0.04
pUG36-*PLC1*^{NES} in WT	2.27 ± 0.05
pUG36-*PLC1*^{PKI} in WT	0.71 ± 0.02

[Significantly different from GFP-Plc1p in WT: $^{***}P<0.001$.]

[Significantly different from GFP-Plc1p^{NES} in WT: $^{+++}P<0.001$.]

[Significantly different from GFP-Plc1p^{PKI} in WT: $^{###}P<0.001$.]

Fluorescence image of logarithmic phase cultures (5 x 10^6 – 1 x 10^7 cells/ml) of BY4742 transformed with the indicated constructs. The left-hand columns show low light DIC images. The left-mid columns show the localisation of the indicated GFP constructs. The right-mid columns show the localisation of nuclei as obtained by transformation of cells with a NLS construct, and the merged images are shown on the right-hand columns. These images are representative of three replicate cultures. All strains were cultured in SC-Ura-Met-His+2% glu medium. The table shows ratio of fluorescence intensity in nucleus and cytosol. Each value represents the mean ± S.E.M. of ten determinations.

So, if the nuclear localisation was the reason for the failure of the Plc1p^{NES} mutant to grow under stressful conditions, it was then hoped this double mutant, which now had most of the Plc1p translocated to the cytosol would show the same ability to grow at high temperature, and high salt as wild-type cells.

I first over-expressed the various compartment restricted GFP-tagged Plc1p mutants from a single copy of the gene with a powerful promoter in *plc1*Δ background to test their phenotypes. This leads to an approximately ten-fold increase in the steady-state level of Plc1p from pMET over that found from endogenous expression, which could be partly suppressed by methionine (0.2g/L) in all media used to grow the cells, but I did not quantify expression levels in the experiments described below after repression.

Wild-type GFP-Plc1p was functional, insofar as it corrected the slow growth of *plc1*Δ mutants at 23ºC (Fig 3.20). It also allowed these same mutant cells to grow at 37ºC and on media containing 0.7M NaCl, as expected (Fig 3.20). The plasma membrane mutant, Plc1p^{CAAX} appeared to be 'wild-type' in phenotype under either stress (Fig 3.20), possibly reflecting the fact that it is present in both nucleus and cytoplasm, at least when over-expressed. Both the over-expressed GFP-tagged Plc1p^{NES} and Plc1p^{PKI} mutants showed the same slow growth phenotype on salt media and the heat sensitivity as the *plc1*Δ strain (Fig 3.20), even when over-expressed. This might indicate that restricting Plc1p to either compartment is harmful to cells and that cells normally need Plc1p in both locales, or it could be that the mutations or insertions in some way inactivate the enzyme.

The Plc1p$^{NES/PKI}$ double mutant grew normally when stressed (Fig 3.20), maybe

Fig 3.20: Growth of various pUG36-PLC1 mutants under Stress

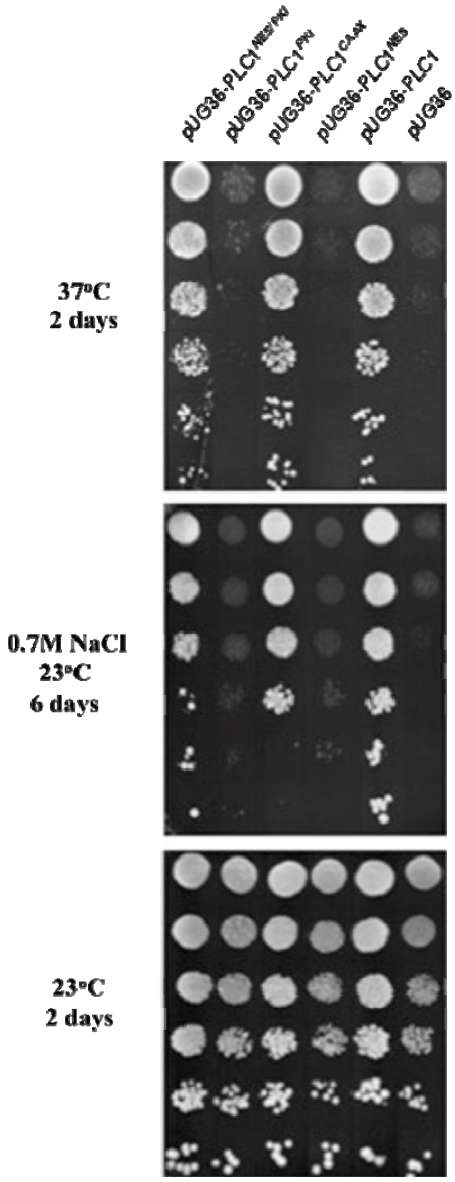

plc1Δ cells transformed with pUG36-*PLC1* constructs were grown to exponential phase (~1 X 10^7 cells/ml) in SC-Ura +2% glu media. Dilution assay was carried out as described in section 2.16. Cells were serially diluted five-fold then grown on an SC-Ura+Met (0.2g/L) +2% glu agar plate at 37 ^oC for 2 days (till wild-type colonies were fully grown) or on the same plates supplemented with 0.7M NaCl at 23 ^oC for 6 days (till wild type colonies were fully grown). The control plate was placed at 23 ^oC for 2 days. These data are representative of three independent experiments.

because it maintained pools of Plc1p in both compartments. This suggests that the mutations introduced into the natural NES of Plc1p did not impair catalytic function. Thus the different growth phenotypes of nuclear and cytoplasmic Plc1p mutants under stress seem to arise primarily from their distinct localisations.

3.7.2 Stress phenotypes of *PLC1* mutants expressed at endogenous levels

Earlier work showed that over-expression of *PLC1* can lead to growth defects and perturb cell function (York *et al*. 1999) and it can be lethal when greatly over-expressed from a powerful promoter (SK Dove and NM Perera 2002, pers. comm.). Expression of GFP-Plc1p from the pUG36 vector, under control of the MET promoter has been previously shown to restore hypo-osmotic stress mediated PtdIns(4,5)P_2 depletion and InsP_6 accumulation in *plc1*Δ cells but the basal level of InsP_6 is higher than wild-type (Perera 2002, p.114).

I therefore sought to insert the *PLC1* mutants as knock-ins. A construct was generated in which the *LEU2* gene was inserted just 3' of the *PLC1* terminator as a selectable marker. Then, mutant *PLC1* constructs were used to replace the coding region of the wild-type *PLC1* gene, so as to achieve wild-type expression of these constructs from the endogenous promoter.

Although I tried to make these knock-in mutants in several strain backgrounds, I could not isolate some of the attempted strains, for unknown reasons. The mutants in the BY4742 background are the ones I have successfully investigated so far. The effects of high temperature and high salt treatments on these knock-in constructs were examined (Fig 3.21).

The Plc1p^{WT} knock in construct appeared to grow faster than the "wild-type" (data not shown), probably as a result of acquisition of a functional *LEU2* gene. The Plc1p^{CAAX} grew normally, but the knock-in Plc1p^{NES} and Plc1p^{PKI} mutants displayed a much slower growth rate and were also much more stress sensitive (Fig 3.21).

Fig 3.21: Growth of various PLC1 mutants under Stress

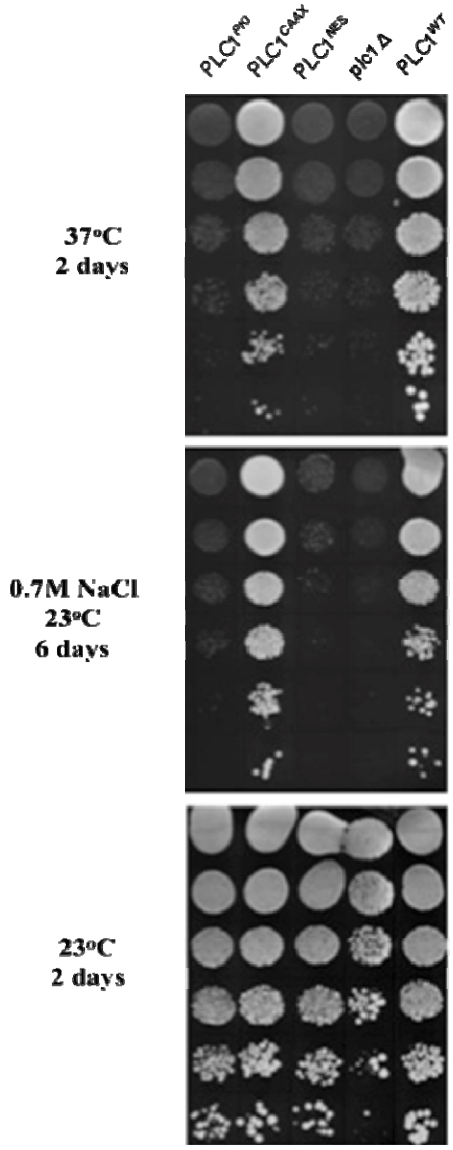

BY4742 cells with various *PLC1* wild type or mutant gene knock-ins were grown to exponential phase till ~1 x 10^7 cells/ml in YPD +2% glu media. A dilution assay was carried out as described in the methodology section. Cells were serially diluted five-fold then grown on YTD+2% glu agar plate at 37 ^oC (till wild type colonies were fully grown) for 2 days or on the same plates supplemented with 0.7M NaCl (till wild type colonies were fully grown) at 23 ^oC for 6 days. The control plate was placed at 23 ^oC for 2 days. Data represents three independent experiments.

Although such results suggest that restricting Plc1p to either the nucleus or cytoplasm during stress is deleterious to cell growth, the fact that Plc1p^{CAAX} behaved normally under stresses seems to indicate that the presence of Plc1p only on the plasma membrane can adequately sustain cells. It is not clear how this is achieved, though it

is likely that cells expressing this mutant maintain a nuclear pool of Plc1p.

These phenotypes have now been seen in more than five independent experiments, albeit with some variations. These data would seem to validate the hypothesis that is the cornerstone of this work: that Plc1p likely performs different roles in the nucleus and cytoplasm of cells.

3.7.3 Fragmented vacuoles in *plc1Δ* and *PLC1* mutants do not re-fuse

Plc1Δ cells are enlarged and become multi-budded after they are shifted to 37°C (Flick and Thorner, 1993). For unknown reasons, vacuoles purified from *plc1Δ* strains still retain PtdIns(4,5)P_2-directed PLC activity (Jun *et al*. 2004), but yeast cells lacking the *PLC1* gene have defects in protein trafficking to the vacuole and in the fusion of vacuole elements: this explains the fragmented vacuole phenotype of *plc1Δ* cells (Seeley *et al*. 2002). I used FM4-64 staining to examine this abnormal vacuole morphology in *plc1Δ* cells. FM4-64 is a lipophillic vacuolar dye and vital stain for studying vacuole morphology. It is taken in via endocytosis and then trafficked to the vacuole (Vida and Emr 1995). It is also a marker for endocytic intermediates, but I exposed the cells to FM4-64 and incubated in FM4-64-free medium for 60 min, under which condition FM4-64 is exclusively on the vacuole membrane (see section 2.17).

Wild-type cells normally have an average of 2-3 vacuole elements per cell, but *plc1Δ* cells have multiple and smaller highly fragmented vacuoles (Fig 3.22, untreated).

Wild-type yeast vacuoles undergo rapid fission and re-fusion upon hyper- and then

hypo-osmotic stress. This was observed by treating wild type BY4742 cells with medium supplemented with 0.6M NaCl and followed by ten-times dilution of the cells with medium lacking the extra NaCl. Their vacuoles quickly fragmented to many small vacuoles in the salt medium (Fig 3.22, 0.6M NaCl 10min), and more than half of these small vacuoles re-fused into one or two large vacuole elements after dilution back into the unsupplemented medium for 60 min (Fig 3.22, 0.06M NaCl 1h).

This re-fusion did not happen in *plc1Δ* cells: the vacuole fragmentation remained the same in the high salt medium (Fig 3.22, 0.6M NaCl 10min) but re-fusion to large vacuoles did not occur after dilution (Fig 3.22, 0.06M NaCl 60min). The abnormal vacuole morphology of *plc1Δ* cells is therefore a consequence of a failure of the re-fusion process.

The *PLC1* knock-in mutants were also examined for their vacuole morphology. Plc1p^{NES} and Plc1p^{PKI} cells both have highly fragmented vacuoles under normal conditions, with Plc1p^{NES} vacuoles appearing more severely fragmented than those in *plc1Δ* (Fig 3.22). The Plc1p^{NES} vacuoles did not re-fuse after hypo-osmotic treatment (Fig3.22), as in the *PLC1* knockout cells. In contrast, vacuoles in Plc1p^{CAAX} appear to be capable of undergoing the fission and re-fusion process, and they seem to undergo excessive fission and fusion in response to stress, when compared to wild-type (Fig3.22).

Here, I observed that vacuole-function in the *PLC1* mutants was in accord with their deficiencies noticed during stress responses. Hence, Plc1p activities seem essential to maintaining a functional vacuole even under normal non-stressed conditions. In

addition, I found both cytoplasmic and nuclear Plc1p are important to obtain normal vacuole morphology.

Figure 3.22: Vacuole morphology in wild-type and PLC1 mutant cells in response to salt stress

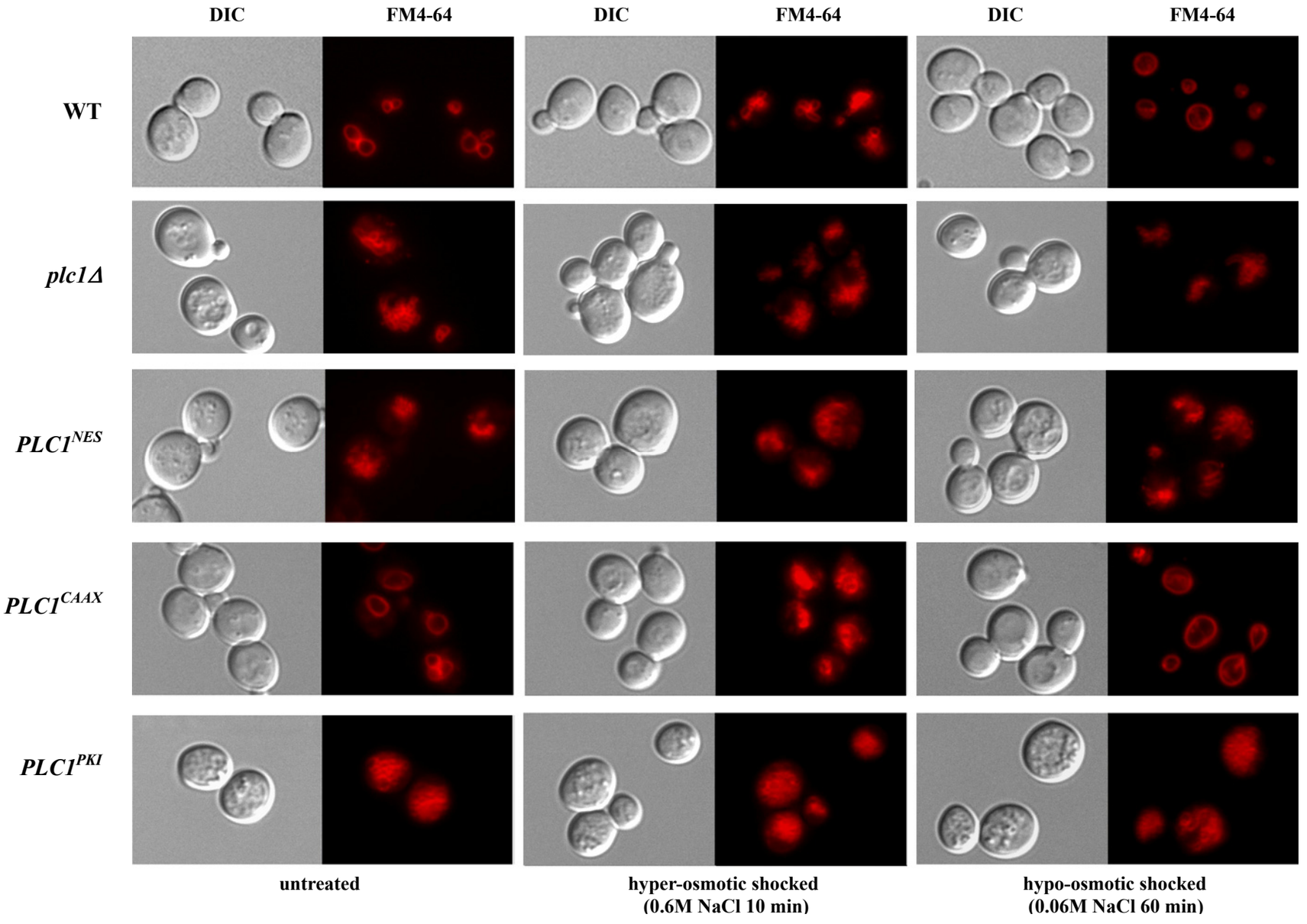

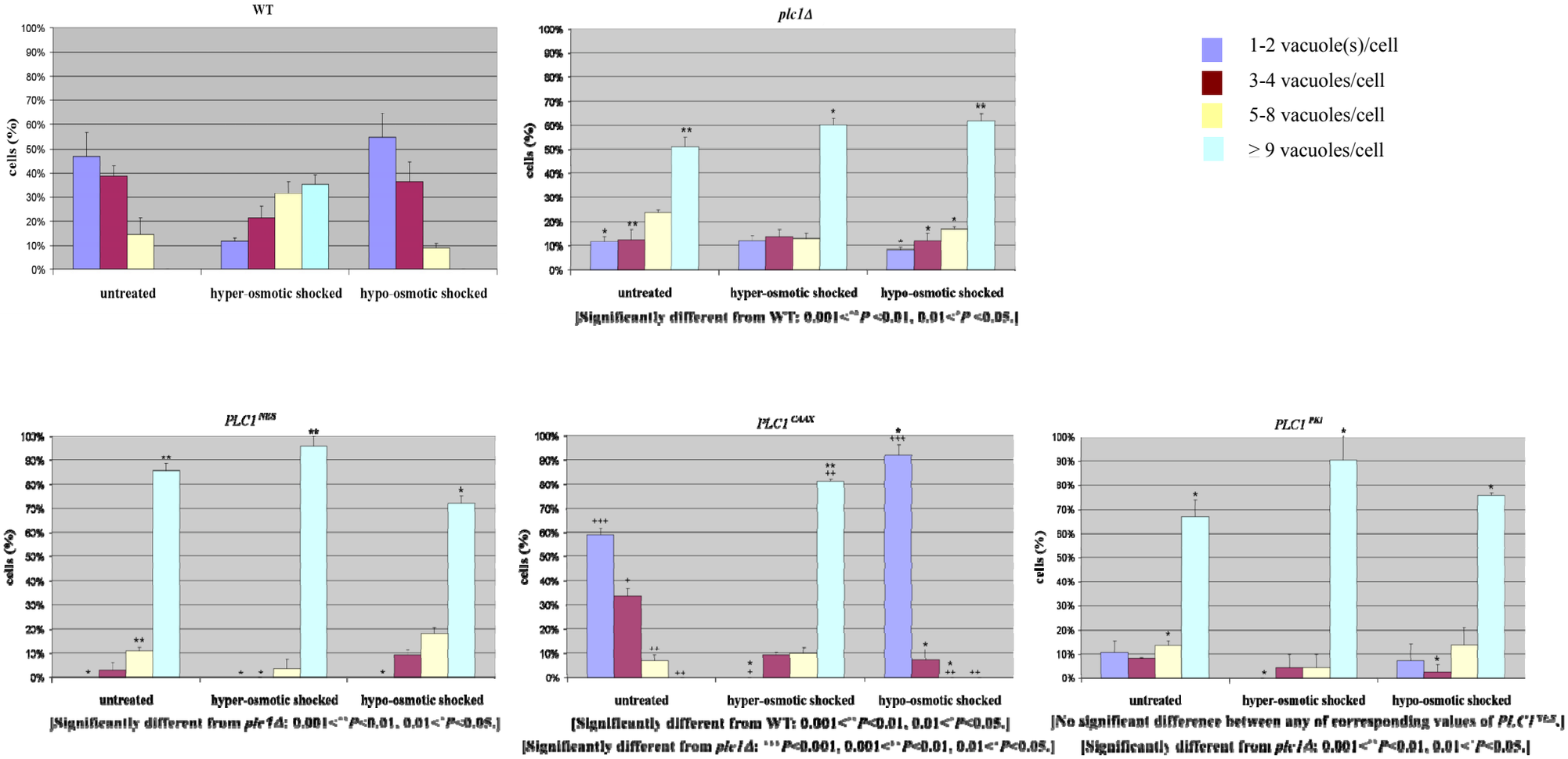

Low light DIC (left) and FM4-64 fluoresence images (right) of logarithmic phase cultures of wild-type and *PLC1* mutant cells grown to 5 x 10^6 – 1 x 10^7 cells/ml at 23°C. Vacuoles were labeled with the fluorescent probe FM4-64 as described in section 2.17. Fields of cells were then photographed before, 10 min after a hyper-osmotic stress and 60 min after a hypo-osmotic stress. The number of vacuoles in each cell was quantified at each stage. These images are representative of three replicate cultures. The graphs show the percentage of cells containing the indicated number of vacuoles after hyper- and hypo- osmotic stresses. Error bars indicate mean ± SEM. Three independent experiments were conducted for each condition.

3.8 Discussion

3.8.1 Is the localisation of Plc1p critical to its functions?

The "bedrock" hypothesis that I wanted to explore in this chapter of work, was whether Plc1p, and possibly PLC-δs in general, might generate compartment-specific signals that help cells adapt to external conditions. Some of these signals could be the inositol phosphates, but other "signals" could include protein-protein interactions.

This hypothesis arises from the observation that Plc1p seems to be distributed between the nucleus and cytoplasm of normally dividing yeast cells. Tagging Plc1p with N-terminal GFP and expressing the GFP-Plc1p construct under a powerful *MET25* promoter enhances Plc1p expression to about ten times the level found in wild type cells: others have shown that native expression of *PLC1* is surprisingly low (Flick and Thorner, 1993; Fratti *et al*. 2004). It has proved difficult to detect Plc1p activity in cell lysates from *S. cerevisiae*, even though similar experiments with animal tissues yield a robust hydrolysis of PtdIns(4,5)P_2 (SK Dove 2003, pers. Comm. and Fratti *et al*. 2004). GFP-Plc1p should be valuable for visualizing such endogenously low levels of expressed protein, provided that the localisation I observe with this construct faithfully reproduce the behaviour of the endogenous Plc1p. The early signs were favourable. The full length GFP-Plc1p construct is stable (APPX. Fig A). Our GFP-Plc1p expression system proved to not alter the cell phenotypically, nor did it result in aberrant inositol phosphate production in an earlier study, although there was some evidence that the basal pathway was more active (NM Perera and SK Dove 2002, per. comm.). I also saw localisation shifts with various Plc1p mutants, and these gave rise to mutant phenotypes even when there was a functional, native Plc1p in the cell. That I was able to observe this even despite the over-expression

suggests our system is in no-way 'saturated' with Plc1p and therefore is capable of reporting where this protein truly resides.

My data suggest that wild-type GFP-Plc1p is distributed in a manner whereby its fluorescence in the nucleus exceeds that in the cytoplasm (Fig 3.2) by at least a factor of 1.6-1.7. However, they are not confocal microscope images. I was rather recording a 'thin' slice of whole-cell image. Therefore, the 'nuclear' fluorescence will be a sum of the nuclear fluorescence and some of the underlying and overlying fluorescence from the cytoplasm.

This distribution is consistent with the proposed nucleo-cytoplasmic shuttling of Plc1p (York, 2006), with the nuclear Plc1p concentration maybe 3 times to the cytoplasmic concentration. Movement of Plc1p into and out of the nucleus must be a regulated event since the mass of GFP-Plc1p is ~130 kD and the molecular weight cutoff of the nuclear pore complex is only 30 kD. Our experiment using an *xpo1-1* mutant in which GFP-Plc1p became substantially more nuclear at restrictive temperature lends weight to the idea of regulated nuclear export of Plc1p (Fig 3.5), and that it uses this exportin to leave the nucleus. The relatively modest increase in nuclear GFP-Plc1p in this experiment may indicate that this enzyme can utilize other exportin pathways to leave the nucleus. In addition, I did not use heated microscope stage, so it is possible that Xpo1p activity might partially returned while I was recording images.

If the steady-state localisation of Plc1p is compared to mammalian PLC-δ_1 or PLC-δ_4

then some differences are immediately apparent. For most of the time, PLC-δ_1 is localized to the plasma membrane in animal cells during growth (Yagisawa *et al*., 2002). In contrast, PLC-δ_4 is present only in the nucleus of animal cells (D'Santos *et al*., 1998; Divecha *et al*., 1997; Liu *et al*., 1996; Martelli *et al*., 1992). The localization of Plc1p is intermediate between these localisation patterns.

3.8.2 Plc1p localisation at different stages of the cell cycle and in response to stress

Having a tool for tracking Plc1p made me want to determine if Plc1p might undergo the same regulated localisation changes that are observed for mammalian PLCs. Such shifts in location can provide clues to the regulation of a protein, though they alone are not a very reliable indicator.

Cell cycle progression can alter the equilibrium between NES and NLS signals and cause the intracellular shuttling of PLC isoforms in animal cells. For example, the 'plasma membrane' enzyme, PLC-δ_1, can enter the nucleus at some stages of the cell cycle in mammalian cells (Yagisawa *et al*., 2002). The fact that PLC-β_1 and PLC-γ_1 are associated with the nuclear matrix while PLC-δ_1 binds to chromatin implies that PLCs might be associated with specific functions during the cell cycle (Crljen *et al.*, 2004). Genetic studies have revealed a link between Plc1p, the C-type cyclin Ume3p (Cooper *et al*. 1999) and the cyclin-dependent protein kinase complex Pho80p/Pho85p (Flick and Thorner 1998), so we were eager to determine if we could see any associated changes in Plc1p localisation. Plc1p has previously been found associated with chromosomes at the division site (DeLillo *et al*., 2003; Lin *et al*., 2000). Although this suggested there might be a cell cycle-regulated change of Plc1p

localisation within the nucleus. However, our attempt to observe this in cells treated with cell cycle modifying drugs was unsuccessful, I did see an efflux of Plc1p from the nucleus during S phase (Fig 3.7). This is when bud emergence occurs and when the cell prepares for mitosis and carries out DNA synthesis. Whether this event is specifically related to Plc1p or just reflects a general shift in nucleo-cytoplasmic shuttling at this time, remains to be determined.

Strains lacking *PLC1* grow slowly at raised temperatures (Flick and Thorner 1998). Synthesis of InsP_6 downstream of Plc1p-catalysed InsP_3 release is stimulated in yeast incubated at 37ºC and in mammalian cells subjected to heat stress (Calderwood and Stevenson 1993; Perera 2002, p.188). The presence of a heat shock binding consensus motif in the *PLC1* promoter suggests that yeasts may require elevated levels of Plc1p to survive at higher temperatures, so I determined if heat stress would induce changes in Plc1p localization. To our surprise, the distribution of GFP-Plc1p remained largely unchanged after 2 hours at 37°C.

There was, though, an obvious translocation of Plc1p after cells were exposed to osmotic challenge, with some GFP-Plc1p leaving the nucleus within 2 minutes, followed by a gradual restoration of its normal nuclear/cytoplasmic distribution (Fig 3.10). An earlier study in our lab showed that InsP_6 derived from Plc1p activity rapidly accumulates after hypo-osmotic shock, peaking at 2 minutes, and that much of the PtdIns(4,5)P_2 hydrolysed by Plc1p was located at the plasma membrane (Perera *et al*., 2004).

Why should the vacuole fusion that occurs after hypo-osmotic shock be inhibited in a

plc1 mutant? Recent data suggest a role for Plc1p in regulating Apl5p, a subunit of the AP-3 complex that is required for vacuolar trafficking (Saiardi *et al*., 2004), and Vps41p, a subunit of HOPS that mediates vacuole-vacuole fusion (K Dong and SK Dove 2009, pers. Comm.).

Hyper-osmotic stress also seems to cause a translocation of Plc1p. Cells deleted for *PLC1* are unable to grow in hyper-osmotic media, possibly because Plc1p functions in parallel to Hog1p in upregulation of glycerol synthesis. The two signaling pathways converge at Sgd1p, which resides in the nucleus and is a suppressor of the osmo-sensitive phenotypes of both *plc1* and *hog1* deletions. It interacts with Plc1p physically, and this may be the mode of regulation instead of involving inositol phosphates, though this is unlikely to be the whole story since *arg82* and *kcs1* mutants also display a profound salt-sensitive phenotype (Dubois *et al*., 2002; El Alami *et al*., 2003; and see Fig 4.31 in this work).

One intriguing question arising from the above observations is to ask how both hyper and hypo osmotic stress can trigger the activation of Plc1p? Or heat stress for that matter? Previous studies suggest that Plc1p might be regulated in response to membrane stretching (Cooper *et al*., 1999). Since heat, hyper and hypo osmotic stress all produce an increase in plasma membrane flexing and bending, that might produce the signal that activates Plc1p.

Another important question is why should all of these disparate stresses cause an activation of Plc1p, or in to ask this another way, what is Plc1p activation supposed to achieve? Since Plc1p has been shown to regulate expression of a number of the so-

called general stress response genes, whose levels are up or down regulated in response to stresses, it might be anticipated that this is the major function of Plc1p during hypo, hyper and heat stress (Ansari *et al*., 1999; Cooper *et al*., 1999; Demczuk *et al*., 2008; Rebecchi and Pentyala, 2000; York, 2006).

3.8.3 Nuclear localisation and export

Having observed a potential nucleo-cytoplasmic shuttling of Plc1p during the cell cycle and under some stimulated conditions, the next question was to examine how Plc1p was entering and leaving the nucleus. As discussed in the Introduction, nucleo-cytoplasmic shuttling usually relies upon signal sequences, known as nuclear localization and export sequences (NLS and NES) within the protein.

The NES of Plc1p was easily found and is located in the PH domain of this protein close to the EF hand. It conforms to a canonical consensus sequence (Kunzler *et al*., 2000), and its mutation led to an almost complete redistribution of Plc1p into the nucleus (Fig 3.11). A consequence of this relocation was that cells expressing the $Plc1p^{NES}$ mutant as their only Plc1p activity did not grow normally and behaved like cells lacking *PLC1* (Fig 3.20 and Fig 3.21). That this was a consequence of the mis-localisation of Plc1p was demonstrated when it was observed that adding an exogenous NES sequence from the protein PKI to $Plc1p^{NES}$ restored both its cytoplasmic localisation and all normal growth phenotypes (Fig 3.20 and Fig 3.21). This strongly suggests that the NES I have identified is the sole NES in Plc1p, and that either that too much nuclear Plc1p is deleterious to cells or Plc1p is required in both compartments to fulfil.

Finding the NLS proved more challenging. Our first attempt focussed on the X-Y inter-domain linker since many mammalian PLCs have an NLS in this region, and Plc1p does have a highly basic cluster located there. However, the X-Y basic patch had no effect on nuclear localisation (data not shown). I therefore turned to a truncation strategy and discovered that a construct encoding only the first one-third of Plc1p displayed the same localisation as the full-length protein, suggesting that NLS and NES activities both reside in the N-terminal one third of Plc1p (Fig 3.12). The N-terminus also seems important for nuclear export as the Plc1p$^{110\text{-end}}$ mutant displayed an increased ratio of nuclear/cytoplasmic fluorescence (Fig 3.14). The very nuclear mutant Plc1p$^{220\text{-end}}$ further indicates that an NLS exists in between amino-acids 220–333 (Fig 3.14). However, my data suggest that there could be more than one sequence mediating nuclear localization, as two further non-overlapping truncation mutants showed nuclear localization: Plc1p$^{1\text{-}220}$ and Plc1p$^{220\text{-}333}$ (Fig 3.13) although both were partially unstable (APPX. Fig A). However, despite creating two stable mutants, Plc1p^{4R} and Plc1p^{KRLR}, that have a number of potential basic sequences in this region of Plc1p mutated, neither of them abolished the nuclear localization of Plc1p completely (Fig 3.15). So I was unable to definitively identify these NLS motifs.

3.8.4 Both nuclear and cytoplasmic pools of Plc1p are required for normal Plc1p function

Having identified the NES sequence my attention turned to examining mutant forms of Plc1p that were tagged to the plasma-membrane (Plc1p^{CAAX}), cytoplasm (Plc1p^{PKI}) or nucleus (Plc1p^{NES}), I investigated the consequences of restricting Plc1p to different

compartments. This was to determine if there are the compartment specific functions of Plc1p either because of the signaling cascade it controls or because of protein-protein interactions.

Plc1p^{CAAX} is concentrated on the plasma membrane but also has a detectable nuclear pool (Fig 3.16). The Plc1p^{PKI} mutant however, is almost completely cytoplasmic: it appeared that the two virally derived NES sequences that were inserted into the N-terminus were so effective that the nuclei of cells expressing this construct were almost devoid of fluorescence (Fig 3.17). The reverse is true of the Plc1p^{NES}–expressing cells, in which cytoplasmic fluorescence was very low. These constructs were stable (APPX. Fig A) and were suitable reagents to test the functions of the separate pools of Plc1p.

Many of the known functions of Plc1p and inositol phosphates are nuclear functions (Irvine, 2003). However, my data make it clear that a functional, nucleus-restricted Plc1p^{NES} is not sufficient to rescue the slow growth of salt- or heat-sensitive phenotypes of a *plc1*Δ cell even when over-expressed (Fig 3.20 and Fig 3.21). This is not a consequence of the GFP tag or of a loss of activity of this mutant because restoring Plc1p^{NES} to the cytoplasm by adding extra NESs rescued the stress phenotypes in these cells (Fig 3.20).

Two possible explanations are that Plc1p-derived inositol phosphates have to be locally generated in each compartment in order for cells to function normally, or that Plc1p protein is required in both compartments for some other reason. A catalytically dead Plc1p that combines either the PKI tag or the NES mutations would be useful to

distinguish between these two possibilities, such as Plc1p$^{PKI/E425G}$ and Plc1p$^{NES/E425G}$ (regarding Plc1p^{E425G} mutant, see section 4.7) Cells expressing pairs of Plc1p mutants, one catalytically dead and one active i.e. *plc1*Δ cells expressing Plc1p^{NES} and Plc1p$^{PKI/E425G}$ and a separate set expressing Plc1p^{PKI} and Plc1p$^{NES/E425G}$. This would then allow us to tell where inositol phosphates are needed and where it is protein-protein interactions only that are required for a normal phenotype.

The phenotypes of the cytosol restricted Plc1p^{PKI} mutant which does not rescue any of the stress phenotypes, reinforces the view that Plc1p is required in both compartments. It was unexpected to find that vacuoles from this mutant, like those of *plc1*Δ cells are abnormally fragmented (Fig 3.22), and thus that nuclear and cytoplasmic pools of Plc1p are both required for normal vacuolar homeostasis. As vacuole morphology is regulated by both Pho85p controlled gene expression and by the cell cycle, it is possible that these phenomena are indirect effects on the vacuole that arise that from primary defects in these two processes. However, there must also be a cytoplasmic component to Plc1p mediated control of vacuole morphology, or else the Plc1p^{NES} mutant would have displayed normal vacuoles.

Why should all these phenotypes require both nuclear and cytoplasmic Plc1p? This could reflect that fact that all of my assays are growth based and so are actually requiring the mutant cells to carry-out the complete life-cycle of *S. cerevisiae* in order to report the phenotype. Better assays would be those focused at the molecular level that would test for events happening over a shorter timescale, and so are more likely to show some discrimination between the two localisation restricted mutants. Alternatively, it could be that many of the phenotypes I have examined are actually

indirect consequences of the failure to export mRNA properly in *plc1*Δ mutants. If this is the case then it is possible that, as part of mRNA export, Plc1p itself must associate normally with the nuclear import and export machinery and my mutants prevent this from happening and so appear defective.

Chapter 4 Regulation of the plasma membrane association of Plc1p

4.1 The intracellular distribution of the Ins(1,4,5)P_3 kinase Arg82p is similar to that of Plc1p

One hypothesis I examined in our attempts to determine why the NLS of Plc1p was so difficult to define was the idea that another protein might be taking Plc1p to the nucleus. Earlier work in our lab showed that when Plc1p was activated, InsP_3 (InsP_3) never accumulated to detectable levels: the 'higher' inositol phosphates appeared straightaway (Perera *et al*., 2004). This made us wonder whether Plc1p might be physically associated with one or more of the inositol phosphate kinases, facilitating the rapid synthesis of higher inositol phosphates. The first candidate I tested was the inositol phosphate kinase Arg82p.

Arg82p is a dual function protein. It is the first kinase in the pathway of phosphorylation of InsP_3, via inositol (1,4,5,6) tetrakisphosphate (InsP_4) and inositol (1,3,4,5,6) pentakisphosphate (InsP_5) to InsP_6, InsP_7 and InsP_8, but it was discovered earlier as a regulator of arginine metabolism in yeast that stabilizes the Arg80-Arg81-Mcm1 transcriptional complex (Bechet *et al*., 1970).

To examine the localization of Arg82p, GFP-tagged Arg82p was expressed in wild-type and *arg82Δ* cells, and its distribution compared with that of the nuclear marker pUR34*NLS* by fluorescence microscopy. GFP-Arg82p was distributed in a similar fashion to Plc1p under normal conditions: it was more concentrated in the nucleus than the cytoplasm (Fig 4.1). Indeed the ratio of nuclear to cytoplasmic GFP-Arg82p

Figure 4.1: Localisation of GFP-Arg82p in wild type and arg82Δ cells

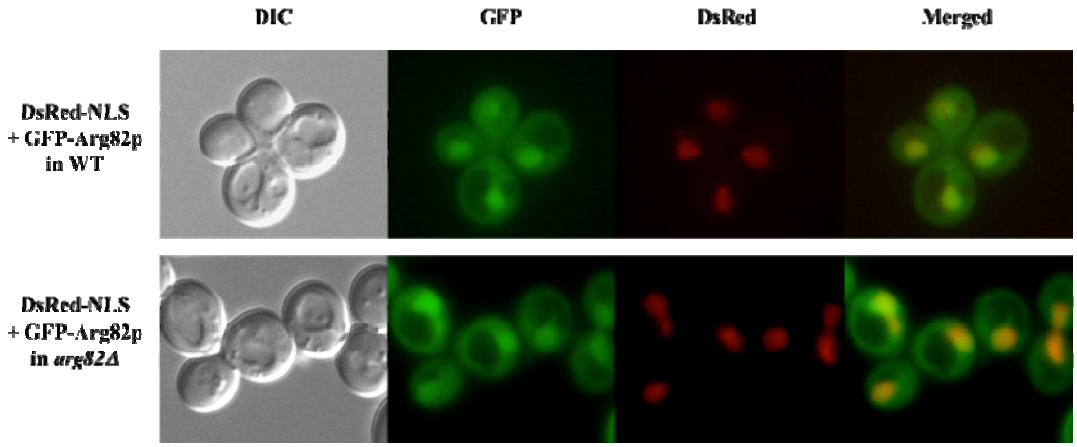

Genotype	Fluorescence Ratio (Nuclear/Cytosolic)
pUG36-*ARG82* in WT	1.64±0.04
pUG36-*ARG82* in *arg82Δ*	1.62±0.03
pUG36-*PLC1* in WT	1.70±0.08

[There was no significantly difference between the corresponding values of GFP-Arg82p in WT and GFP-Arg82p in *arg82Δ* cells and no significantly difference between the corresponding values of GFP-Arg82p and GFP-Plc1p in WT cells.]

Fluorescence images of logarithmic phase cultures (5 x 10^6 – 1 x 10^7 cells/ml) of wild type BY4742 (top) and *arg82Δ* (bottom) transformed with pUG36–*ARG82* and pUR34*NLS*, respectively. The left-hand columns show low light DIC images. The left-mid columns show the localisation of the indicated GFP constructs. The right-mid columns show the localisation of nuclei, as reported by the DsRed-tagged NLS construct, and the merged images are shown on the right-hand columns. These images are representative of three replicate cultures. All strains were cultured in SC-Ura-Met-His+2% glu medium. The table shows ratio of fluorescence intensity of plasma membrane (PM), nucleus and cytosol. Each value represents the mean ± S.E.M. of ten determinations.

fluorescence was similar to the equivalent ratio for Plc1p (~1.6-1.7).

4.2 GFP-Plc1p associates with plasma membrane in *arg82Δ* cells

Accordingly I then tested whether Arg82p participated in the regulation of Plc1p localization. First, I examined the localization of Plc1p in cells depleted of Arg82p to see whether there would be ablation or the reduction of the nuclear localization of Plc1p. Unexpectedly, some GFP-Plc1p was now associated with cell periphery. It seems that the *arg82Δ* cells had a normal ratio of nuclear to cytosolic Plc1p, but some of the Plc1p was now concentrated on the plasma membrane (Fig 4.2).

This localisation has never before been observed in wild-type cells (Fig 4.2) which suggested that normally Arg82p somehow negatively regulates the association of Plc1p with the plasma membrane. Where I re-introduced wild-type Arg82p (pYCplac111-*ARG82*) into *arg82Δ* cells, Plc1p reverted to its normal nuclear/cytoplasmic distribution (Fig 4.2). Empty pYCplac111 vector had no effect on the localisation of Plc1p in *arg82Δ* cells (Fig 4.2).

It is worth noting that the Arg82p constructs were transformed into both *arg82Δ* and *arg82Δ plc1*Δ cells, in case there was some interaction between our GFP tagged constructs and wild-type Plc1p. The same results were obtained in both cases, and only pictures of the *arg82Δ* cells are shown because expression of the constructs was always better in this strain.

4.3 Plc1p is unlikely to form a complex with Arg82p

I also examined the localisation of GFP-Arg82p in *plc1Δ* cells. Its distribution was the same as in wild-type cells (Fig 4.3), indicating that the absence of Plc1p did not change the localization of Arg82p.

I then carried out a co-immunoprecipitation assay to detect if Plc1p and Arg82p were part of a common protein complex. Plc1p was tagged with three tandem copies of the HA epitope and Arg82p was tagged with nine copies of the Myc epitope. These constructs were expressed at wild-type levels in yeast cells as knock-ins at the normal chromosome locus (see section 2.15). A total protein lysate from cells expressing both tagged proteins was incubated with anti-Myc antibodies and Protein G sepharose, followed by incubation with anti-HA and anti-Myc antibodies, respectively (see

Fig 4.2: Localization of GFP-Plc1p in the absence or presence of Arg82p

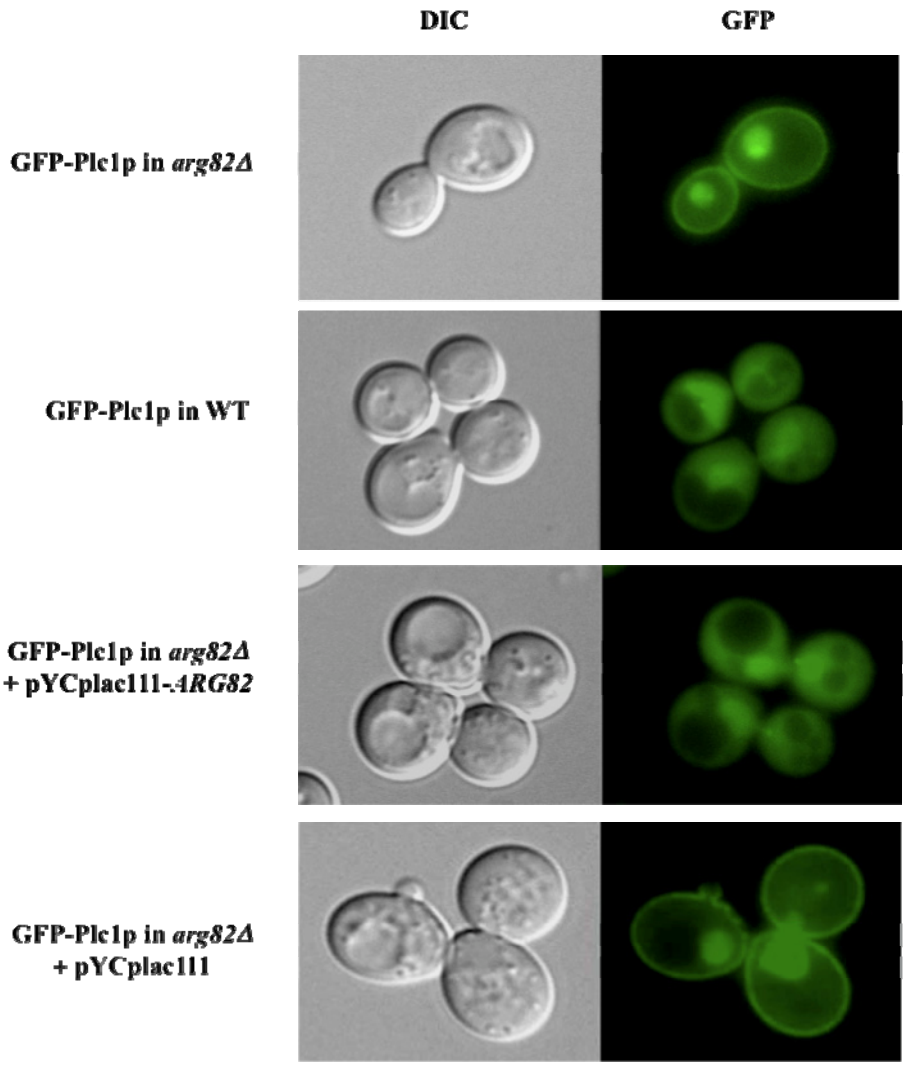

Genotype	Fluorescence Ratio		
	PM/Cytosolic	Nuclear/Cytosolic	PM/Nuclear
pUG36-*PLC1* in *arg82Δ*	1.13± 0.02***	1.74± 0.08	0.66±0.03***
pUG36-*PLC1* in WT	0.74±0.01	1.70±0.08	0.44±0.02
pUG36-*PLC1* in *arg82Δ* + pYCplac111-*ARG82*	0.76± 0.04	1.56± 0.04	0.49±0.03
pUG36-*PLC1* in *arg82Δ* + pYCplac111	1.15± 0.01	1.67 ±0.06	0.70±0.03

[Significantly different from GFP-Plc1p in WT and *arg82Δ*+p*ARG82* cells: ***P<0.001; There was no significant difference from *arg82Δ* with empty vector.]

Logarithmic phase cultures (5 x 10^6 – 1 x 10^7 cells/ml) of *arg82Δ*+pUG36–*PLC1* and BY4742 + pUG36–*PLC1* in SC-Ura-Met+2%glu or *arg82Δ* + pUG36–*PLC1* + pYCplac111-*ARG82* and *arg82Δ* + pUG36–*PLC1* + pYCplac111-*ARG82* in SC-Ura-Met-Leu+2%glu, at 25°C. These images are representative of three replicate cultures. The table shows ratio of fluorescence intensity of plasma membrane (PM), nucleus and cytosol. Each value represents the mean ± S.E.M. of ten determinations.

Fig 4.3: Localization of GFP-Arg82p in plc1Δ cells

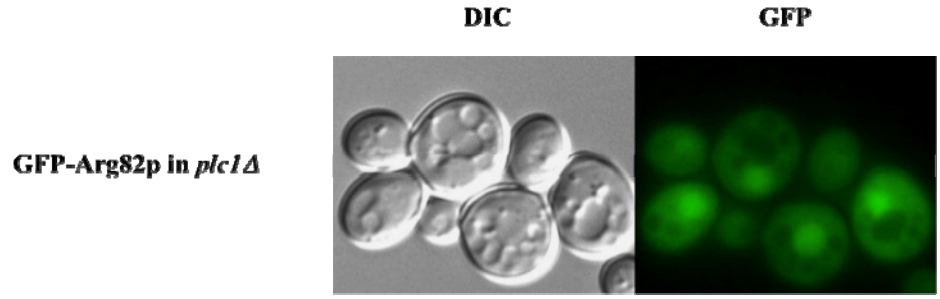

Genotype	Fluorescence Ratio		
	PM/Cytosolic	Nuclear/Cytosolic	PM/Nuclear
pUG36-*ARG82* in *plc1Δ*	0.77±0.03	1.64±0.03	0.47±0.02
pUG36-*ARG82* in WT	0.73±0.02	1.64±0.04	0.45±0.02

[There were no significant differences between the corresponding values of the two cell types.]

Low light DIC (left columns) and Fluorescence images (right columns) of logarithmic phase cultures (5 x 10^6 – 1 x 10^7 cells/ml) of *plc1Δ* + pUG36-*ARG82* at 25°C in SC-Ura-Met+2% glu. These images are representative of three replicate cultures. The table shows the ratio of fluorescence intensity of plasma membrane (PM), nucleus and cytosol. Each value represents the mean ± S.E.M. of ten determinations.

section 2.15). In the anti-Myc pull-down, Arg82p was visualized by anti-Myc, but no Plc1p-3HA was detected by anti-HA (Fig 4.4). The same negative result was obtained even after including the crosslinker such as DSP (Dithiobis (succinimidyl propionate), Pierce).

Plc1p is present at very low levels (section 3.2), so it was possible that a small amount of Plc1p bound to Arg82p was not detected. I therefore used lysates from cells over-expressing GFP-Plc1p from pUG36 in a similar experiment, probing the blots with anti-GFP. Again, no Plc1p was co-immunoprecipitated with Arg82p (Fig 4.5).

These data suggest that Plc1p and Arg82p do not form a complex, though they do not eliminate the possibility of weak and/or transient association between the two proteins.

Fig 4.4: anti-Myc pull-down blot for detecting the putative binding of Plc1p and Arg82p anaylsed by Co-immunoprecipitation

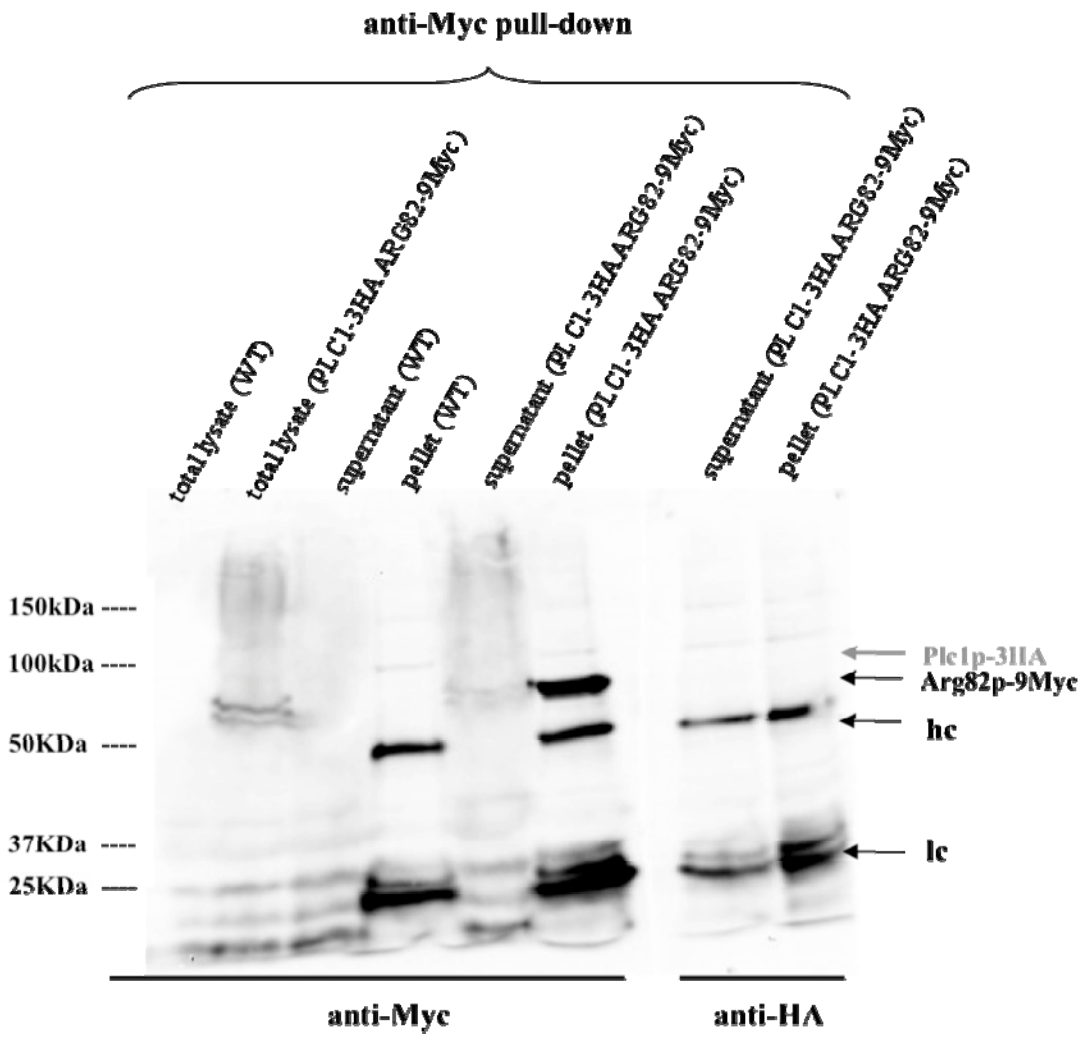

FY833 (PLC1::PLC1-3HA ARG82::ARG82-9Myc) and FY833(WT) culture (control)100ml each, were grown to OD_{600} ~0.7 (1x 10^7 /ml) in YEPD+2% glu media and lysates prepared (section 2.15). 5µl of anti-Myc and 100µl Protein G sepharose were together added to 500µl of total lysate, incubated for 2 hours, and then supernatant and pellet were collected by centrifugation at 500g. The anti-Myc pull-downs were then analyzed by SDS-PAGE gel followed by Western-blotting for immunological analysis. Samples were electrophoretically transferred to a nitrocellulose filter followed by incubation with anti-Myc or anti-HA(1:2000), respectively.

4.4 The kinase activity of Arg82p is required for negative regulation of the interaction of Plc1p with the plasma membrane

The results above make it likely that one or more of the products of Arg82p may regulate Plc1p's association with plasma membrane.

Fig 4.5: anti-Myc pull-down blot for detecting the putative binding of Plc1p and Arg82p analysed by Co-immunoprecipitation

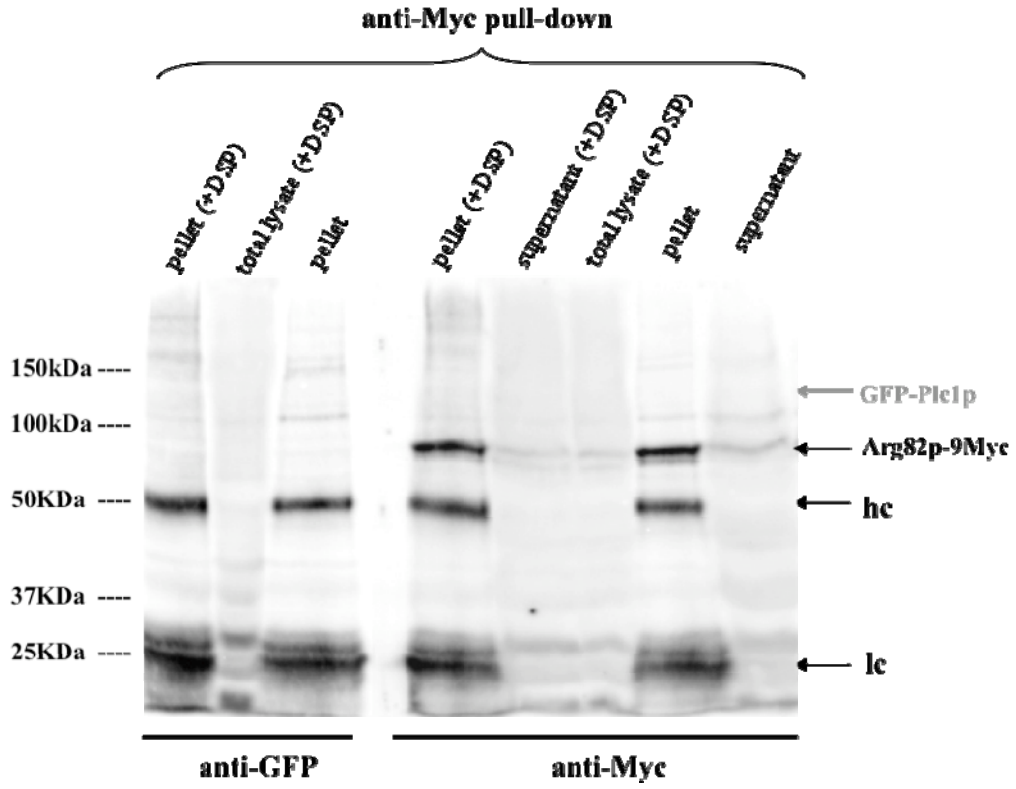

A 100ml culture of FY833 (ARG82::ARG82-9Myc, pUG36-*PLC1*) in SC-Ura-Met+2%glu was grown to OD_{600} ~0.7 (1x 10^7 /ml), with or without 5mM DSP added to each cell culture in 500µl of lysis buffer before cell breakage (section 2.15). 5µl of anti-Myc and 100µl Protein G sepharose were together added to 500µl total lysate, incubated for 2 hours, and then supernatant and pellet collected by centrifugation at 500g. The anti-Myc pull-downs were then analyzed by SDS-PAGE gel followed by Western-blotting for immunological analysis. Samples were electrophoretically transferred to a nitrocellulose filter followed by incubation with anti-Myc (1:2000), or anti-GFP (1:1000), respectively.

The inositol phosphate binding domain of Arg82p (residues 127 to 135), one of several well-conserved motifs found in Ins*P* kinases, is required for its inositol kinase activity (Fig 4.6A). Mutations in such domains disrupt kinase activity but do not affect protein stability (Dubois *et al*., 2002). An aspartic acid to alanine amino-acid mutation at 131 ($ARG82^{D131A}$) in the Ins*P* binding domain eliminates kinase activity (Fig 4.6B). In contrast, the polyaspartate stretch close to the C-terminus (residues 282-303) of Arg82p is involved in the regulation of arginine metabolism (Fig 4.6A), but not in kinase activity (Dubois *et al*., 2000). Removing the polyaspartate stretch

Fig 4.6:

A. Schematic representation of Arg82p

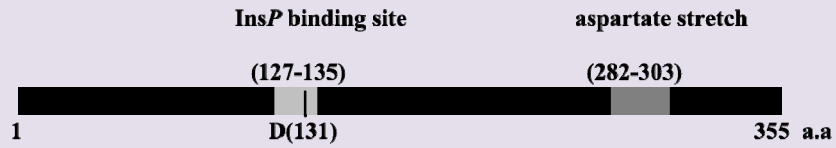

B. Effect of mutations in GST–Arg82p on Arg82p activity (Dubois et al. 2000)

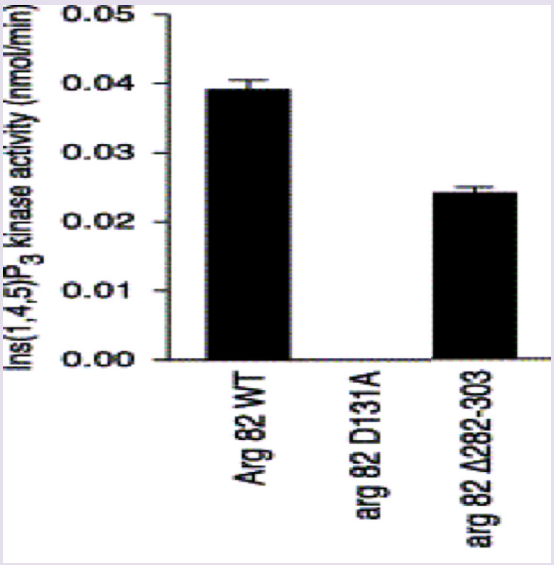

results in a mutant that does not regulate arginine metabolism but retains InsP_3 kinase activity (Dubois *et al*., 2000) (Fig 4.6B).

I obtained these two *arg82* mutants, *ARG82*^{D131A} and *ARG82*$^{\Delta asp}$ (*ARG82*$^{\Delta(282\text{-}303)}$), from Dr Evelyne Dubois (Brussels, Belgium) and cloned them into the pYCplac111 vector. When I put the kinase-dead mutant, p*ARG82*^{D131A}, into cells lacking *ARG82*, Plc1p remained associated with the plasma membrane (Fig 4.7), but when I put the aspartate mutant p*ARG82*$^{\Delta asp}$ into cells, they regained the Plc1p distribution characteristic of wild-type cells (Fig 4.7).

Fig 4.7: Localization of GFP-Plc1p in ARG82 mutants

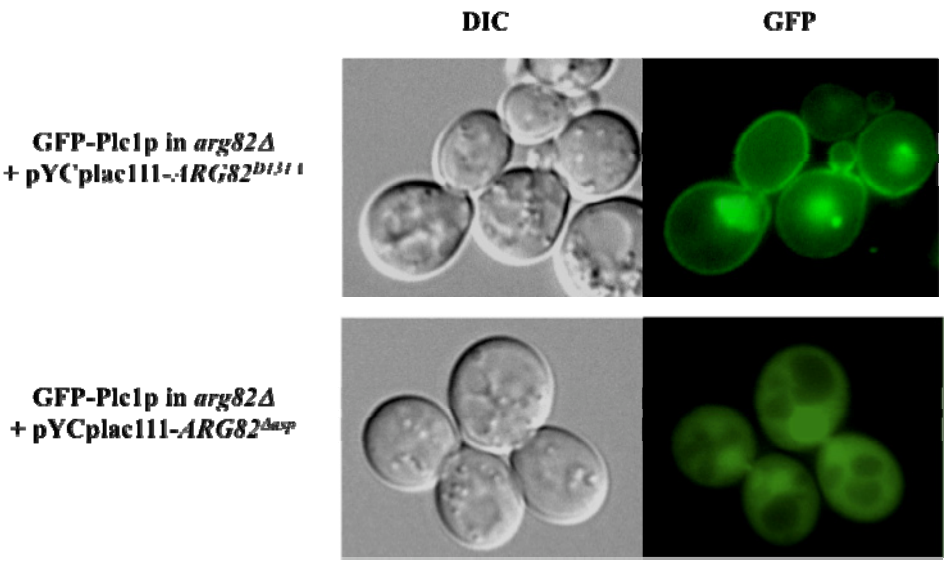

Genotype	Fluorescence Ratio		
	PM/Cytosolic	Nuclear/Cytosolic	PM/Nuclear
pUG36-*PLC1* in *arg82Δ* + pYCplac111-*ARG82*^{D131A}	1.16±0.04***	1.86±0.09*	0.63±0.03**
pUG36-*PLC1* in *arg82Δ* + pYCplac111-*ARG82*^{Δasp}	0.72±0.02^{+++}	1.61±0.03	0.45±0.02^{+++}
pUG36-*PLC1* in *arg82Δ*	1.13±0.02	1.74±0.08	0.66±0.03
pUG36-*PLC1* in *arg82Δ* + pYCplac111-*ARG82*	0.76±0.04	1.56±0.04	0.49±0.03

[Significantly different from GFP-Plc1p in *arg82Δ*+p*ARG82*: $^{***}P<0.001$, $^{**}0.001<P<0.01$, $^{*}0.01<P<0.05$, and not significantly different from GFP-Plc1p in *arg82Δ*.]
[Significantly different from GFP-Plc1p in *arg82Δ*: $^{+++}P<0.001$, and not significantly different from GFP-Plc1p in *arg82Δ*+p*ARG82*.]

Low light DIC (left columns) and Fluorescence images (right columns) of logarithmic phase cultures (5 x 10^6 – 1 x 10^7 cells/ml) of *arg82Δ* + pUG36-*PLC1* transformed with pYCplac111-*ARG82*^{D131A} or pYCplac111-*ARG82*^{Δasp}, respectively, in SC-Ura-Met-Leu+2%glu at 25°C. These images are representative of three replicate cultures. The table shows ratio of fluorescence intensity of plasma membrane (PM), nucleus and cytosol. Each value represents the mean ± S.E.M. of ten determinations

This suggests that the kinase activity of Arg82p is required for regulation of Plc1p distribution, and that inositol polyphosphates downstream of the kinase activity of Arg82p are likely to negatively regulate the interaction between Plc1p and plasma membrane.

4.5 GFP-ARG82p^{D131A} is not on the plasma membrane in *arg82Δ* cells -- further confirming that Plc1p and Arg82p don't physically associate

Some Plc1p is redirected to the plasma membrane in cells lacking Arg82p or harbouring the kinase-dead Arg82p^{D131A}, so what would be the distribution of Arg82p^{D131A} if we linked it to GFP and expressed it in *arg82*Δ cells?

The intracellular distribution of GFP-Arg82p^{D131A} was the same as of wild-type GFP-Arg82p: it showed no plasma membrane localisation in *arg82Δ* cells (Fig 4.8) despite the fact that some Plc1p was clearly on the plasma membrane in these cells (Fig 4.2). This reinforced our conclusion that Plc1p and Arg82p are unlikely to associate with each other directly.

Fig 4.8: Localization of GFP-Arg82p^{D131A} in arg82Δ cell

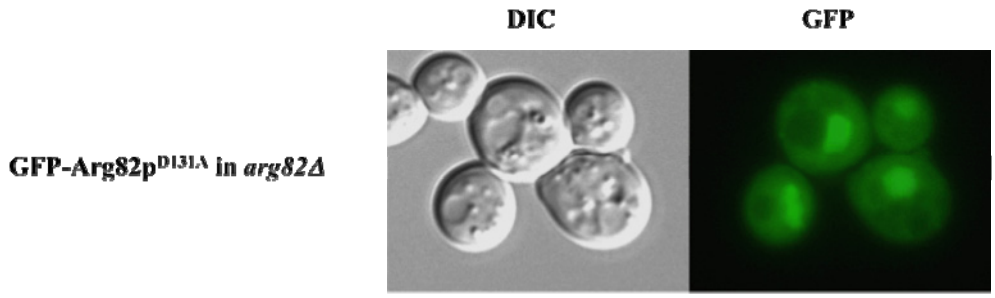

Genotype	Fluorescence Ratio		
	PM/Cytosolic	Nuclear/Cytosolic	PM/Nuclear
pUG36-*ARG82*^{D131A} in *arg82Δ*	0.74 ± 0.01	1.58 ± 0.01	0.47 ± 0.005
pUG36-*ARG82* in *arg82Δ*	0.72 ± 0.01	1.62 ± 0.03	0.45 ± 0.004

[There were no significant differences between the corresponding values of the two cell populations.]

Low light DIC (left columns) and fluorescence images (right columns) of logarithmic phase cultures (5 x 10^6 – 1 x 10^7 cells/ml) of *arg82Δ* + pUG36-*ARG82*^{D131A} were grown in SC-Ura-Met+2% glu at 25°C. These images are representative of three replicate cultures. The table shows ratio of fluorescence intensity of plasma membrane (PM), nucleus and cytosol. Each value represents the mean ± S.E.M. of ten determinations.

4.6 Inhibiting Plc1p activity by U73122 doesn't result in the plasma membrane association of Plc1p

If the interaction of Plc1p with the plasma membrane is inhibited by inositol polyphosphates, then blocking Plc1p activity should also have the same effect as deleting *ARG82*, because the InsP_3 that Arg82p phosphorylates is all produced by Plc1p activity in *S. cerevisiae*. To examine this, I first tried to inhibit Plc1p by using U73122 (Sigma), an inhibitor of inositol lipid hydrolysis by phosphoinositidase C (Smith *et al*., 1990). In an earlier study by Dr. Perera, U73122 inhibited the Plc1p-catalysed PtdIns(4,5)P_2 hydrolysis in response to hypo-osmotic stress in a dose-dependant manner, with a near-complete inhibition at ~5 μM, at which concentration most cells are still viable (Perera *et al.*, 2004). However, U73122 did not inhibit the basal production of InsP_6.

I treated wild-type BY4742 cells transformed with pUG36-*PLC1* with 5 μM U73122 for an hour with gentle shaking at 23°C. There was no concentration of GFP-Plc1p fluorescence on the plasma membrane after treatment with U73122 or with 0.26%(v/v) DMSO, in which it was added (Fig 4.9). However, before I ruled out that the association of Plc1p with plasma membrane was negatively regulated by the inositol phosphates, it was necessary to know if U73122's inhibition on Plc1p activity could have any effect on the enzyme's binding affinity to its substrate and the plasma membrane.

I also examined the localization of Plc1p in *arg82Δ* cells treated with U73122. Unexpectedly, there was hardly any GFP-Plc1p fluorescence at the plasma membrane

Fig 4.9: Localization of GFP-Plc1p in wild-type cells treated with U73122

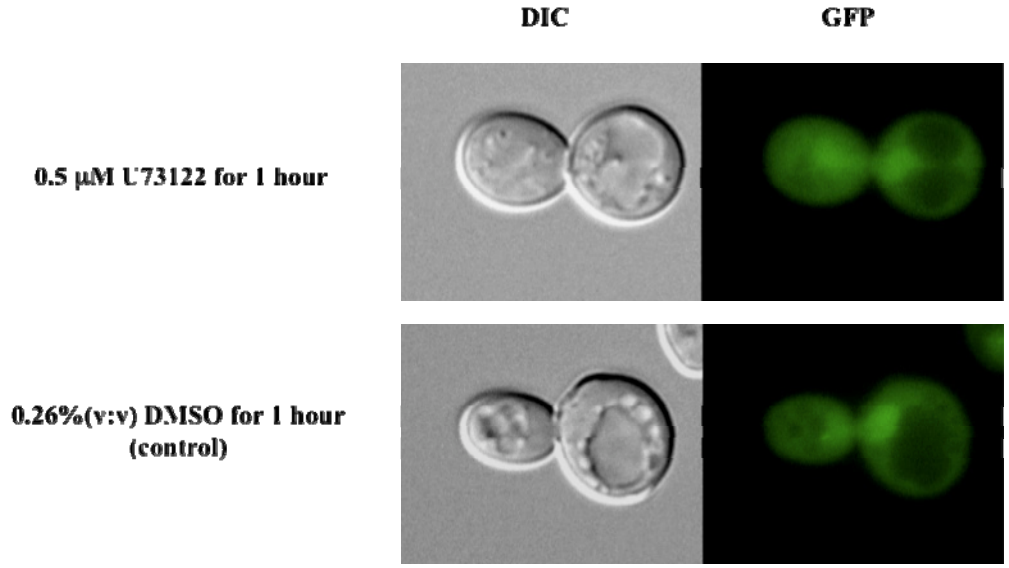

pUG36-*PLC1* in WT	Fluorescence Ratio		
	PM/Cytosolic	Nuclear/Cytosolic	PM/Nuclear
5 μM U73122 1h	0.76±0.01	1.63±0.11	0.48±0.02
0.26%(v:v) DMSO 1h	0.78±0.02	1.63±0.04	0.48±0.02
untreated	0.74±0.01	1.70±0.08	0.44±0.02

[There were no significant differences between the corresponding values of the untreated and the treated cell populations with U73122 or DMSO.]

Low light DIC (left columns) and fluorescence images (right columns) of logarithmic phase cultures (5 x 10^6 – 1 x 10^7 cells/ml) of BY4742 transformed with pUG36-*PLC1* were grown in SC-Ura-Met+2% glu at 25°C and pre-treated for 1 hour with 5 μM U73122 or its vehicle 0.26%(v:v) DMSO. These images are representative of three replicate cultures. The table shows ratio of fluorescence intensity of plasma membrane (PM), nucleus and cytosol. Each value represents the mean ± S.E.M. of ten determinations.

in the *arg82Δ* cells. Rather, fluorescence was concentrated at the nuclear envelope (Fig 4.10). The meaning of these U73122 results is not clear, but my data indicate that it was not acting solely as a PLC inhibitor and therefore that it was not an appropriate tool for these experiments.

4.7 A catalytically dead *PLC1*^{E425G} mutant associates with the plasma membrane stably

Another way to determine whether these inositol phosphates might influence the

Fig 4.10: Localization of GFP-Plc1p in arg82Δ cells treated with U73122

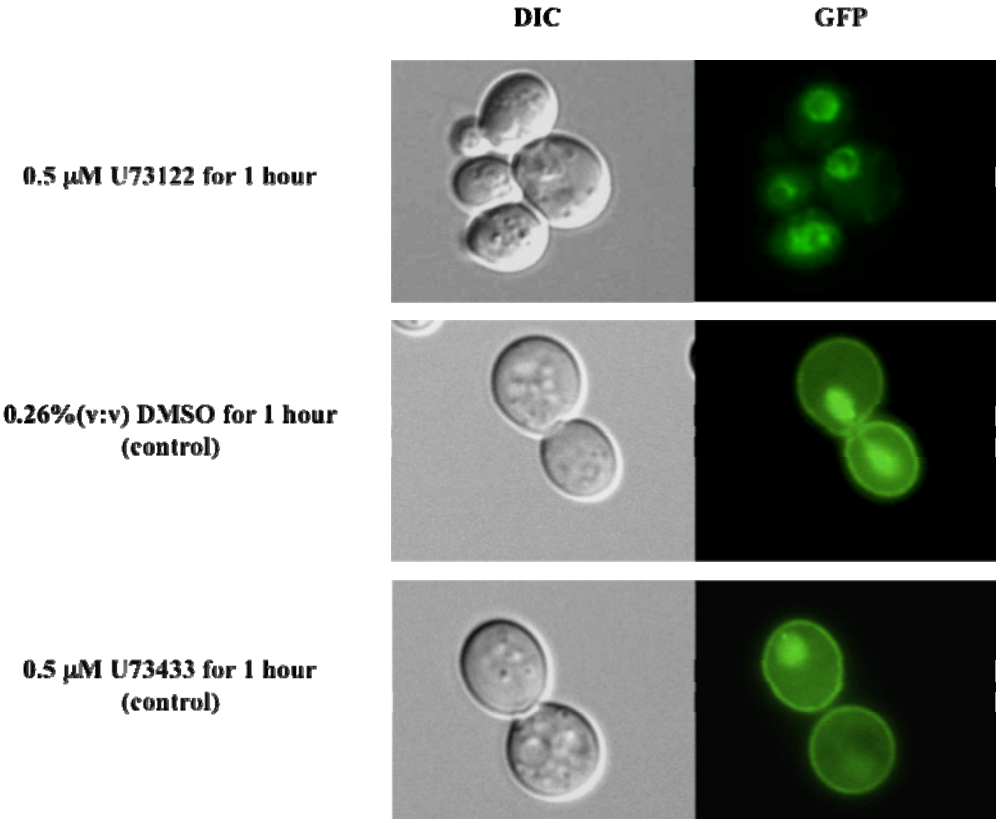

pUG36-*PLC1* in *arg82Δ*	Fluorescence Ratio		
	PM/Cytosolic	Nuclear/Cytosolic	PM/Nuclear
5 μM U73122 1h	0.82±0.02***	1.66±0.05	0.50±0.02***
0.26%(v:v) DMSO 1h	1.16±0.02	1.61±0.07	0.73±0.03
5 μM U73433 1h	1.14±0.02	1.60±0.06	0.73±0.03
untreated	1.13±0.02	1.74±0.08	0.66±0.03

[Significantly different from the untreated for each corresponding values: ***P<0.001; There were no significant differences between the corresponding values of the untreated with either DMSO or U73433 treated.]

Low light DIC (left columns) and fluorescence images (right columns) of logarithmic phase cultures (5 x 10^6 – 1 x 10^7 cells/ml) of *arg82Δ*+pUG36-*PLC1* in SC-Ura-Met+2%glu at 25°C and pre-treated for 1 hour with 5 μM U73122 or its vehicle 0.26% DMSO or 5 μM its inactive analogue U73433. These images are representative of three replicate cultures. The table shows ratio of fluorescence intensity of plasma membrane (PM), nucleus and cytosol. Each value represents the mean ± S.E.M. of ten determinations.

intracellular distribution of Plc1p was to make a catalytically inactive Plc1p mutant and express it in *plc1Δ* cells. A possible prediction would be that this mutant might be at the plasma membrane, since it would not liberate any Plc1p derived inositol phosphates. Cheng *et al*. have previously made a variety of mutations in the X region

of human PLC-δ_1. Amongst these, the Glu^{341} to Gly, or His ^{356} to Leu mutations abolished enzyme activity but yielded proteins that still bound to PtdIns(4,5)P_2 with affinities similar to the wild-type enzyme and maintained a normal expression level (Cheng *et al*., 1995)(Fig 4.11 A). I located the corresponding Glu and His in Plc1p by aligning the highly conserved X region sequences of PLC isoforms from different species (Fig 4.11 B**),** and mutated the corresponding Glu^{425} to Gly (Plc1p^{E425G}) and His^{439} to Leu (Plc1p^{H439L}).

Fig 4.11

A. Characterization of human PLCδ1 mutants (Cheng et al., 1995)

TABLE II

In vitro characterization of human PLCδ1 mutants

Type of mutant	Enzymatic activity[a]		Protein expression[b]
	PI	PIP_2	
	μmol/mg/min		
E327G (Glu^{327} → Gly)	64 ± 7	37 ± 5	++++
R338L (Arg^{338} → Leu)	<0.1	<0.1	+
E341G (Glu^{341} → Gly)	<0.1	<0.1	++++ *
H356L (His^{356} → Leu)	<0.1	<0.1	++++
S381A (Ser^{381} → Ala)	8 ± 2	5 ± 1	++
S388A (Ser^{388} → Ala)	71 ± 6	40 ± 6	++++
K434Q (Lys^{434} → Asn)	29 ± 3	12 ± 3	++++
K440Q (Lys^{440} → Asn)	68 ± 3	39 ± 4	++++
K441Q (Lys^{441} → Asn)	13 ± 3	7 ± 2	+
R549G (Arg^{549} → Gly)	12 ± 2	<0.1	++++

[a] PIP_2 and PI hydrolysis activities were expressed as release of μmol of IP_3 or IP/min/mg of enzyme (see "Experimental Procedures").

[b] The values are expressed relative to that of wild type enzyme; +, between 10 and 20%; ++, between 20 and 40%; and ++++, between 80 and 120%. The relative level of mutant PLCδ1 from crude extract protein (200 μg) was estimated by Western blotting analysis.

*** The equivalent mutations in Plc1p were examined in this study.**

B: Comparison of the primary structures of the conserved regions of PLC isoenzymes (Cheng, et al., 1995)

```
                                          *          * *              *
Hum PLCδ1(298): MGQPLSHYLVSSSHNTYLLEDQLAGPSSTEAYIRALCK-GCRCLELDCWDG---PNQEPIIYHGYTFTSKILFC
Rat PLCβ1(318): MSQPLSHYFINSSHNTYLTAGQLAGNSSVEMYRQVLLS-GCRCVELDCWKGRT-AEEEPVITHGFTMTTEISFK
Hum PLCβ2(314): MTQPLNHYFINSSHNTYLTAGQFSGLSSAEMYRQVLLS-GCRCVELDCWKGKP-PDEEPIITHGFTMTTDIFFK
Rat PLCβ3(300): MTQPLSAYFINSSHNTYLTAGQLAGTSSVEMYRQALLW-GCRCVELDVWKGRP-PEEEPFITHGFTMTTEVPLR
Dro PLCβ (321): MDQPLAHYYINSSHNTYLSGRQIGGKSSVEMYRQTLLA-GGRCVELDCWNGKG-EDEEPIVTHGHAYCTEILFK
Rat PLCγ1(322): MNNPLSHYWISSSHNTYLTGDQFSSESSLEAYARCLRM-GCRCLELDCWDG---PDGMPVIYHGHTLTTKIKFS
Rat PLCγ2(314): MNNPLSHYWISSSHNTYLTGDQLRSESSTEAYIRCLRA-GCRCIELDCWDG---PDGKPIIYHGWTRTTKIKFD
Yeast PLC(383): -SKPLNHYFIASSHNTYLLGKQIAETPSVEGYIQVLQQ-GCRCVEIDIWDG----ENGPVVCHGF-LTSAIPLK
BAC.PLC  (76):  ----------------------QVWGMTQ-EYDFRYQMDHGARIPDIR---GRLTDDNTIVLHHG-PLYLYVTLH
```

Comparison of the sequences in the conserved X domain of PLC isoenzymes from rat, human, Drosophila, yeast and bacillus. The blue colored font denote amino acids in seven or more sequences are identical or represent conservative substitutions grouped as follows: A and G; T and S; I, L, M and V; K, H and R; W, Y and F; D and E; N and Q. Gaps indicated by hyphens are to optimize the alignment. Identical residues containing functional side chain are indicated by an asteriask and the residues in bold were subjected to mutagenesis in this study.

When I examined the distribution of these two mutants in *arg82Δ* cells, GFP-Plc1p^{H439L} distributed much like wild-type Plc1p does in wild-type cells: there was no obvious association with the plasma membrane (Fig 4.12). By contrast, GFP-Plc1p^{E425G} was clearly associated with the plasma membrane (Fig 4.12), in much the same pattern as Plc1p^{wt} in *arg82Δ* cells.

Fig 4.12: Localization of GFP-Plc1p^{H439L} and GFP-Plc1p^{E425G} in arg82Δ cells

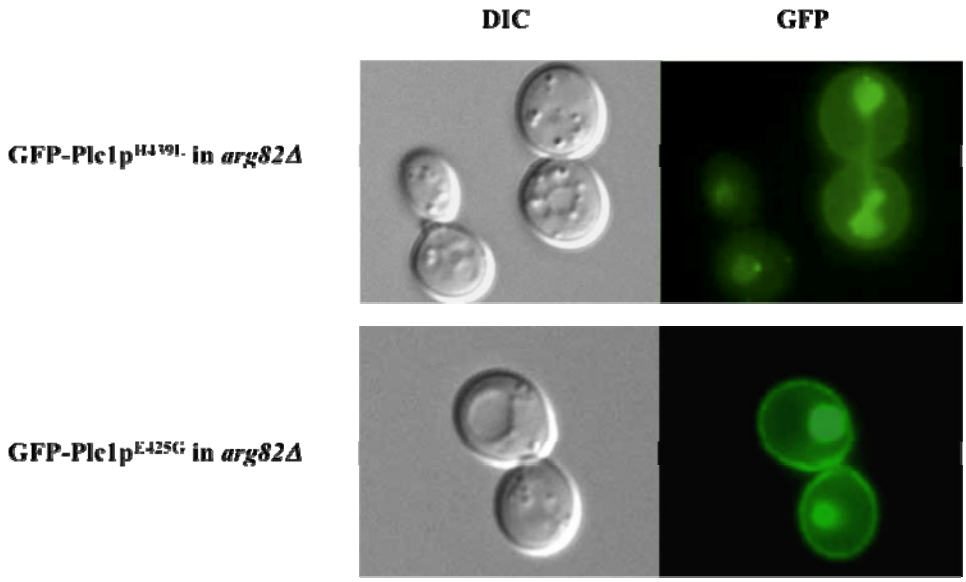

Genotype	Fluorescence Ratio		
	PM/Cytosolic	Nuclear/Cytosolic	PM/Nuclear
pUG36-*PLC1^{H439L}* in *arg82Δ*	0.87±0.02***	1.92±0.08	0.46±0.02***
pUG36-*PLC1^{E425G}* in *arg82Δ*	1.16±0.01	1.70±0.09	0.71±0.05
pUG36-*PLC1* in *arg82Δ*	1.13±0.02	1.74±0.08	0.66±0.03

[Significantly different from the corresponding values of GFP-Plc1p in *arg82Δ*: $^{***}P<0.001$; There were no significant differences between the corresponding values of GFP-Plc1p^{E425G} to GFP-Plc1p in *arg82Δ*.]

Low light DIC (left columns) and fluorescence images (right columns) of logarithmic phase cultures (5 x 10^6 – 1 x 10^7 cells/ml) of *arg82Δ* transformed of the *PLC1* mutant indicated above, in SC-Ura-Met+2% glu at 25°C. These images are representative of three replicate cultures. The table shows ratio of fluorescence intensity of plasma membrane (PM), nucleus and cytosol. Each value represents the mean ± S.E.M. of ten determinations.

One possible explanation of the difference between these mutants is that the H439L mutation reduced the PtdIns(4,5)P_2 affinity of this mutant, but the E425G mutation did not. I therefore decided to use only the Plc1p^{E425G} for the remaining experiments.

To simply test the activity of the Plc1p^{E425G} mutant, I examined its effect on growth at elevated temperature. It hardly grew at 37°C, like *plc1Δ,* suggesting that the mutation probably abolished Plc1p activity (Fig 4.13).

Fig 4.13: Heat stress to PLC1^{E425G} mutant in plc1Δ cells

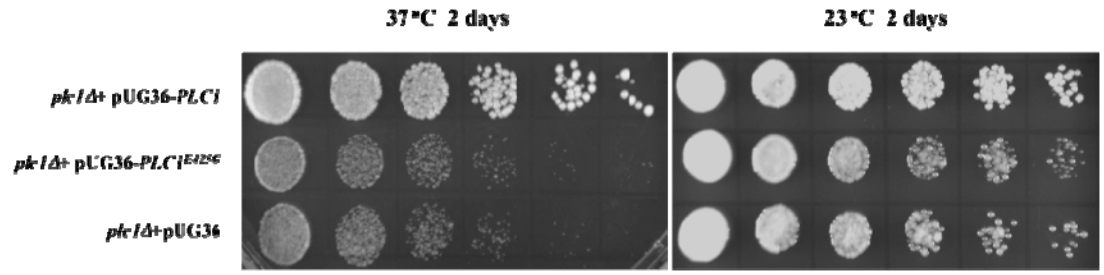

Cells were grown to exponential phase till about ~1 x 10^7 cells/ml in SC-Ura-Met (2% glu) media. A dilution assay was then carried out as described in methodology section. Cells were serially diluted five-fold then grown on YTD agar plates (2% glu) at 37 ^oC (till wild type cells were fully grown) for 2 days. A control plate was grown at 23^oC for 2 days. Data represent three independent experiments.

A lipid dot assay was also carried out to test its binding and catalytic properties. The strips were dotted with 1 nmole of PtdIns(3)*P*, PtdIns(3,5)P_2 and PtdIns(4,5)P_2, and then incubated with purified GST-Plc1p and GST-Plc1p^{E425G}, respectively, followed by antibody detection of the GST tag. After the ECL chemiluminescence reaction, the binding of the proteins to the lipids was shown as black dots on the blot. No binding of wild-type GST-Plc1p was seen, presumably because it hydrolysed the PtdIns(4,5)P_2 on the strip. Binding of Plc1p^{E425G} to PtdIns(4,5)P_2 was observed, showing that it bound and was catalytically inactive (Fig 4.14). PLC-δ_1 PH has been long known to bind with PtdIns3*P* for unknown reasons and Plc1p appears to also do

Fig 4.14: Lipid dot assay for detecting the binding of Plc1p or Plc1p^{E425G} with phosphoinositides

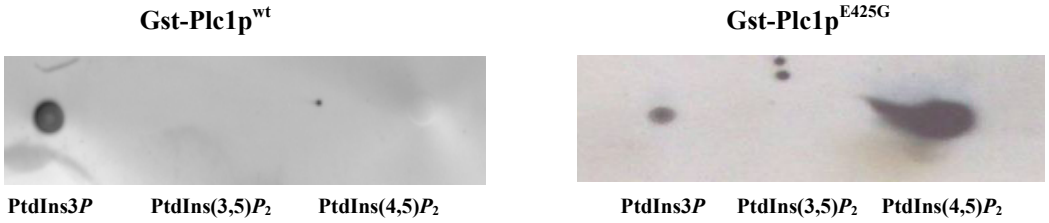

Hi-Bond C+ supported nitrocellulose strips were spotted with ~1µg of each of the following lipids: PtdIns3*P*, PtdIns(3,5)P_2 and PtdIns(4,5)P_2 and incubated with ~ 15µg of Gst-Plc1p^{wt} and Gst-Plc1p^{E425G}, respectively, in 6 ml of TBST, for 2 hours at room temperature, followed up by anti-GST antibody detection.

so (Ferguson *et al.*, 2000). This served as a useful positive control to show the sensitivity of the assay.

Having confirmed that Plc1p^{E425G} associates with the plasma membrane and is probably catalytically inactive, I examined its distribution in *plc1Δ* cells. Again, it was associated with the plasma membrane (Fig 4.15), consistent with the idea that inositol polyphosphates are somehow responsible for preventing Plc1p from associating with the plasma membrane. This removes many of the trivial explanations for how Plc1p might be artificially associating since I have now demonstrated this interaction in two completely different ways.

4.8 Distribution of GFP-Plc1p in cells devoid of the other inositol phosphate kinases

Having evidence that inositol phosphates might regulate Plc1p's interaction with the plasma membrane, I hoped to determine which inositol polyphosphate(s) are responsible for this effect by observing GFP-Plc1p localisation in cells depleted of the

Fig 4.15: Localization of GFP-Plc1p^{E425G} in plc1Δ cells.

Genotype	Fluorescence Ratio		
	PM/Cytosolic	Nuclear/Cytosolic	PM/Nuclear
pUG36-*PLC1*^{E425G} in *plc1Δ*	1.39±0.05$^{***/+++}$	1.74±0.09	0.81±0.03***
pUG36-*PLC1* in *plc1Δ*	0.77±0.01	1.65±0.02	0.47±0.01
pUG36-*PLC1*^{E425G} in *arg82Δ*	1.16±0.01	1.70±0.09	0.71±0.05

[Significantly different from the corresponding values of GFP-Plc1p in *plc1Δ*: $^{***}P<0.001$, and of GFP-Plc1p^{E425G} in *arg82Δ*: $^{+++}P<0.001$.]

Low light DIC (left columns) and fluorescence images (right columns) of logarithmic phase cultures (5 x 10^6 – 1 x 10^7 cells/ml) of BY4742*plc1Δ* transformed with pUG36-*PLC1*^{E425G} in SC-Ura-Met+2% glu at 25°C. These images are representative of three replicate cultures. The table shows ratio of fluorescence intensity of plasma membrane (PM), nucleus and cytosol. Each value represents the mean ± S.E.M. of ten determinations.

other 'higher' inositol phosphates or inositol pyrophosphates that are phosphorylated via InsP_5.

The pathways by which *S. cerevisiae* converts Plc1p-generated InsP_3 to InsP_6 and then to inositol pyrophosphates have been established (Mulugu *et al*., 2007; Odom *et al*., 2000; Zhang *et al*., 2001)(Fig 4.16).

Hence, the localization of GFP-Plc1p was examined in *ipk1Δ, kcs1Δ, vip1Δ* and *kcs1Δvip1Δ* cells. GFP-Plc1p did not associate with the plasma membrane in any of these mutants (Fig 4.17). *Arg82Δ* cells are almost devoid of inositol phosphates possessing more than two phosphates. InsP_5s (probably more than one isomer) are the only abundant Ins*P*s in *ipk*Δ cells (Perera *et al*., 2004), and the inositol polyphosphate

Fig4.16: Pathways of InsP_3 metabolism in S. cerevisiae

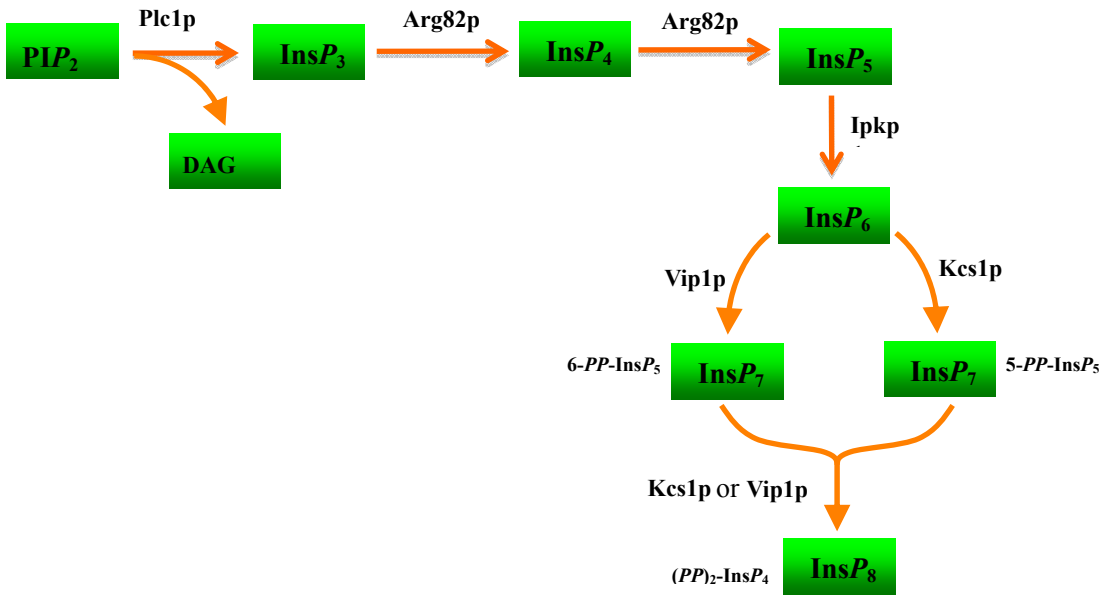

profiles of the other mutants are dominated by InsP_6. This being so, the simplest explanation of the presence of Plc1p at the plasma membrane only in *arg82Δ* cells is that this association only occurs when the cells do not contain a substantial concentration of any inositol polyphosphate with 5 or more phosphate groups.

There was somewhat less GFP-Plc1p in the nucleus in *kcs1Δ*, *vip1Δ*, and *vip1Δkcs1Δ* cells than in the wild-type or *arg82Δ* cells (Fig 4.17). All of these mutants contain abnormally high levels of InsP_6: might this suppress nuclear Plc1p localization?

4.9 The Ins(1,4,5,6)P_4 kinase activity of Arg82p is responsible for destabilizing the Plc1p-plasma membrane interaction

Arg82p is a dual InsP_3 kinase: It first phosphorylates InsP_3 at the D6 hydroxyl to form

Fig 4.17: Localization of GFP-Plc1p in ipk1Δ, kcs1Δ, vip1Δ and vip1Δkcs1Δcells

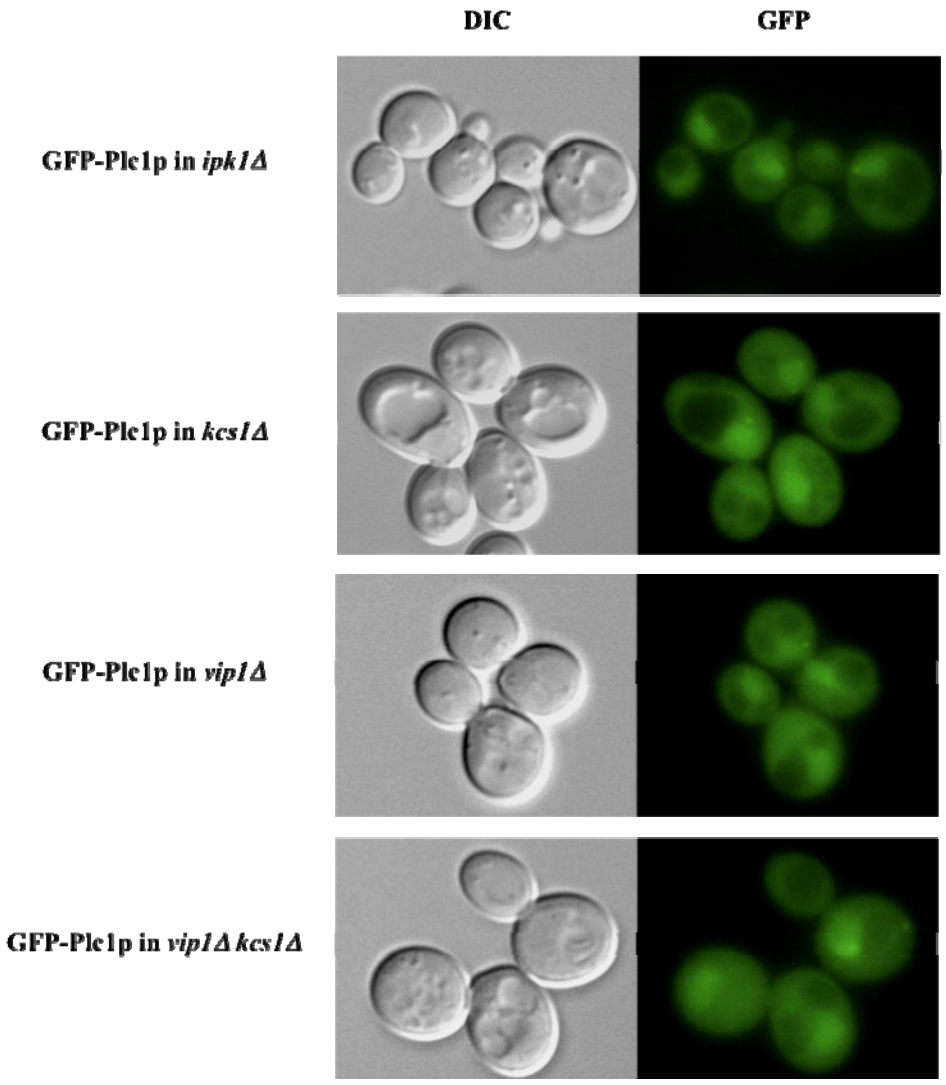

Genotype	Fluorescence Ratio		
	PM/Cytosolic	Nuclear/Cytosolic	PM/Nuclear
pUG36-*PLC1* in *ipk1Δ*	$0.77\pm0.02^{***}$	1.59 ± 0.06	$0.49\pm0.02^{***}$
pUG36-*PLC1* in *kcs1Δ*	$0.71\pm0.01^{***}$	$1.46\pm0.05^{**/+}$	$0.49\pm0.02^{***}$
pUG36-*PLC1* in *vip1Δ*	$0.73\pm0.02^{***}$	$1.50\pm0.04^{*/+}$	$0.48\pm0.01^{***}$
pUG36-*PLC1* in *vip1Δkcs1Δ*	$0.72\pm0.02^{***}$	$1.50\pm0.04^{*/+}$	$0.49\pm0.01^{***}$
pUG36-*PLC1* in WT	0.74 ± 0.01	1.70 ± 0.08	0.44 ± 0.02
pUG36-*PLC1* in *arg82Δ*	1.13 ± 0.02	1.74 ± 0.08	0.66 ± 0.03

[Significantly different from the corresponding values of GFP-Plc1p in *arg82Δ*: $^{***}P<0.001$, $0.001<^{**}P<0.01$, $0.01<^{*}P<0.05$; Significantly different from the corresponding values of GFP-Plc1p in WT: $0.01<^{+}P<0.05$.]

Low light DIC (left columns) and fluorescence images (right columns) of logarithmic phase cultures ($5 \times 10^6 - 1 \times 10^7$ cells/ml) of *ipk1Δ* (BY4742 *ipk1::kanMX4*), *kcs1Δ* (BY4742 *kcs1::kanMX4*), *vip1Δ* (BY4742 *vip1::kanMX4*), *vip1Δkcs1Δ* (BY4742 *vip1::LEU2, kcs1::kanMX4*), transformed of pUG36-*PLC1*, respectively, was grown in SC-Ura-Met+2%glu at 25°C. These images are representative of three replicate cultures. The table shows ratio of fluorescence intensity of plasma membrane (PM), nucleus and cytosol. Each value represents the mean ± S.E.M. of ten determinations.

Ins(1,4,5,6)P_4, then at D3, leading to the synthesis of Ins(1,3,4,5,6)P_5 (see diagram below).

$$\text{Ins}(1,4,5)P_3 \xrightarrow{\text{Arg82p}} \text{Ins}(1,4,5,6)P_4 \xrightarrow{\text{Arg82p}} \text{Ins}(1,3,4,5,6)P_5$$

To discover which of these inositol polyphosphates might have the dominant role in suppressing the Plc1p-plasma membrane interaction, I transformed a plasmid carrying an *arg82* mutant *ipk2-3* from Dr John York, which has a glycine at 344 converted to arginine, pUG34-*ARG82*^{G344R}. This mutant makes only Ins(1,4,5,6)P_4 (Chang *et al*., 2002)(Fig 4.18).

Fig 4.18: HPLC analysis of soluble inositol phosphates isolated from ARG82^{G344R} (ipk2-3) strain grown in the presence of 30 µCi/ml [3H]inositol at 23 °C, which can synthesize InsP$_4$. (Chang et al. 2002)

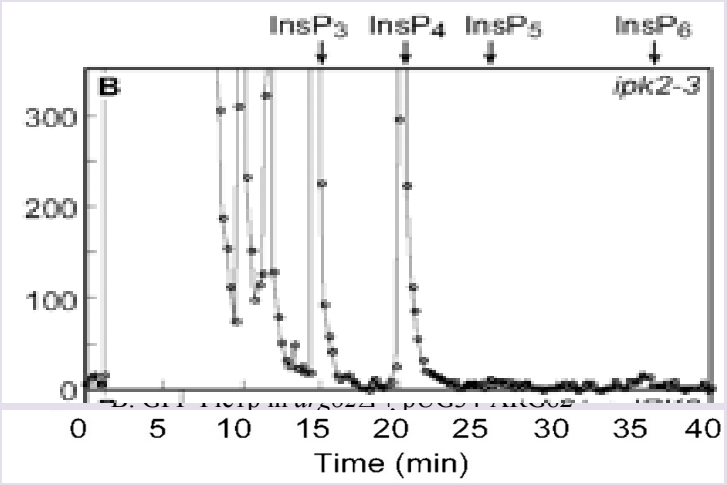

When p*ARG82*^{G344R} was introduced into *arg82Δ* cells, GFP-Plc1p associated with the plasma membrane, as in cells devoid of Arg82p (Fig 4.19). Since Plc1p associated with the plasma membrane when cells could make Ins(1,4,5,6)P_4 but not Ins(1,3,4,5,6)P_5, it seems that Ins(1,3,4,5,6)P_5 can inhibit the association of Plc1p with the plasma membrane.

Fig 4.19: Localization of GFP-Plc1p is affected in ARG82^{G344R} mutant

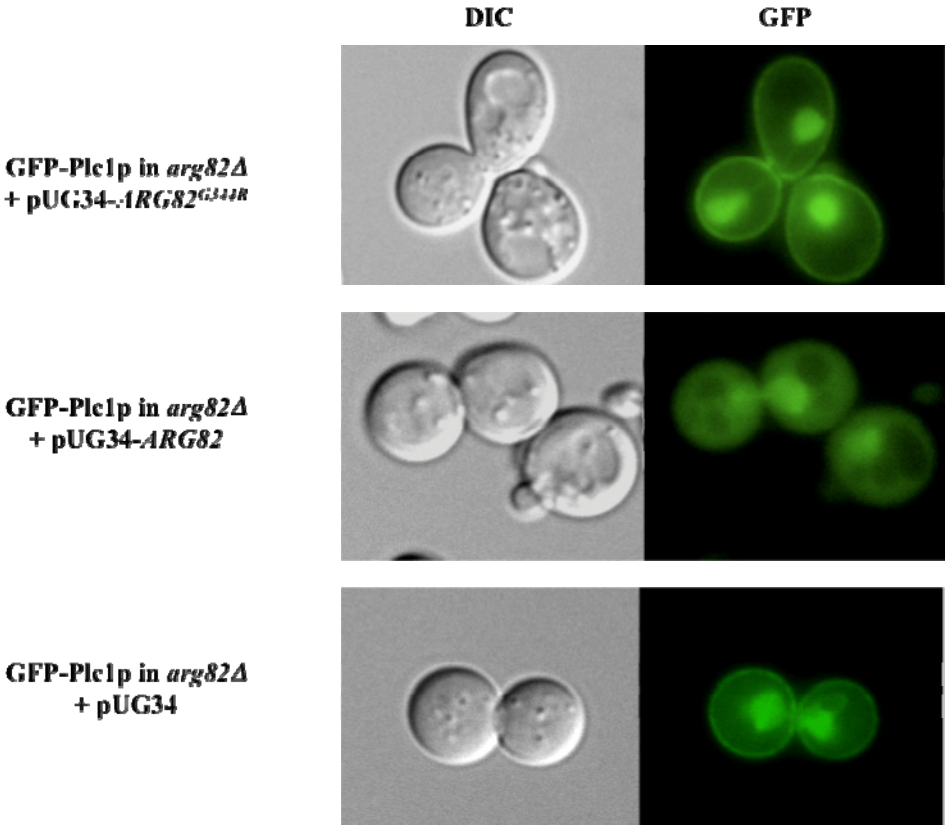

Genotype	Fluorescence Ratio		
	PM/Cytosolic	Nuclear/Cytosolic	PM/Nuclear
pUG36-*PLC1* in *arg82Δ* + pUG34-*ARG82*^{G344R}	1.15±0.03	1.70±0.07	0.67±0.03
pUG36-*PLC1* in *arg82Δ* + pUG34-*ARG82*	0.71±0.02	1.56±0.06	0.46±0.019
pUG36-*PLC1* in *arg82Δ* + pUG34	1.16±0.02	1.84±0.09	0.64±0.02
pUG36-*PLC1* in *arg82Δ*	1.13±0.02	1.74±0.08	0.66±0.03
pUG36-*PLC1* in WT	0.74±0.01	1.70±0.08	0.44±0.02

[There were no significant differences between the corresponding values of GFP-Plc1p in *arg82Δ*+ p*ARG82*^{G344R} and in *arg82Δ*, GFP-Plc1p in *arg82Δ*+p*ARG82* and in WT, GFP-Plc1p in *arg82Δ* with empty vector and in *arg82Δ*.]

Low light DIC (left columns) and Fluorescence images (right columns) of logarithmic phase cultures (5 x 10^6 – 1 x 10^7 cells/ml) of *arg82Δ*+pUG36-*PLC1* transformed with p*ARG82* and its mutant plasmid as indicated, respectively, were grown in SC-Ura-Met-His+2%glu at 25°C. These images are representative of three replicate cultures. The table shows ratio of fluorescence intensity of plasma membrane (PM), nucleus and cytosol. Each value represents the mean ± S.E.M. of ten determinations.

One way to ask whether InsP_5 can be sufficient to prevent Plc1p from associating with the plasma membrane is to determine whether Plc1p in *arg82*Δ cells could leave the plasma membrane if cells are loaded with exogenous InsP_5.

I attempted to test this by incubating *arg82Δ* cells expressing wild-type GFP-Plc1p and *plc1Δ* cells expressing GFP-Plc1p^{E425G} mutant with a membrane-permeant InsP_5, 2-O-Butyryl-Ins(1,3,4,5,6)P_5/PM (100μM) (Echelon) (Rudolf *et al*., 1998; Yang *et al*., 1999) (Fig 4.20 and Fig 4.21). Cells were treated for 2 hours in total, and examined after 15 min and 2 hours. After the treatment with membrane-permeant Ins(1,3,4,5,6)P_5 for 15 min, there was a modest redistribution of GFP-Plc1p to the plasma membrane, which partially reversed after 2 hours. This was the opposite of what we had hoped might happen.

This experiment was made difficult to interpret because I lacked a positive control and was also unsure if the InsP_5 was actually taken into the cells because of the yeast cell wall. I did try spheroplasting the cells before adding the InsP_5. However, apart from ending up having diffused fluorescence that affected the microscopy results in most of the cells, I didn't detect any changes in the localization of Plc1p on the plasma membrane (data not shown). Hence these add-back experiments were inconclusive.

However, it is unlikely that InsP_5 itself destabilizes Plc1p's association with plasma membrane in normal cells since previous work by Dr Perera showed there are no significant levels of InsP_5 in wild type cells according to the [^{3}H]inositol polyphosphate elution profiles from wild-type cells obtained by HPLC analysis (Perera *et al*., 2004). All InsP_5 generated is rapidly phosphorylated, and only the InsP_6 level is substantial, at least in resting cells. At such an undetectable level, InsP_5 would be unlikely to play a regulatory role on its own: though it is likely it can when it accumulates. It is therefore possible that InsP_5, together with InsP_6 and/or facilitated by the inositol pyrophosphates, are jointly responsible for directing Plc1p off from the

plasma membrane. At the moment, it is unsure if InsP_5 alone is sufficient for de-stabilizing Plc1p from the plasma membrane.

Fig 4.20: Localization of GFP-Plc1p in arg82Δ incubated with Ins(1,3,4,5,6)P_5/PM for indicated time course

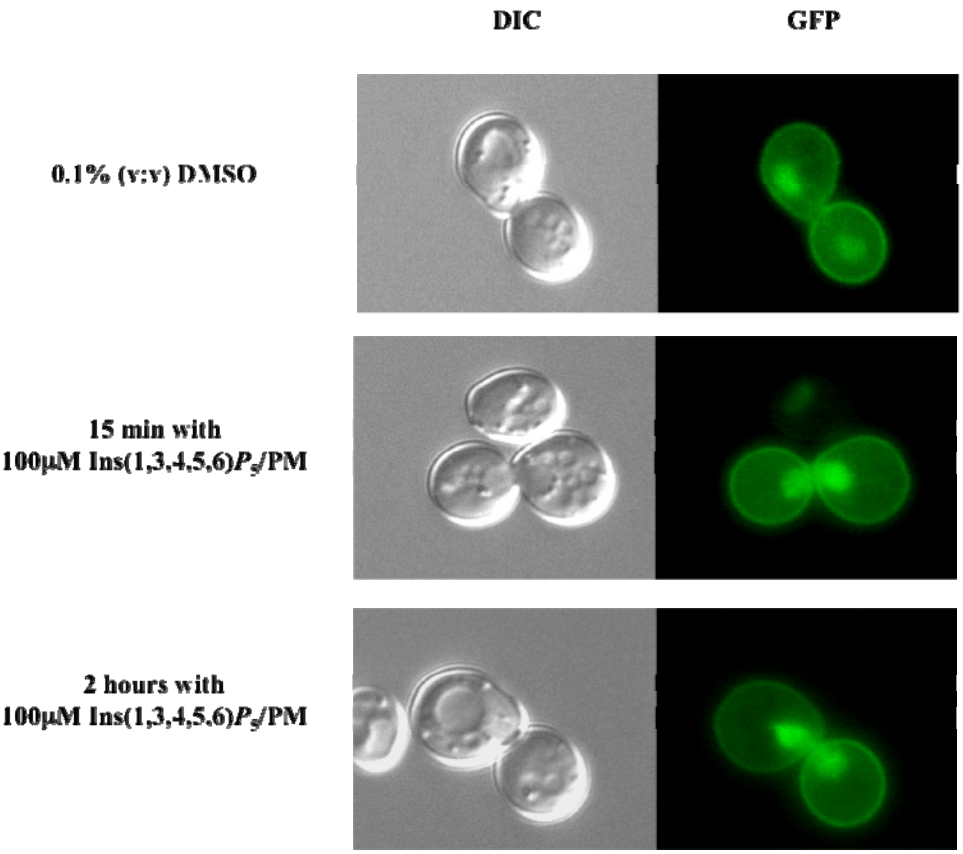

pUG36-*PLC1* in *arg82Δ*	Fluorescence Ratio		
	PM/Cytosolic	Nuclear/Cytosolic	PM/Nuclear
0.1% (v:v) DMSO	1.17±0.02	1.65±0.07	0.72±0.04
100μM Ins(1,3,4,5,6)P_5 15min	1.36±0.05***	1.82±0.09	0.76±0.04*
100μM Ins(1,3,4,5,6)P_5 2hrs	1.29±0.04***	1.80±0.05	0.72±0.02
untreated	1.13±0.02	1.74±0.08	0.66±0.03

[Significantly different from the corresponding values of the untreated: $^{***}P<0.001$, $0.01<^{*}P<0.05$. There were no significant differences between the corresponding values of the untreated with the DMSO treated, or between the treated for 15 min and for 2 hrs.]

Low light DIC (left columns) and Fluorescence images (right columns) of logarithmic phase cultures (5 x 10^6 – 1 x 10^7 cells/ml) of *arg82Δ*+pUG36-*PLC1* were grown in SC-Ura-Met+2%glu at 25°C. 100μM of Ins(1,3,4,5,6)P_5/PM were added and incubated for 15 min and 2 hours. Control was cells treated with drug carrier 0.1% (v:v) DMSO. These images are representative of three replicate cultures. The table shows ratio of fluorescence intensity of plasma membrane (PM), nucleus and cytosol. Each value represents the mean ± S.E.M. of ten determinations.

Fig 4.21: Localization of GFP-Plc1p^{E425G} in plc1Δ incubated with Ins(1,3,4,5,6)P_5/PM for indicated time course

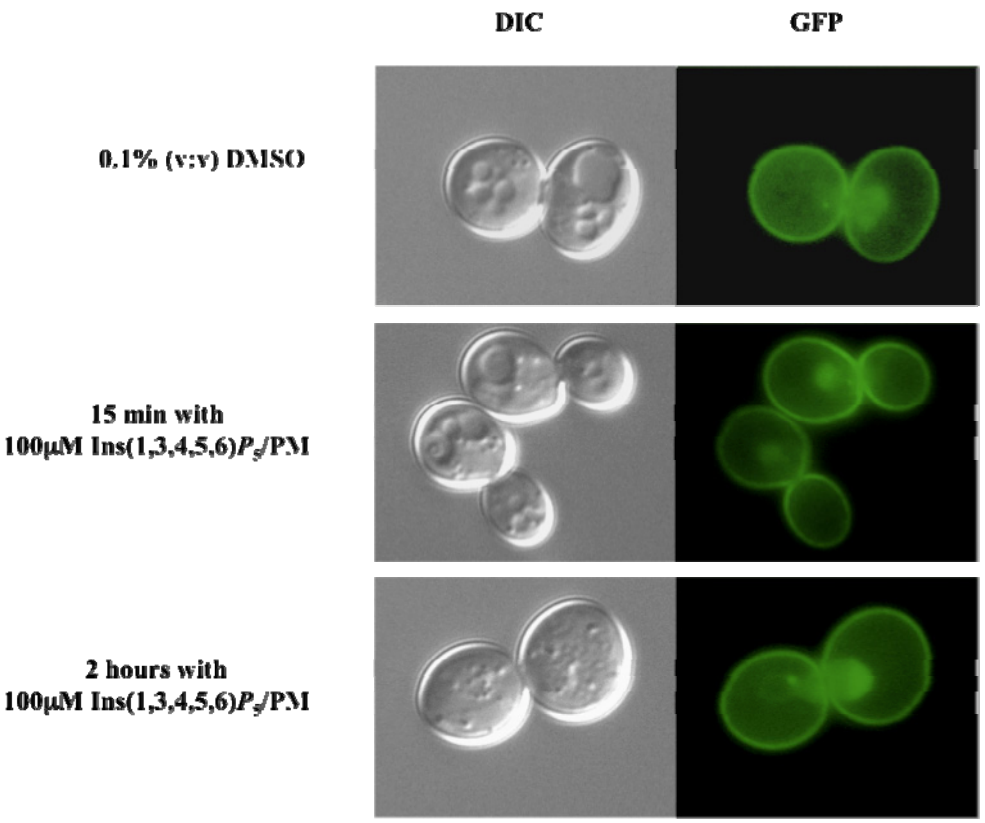

pUG36-*PLC1*^{E425G} in *plc1Δ*	Fluorescence Ratio		
	PM/Cytosolic	Nuclear/Cytosolic	PM/Nuclear
0.1% (v:v) DMSO	1.39±0.02	1.67±0.08	0.85±0.03
100μM Ins(1,3,4,5,6)P_5 15min	1.38±0.04	1.57±0.05	0.89±0.01*
100μM Ins(1,3,4,5,6)P_5 2hrs	1.44±0.04	1.57±0.08	0.93±0.04**
untreated	1.39±0.05	1.74±0.09	0.81±0.03

[Significantly different from the corresponding values of the untreated: $0.001<^{**}P<0.01$, $0.01<^{*}P<0.05$. There were no significant differences between the corresponding values of the untreated with the DMSO treated, or between the treated for 15 min and for 2 hrs.]

Low light DIC (left columns) and fluorescence images (right columns) of logarithmic phase cultures (5 x 10^6 – 1 x 10^7 cells/ml) of *plc1Δ*+pUG36-*PLC1*^{E425G} were grown in SC-Ura-Met+2%glu at 25°C. 100μM of Ins(1,3,4,5,6)P_5/PM were added and incubated for 15 min and 2 hours. Control was cells treated with drug carrier 0.1% (v:v) DMSO. These images are representative of three replicate cultures. The table shows ratio of fluorescence intensity of plasma membrane (PM), nucleus and cytosol. Each value represents the mean ± S.E.M. of ten determinations.

4.10 The PH domain of Plc1p is involved in its interaction with the plasma membrane

The above experiments raised the question of how Plc1p associates with the plasma

membrane in cells lacking Arg82p and/or the downstream inositol polyphosphates. The PH domain of many PLC-δs is required for the processive hydrolysis of its substrate PtdIns(4,5)P_2 at the plasma membrane, at least in animal cells. It is known that the high affinity binding of Ins(1,4,5)P_3 to PLC-δ_1 via its PH domain inhibits its binding to PtdIns(4,5)P_2 (Cifuentes *et al*., 1994; Lemmon *et al.*, 1995). In addition, a number of studies suggest that several inositol polyphosphates can inhibit interactions between various PH domains and phosphoinositides (Hirata *et al*., 1998). Hence we wondered if it was a PtdIns(4,5)P_2-PH domain interaction in this case.

I had made two stable mutants with mutations in or around the PH domain of Plc1p when I was seeking the nuclear localization signal: Plc1p$^{R111L/R117S/R120S/R123E}$ (Plc1p^{4R}) and Plc1p$^{K170A/R171A/R173A}$ (Plc1p^{KRLR}) (Section 3.6.2.2). Transformation into *arg82Δ* of GFP-Plc1p^{KRLR} did not reduce the plasma membrane association of the protein in *arg82Δ* cells: nuclear localization was also affected as in wild-type cells (Fig 4.22 and Fig 3.15). The Plc1p^{4R} mutant did not associate with the plasma membrane, and it was noticeably more concentrated in the nucleus in *arg82Δ* than in wild-type cells (Fig 4.22).

The four arginines mutated in Plc1p^{4R} are located at the start of the PH domain with the first arginine, R111, in the N-terminal extension before PH domain (see diagram below). This strongly suggests that some amino acid residues in the PH domain may be important for Plc1p's interaction with plasma membrane.

However, although these mutations alter the binding affinity of Plc1p for PtdIns(4,5)P_2, they aren't likely to affect Plc1p's activities during stress responses, at

Fig 4.22: Localization of GFP-Plc1p^{KRLR} and GFP-Plc1p^{4R} in arg82Δ cells

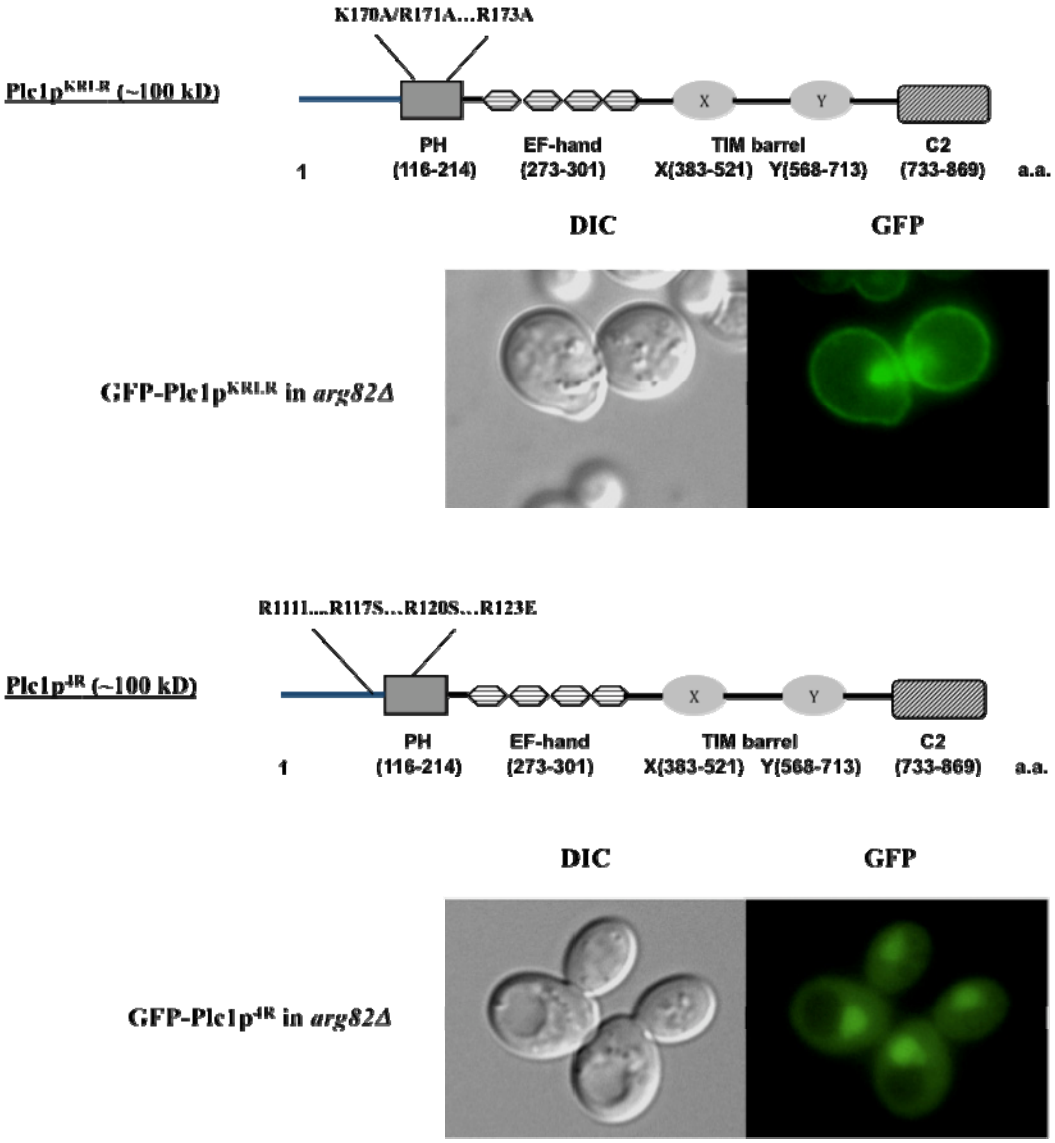

Genotype	Fluorescence Ratio		
	PM/Cytosolic	Nuclear/Cytosolic	PM/Nuclear
pUG36-*PLC1*^{KRLR} in *arg82Δ*	1.16±0.02	1.49±0.04**	0.78±0.02**
pUG36- *PLC1*^{4R} in *arg82Δ*	0.70±0.02***	1.80±0.05	0.39±0.01***
pUG36-*PLC1* in *arg82Δ*	1.13±0.02	1.74±0.08	0.66±0.03

[Significantly different from the corresponding values of GFP-Plc1p in *arg82Δ*: $^{***}P<0.001$, $0.001<^{**}P<0.01$.]

Low light DIC (left columns) and fluorescence images (right columns) of logarithmic phase cultures (5 x 10^6 – 1 x 10^7 cells/ml) of *arg82Δ* transformed with pUG36-*PLC1*^{KRLR} or pUG36-*PLC1*^{4R}, respectively, were grown in SC-Ura-Met + 2%glu at 25°C. These images are representative of three replicate cultures. The table shows ratio of fluorescence intensity of plasma membrane (PM), nucleus and cytosol. Each value represents the mean ± S.E.M. of ten determinations.

least phenotypically – as this mutant grew as well as cells having wild type Plc1p transformed at elevated temperature (Fig 4.23).

Fig 4.23: Heat stress response of the Plc1p^{4R} mutant

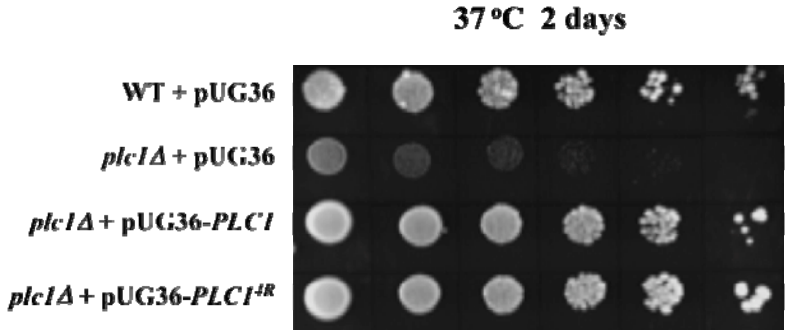

Cells were grown to exponential phase (about ~1 x 10^7 cells/ml) in SC-Ura-Met (2% glu) media. A dilution assay was then carried out as described in the methodology section. Cells were serially diluted five-fold then grown on YTD agar plate (2% glu) at 37 °C for 2 days (till wild type colonies were fully grown).

I also mutated some of these arginine residues in pairs: Plc1p$^{R117S/R120S}$ (Plc1p$^{R2/3}$), Plc1p$^{R117S/R123E}$ (Plc1p$^{R2/4}$), and Plc1p$^{R120S/R123E}$ (Plc1p$^{R3/4}$). None of these three mutants were disassociated as effectively from the plasma membrane as was Plc1p^{4R} (Fig 4.24). Though the Plc1p$^{R3/4}$ mutant does appear to have more effect on GFP-Plc1p association with the plasma membrane than the Plc1p$^{R2/3}$ and Plc1p$^{R2/4}$ mutants both appeared to have only slight effects, and still displayed somewhat more plasma membrane associated GFP-Plc1p protein than the Plc1p^{4R} mutant.

I then looked at the single mutation of the first of these four arginines, GFP-Plc1p^{R1}. The single R111L change decreased the association of GFP-Plc1p with the plasma membrane as effectively as the Plc1p$^{R3/4}$ construct. The Plc1p^{R1} mutant also showed a high level of nuclear localization (Fig 4.24).

Fig 4.24: Localization of* GFP-Plc1p$^{R2/3}$, GFP- Plc1p$^{R2/4}$, GFP- Plc1p$^{R3/4}$ and GFP- Plc1p^{R1} *in arg82Δ cells

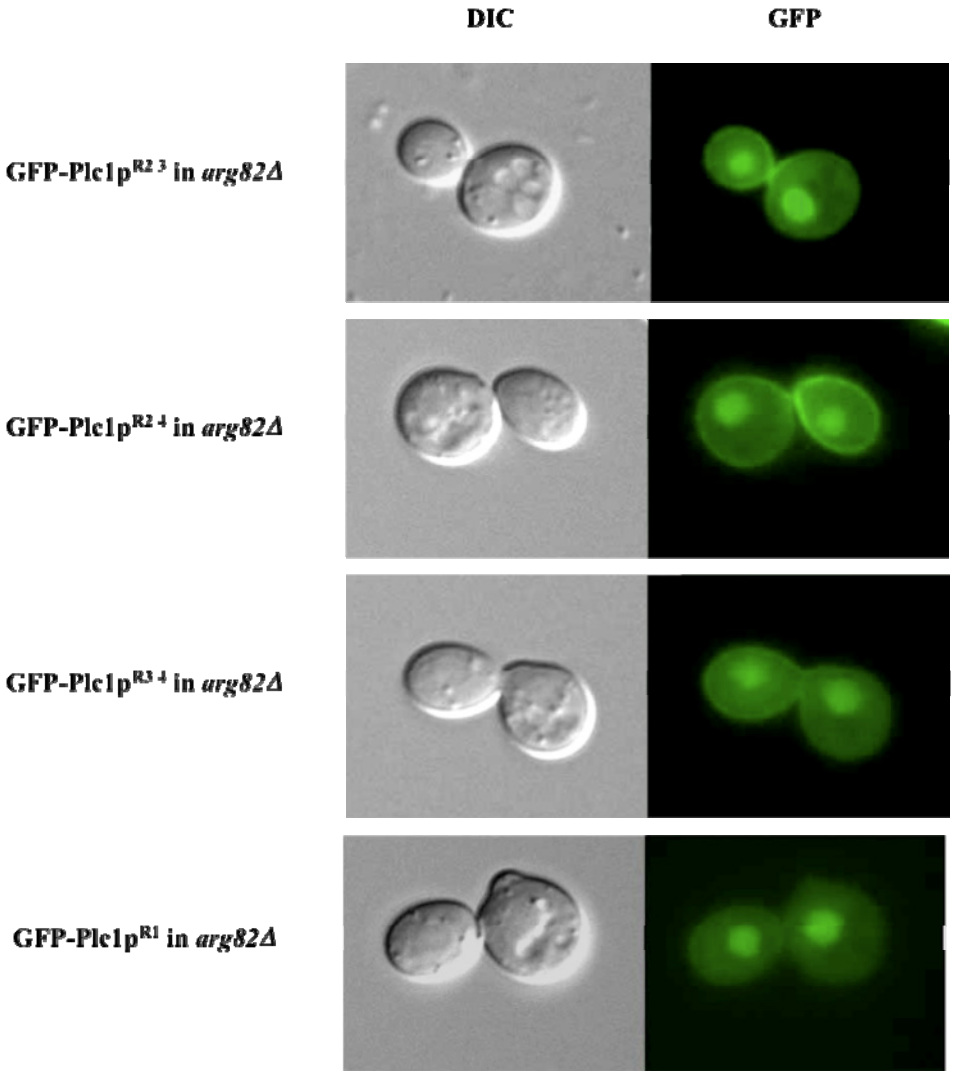

Genotype	Fluorescence Ratio		
	PM/Cytosolic	Nuclear/Cytosolic	PM/Nuclear
pUG36-*PLC1*$^{R2/3}$ in *arg82Δ*	1.02±0.03$^{**/+++}$	1.45±0.06$^{**/+++}$	0.71±0.03^{+++}
pUG36-*PLC1*$^{R2/4}$ in *arg82Δ*	1.13±0.02^{+++}	1.40±0.05$^{**/+++}$	0.82±0.03$^{**/+++}$
pUG36-*PLC1*$^{R3/4}$ in *arg82Δ*	0.84±0.04$^{***/++}$	1.47±0.06$^{*/+++}$	0.59±0.04^{+++}
pUG36-*PLC1*^{R1} in *arg82Δ*	0.83±0.03$^{***/++}$	1.99±0.11*	0.43±0.03***
pUG36-*PLC1* in *arg82Δ*	1.13±0.02	1.74±0.08	0.66±0.03
pUG36- *PLC1*^{4R} in *arg82Δ*	0.70±0.02	1.80±0.05	0.39±0.01

[Significantly different from the corresponding values of GFP-Plc1p in *arg82Δ*: $^{***}P<0.001$, $0.001<^{**}P<0.01$, $0.01<^{**}P<0.05$.]

[Significantly different from the corresponding values of GFP-Plc1p^{4R} in *arg82Δ*: $^{+++}P<0.001$, $0.001<^{++}P<0.01$.]

Low light DIC (left columns) and fluorescence images (right columns) of logarithmic phase cultures (5 x 10^6 – 1 x 10^7 cells/ml) of *arg82Δ* transformed with various *PLC1* mutant as indicated, respectively. Cells were grown in SC-Ura-Met+2%glu at 25°C. These images are representative of three replicate cultures. The table shows ratio of fluorescence intensity of plasma membrane (PM), nucleus and cytosol. Each value represents the mean ± S.E.M. of ten determinations.

These experiments didn't isolate a single arginine that was responsible for the association of Plc1p and plasma membrane. R111 seems very effective, but it is possible that all of these arginine residues are important.

4.11 GFP-Plc1p$^{4R/E425G}$ is not on the plasma membrane in *plc1Δ*

A catalytically dead Plc1p mutant, GFP-Plc1p^{E425G} was associated with the plasma membrane in *plc1Δ* cells, and mutations in or near the PH domain (R111L/R117S/R120S/R123E), disrupted this association. So how would the mutant that combines the R111L/R117S/R120S/R123E (4R) and E425G mutations behave? As expected, GFP-Plc1p$^{4R/E425G}$ was not associated with the plasma membrane in either *plc1Δ* or *arg82Δ* cells, presumably because of the mutations in the four arginines (Fig 4.25). However, this mutant had also lost much of its nuclear concentration. To test the reliability of these observations, I examined the stability of the various arginine mutants and Plc1p^{E425G}. GFP-Plc1p$^{4R/E425G}$ are relatively stable, but some free GFP was also seen on the blot (APPX. Fig A).

I am therefore confident that this construct does reliably represent the localisation of the catalytically inactive Plc1p^{E425G} and that this mutant was truly no longer capable of binding with the plasma membrane when four arginines in its PH domain were disrupted. Therefore the PH domain does indeed appear to participate in the interaction of Plc1p with plasma membrane.

4.12 Localisation of Plc1p truncation mutants in *arg82Δ* cells

Having established that some mutations in the PH domain and the X-Y region appear to be important for Plc1p to interact with the plasma membrane, we wondered

Fig 4.25: Localization of GFP-Plc1p$^{4R/E425G}$ in plc1Δ and arg82Δ cells

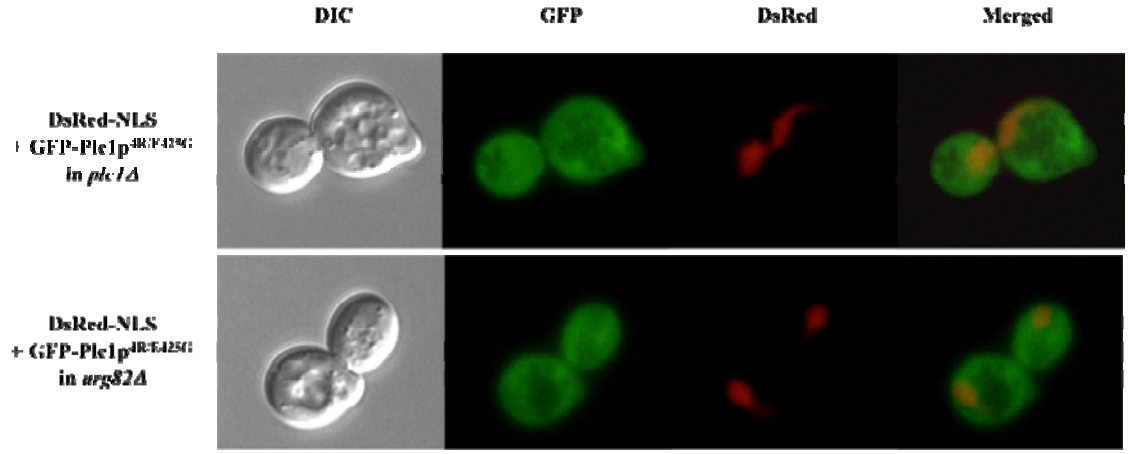

Genotype	Fluorescence Ratio		
	PM/Cytosolic	Nuclear/Cytosolic	PM/Nuclear
pUG36-*PLC1*$^{4R/E425G}$ in *plc1Δ*	0.77±0.02$^{\#\#\#}$	1.17±0.02$^{***/+++/\#\#\#}$	0.67±0.02$^{***/+++/\#\#\#}$
pUG36-*PLC1*$^{4R/E425G}$ in *arg82Δ*	0.79±0.02$^{\underline{***/+++/\#\#\#}}$	1.16±0.03$^{\underline{***/+++/\#\#\#}}$	0.69±0.02$^{\underline{+++}}$
pUG36-PLC1 in *plc1Δ*	0.77±0.01	1.65±0.02	0.47±0.01
pUG36-*PLC1*^{4R} in *plc1Δ*	0.80±0.02	1.48±0.03	0.54±0.01
pUG36-*PLC1*^{E425G} in *plc1Δ*	1.39±0.05	1.74±0.09	0.81±0.03
pUG36-*PLC1* in *arg82Δ*	1.13±0.02	1.74±0.08	0.66±0.03
pUG36-*PLC1*^{4R} in *arg82Δ*	0.70±0.02	1.80±0.05	0.39±0.01
pUG36-*PLC1*^{E425G} in *arg82Δ*	1.16±0.01	1.70±0.09	0.71±0.05

[Significantly different from the corresponding values of GFP-Plc1p in *plc1Δ*: $^{***}P$<0.001; of GFP-Plc1p^{4R} in *plc1Δ*: ^{+++}P<0.001; of GFP-Plc1p^{E425G} in *plc1Δ*: $^{\#\#\#}P$<0.001.]
[Significantly different from the corresponding values of GFP-Plc1p in *arg82Δ*: $\underline{^{***}}P$<0.001; of GFP-Plc1p^{4R} in *arg82Δ*: $\underline{^{+++}}P$<0.001; of GFP-Plc1p^{E425G} in arg82*Δ*: $\underline{^{\#\#\#}}P$<0.001.]

Fluorescence images of logarithmic phase cultures (5 x 10^6 – 1 x 10^7 cells/ml) of *plc1Δ* (top) and *arg82Δ* (bottom) transformed with pUG36–*PLC1*$^{4R/E425G}$ and pUR34*NLS*, respectively. The left-hand columns show low light DIC images. The left-mid columns show the localisation of the indicated GFP constructs. The right-mid columns show the localisation of nuclei as obtained by transformation of cells with a NLS construct, and the merged images are shown on the right-hand columns. These images are representative of three replicate cultures. All strains were cultured in SC-Ura-Met-His+2% glu medium. The table shows ratio of fluorescence intensity of plasma membrane (PM), nucleus and cytosol. Each value represents the mean ± S.E.M. of ten determinations.

whether other domains of Plc1p might also be required for the association with the plasma membrane. I tested this by examining the localization of the truncation mutants, Plc1p$^{1\text{-}333}$, Plc1p$^{220\text{-end}}$ and Plc1p$^{(1\text{-}333)+C2}$ in *arg82Δ* cells. GFP-Plc1p$^{1\text{-}333}$ and GFP-Plc1p$^{220\text{-end}}$ are both stable (APPX. Fig A), and I also confirmed the stability of GFP-Plc1p$^{(1\text{-}333)+C2}$ (APPX. Fig A). As shown in Fig 4.26, Plc1p$^{1\text{-}333}$ includes the

entire PH domain, Plc1p$^{220\text{-end}}$ includes the XY and C2 domains, and the Plc1p$^{(1\text{-}333)+C2}$ mutant has the XY region deleted.

Fig 4.26: Diagram of the Plc1p truncation mutants

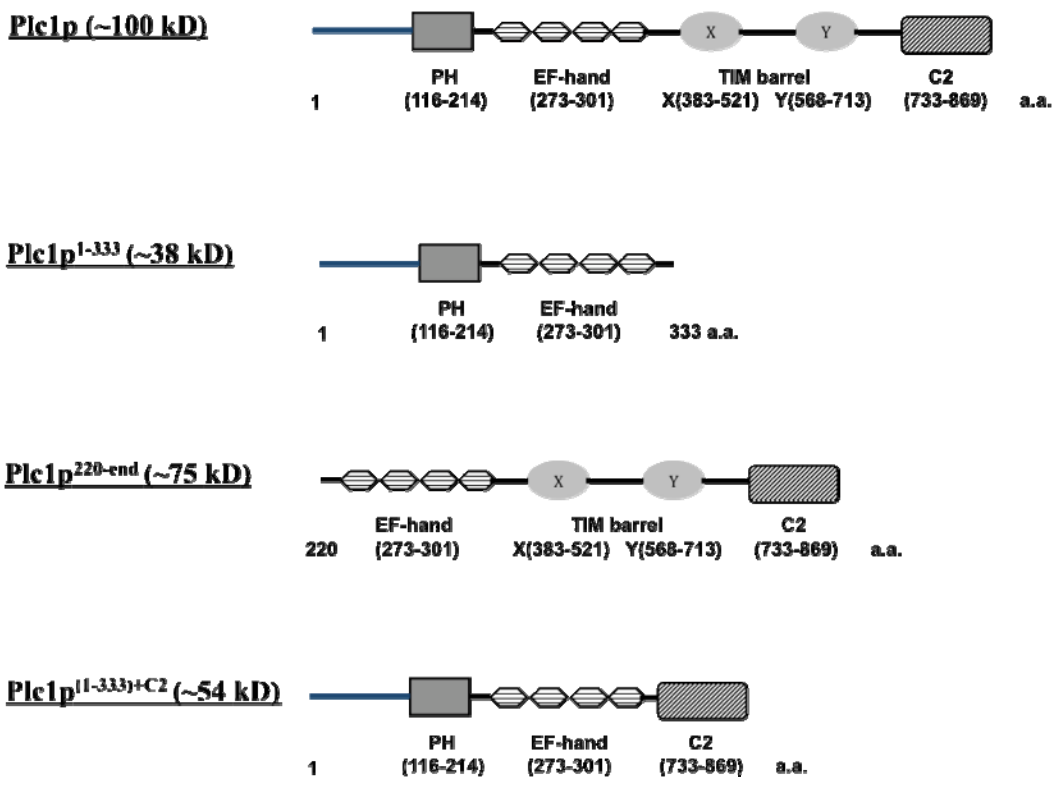

Thus, in *arg82Δ*, the GFP-Plc1p$^{1\text{-}333}$ tests the requirement for the XY and C2 region for its association with plasma membrane. The localization of GFP-Plc1p$^{220\text{-end}}$ meanwhile, and GFP-Plc1p$^{(1\text{-}333)+C2}$ were used to tell us if the PH domain and/or XY domain are indispensable for binding, respectively.

None of these truncation mutant constructs associated with the plasma membrane in *arg82*Δ cells, and GFP-Plc1p$^{220\text{-end}}$ and GFP-Plc1p$^{(1\text{-}333)+C2}$ were very concentrated in

the nucleus (Fig 4.27). Therefore, these latter two constructs were provided less useful insights into the association of Plc1p with the plasma membrane in *arg82*Δ cells.

Fig 4.27: Localization of GFP-Plc1p$^{1-333}$, GFP-Plc1p$^{220-end}$ and GFP-Plc1p$^{(1-333)+C2}$ in arg82Δ cells

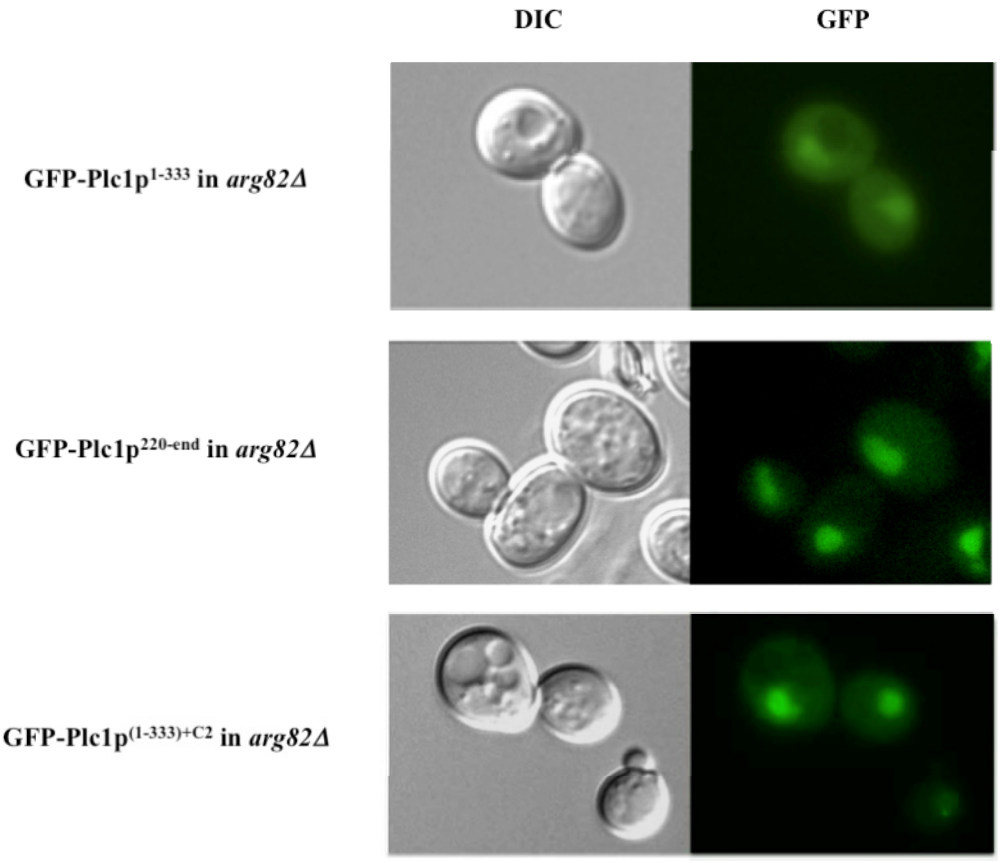

Genotype	Fluorescence Ratio		
	PM/Cytosolic	Nuclear/Cytosolic	PM/Nuclear
pUG36-*PLC1*$^{1-333}$ in *arg82Δ*	0.82±0.02***	1.44±0.06**	0.58±0.03*
pUG36-*PLC1*$^{220-end}$ in *arg82Δ*	0.79±0.02***	2.83±0.30**	0.33±0.05***
pUG36-*PLC1*$^{(1-333)+C2}$ in *arg82Δ*	0.78±0.01***	2.17±0.14*	0.37±0.02***
pUG36-*PLC1* in *arg82Δ*	1.13±0.02	1.74±0.08	0.66±0.03

[Significantly different from the corresponding values of GFP-Plc1p in *arg82Δ*: $^{***}P<0.001$, $0.001<^{**}P<0.01$, $0.01<^{*}P<0.05$.]

Low light DIC (left columns) and fluorescence images (right columns) of logarithmic phase cultures (5 x 10^6 – 1 x 10^7 cells/ml) of *arg82Δ* transformed with *PLC1* mutants indicated, respectively. Cells were grown in SC-Ura-Met+2% glu at 25°C. These images are representative of three replicate cultures. The table show the ratio of fluorescence intensity of plasma membrane (PM), nucleus and cytosol. Each value represents the mean ± S.E.M. of ten determinations.

4.13 Plc1p associates with the plasma membrane in *arg82Δvps41Δ* cells which have a reduced complement of PtdIns(4,5)P_2

The catalytically dead and PH domain mutants of Plc1p no longer associate with the plasma membrane. We wondered whether PtdIns(4,5)P_2 was involved in this binding of Plc1p with the plasma membrane.

Vps41p is a vacuolar membrane protein that is a subunit of the homotypic vacuole fusion and vacuole protein sorting (HOPS) complex (Nakamura *et al*., 1997). Mutations in *VPS41* cause many defects, including poor growth on low iron medium, altered vacuolar morphology, mis-sorting of membranous and soluble vacuolar proteins. One of our previous studies on Vps41p uncovered another defect: decreased levels of intracellular PtdIns(4,5)P_2 in *vps41Δ* cells (SK Dove 2008, unpublished.). I therefore constructed a *arg82Δvps41Δ* double mutant, to observe GFP-Plc1p's localization in the cells with a relatively low level of PtdIns(4,5)P_2.

arg82Δvps41Δ cells were very compromised, with slow growth and highly fragmented vacuoles. However, GFP-Plc1p was still on the plasma membrane, indicating that this localisation can be achieved despite a subnormal PtdIns(4,5)P_2 complement (Fig 4.28).

4.14 Localisation of GFP-Plc1p in *arg82Δ* cells after hypo-osmotic shock activation

Plc1p associates with the plasma membrane in unstressed *arg82Δ* cells. We were interested in knowing whether this association would change when cells were stressed. Dr Perera had earlier determined the phosphoinositide complements after

Fig 4.28: Localization of GFP-Plc1p in arg82Δvps41Δ

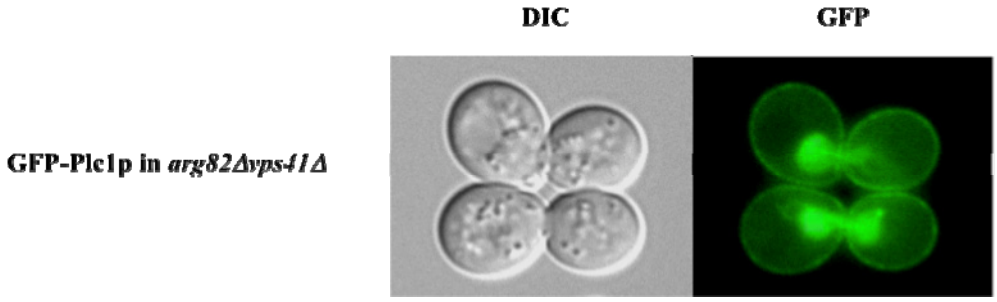

Genotype	Fluorescence Ratio		
	PM/Cytosolic	Nuclear/Cytosolic	PM/Nuclear
pUG36-*PLC1* in *arg82Δ vps41Δ*	1.14±0.03	1.68±0.03	0.68±0.01
pUG36-*PLC1* in *arg82Δ*	1.13±0.02	1.74±0.08	0.66±0.03

[There were no significant differences between the corresponding values of the two.]

Low light DIC (left columns) and fluorescence images (right columns) of logarithmic phase cultures (5 x 10^6 – 1 x 10^7 cells/ml) of *arg82Δvps41Δ* transformed with pUG36-*PLC1* were grown in SC-Ura-Met+2% glu at 25°C. These images are representative of three replicate cultures. The table shows the ratio of fluorescence intensity of plasma membrane (PM), nucleus and cytosol. Each value represents the mean ± S.E.M. of ten determinations.

hypo-osmotic challenge of wild-type, *plc1Δ* and *arg82Δ* cells. After Plc1p was activated, the basal level of PtdIns(4,5)P_2 was reduced by ~ 40% in wild-type and *arg82Δ* cells, but was unchanged in *plc1Δ* cells (Perera *et al*. 2004).

I investigated whether the distribution of GFP-Plc1p in *arg82Δ* cells would change after hypo-osmotic shock. I grew cells in medium supplemented with 0.9M NaCl (through two steps: 0.5M NaCl and then 0.9M NaCl) into exponential phase, and then quickly diluted them into 10 volumes of the same medium lacking salt. After cells had been grown with a high concentration of salt for several generations, their plasma membrane GFP-Plc1p fluorescence increased, and there was less fluorescence in the nucleus. After hypo-osmotic shock, plasma membrane GFP-Plc1p declined somewhat and nuclear GFP-Plc1p gradually reverted to the normal levels. 30 minutes after the hypo-osmotic shock, Plc1p had regained its usual intracellular distribution in *arg82Δ*

cells (Fig 4.29). Although it is possible that the loss of PtdIns(4,5)P_2 during Plc1p activation might have contributed to the dissociation of Plc1p from the plasma membrane upon activation, it should be remembered that the PtdIns(4,5)P_2 complement of cells grown in high salt is, as far as we know, normal.

Figure 4.29: Localization of GFP-Plc1p in arg82Δ during hypo-osmotic shock

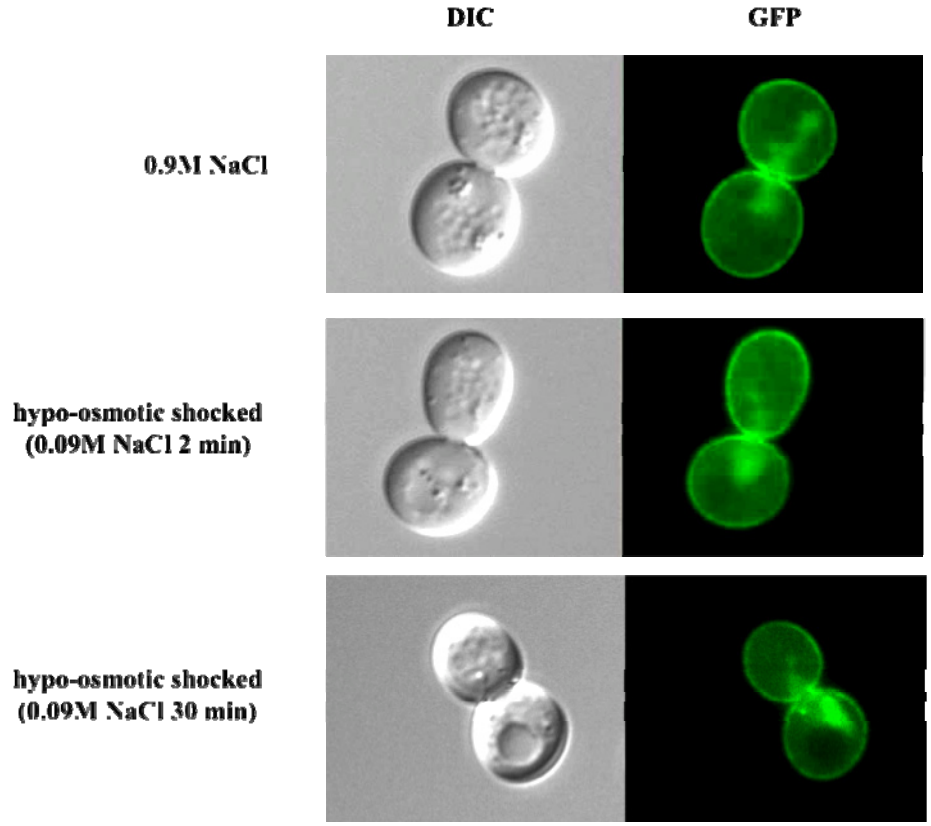

pUG36-*PLC1* in *arg82Δ*	Fluorescence Ratio		
	PM/Cytosolic	Nuclear/Cytosolic	PM/Nuclear
untreated	1.13±0.02	1.74±0.08	0.66±0.03
in 0.9M NaCl	1.30±0.03***	1.28±0.04***	1.03±0.05***
hypo-osmotic shocked - 0.09M NaCl 2 min	1.26±0.04**	1.44±0.06$^{**/+}$	0.88±0.04$^{***/+}$
hypo-osmotic shocked - 0.09M NaCl 30 min	1.20±0.05	1.66±0.11	0.77±0.07

[Significantly different from the corresponding values of the untreated: $^{***}P<0.001$, $0.001<^{**}P<0.01$; There were no significant differences between the untreated and the hypo-osmotic shocked for 30 min.] [Significantly different from the corresponding values of the cells grown in 0.9M NaCl: $0.01<^{+}P<0.05$; There were no significant differences from the hypo-osmotic shocked for 30 min.]

Low light DIC (left columns) and fluorescence images (right columns) of logarithmic phase cultures (5 x 10^6 – 1 x 10^7 cells/ml) of *arg82Δ*+ pUG36–*PLC1* grown at 25°C in SC-Ura-Met + 2% glu + 0.9M NaCl media followed by a rapid shift to 10 volumes of medium lacking salt for 2 min and 30 min. These images are representative of three replicate cultures. The table shows ratio of fluorescence intensity of plasma membrane (PM), nucleus and cytosol. Each value represents the mean ± S.E.M. of ten determinations.

4.15 Plc1p's localisation in *gpr1Δ* & *gpr1Δarg82Δ* cells

The plasma membrane glucose response protein, Gpr1p, is coupled to a G-protein α-subunit Gpa2p which regulates cAMP synthesis and PKA activity. Plc1p has been implicated in PKA signalling by affecting cAMP synthesis via an interaction with the Gpr1p/Gpa2p pathway (Ansari *et al*., 1999). Plc1p may physically interact with Gpr1p and Gpa2p**,** and Gpr1p may regulate Plc1p activity (Demczuk *et al*., 2008). I therefore determined whether deleting Gpr1p would influence the association between Plc1p and the plasma membrane.

I examined the localization of GFP-Plc1p in *gpr1Δ* and *gpr1Δ arg82Δ* cells. Plc1p was distributed between the nucleus and cytoplasm in *gpr1Δ*, as in wild-type cells, and it still associated with the plasma membrane in cells devoid of both Gpr1p and Arg82p (Fig 4.30). Therefore, Gpr1p seems to have no role in the association of Plc1p with the plasma membrane.

4.16 Inositol polyphosphates are involved in stress responses

PLC1 is not an essential gene, but cells devoid of Plc1p do not grow in stressed environments. Plc1p-mediated hydrolysis of PtdIns(4,5)P_2 is the only pathway for InsP_3 synthesis in *S. cerevisiae* (Odom *et al*., 2000; York *et al*., 1999), and the higher Ins*P*s generated from InsP_3 participate in multiple intracellular activities. Earlier, I presented evidence that correct intracellular localisation of Plc1p may be necessary for cells to maintain healthy growth under stress (section 3.7), and the fact that *arg82Δ* cells display increased transcription of Msn2p-dependent stress-responsive genes may indicate that synthesis of Ins*P*s are required for normal PKA signalling (Demczuk *et al*., 2008). I tested this idea with *arg82* mutants.

Fig 4.30: Localization of GFP-Plc1p in gpr1Δ and gpr1Δ arg82Δ cells

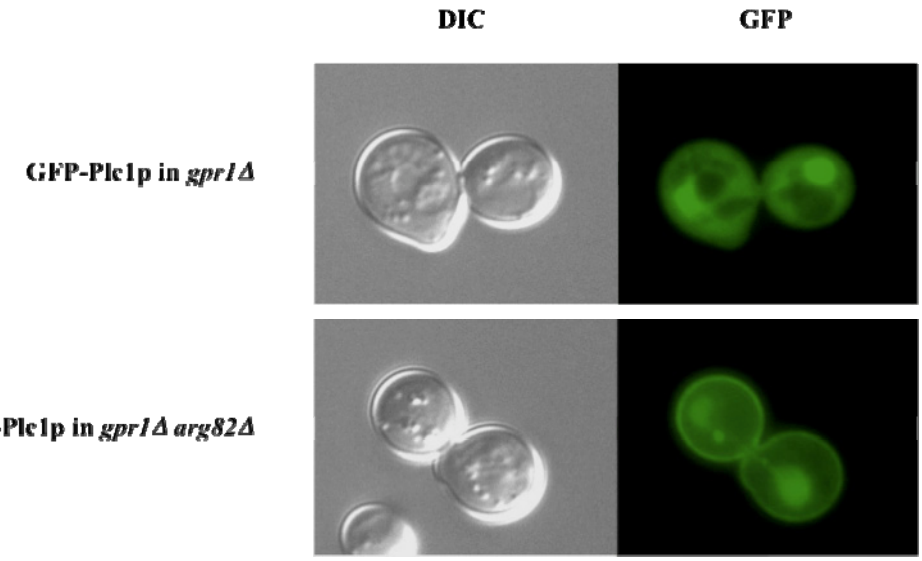

Genotype	Fluorescence Ratio		
	PM/Cytosolic	Nuclear/Cytosolic	PM/Nuclear
pUG36-*PLC1* in *gpr1Δ*	0.71±0.02	1.64±0.06	0.44±0.02
pUG36-*PLC1* in *gpr1Δ arg82Δ*	1.17±0.06***	1.77±0.08	0.68±0.05***
pUG36-*PLC1* in WT	0.74±0.01	1.70±0.08	0.44±0.02
pUG36-*PLC1* in *arg82Δ*	1.13±0.02	1.74±0.08	0.66±0.03

[Significantly different from the corresponding values of *gpr1Δ*: ***$P<0.001$. There were no significant differences between the corresponding values of GFP-Plc1p in WT and in *gpr1Δ*, in *arg82Δ* and in *gpr1Δ arg82Δ*.]

Low light DIC (left columns) and fluorescence images (right columns) of logarithmic phase cultures (5 x 10^6 – 1 x 10^7 cells/ml) of *gpr1Δ* and *gpr1Δarg82Δ* transformed with pUG36-*PLC1*, respectively, were grown in SC-Ura-Met+2% glu at 25°C. These images are representative of three replicate cultures. The table shows the ratio of fluorescence intensity of plasma membrane (PM), nucleus and cytosol. Each value represents the mean ± S.E.M. of ten determinations.

Plasmids expressing $ARG82^{D131A}$, $ARG82^{\Delta asp}$ and $ARG82^{G344R}$ were used here to investigate whether inositol polyphosphates downstream of Plc1p activation were essential to cell survival in stressed conditions. As shown in Fig 4.31, cells expressing $ARG82^{D131A}$ and $ARG82^{G344R}$, which make no InsP_5, both appeared sick at 37°C and in the presence of high salt (0.7M NaCl). In contrast, Arg82p$^{\Delta asp}$, a kinase-active mutant with an ablated DNA binding domain, grew as well as the cells harbouring wild type Arg82p. This strengthens the evidence that Plc1p alleviates stress responses as a result of the synthesis of inositol polyphosphates.

Fig 4.31: Growth of various ARG82 mutants under Stresses

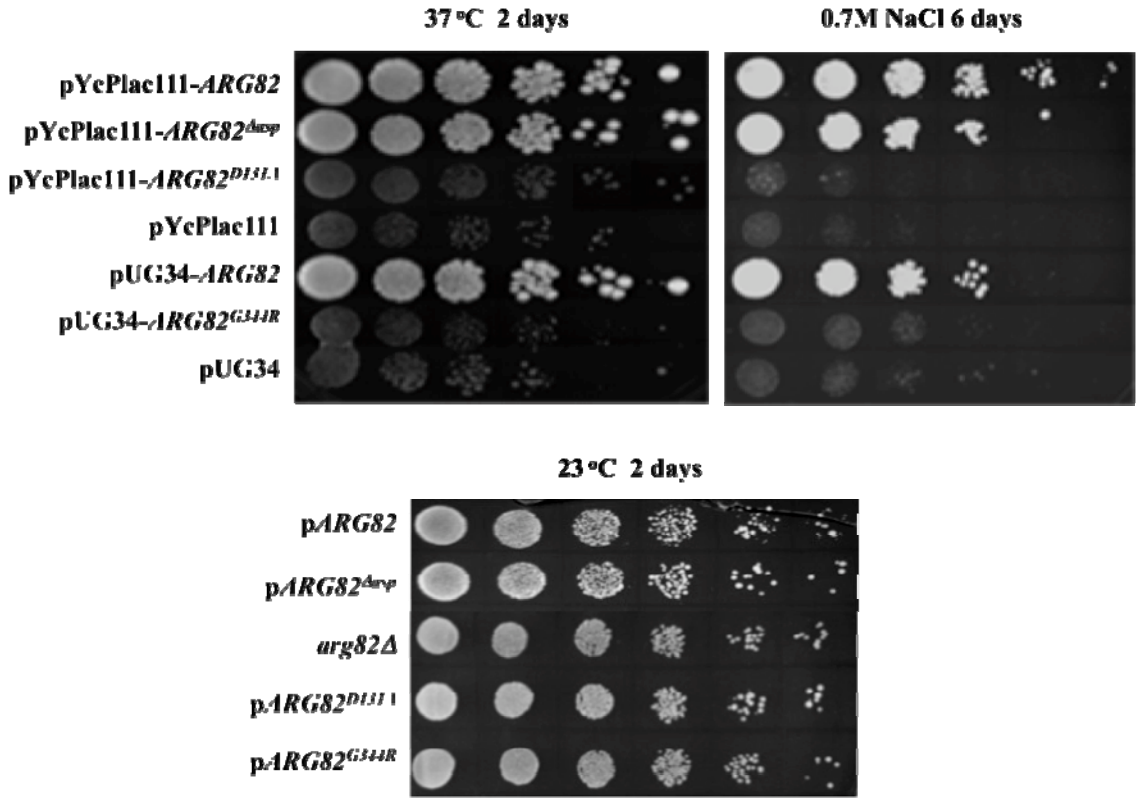

arg82Δ cells transformed with various plasmids as indicated were grown to exponential phase till about ~1 x 10^7 cells/ml in YPD (for *arg82Δ* cells), SC-His + 2% glu (for pUG34 plasmids) or SC-Leu+2% glu (for pYcPlac111 plasmids). Dilution assay was carried out as described in methodology section. Cells were serially diluted five-fold then grown on YTD+2% glu agar plates at 37 ^{o}C (till wild-type was fully grown) for 2 days or on the same plate but with 0.7M NaCl (till wild-type was fully grown) for 6 days. Control plate was grown at 23^{o}C for 2 days. Data represents three independent experiments.

4.17 Discussion

4.17.1 Arg82p can negatively regulate the interaction between Plc1p and the plasma membrane

In wild-type cells, GFP-Plc1p is distributed between the nucleus and the cytoplasm and displays no obvious interactions with any membranes. It was therefore unexpected to find GFP-Plc1p associated with the plasma membrane in *arg82Δ* cells (Fig 4.2). This is consistent with the idea that Plc1p has some kinship with PLC-δ_1: both can associate with the plasma membrane and can enter the nucleus. To what

degree the plasma-membrane association of Plc1p ever occurs, even transiently, in wild-type cells remains uncertain. The functional consequences of this membrane binding by Plc1p are also unclear, as Plc1p activation in *arg82Δ* cells in response to hypo-osmotic shock seems normal (Perera *et al*., 2004).

So, how does Arg82p influence membrane binding? I first confirmed that wild-type *ARG82* restores wild-type Plc1p localisation to *arg82Δ* cells. This rules out the trivial possibility that the observed localisation shift was the result of an unlinked mutation (Fig 4.2).

Arg82p was first discovered as a protein chaperon required to stabilize the Arg80p-Mcm1p complex during the control of expression of arginine-responsive genes. This requires the Arg82p poly-aspartate domain (residues 282-303) but not the Ins*P* kinase domain (residues 127-135) for Ins(1,3,4,5,6)P_5 synthesis, although there is considerable controversy over this point (Odom *et al*., 2000; Dubois *et al*., 2000). The two domains and functions do indeed appear to be independent from each other in our hands, as was originally reported (Dubois *et al*., 2000). Indeed, the Arg82p kinase dead mutant is sensitive to stresses (Fig 4.31) in a manner similar to a *PLC1* knock-out strain, whereas the DNA binding function of Arg82p is not essential when growing in normal media under stresses as mutants deficient in arginine metabolism displayed a 'wild type' phenotype in response to stress (Fig 4.31).

Various observations made us wonder whether Arg82p might physically interact with Plc1p and so facilitate the rapid metabolism of InsP_3 to InsP_6, an idea that became more attractive when it was observed that Arg82p and Plc1p sometimes show similar

intracellular distributions (Fig 4.1). However, Arg82p localisation did not change following deletion of *PLC1* (Fig 4.3), and I obtained no evidence for a physical association between Plc1p and Arg82p by co-immunoprecipitation experiments (Fig 4.4 and Fig 4.5) or by the observation that a catalytically inactive GFP-Arg82p^{D131A} and Plc1p showed different distributions in *arg82Δ* cells (Fig 4.8).

It therefore seemed likely that the products of Arg82p were preventing Plc1p from associating with the plasma membrane in normal cells. I tried to test this idea by inhibiting Plc1p activity and so removed all inositol phosphates, since they all derive from Plc1p mediated cleavage of PtdIns(4,5)P_2. This method is an independent way to achieve an even greater loss of inositol phosphates than is the case in *arg82Δ* cells (York *et al*., 1999).

I first attempted to use the PLC-inhibitor U73122 to arrest Plc1p activity. U73122 partially inhibits Plc1p (Perera *et al*., 2004), but the mechanism of inhibition is ill-defined. Plc1p was dissociated from the plasma membrane of *arg82Δ* cells by U73122 treatment, maybe because of inhibition of active site binding to PtdIns(4,5)P_2. This hypothesis was strengthened when I made several active site mutants of Plc1p. The catalytically inactive Plc1p^{H439L} was also no longer able to associate with the plasma membrane of *arg82Δ* cells (Fig 4.12). This mutant contains only a single amino acid substitution in the active site, supporting the idea that substrate binding may be required for membrane association.

A second Plc1p mutant, Plc1p^{E452G}, was still plasma membrane bound in *arg82Δ* cells (Fig 4.12) but was also catalytically compromised, as indicated by the heat sensitivity

of strains expressing this construct as their sole Plc1p (Fig 4.13). This suggested that Plc1p^{E452G} might also be plasma membrane-bound in *plc1*Δ cells, and this was indeed the case (Fig 4.15). These results are all consistent with a hypothesis that Plc1p binds to the plasma membrane via its active site and that inositol polyphosphates inhibit this association.

The question now turned to which inositol phosphates might inhibit Plc1p membrane binding? To examine this question the localisation of GFP-Plc1p was examined in strains bearing deletions of the genes encoding the other known inositol phosphate kinases, Ipk1p, Kcs1p and Vip1p. As shown in Figure 4.17, inactivating these kinases did not cause a localisation shift of GFP-Plc1p to the plasma membrane. This refocused attention on Arg82p, and I analysed a mutant from Dr John York's lab (Arg82p^{G344R}) that can synthesize Ins(1,4,5,6)P_4 but not Ins(1,3,4,5,6)P_5. GFP-Plc1p remained associated with the plasma-membrane in this mutant (Fig 4.19), indicating that Ins(1,4,5,6)P_4 does not dissociate Plc1p from the plasma membrane.

To address the notion that Arg82p-generated Ins(1,3,4,5,6)P_5 can dissociate Plc1p from the plasma membrane, I attempted to "add back" InsP_5 to cells as a cell permeant 2-O-Butyryl-Ins(1,3,4,5,6)P_5 but was unsuccessful. This molecule can cross the plasma membrane of mammalian cells and becomes trapped when the butyryl ester is removed by esterases. This experiment failed to destablise GFP-Plc1p from the plasma membrane in *arg82Δ* cells (Fig 4.20) or of GFP-Plc1p^{E425G} in *plc1*Δ cells (Fig 4.21). Indeed, the reverse was true: there appeared to be more Plc1p on the membrane after treatment, though this might have been a consequence of a decrease in nuclear Plc1p. The reason for this decrease in nuclear Plc1p is not clear, but may be a result of

elevated inositol phosphates, since I also observed a similar reduction in nuclear Plc1p in *kcs1Δ*, *vip1Δ* and *kcs1Δvip1Δ* mutants (Fig 4.17), all of which exhibit abnormally high levels of certain higher inositol phosphates. Why exogenous InsP_5 was not able to destablise Plc1p at the same time is not clear. However, knowing InsP_5 is involved in such association does not rule out more phosphorylated inositol phosphates playing a role since the other kinases were intact in *arg82*Δ cells.

The kinases involved in the Ins*P*s synthesis pathway sequentially phosphorylate specific substrates and must work closely together as no isomer of InsP_3, Ins(1,4,5,6)P_4 or Ins(1,3,4,5,6,)P_5 consistently accumulates in the control and stimulated wild-type cells (Perera *et al*., 2004). When depleted of a certain Ins*P* kinase, yeast cells tend to accumulate the substrate of this kinase (or products of its degradation by an alternative route) (Perera *et al*., 2004), and these inositol phosphates are also subjected to increased dephosphorylation by specific phosphatase which results in a characteristic inositol polyphosphate profile that is distinct for each inositol phosphate kinase mutant. Various workers, including Dr Perera from our lab, have previously analyzed the inositol polyphosphate accumulation in cells lacking the inositol polyphosphate kinases Arg82p, Ipk1p and Kcs1p (Perera *et al*., 2004). Fig 4.32 shows the inositol polyphosphates that accumulate in inositol polyphosphate kinase knock-out strains. Compared with the wild type, the major change in *arg82Δ* cells was a complete loss of higher inositol phosphates and a massive increase in the amount of Ins(1,4)P_2 (InsP_2) most likely resulting from an enhanced rate of InsP_3 dephosphorylation. In *ipk1Δ* cells, an accumulation of InsP_5 and *PP*-InsP_4 was seen and a huge peak of InsP_6 plus some forms of InsP_4 were found in *kcs1Δ* cells (Fig 4.32). Since Dr Perera's work, Vip1p was discovered as a second inositol

pyrophosphate synthase, with products that are structurally different from those produced by Kcs1p (Mulugu *et al*., 2007). *vip1Δ* cells would therefore be expected to have a profile of inositol polyphosphate accumulation largely similar to that of to *kcs1Δ.*

Fig 4.32: Composite HPLC chromatogram showing the combined elution profiles of [^{3}H]labelled inositol polyphosphates in wild-type, arg82Δ, ipk1Δ, and kcs1Δ of BY4742 cells, respectively, after hypo-osmotic shock. Figure does not show the Ins(1,4)P2 that accumulated in arg82Δ cells. (Perera 2002, p.124)

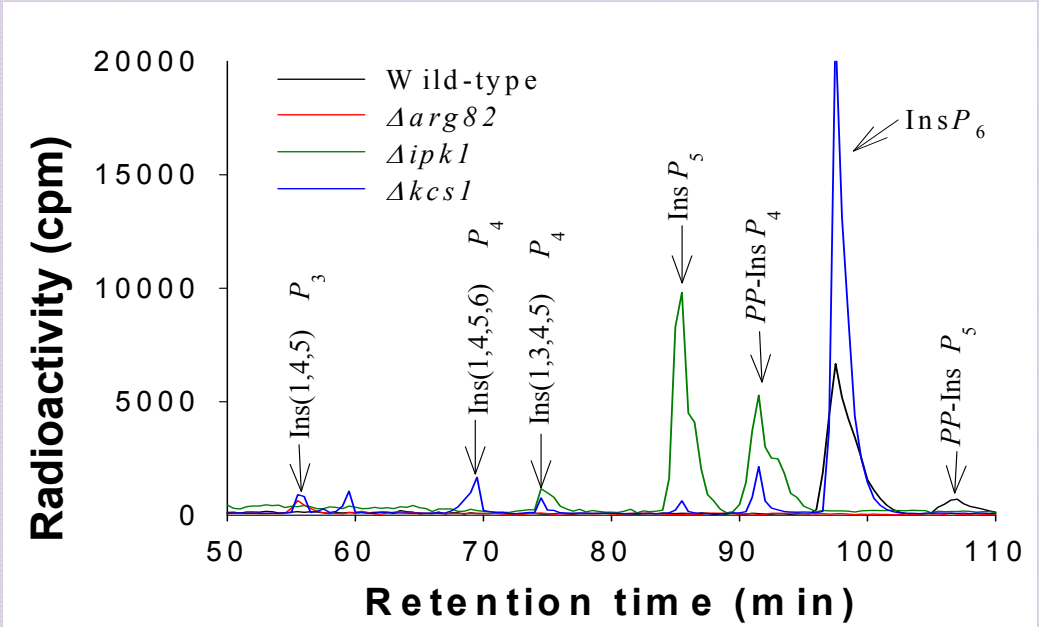

The accumulation of Ins(1,4)P_2 and the lack of InsP_5/*PP*-InsP_4 in *arg82Δ* indicates that either InsP_5 or a pyrophosphorylated inositol phosphate generated from InsP_5 might regulate the association of Plc1p with the plasma membrane.

Inositol pyrophosphates are now recognized as a group of important multi-functional molecules that regulate diverse cellular processes, including endocytic trafficking (Saiardi *et al*., 2002), DNA recombination (Luo *et al*., 2002) and are required for

vacuole morphogenesis (Saiardi *et al*., 2000b), cell wall integrity and resistance to salt stress (Dubois *et al*., 2002).

Alternatively, it could be that any of the more highly phosphorylated inositol phosphate than InsP_5 might be able to fulfil this role in cells. I favour this latter hypothesis because the only inositol phosphate to reach substantial levels in wild-type cells is InsP_6 (Fig 4.31). Yet if only InsP_6 were required, then GFP-Plc1p should be on the plasma membrane in *ipk1*Δ cells. Hence I suggest that InsP_6 normally inhibits Plc1p associating with the membrane but that other inositol phosphates, such as InsP_5 and *PP*-InsP_4, can also mediate this effect if their levels become elevated. Surely, the simplest explanation is that any Ins*P*s with 5 or more phosphates keeps Plc1p off the plasma membrane. However, even some InsP_2 could weakly interfere with Plc1p's interaction with plasma membrane because it is notable that the GFP-Plc1p^{E425G} gives a higher level of plasma membrane fluorescence in *plcΔ* than GFP-Plc1p does in *arg82Δ* cells: the former has no inositol phosphates whilst the latter has very high levels of InsP_2.

4.17.2 How does Plc1p interact the plasma membrane?

Having defined as closely as possible that inositol polyphosphates, primarily InsP_5 and/or InsP_6, prevent Plc1p from associating with the plasma membrane, I next tried to understand what features of the Plc1p molecule are involved in its interaction with the plasma membrane in *arg82Δ* cells that lack inositol polyphosphates.

I already had evidence that PtdIns(4,5)P_2 binding by the active site was probably needed, and I next tested if an intact PH domain was required. The PH domain and C2

domain are known as a membrane-targeting domain for most PLCs. The binding of Plcδ_1 to PtdIns(4,5)P_2 via its PH domain is important for processive hydrolysis in animal cells (Cifuentes *et al*., 1993; Lomasney *et al.*, 1996), and the PH domain of PLC-δ_1 is also known to bind to inositol polyphosphates. For example, InsP_3 binds to PLC-δ_1 via its PH domain with high affinity and competitively with PtdIns(4,5)P_2 (Cifuentes *et al*., 1994; Lemmon *et al*., 1995). Indeed, there is a substantial body of literature that suggests that inositol phosphates can inhibit the interactions between many PH domains and phosphoinositides (Hirata *et al*., 1998). This begged the question of whether the PH domain of Plc1p is the region that the inositol polyphosphates interact with in order to prevent membrane binding Plc1p?

As shown in Fig 4.22, several basic residues in the PH domain are required for membrane binding, as the Plc1p^{4R} mutant did not associate with the plasma membrane in *arg82Δ* cells. Oddly, this over-expressed mutant Plc1p did allow *plc1*Δ cells to grow at 37ºC (Fig 4.23), suggesting that growth at 37ºC does not need Plc1p to associate with the plasma membrane stable enough to be seen in our experiments.

Unsurprisingly, the same 4R mutant also destabilized the plasma-membrane binding of the Plc1p^{E425G} mutant in *plc1*Δ cells (Fig 4.25) as expected. The fluorescence looked rather diffuse though GFP-Plc1p$^{4R/E425G}$ was fairly a stable construct (APPX. Fig A), and it was intriguing that the nuclear fluorescence was dramatically decreased in the combined mutant while both GFP-Plc1p^{4R} and GFP- Plc1p^{E425G} were fairly nuclear. This might suggest that PtdIns(4,5)P_2 binding may somehow contribute to nuclear localisation, since both of these domains are likely to interact with this lipid.

Much of the effect of the 4R mutant could derive from the loss of the R111 residue since a Plc1p^{R1} mutant had almost as little plasma-membrane binding as the Plc1p^{4R} mutant (Fig 4.24). Therefore, sequence in the link of N-terminal extension and the PH domain are especially important. This was also confirmed by a truncation mutant Plc1p$^{220\text{-end}}$ which has no N-terminal 220 residue including the whole PH domain and failed to associate with plasma membrane in *arg82Δ* cells (Fig 4.27).

That neither the truncation mutants of Plc1p (Plc1p$^{1\text{-}333}$ and Plc1p$^{(1\text{-}333)+C2}$) or Plc1p^{H439L} associated with the plasma membrane in *arg82Δ* cells (Fig 4.27), suggested that domains other than the PH domain are also required for the plasma membrane interaction.

The XY domain interacts with substrates, the membrane surface and the activating Ca^{2+}. A ridge of hydrophobic residues surrounding the active site is important for the interaction with and insertion into the membrane (Rebecchi and Pentyala, 2000). However, what the PH and C2 domains of Plc1p are binding to is unclear (Flick and Thorner, 1993). Previous studies have demonstrated strong evidence that the C2 domain in other proteins binds to lipids, usually either PtdSer and/or PtdIns(4,5)P_2 (Sutton *et al*., 1995; Rhee, 2001). The C2 domain of PLC-ζ was found interact with phosphoinositides, namely PtdIns3*P* or PtdIns5*P*, and this seemed to negatively regulate the PLC-ζ (Kouchi *et al*., 2005).

That Plc1p can associate with the plasma membrane, even when it is over-expressed, suggests that at least some of its binding partners are reasonably abundant molecules, probably lipids. Which of these interactions is regulated by inositol phosphates is also

undefined, although the known propensity of PH domains to bind inositol phosphates is established and it would be surprising if this was not the site of lipid-inositol phosphate competition.

In an attempt to define possible protein ligands for the various domains of Plc1p, I tried looking at GFP-Plc1p localisation in mutants that remove or reduce several known Plc1p-interactors. The first was Gpr1p, as Plc1p has recently been implicated as a possible component of the Gpr1p-Gpa2p signaling module, participating in PKA signalling by affecting cAMP synthesis (Ansari *et al*., 1999). The Plc1p/Grp1p/Gpa2p complex operates in a growth control pathway parallel to Ras2p (Demczuk *et al*., 2008). The requirement for Plc1p in this pathway is unclear, as there is some suggestion that the protein merely acts as some sort of scaffold. Gpr1p is resident on the plasma membrane and was reported to enhance PtdIns(4,5)P_2 hydrolysis by Plc1p through either a direct regulation of Plc1p or by mediating the recruitment of Plc1p to the plasma membrane and to PtdIns(4,5)P_2 (Demczuk *et al*., 2008). However, deletion of *GPR1* had no effect on GFP-Plc1p membrane interaction in a double *gpr1Δ arg82Δ* cells (Fig 4.30).

Similarly, an attempt to reduce PtdIns(4,5)P_2 levels by making a *VPS41* deletion was also not successful in altering the binding of Plc1p to the cell surface (Fig 4.28). *VPS41* encodes a vacuole membrane protein (Nakamura *et al*., 1997) and *vps41Δ* cells were found having relatively low level of membrane PtdIns(4,5)P_2 (SK Dove 2008, pers. comm.). The reason the double mutant may still have displayed plasma membrane fluorescence could be because this strain still retains substantial PtdIns(4,5)P_2 (about ¼ to ½ or normal SK Dove 2008, unpublished) or because the

levels of PtdIns(4,5)P_2 are altered or restored in the *arg82Δvps41*Δ cells used in this experiment, as I did not measure this in the double mutant. This needs be further addressed by looking at GFP-Plc1p localisation in *mss4-1*, a mutant of the yeast PtdIns4*P* 5-kinase Mss4p, that have even lower levels of PtdIns(4,5)P_2.

Finally, I used the above system to see if plasma membrane localized Plc1p could be used as a tool to study activation of Plc1p. I tried using hyper-osmotic stress and demonstrated that changes in the localisation of Plc1p were detected during activation: a decrease in GFP tagged protein signal on the plasma membrane (Fig 4.29). This would be expected if PtdIns(4,5)P_2 hydrolysis was destabilizing Plc1p's membrane association. It is a very interesting set of results because previously, Dr Perera demonstrated that when yeast cells are incubated at 37ºC, the complement of PtdIns(4,5)P_2 increases by 2-4 fold, as do the levels of inositol phosphates (Perera *et al*., 2004). We wonder if the same is true of yeast exposed to salt for long periods because Plc1p is known to be required for growth under both these stressful conditions. If so, then this would explain why more Plc1p is on the plasma membrane immediately before dilution. These data also seem consistent with the idea that plasma membrane GFP-Plc1p could be used to monitor Plc1p activation in cells.

4.17.3 Models

Overall our data are consistent with a role for Arg82p derived inositol phosphates in the negative regulation of Plc1p-plasma membrane interaction and confirmed by the association of a catalytically inactive mutant GFP-Plc1p^{E425G} with plasma membrane in *plc1*Δ cells.

The above study allows me to propose the following model:

In cells devoid of Arg82p where the normal inositol phosphate profile consists of almost no InsP_3 and mainly Ins(1,4)P_2, Plc1p is associated with plasma membrane via binding with PtdIns(4,5)P_2 through the concert effort of PH domain, XY region and C2 domain presumably.

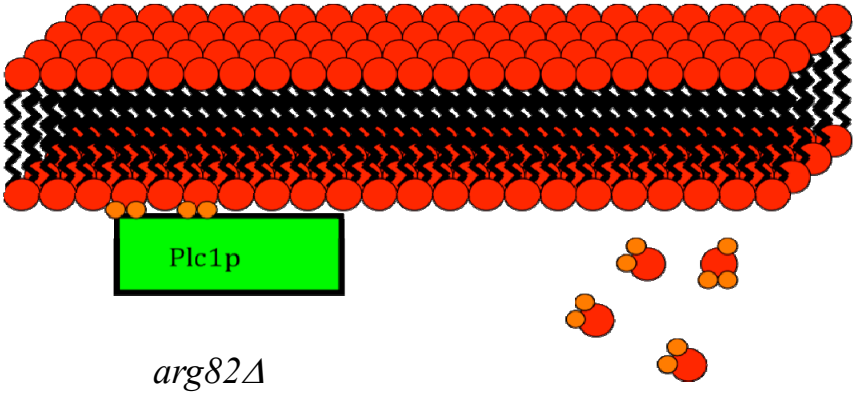

arg82Δ

In wild-type cells where InsP_6/Ins(1,3,4,5,6)P_5 levels are substantial, Plc1p interacts with Ins*P*s. This creates negative feedback and prevents the association of Plc1p with the plasma membrane. Exactly how this interaction inhibits binding is not clear but is likely to involve a competition with the PH domain. Despite the fact that a number of PH domain-inositol phosphate interactions are known, most of these interactions have only been found *in vitro*. There are in fact very few examples where inositol phosphates are actual physiological regulators of protein-lipid interactions and it is gratifying to have added another such phenomena to the overall picture.

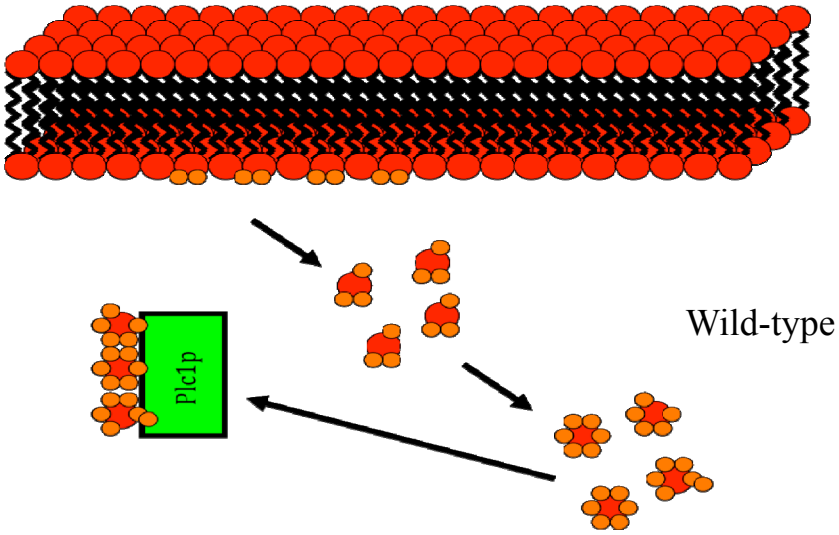
Plc1p
Wild-type

Chapter 5 Concluding remarks and future work

5.1 Identification of the signals that direct nuclear localisation of Plc1p

Further attempts to identify the NLS sequence(s) of Plc1p should focus on the region defined by amino-acid residues 220 to 333 using a random screen. The key to this type of approach is to find a protein that is deleterious when constitutively nuclear e.g. Pka3p. If time had allowed I would have first randomly mutagenised the 220-333 amino-acids tract of DNA by error prone PCR. I would then have created a library of these mutant *PLC1* truncation mutants fused to the *PKA3* gene and tagged with GFP at the C-terminus. The whole library of constructs would have been placed under control of an inducible promoter (e.g *GAL1* promoter that is repressed by growth in glucose containing media and is induced by galactose). The library would then have been transformed into yeast and proteins bearing a non-functional Plc1p-NLS sequence isolated via growth on galactose (If the NLS is mutated, Pka3p will be cytoplasmic and unable to affect cell growth; hence cytoplasmic mutants will grow much faster on galactose medium). Mutants with in frame stop codons could be identified since they would not express any GFP: since GFP is at the C-terminus of the construct. Genuinely cytoplasmic proteins could then be identified using visualisation of the relevant fusion proteins by microscopy. The plasmids would then be isolated and sequenced to determine which residues are mutated and hence lead to disruption of the NLS, creating a $Plc1p^{NLS}$ mutant.

The challenge to this type of screen would be the stability of the GFP tagged mutant and the activity of Pka3p as a fusion protein. Also, as several PH domain mutations can weaken the nuclear localisation signal of Plc1p but neither completely abolishes

the nuclear translocation, we are expecting that a structural-fold might direct nuclear localisation of Plc1p, rather than a simple sequence motif.

Yeast two hybrid screens could also be utilized to find proteins that interact with Plc1p, and deletion mutants of each one of them examined for Plc1p-localisation: if any displayed a completely cytoplasmic Plc1p then this would be a good indication that it is not a true NLS that is directing Plc1p to the nucleus, but instead it is a protein-protein interaction.

5.2 Inositol polyphosphates accumulation profile in *PLC1* mutants

Both $Plc1p^{NES}$ and $Plc1p^{PKI}$ failed to respond to stress, while $Plc1p^{CAAX}$ and $Plc1p^{PKI/NES}$, which maintain Plc1p in both nucleus and cytoplasm, displayed full growth under these stresses. All these results strongly suggest that Plc1p function is localisation dependent and Plc1p is required in both cytoplasm and nucleus to exert control.

Based on the fact that yeast has no InsP_3 receptor and that the yeast PKC homolog doesn't respond to DAG, most of the functions of Plc1p must be mediated via inositol polyphosphates. Plc1p regulated stress responses are at least partially through the inositol polyphosphates as indicated by the failure of growth under stresses of various Arg82p, and Kcs1p kinase disrupted mutants, as well as the catalytically inactive mutant I have described in this work. Water soluble inositol phosphates have been an area of active study in recent years and their diverse functions in multiple cellular processes have been revealed. It has been suggested that these inositol phosphates act as "second messengers", yet the available evidence supports a different conclusion as

the concentration of these molecules is normally high, even in unstimulated cells. This implies a more fundamental 'house-keeping' role for these molecules, where changes in their concentration are not so important, though it does not rule out a second messenger role.

A very important set of experiments would be to look at the generation of inositol phosphates in the knock-in constructs I have created, especially in response to heat, salt and hypo-osmotic stress, using a [^{3}H]inositol labelling approach. Plc1p is activated under all these stress conditions and it will be interesting to determine to what extent this activation still happens in the nuclear versus cytoplasmically restricted Plc1p mutants. It will also be instructive to determine if the isomers of inositol phosphates produced change once Plc1p is restricted in one compartment or another. The answer to this question should give us an insight into whether the inositol phosphate kinases are physically associated with Plc1p: I have found no evidence for this so far but neither have I ruled it out.

One important issue will be to learn where the "basal" pool of higher inositol phosphates is located and compare this with the location of the "stimulated" pool that appears during heat or salt or hypo-osmotic stress. Will this be the same compartment for all of these stresses or will it be different? Higher inositol phosphates, with six or more phosphate groups, are soluble molecules and there are pores in the nuclear envelope that would seem to make restricting their subcellular localisation unlikely. However, higher inositol phosphates are not as mobile as might be expected. A large hydration shell of ordered water probably surrounds the highly charged inositides and this seems to result in a much slower and more restricted diffusion than might be

expected (Van der Kaay and Van Haastert, 1995). Higher inositol phosphates generated in one of the compartments could therefore conceivably be retained and unable to diffuse through the nuclear pores. What's more, there are high concentrations of inositol phosphate phosphatases in the cytoplasm which could soak up any small leakage from the nucleus, rendering the cytoplasm inositol phosphate poor relative to the nucleus.

The above assumptions are possible but have yet to be confirmed. Many of the functions of higher inositol phosphates elucidated so far appear to be nuclear functions that are essentially "house-keeping", but the osmotic shock induced InsP_6 accumulation appears to be a cytoplasmic event (Perera *et al*., 2004). The Plc1p^{NES} and Plc1p^{PKI} constructs that are restricted to either the nucleus or the cytoplasm will help to test these hypotheses and to see if pools of spatially restricted higher inositol phosphates really occur *in vivo*.

The next major question is how inositol phosphates actually function? One hypothesis is that the inositol pyrophosphates can pyrophosphorylate proteins that have already been "primed" with a serine phosphorylation by casein kinase I isoforms. However, some inositol pyrophosphates also seem to act as simple allosteric regulators, for example, InsP_7 and Pho81p. Whatever the case, it is likely that additional effectors remain to be found and if time allowed I would have enjoyed making some high specific activity InsP_7 and InsP_8 and using them to probe for inositol phosphate binding proteins in yeast cell lysates. I would have followed this by FPLC mediated protein fractionation, to reduce the complexity of the mixture to distinct but resolved bands on an SDS-PAGE gel, and then used FT-ICR Mass spectrometry to determine

which proteins were in each band: an analysis of the phenotypes of deletion mutants for each identified protein should quickly expose any potential binding proteins.

5.3 Upstream activator(s) for Plc1p

The upstream activator of Plc1p remains undefined and this is an area I would have relished having time to dissect. An increase in Ca^{2+} concentration from entry of extracellular Ca^{2+} is proposed as a general mechanism of activation of Plc-δs (Das *et al.*, 1993; Kim *et al.*, 1999; Rebecchi and Pentyala, 2000; Rhee, 2001). Plc1p activation is regulated in response to a hypo-osmotic shock (Batiza *et al.*, 1996) and Ca^{2+} influx is triggered by this stress, although Perera *et al.* (2004) observed no change in Plc1p activation when yeast cells were cultured in medium devoid of all divalent cations. I have noticed the hypo-osmotic shock induced localisation change of Plc1p which may indicate activation. Dr Nevin Perera noticed that several genes from the PKC1-MAP kinase pathway seemed to affect Plc1p activation when deleted: namely *WSC1*, *WSC2*, and *WSC3* (for cell wall integrity and stress response component) (Perera 2002, p141). It seems unlikely that these are the direct upstream activators since these proteins are only found in ascomycete yeast, though they do have homology with some other protein families with a wider distribution. Since Plc-δs are present in most eukaryotes, it seems likely that there will turn out to be some conservation in the way these enzymes are activated: perhaps one of the GTPases downstream of the WSC proteins will turn out to be this activator. I would therefore check regulation of Plc1p in deletion mutants of the entire Pkc1p MAPK pathway if time allowed.

5.4 What is the key factor that prevents Plc1p from associating with the plasma membrane in normal cells?

Evidence has been presented in this work to suggest that inositol phosphates might be generating negative feedback: destabilizing Plc1p's interaction with the plasma membrane and hence no plasma membrane localised GFP-Plc1p is seen in normally growing cells. However, the exact nature of this interaction remains ill-defined and needs further work.

The [^{3}H]inositol labelling assay would help to understand the inositol polyphosphates and PPIn accumulation in *arg82Δ*, $ARG82^{G344R}$ and $PLC1^{E425G}$ cells, and therefore might give clues to decipher the increased level of interaction of Plc1p with the plasma membrane in these mutants.

Since mutations that interrupt the PH domain of Plc1p result in a loss of interaction with plasma membrane, it seems reasonable to try and test if an increase in the levels of PtdIns(4,5)P_2 might be responsible for Plc1p binding to the plasma membrane in *arg82*Δ mutants. Most PtdIns(4,5)P_2 is in the plasma membrane and regulates various cellular processes, many of which seem to occur constitutively, such as its role in the actin cytoskeleton and as an essential co-factor for a number of ion channels.

An *in vitro* vesicle binding assay would be ideal to decide the potential negative feedback on Plc1p by inositol phosphates. Highly purified recombinant Plc1p and its catalytically dead form Plc1p^{E425G} would be essential for this assay: this has been a serious impediment to setting up this experiment since Plc1p is not expressed well in *E.coli*. If I had had time to produced recombinant Plc1p via another expression system

then I would have liked to have tested whether InsP_5, InsP_6 and *PP*-InsP_4 could affect the binding of Plc1p to PtdCho vesicles doped with 3 mol % PtdIns(4,5)P_2.

References

Adam, A., Goccschling, D. E., Kaiser, C. A., and Sterns, T., eds., *Methods in Yeast Genetics,* Cold Springs Harbour Laboratory Manual [1997]

Akhtar, N., Pahlman, A.K., Larsson, K., Corbett, A.H., and Adler, L. (2000). SGD1 encodes an essential nuclear protein of Saccharomyces cerevisiae that affects expression of the GPD1 gene for glycerol 3-phosphate dehydrogenase. FEBS Lett *483*, 87-92.

Alcazar-Roman, A.R., Tran, E.J., Guo, S., and Wente, S.R. (2006). Inositol hexakisphosphate and Gle1 activate the DEAD-box protein Dbp5 for nuclear mRNA export. Nat Cell Biol *8*, 711-716.

Anderson, R.a.R., EG (1930). The chemistry of the lipids of tubercle bacilli.xx. the occurrence of mannose and inosite in the phosphatide fractions from the human, avian, and bovine tubercle bacilli. J Biol Chem *89*, 611-617.

Ansari, K., Martin, S., Farkasovsky, M., Ehbrecht, I.M., and Kuntzel, H. (1999). Phospholipase C binds to the receptor-like GPR1 protein and controls pseudohyphal differentiation in Saccharomyces cerevisiae. J Biol Chem *274*, 30052-30058.

Atherton, R.S., and Hawthorne, J.N. (1968). The phosphoinositide inositolphosphohydrolase of guinea-pig intestinal mucosa. Eur J Biochem *4*, 68-75.

Auesukaree, C., Tochio, H., Shirakawa, M., Kaneko, Y., and Harashima, S. (2005). Plc1p, Arg82p, and Kcs1p, enzymes involved in inositol pyrophosphate synthesis, are essential for phosphate regulation and polyphosphate accumulation in Saccharomyces cerevisiae. J Biol Chem *280*, 25127-25133.

Bae, Y.S., Cantley, L.G., Chen, C.S., Kim, S.R., Kwon, K.S., and Rhee, S.G. (1998). Activation of phospholipase C-gamma by phosphatidylinositol 3,4,5-trisphosphate. J Biol Chem *273*, 4465-4469.

Balla, T. (2006). Phosphoinositide-derived messengers in endocrine signaling. J Endocrinol *188*, 135-153.

Baird, G.S., Zacharias, D.A., and Tsien, R.Y. (2000). Biochemistry, mutagenesis, and oligomerization of DsRed, a red fluorescent protein from coral. Proc Natl Acad Sci U S A *97*, 11984-11989.

Barret, C., Roy, C., Montcourrier, P., Mangeat, P., and Niggli, V. (2000). Mutagenesis of the phosphatidylinositol 4,5-bisphosphate (PIP(2)) binding site in the NH(2)-terminal domain of ezrin correlates with its altered cellular distribution. J Cell Biol *151*, 1067-1080.

Batiza, A.F., Schulz, T., and Masson, P.H. (1996). Yeast respond to hypotonic shock with a calcium pulse. J Biol Chem *271*, 23357-23362.

Bechet, J., Greenson, M., and Wiame, J.M. (1970). Mutations affecting the repressibility of arginine biosynthetic enzymes in Saccharomyces cerevisiae. Eur J Biochem *12*, 31-39.

Beck, T., and Hall, M.N. (1999). The TOR signalling pathway controls nuclear localization of nutrient-regulated transcription factors. Nature *402*, 689-692.

Bender, A.S., Neary, J.T., and Norenberg, M.D. (1993). Role of phosphoinositide hydrolysis in astrocyte volume regulation. J Neurochem *61*, 1506-1514.

Bennett, D.E., McCreary, C.E., and Coleman, D.C. (1998). Genetic characterization of a phospholipase C gene from Candida albicans: presence of homologous sequences in Candida species other than Candida albicans. Microbiology *144 (Pt 1)*, 55-72.

Berridge, M.J., and Irvine, R.F. (1989). Inositol phosphates and cell signalling. Nature *341*, 197-205.

Berridge, M.J. (1983). Rapid accumulation of inositol trisphosphate reveals that agonists hydrolyse polyphosphoinositides instead of phosphatidylinositol. Biochem J *212*, 849-858.

Bertagnolo, V., Mazzoni, M., Ricci, D., Carini, C., Neri, L.M., Previati, M., and Capitani, S. (1995). Identification of PI-PLC beta 1, gamma 1, and delta 1 in rat liver: subcellular distribution and relationship to inositol lipid nuclear signalling. Cell Signal *7*, 669-678.

Bhandari, R., Saiardi, A., Ahmadibeni, Y., Snowman, A.M., Resnick, A.C., Kristiansen, T.Z., Molina, H., Pandey, A., Werner, J.K., Jr., Juluri, K.R., *et al.* (2007). Protein pyrophosphorylation by inositol pyrophosphates is a posttranslational event. Proc Natl Acad Sci U S A *104*, 15305-15310.

Bolger, T.A., Folkmann, A.W., Tran, E.J., and Wente, S.R. (2008). The mRNA export factor Gle1 and inositol hexakisphosphate regulate distinct stages of translation. Cell *134*, 624-633.

Bottomley, M.J., Salim, K., and Panayotou, G. (1998). Phospholipid-binding protein domains. Biochim Biophys Acta *1436*, 165-183.

Boyer, J.L., Hepler, J.R., and Harden, T.K. (1989). Hormone and growth factor receptor-mediated regulation of phospholipase C activity. Trends Pharmacol Sci *10*, 360-364.

Brearley, C.A., and Hanke, D.E. (1996). Metabolic evidence for the order of addition of individual phosphate esters in the myo-inositol moiety of inositol hexakisphosphate in the duckweed Spirodela polyrhiza L. Biochem J *314 (Pt 1)*, 227-233.

Brewster, J.L., de Valoir, T., Dwyer, N.D., Winter, E., and Gustin, M.C. (1993). An osmosensing signal transduction pathway in yeast. Science *259*, 1760-1763.

Bruzik, K.S., and Tsai, M.D. (1994). Toward the mechanism of phosphoinositide-specific phospholipases C. Bioorg Med Chem *2*, 49-72.

Calderwood, S.K., and Stevenson, M.A. (1993). Inducers of the heat shock response stimulate phospholipase C and phospholipase A2 activity in mammalian cells. J Cell Physiol *155*, 248-256.

Camps, M., Carozzi, A., Schnabel, P., Scheer, A., Parker, P.J., and Gierschik, P. (1992). Isozyme-selective stimulation of phospholipase C-beta 2 by G protein beta gamma-subunits. Nature *360*, 684-686.

Chang, S.C., Miller, A.L., Feng, Y., Wente, S.R., and Majerus, P.W. (2002). The human homolog of the rat inositol phosphate multikinase is an inositol 1,3,4,6-tetrakisphosphate 5-kinase. J Biol Chem *277*, 43836-43843.

Chen, S., Lin, F., Iismaa, S., Lee, K.N., Birckbichler, P.J., and Graham, R.M. (1996). Alpha1-adrenergic receptor signaling via Gh is subtype specific and independent of its transglutaminase activity. J Biol Chem *271*, 32385-32391.

Cheng, H.F., Jiang, M.J., Chen, C.L., Liu, S.M., Wong, L.P., Lomasney, J.W., and King, K. (1995). Cloning and identification of amino acid residues of human phospholipase C delta 1

essential for catalysis. J Biol Chem *270*, 5495-5505.

Chi, Y., Huddleston, M.J., Zhang, X., Young, R.A., Annan, R.S., Carr, S.A., and Deshaies, R.J. (2001). Negative regulation of Gcn4 and Msn2 transcription factors by Srb10 cyclin-dependent kinase. Genes Dev *15*, 1078-1092.

Chi, T.H., and Crabtree, G.R. (2000). Perspectives: signal transduction. Inositol phosphates in the nucleus. Science *287*, 1937-1939.

Cifuentes, M.E., Delaney, T., and Rebecchi, M.J. (1994). D-myo-inositol 1,4,5-trisphosphate inhibits binding of phospholipase C-delta 1 to bilayer membranes. J Biol Chem *269*, 1945-1948.

Cifuentes, M.E., Honkanen, L., and Rebecchi, M.J. (1993). Proteolytic fragments of phosphoinositide-specific phospholipase C-delta 1. Catalytic and membrane binding properties. J Biol Chem *268*, 11586-11593.

Clarke, J.H. (2003). Lipid signalling: picking out the PIPs. Curr Biol *13*, R815-817.

Cocco, L., Martelli, A.M., Barnabei, O., and Manzoli, F.A. (2001a). Nuclear inositol lipid signaling. Adv Enzyme Regul *41*, 361-384.

Cocco, L., Martelli, A.M., Gilmour, R.S., Rhee, S.G., and Manzoli, F.A. (2001b). Nuclear phospholipase C and signaling. Biochim Biophys Acta *1530*, 1-14.

Cocco, L., Capitani, S., Maraldi, N.M., Mazzotti, G., Barnabei, O., Rizzoli, R., Gilmour, R.S., Wirtz, K.W., Rhee, S.G., and Manzoli, F.A. (1998). Inositides in the nucleus: taking stock of PLC beta 1. Adv Enzyme Regul *38*, 351-363.

Cockcroft, S. (2006). The latest phospholipase C, PLCeta, is implicated in neuronal function. Trends Biochem Sci *31*, 4-7.

Cockcroft, S., and Thomas, G.M. (1992). Inositol-lipid-specific phospholipase C isoenzymes and their differential regulation by receptors. Biochem J *288 (Pt 1)*, 1-14.

Cockcroft, S., and Stutchfield, J. (1988a). Effect of pertussis toxin and neomycin on G-protein-regulated polyphosphoinositide phosphodiesterase. A comparison between HL60 membranes and permeabilized HL60 cells. Biochem J *256*, 343-350.

Cockcroft, S., and Stutchfield, J. (1988b). G-proteins, the inositol lipid signalling pathway, and secretion. Philos Trans R Soc Lond B Biol Sci *320*, 247-265.

Cockcroft, S., and Gomperts, B.D. (1985). Role of guanine nucleotide binding protein in the activation of polyphosphoinositide phosphodiesterase. Nature *314*, 534-536.

Cooper, K.F., Mallory, M.J., and Strich, R. (1999). Oxidative stress-induced destruction of the yeast C-type cyclin Ume3p requires phosphatidylinositol-specific phospholipase C and the 26S proteasome. Mol Cell Biol *19*, 3338-3348.

Cooper, K.F., Mallory, M.J., Smith, J.B., and Strich, R. (1997). Stress and developmental regulation of the yeast C-type cyclin Ume3p (Srb11p/Ssn8p). Embo J *16*, 4665-4675.

Corvera, S. (2001). Phosphatidylinositol 3-kinase and the control of endosome dynamics: new players defined by structural motifs. Traffic *2*, 859-866.

Costigan, C., Gehrung, S., and Snyder, M. (1992). A synthetic lethal screen identifies SLK1, a

novel protein kinase homolog implicated in yeast cell morphogenesis and cell growth. Mol Cell Biol *12*, 1162-1178.

Crabeel, M., de Rijcke, M., Seneca, S., Heimberg, H., Pfeiffer, I., and Matisova, A. (1995). Further definition of the sequence and position requirements of the arginine control element that mediates repression and induction by arginine in Saccharomyces cerevisiae. Yeast *11*, 1367-1380.

Craig, E.A., Gambill, B.D., and Nelson, R.J. (1993). Heat shock proteins: molecular chaperones of protein biogenesis. Microbiol Rev *57*, 402-414.

Creba, J.A., Downes, C.P., Hawkins, P.T., Brewster, G., Michell, R.H., and Kirk, C.J. (1983). Rapid breakdown of phosphatidylinositol 4-phosphate and phosphatidylinositol 4,5-bisphosphate in rat hepatocytes stimulated by vasopressin and other Ca2+-mobilizing hormones. Biochem J *212*, 733-747.

Crljen, V., Visnjic, D., and Banfic, H. (2004). Presence of different phospholipase C isoforms in the nucleus and their activation during compensatory liver growth. FEBS Lett *571*, 35-42.

Culjkovic, B., Topisirovic, I., Skrabanek, L., Ruiz-Gutierrez, M., and Borden, K.L. (2006). eIF4E is a central node of an RNA regulon that governs cellular proliferation. J Cell Biol *175*, 415-426.

D'Santos, C.S., Clarke, J.H., Irvine, R.F., and Divecha, N. (1999). Nuclei contain two differentially regulated pools of diacylglycerol. Curr Biol *9*, 437-440.

D'Santos, C.S., Clarke, J.H., and Divecha, N. (1998). Phospholipid signalling in the nucleus. Een DAG uit het leven van de inositide signalering in de nucleus. Biochim Biophys Acta *1436*, 201-232.

Davenport, K.R., Sohaskey, M., Kamada, Y., Levin, D.E., and Gustin, M.C. (1995). A second osmosensing signal transduction pathway in yeast. Hypotonic shock activates the PKC1 protein kinase-regulated cell integrity pathway. J Biol Chem *270*, 30157-30161.

Das, T., Baek, K.J., Gray, C., and Im, M.J. (1993). Evidence that the Gh protein is a signal mediator from alpha 1-adrenoceptor to a phospholipase C. II. Purification and characterization of a Gh-coupled 69-kDa phospholipase C and reconstitution of alpha 1-adrenoceptor, Gh family, and phospholipase C. J Biol Chem *268*, 27398-27405.

Dawson, R.M. (1959). Studies on the enzymic hydrolysis of monophosphoinositide by phospholipase preparations from P. notatum and ox pancreas. Biochim Biophys Acta *33*, 68-77.

DeLillo, N., Romero, C., Lin, H., and Vancura, A. (2003). Genetic evidence for a role of phospholipase C at the budding yeast kinetochore. Mol Genet Genomics *269*, 261-270.

Demczuk, A., Guha, N., Nguyen, P.H., Desai, P., Chang, J., Guzinska, K., Rollins, J., Ghosh, C.C., Goodwin, L., and Vancura, A. (2008). Saccharomyces cerevisiae phospholipase C regulates transcription of Msn2p-dependent stress-responsive genes. Eukaryot Cell *7*, 967-979.

Di Paolo, G., and De Camilli, P. (2006). Phosphoinositides in cell regulation and membrane dynamics. Nature *443*, 651-657.

Diakonova, M., Chilov, D., Arnaoutov, A., Alexeyev, V., Nikolsky, N., and Medvedeva, N. (1997). Intracellular distribution of phospholipase C gamma 1 in cell lines with different levels of transformation. Eur J Cell Biol *73*, 360-367.

Divecha, N., Treagus, J., Vann, L., and D'Santos, C. (1997). Phospholipases in the nucleus. Semin Cell Dev Biol *8*, 323-331.

Divecha, N., Banfic, H., and Irvine, R.F. (1991). The polyphosphoinositide cycle exists in the nuclei of Swiss 3T3 cells under the control of a receptor (for IGF-I) in the plasma membrane, and stimulation of the cycle increases nuclear diacylglycerol and apparently induces translocation of protein kinase C to the nucleus. Embo J *10*, 3207-3214.

Dove, S.K., Cooke, F.T., Douglas, M.R., Sayers, L.G., Parker, P.J., and Michell, R.H. (1997). Osmotic stress activates phosphatidylinositol-3,5-bisphosphate synthesis. Nature *390*, 187-192.

Downes, C.P., Gray, A., and Lucocq, J.M. (2005). Probing phosphoinositide functions in signaling and membrane trafficking. Trends Cell Biol *15*, 259-268.

Downes, C.P., and Currie, R.A. (1998). Lipid signalling. Curr Biol *8*, R865-867.

Downes, C.P., and Michell, R.H. (1985). Inositol phospholipid breakdown as a receptor-controlled generator of second messengers, in Molecular Mechanisms of Transmembrane Signalling (Cohen P. and Houslay M. D., eds.). Elsevier Science, Amsterdam *4*, pp. 3–56.

Downes, C.P., and Michell, R.H. (1982). Phosphatidylinositol 4-phosphate and phosphatidylinositol 4,5-bisphosphate: lipids in search of a function. Cell Calcium *3*, 467-502.

Drayer, A.L., Van der Kaay, J., Mayr, G.W., and Van Haastert, P.J. (1994). Role of phospholipase C in Dictyostelium: formation of inositol 1,4,5-trisphosphate and normal development in cells lacking phospholipase C activity. Embo J *13*, 1601-1609.

Dubois, E., Scherens, B., Vierendeels, F., Ho, M.M., Messenguy, F., and Shears, S.B. (2002). In Saccharomyces cerevisiae, the inositol polyphosphate kinase activity of Kcs1p is required for resistance to salt stress, cell wall integrity, and vacuolar morphogenesis. J Biol Chem *277*, 23755-23763.

Dubois, E., Dewaste, V., Erneux, C., and Messenguy, F. (2000). Inositol polyphosphate kinase activity of Arg82/ArgRIII is not required for the regulation of the arginine metabolism in yeast. FEBS Lett *486*, 300-304.

Dubois, E., and Messenguy, F. (1994). Pleiotropic function of ArgRIIIp (Arg82p), one of the regulators of arginine metabolism in Saccharomyces cerevisiae. Role in expression of cell-type-specific genes. Mol Gen Genet *243*, 315-324.

Einspahr, K.J., Peeler, T.C., and Thompson, G.A., Jr. (1988). Rapid changes in polyphosphoinositide metabolism associated with the response of Dunaliella salina to hypoosmotic shock. J Biol Chem *263*, 5775-5779.

El Alami, M., Messenguy, F., Scherens, B., and Dubois, E. (2003). Arg82p is a bifunctional protein whose inositol polyphosphate kinase activity is essential for nitrogen and PHO gene expression but not for Mcm1p chaperoning in yeast. Mol Microbiol *49*, 457-468.

El Bakkoury, M., Dubois, E., and Messenguy, F. (2000). Recruitment of the yeast MADS-box proteins, ArgRI and Mcm1 by the pleiotropic factor ArgRIII is required for their stability. Mol Microbiol *35*, 15-31.

Emoto, K., Inadome, H., Kanaho, Y., Narumiya, S., and Umeda, M. (2005). Local change in phospholipid composition at the cleavage furrow is essential for completion of cytokinesis. J Biol Chem *280*, 37901-37907.

Essen, L.O., Perisic, O., Lynch, D.E., Katan, M., and Williams, R.L. (1997). A ternary metal binding site in the C2 domain of phosphoinositide-specific phospholipase C-delta1. Biochemistry *36*, 2753-2762.

Essen, L.O., Perisic, O., Cheung, R., Katan, M., and Williams, R.L. (1996). Crystal structure of a mammalian phosphoinositide-specific phospholipase C delta. Nature *380*, 595-602.
Estruch, F. (2000). Stress-controlled transcription factors, stress-induced genes and stress tolerance in budding yeast. FEMS Microbiol Rev *24*, 469-486.

Estruch, F., and Carlson, M. (1993). Two homologous zinc finger genes identified by multicopy suppression in a SNF1 protein kinase mutant of Saccharomyces cerevisiae. Mol Cell Biol *13*, 3872-3881.

Faenza, I., Billi, A.M., Follo, M.Y., Fiume, R., Martelli, A.M., Cocco, L., and Manzoli, L. (2005). Nuclear phospholipase C signaling through type 1 IGF receptor and its involvement in cell growth and differentiation. Anticancer Res *25*, 2039-2041.

Faenza, I., Matteucci, A., Bavelloni, A., Marmiroli, S., Martelli, A.M., Gilmour, R.S., Suh, P.G., Manzoli, L., and Cocco, L. (2002). Nuclear PLCbeta(1) acts as a negative regulator of p45/NF-E2 expression levels in Friend erythroleukemia cells. Biochim Biophys Acta *1589*, 305-310.

Faenza, I., Matteucci, A., Manzoli, L., Billi, A.M., Aluigi, M., Peruzzi, D., Vitale, M., Castorina, S., Suh, P.G., and Cocco, L. (2000). A role for nuclear phospholipase Cbeta 1 in cell cycle control. J Biol Chem *275*, 30520-30524.

Fain, J.N., Wallace, M.A., and Wojcikiewicz, R.J. (1988). Evidence for involvement of guanine nucleotide-binding regulatory proteins in the activation of phospholipases by hormones. Faseb J *2*, 2569-2574.

Falasca, M., Logan, S.K., Lehto, V.P., Baccante, G., Lemmon, M.A., and Schlessinger, J. (1998). Activation of phospholipase C gamma by PI 3-kinase-induced PH domain-mediated membrane targeting. Embo J *17*, 414-422.

Feng, Y., Wente, S.R., and Majerus, P.W. (2001). Overexpression of the inositol phosphatase SopB in human 293 cells stimulates cellular chloride influx and inhibits nuclear mRNA export. Proc Natl Acad Sci U S A *98*, 875-879.

Feng, J.F., Rhee, S.G., and Im, M.J. (1996). Evidence that phospholipase delta1 is the effector in the Gh (transglutaminase II)-mediated signaling. J Biol Chem *271*, 16451-16454.

Ferguson, K.M., Kavran, J.M., Sankaran, V.G., Fournier, E., Isakoff, S.J., Skolnik, E.Y., and Lemmon, M.A. (2000). Structural basis for discrimination of 3-phosphoinositides by pleckstrin homology domains. Mol Cell *6*, 373-384.

Ferguson, K.M., Lemmon, M.A., Schlessinger, J., and Sigler, P.B. (1995). Structure of the high affinity complex of inositol trisphosphate with a phospholipase C pleckstrin homology domain. Cell *83*, 1037-1046.

Field, S.J., Madson, N., Kerr, M.L., Galbraith, K.A., Kennedy, C.E., Tahiliani, M., Wilkins, A., and Cantley, L.C. (2005). PtdIns(4,5)P2 functions at the cleavage furrow during cytokinesis. Curr Biol *15*, 1407-1412.

Fleischer, B., Xie, J., Mayrleitner, M., Shears, S.B., Palmer, D.J., and Fleischer, S. (1994). Golgi coatomer binds, and forms K(+)-selective channels gated by, inositol polyphosphates. J Biol Chem *269*, 17826-17832.

Flick, J.S., and Thorner, J. (1998). An essential function of a phosphoinositide-specific phospholipase C is relieved by inhibition of a cyclin-dependent protein kinase in the yeast Saccharomyces cerevisiae. Genetics *148*, 33-47.

Flick, J.S., and Thorner, J. (1993). Genetic and biochemical characterization of a phosphatidylinositol-specific phospholipase C in Saccharomyces cerevisiae. Mol Cell Biol *13*, 5861-5876.

Fluckiger, A.C., Li, Z., Kato, R.M., Wahl, M.I., Ochs, H.D., Longnecker, R., Kinet, J.P., Witte, O.N., Scharenberg, A.M., and Rawlings, D.J. (1998). Btk/Tec kinases regulate sustained increases in intracellular Ca2+ following B-cell receptor activation. Embo J *17*, 1973-1985.

Folch, J., Casals, J., Pope, A., Meath, J. A., LeBaron, F. N., Lees, M. (1959). Biology of Myelin (London: Cassell and Co.).

Folch, J. (1949). Complete fractionation of brain cephalin; isolation from it of phosphatidyl serine, phosphatidyl ethanolamine, and diphosphoinositide. J Biol Chem *177*, 497-504.

Fratti, R.A., Jun, Y., Merz, A.J., Margolis, N., and Wickner, W. (2004). Interdependent assembly of specific regulatory lipids and membrane fusion proteins into the vertex ring domain of docked vacuoles. J Cell Biol *167*, 1087-1098.

Frederick, J.P., Mattiske, D., Wofford, J.A., Megosh, L.C., Drake, L.Y., Chiou, S.T., Hogan, B.L., and York, J.D. (2005). An essential role for an inositol polyphosphate multikinase, Ipk2, in mouse embryogenesis and second messenger production. Proc Natl Acad Sci U S A *102*, 8454-8459.

Garcia, P., Gupta, R., Shah, S., Morris, A.J., Rudge, S.A., Scarlata, S., Petrova, V., McLaughlin, S., and Rebecchi, M.J. (1995). The pleckstrin homology domain of phospholipase C-delta 1 binds with high affinity to phosphatidylinositol 4,5-bisphosphate in bilayer membranes. Biochemistry *34*, 16228-16234.

Gerasimenko, O., and Gerasimenko, J. (2004). New aspects of nuclear calcium signalling. J Cell Sci *117*, 3087-3094.

Gietz, R.D., and Sugino, A. (1988). New yeast-Escherichia coli shuttle vectors constructed with in vitro mutagenized yeast genes lacking six-base pair restriction sites. Gene *74*, 527-534.

Godin, C.M., Ferreira, L.T., Dale, L.B., Gros, R., Cregan, S.P., and Ferguson, S.S.G. (2010). The small GTPase Ral couples the angiotensin II type 1 receptor to the activation of phospholipase-delta1. Molecular Pharmacology (in press)

Gorner, W., Durchschlag, E., Wolf, J., Brown, E.L., Ammerer, G., Ruis, H., and Schuller, C. (2002). Acute glucose starvation activates the nuclear localization signal of a stress-specific yeast transcription factor. Embo J *21*, 135-144.

Gorner, W., Durchschlag, E., Martinez-Pastor, M.T., Estruch, F., Ammerer, G., Hamilton, B., Ruis, H., and Schuller, C. (1998). Nuclear localization of the C2H2 zinc finger protein Msn2p is regulated by stress and protein kinase A activity. Genes Dev *12*, 586-597.

Graf, E., Empson, K.L., and Eaton, J.W. (1987). Phytic acid. A natural antioxidant. J Biol Chem *262*, 11647-11650.

Grobler, J.A., and Hurley, J.H. (1998). Catalysis by phospholipase C delta1 requires that Ca2+ bind to the catalytic domain, but not the C2 domain. Biochemistry *37*, 5020-5028.

Gross, T., Siepmann, A., Sturm, D., Windgassen, M., Scarcelli, J.J., Seedorf, M., Cole, C.N., and Krebber, H. (2007). The DEAD-box RNA helicase Dbp5 functions in translation termination. Science *315*, 646-649.

Guha, N., Desai, P., and Vancura, A. (2007). Plc1p is required for SAGA recruitment and derepression of Sko1p-regulated genes. Mol Biol Cell *18*, 2419-2428.

Gusovsky, F., Lueders, J.E., Kohn, E.C., and Felder, C.C. (1993). Muscarinic receptor-mediated tyrosine phosphorylation of phospholipase C-gamma. An alternative mechanism for cholinergic-induced phosphoinositide breakdown. J Biol Chem *268*, 7768-7772.

Gustin, M.C., Albertyn, J., Alexander, M., and Davenport, K. (1998). MAP kinase pathways in the yeast Saccharomyces cerevisiae. Microbiol Mol Biol Rev *62*, 1264-1300.

Halstead, J.R., Jalink, K., and Divecha, N. (2005). An emerging role for PtdIns(4,5)P2-mediated signalling in human disease. Trends Pharmacol Sci *26*, 654-660.

Han, J., Lee, J.D., Bibbs, L., and Ulevitch, R.J. (1994). A MAP kinase targeted by endotoxin and hyperosmolarity in mammalian cells. Science *265*, 808-811.

Hanakahi, L.A., and West, S.C. (2002). Specific interaction of IP6 with human Ku70/80, the DNA-binding subunit of DNA-PK. Embo J *21*, 2038-2044.

Heilmann, I. (2008). Towards understanding the function of stress-inducible PtdIns(4,5)P(2) in plants. Commun Integr Biol *1*, 204-206.

Heinz, D.W., Essen, L.O., and Williams, R.L. (1998). Structural and mechanistic comparison of prokaryotic and eukaryotic phosphoinositide-specific phospholipases C. J Mol Biol *275*, 635-650.

Heitman, J., Movva, N.R., and Hall, M.N. (1991). Targets for cell cycle arrest by the immunosuppressant rapamycin in yeast. Science *253*, 905-909.

Hinchliffe, K.A., Ciruela, A., and Irvine, R.F. (1998). PIPkins1, their substrates and their products: new functions for old enzymes. Biochim Biophys Acta *1436*, 87-104.

Hirao, M., Sato, N., Kondo, T., Yonemura, S., Monden, M., Sasaki, T., Takai, Y., and Tsukita, S. (1996). Regulation mechanism of ERM (ezrin/radixin/moesin) protein/plasma membrane association: possible involvement of phosphatidylinositol turnover and Rho-dependent signaling pathway. J Cell Biol *135*, 37-51.

Hirata, Y., Andoh, T., Asahara, T., and Kikuchi, A. (2003). Yeast glycogen synthase kinase-3 activates Msn2p-dependent transcription of stress responsive genes. Mol Biol Cell *14*, 302-312.

Hirata, M., Kanematsu, T., Takeuchi, H., and Yagisawa, H. (1998). Pleckstrin homology domain as an inositol compound binding module. Jpn J Pharmacol *76*, 255-263.

Hohmann, S. (2002). Osmotic stress signaling and osmoadaptation in yeasts. Microbiol Mol Biol Rev *66*, 300-372.

Hokin, M.R., and Hokin, L.E. (1964). The Synthesis of Phosphatidic Acid and Protein-Bound Phosphorylserine in Salt Gland Homogenates. J Biol Chem *239*, 2116-2122.

Hokin, L.E., and Hokin, M.R. (1955a). Effects of acetylcholine on phosphate turnover in phospholipides of brain cortex in vitro. Biochim Biophys Acta *16*, 229-237.

Hokin, L.E., and Hokin, M.R. (1955b). Effects of acetylcholine on the turnover of phosphoryl units in individual phospholipids of pancreas slices and brain cortex slices. Biochim Biophys Acta *18*, 102-110.

Hokin, M.R., and Hokin, L.E. (1953). Enzyme secretion and the incorporation of P32 into phospholipides of pancreas slices. J Biol Chem *203*, 967-977.

Homma, Y., and Emori, Y. (1995). A dual functional signal mediator showing RhoGAP and phospholipase C-delta stimulating activities. Embo J *14*, 286-291.

Huang, K.N., and Symington, L.S. (1995). Suppressors of a Saccharomyces cerevisiae pkc1 mutation identify alleles of the phosphatase gene PTC1 and of a novel gene encoding a putative basic leucine zipper protein. Genetics *141*, 1275-1285.

Im, M.J., Russell, M.A., and Feng, J.F. (1997). Transglutaminase II: a new class of GTP-binding protein with new biological functions. Cell Signal *9*, 477-482.

Insall, R.H., and Weiner, O.D. (2001). PIP3, PIP2, and cell movement--similar messages, different meanings? Dev Cell *1*, 743-747.

Irie, K., Takase, M., Lee, K.S., Levin, D.E., Araki, H., Matsumoto, K., and Oshima, Y. (1993). MKK1 and MKK2, which encode Saccharomyces cerevisiae mitogen-activated protein kinase-kinase homologs, function in the pathway mediated by protein kinase C. Mol Cell Biol *13*, 3076-3083.

Irvine, R.F. (2003). Nuclear lipid signalling. Nat Rev Mol Cell Biol *4*, 349-360.

Irvine, R. (2000). Nuclear lipid signaling. Sci STKE *2000*, RE1.

Iwaki, S., Sano, T., Takagi, T., Osumi, M., Kihara, A., and Igarashi, Y. (2007). Intracellular trafficking pathway of yeast long-chain base kinase Lcb4, from its synthesis to its degradation. J Biol Chem *282*, 28485-28492.

Jin, L., Guzik, B.W., Bor, Y.C., Rekosh, D., and Hammarskjold, M.L. (2003). Tap and NXT promote translation of unspliced mRNA. Genes Dev *17*, 3075-3086.

Jun, Y., Fratti, R.A., and Wickner, W. (2004). Diacylglycerol and its formation by phospholipase C regulate Rab- and SNARE-dependent yeast vacuole fusion. J Biol Chem *279*, 53186-53195.

Kaffman, A., Rank, N.M., O'Neill, E.M., Huang, L.S., and O'Shea, E.K. (1998). The receptor Msn5 exports the phosphorylated transcription factor Pho4 out of the nucleus. Nature *396*, 482-486.

Kaffman, A., Herskowitz, I., Tjian, R., and O'Shea, E.K. (1994). Phosphorylation of the transcription factor PHO4 by a cyclin-CDK complex, PHO80-PHO85. Science *263*, 1153-1156.

Kai, M., Salway, J.G., Michell, R.H., Hawthorne, J.N. (1966). The biosynthesis of triphosphoinositide by rat brain in vitro." Biochem. Biophys. Res. Commun. *22*: 370-5.

Katan, M. (2005). New insights into the families of PLC enzymes: looking back and going forward. Biochem J *391*, e7-9.

Katan, M. (1998). Families of phosphoinositide-specific phospholipase C: structure and function. Biochim Biophys Acta *1436*, 5-17.

Kemp, P., Hubscher, G., and Hawthorne, J.N. (1961). Phosphoinositides. 3. Enzymic hydrolysis of inositol-containing phospholipids. Biochem J *79*, 193-200.

Kim, Y.H., Park, T.J., Lee, Y.H., Baek, K.J., Suh, P.G., Ryu, S.H., and Kim, K.T. (1999). Phospholipase C-delta1 is activated by capacitative calcium entry that follows phospholipase C-beta activation upon bradykinin stimulation. J Biol Chem *274*, 26127-26134.

Kim, C.G., Park, D., and Rhee, S.G. (1996). The role of carboxyl-terminal basic amino acids in Gqalpha-dependent activation, particulate association, and nuclear localization of phospholipase C-beta1. J Biol Chem *271*, 21187-21192.

Kim, U.H., Fink, D., Jr., Kim, H.S., Park, D.J., Contreras, M.L., Guroff, G., and Rhee, S.G. (1991). Nerve growth factor stimulates phosphorylation of phospholipase C-gamma in PC12 cells. J Biol Chem *266*, 1359-1362.

Kim, J.W., Sim, S.S., Kim, U.H., Nishibe, S., Wahl, M.I., Carpenter, G., and Rhee, S.G. (1990). Tyrosine residues in bovine phospholipase C-gamma phosphorylated by the epidermal growth factor receptor in vitro. J Biol Chem *265*, 3940-3943.

Kirk, C.J. (1990). Recent developments in our understanding of the inositol lipid signalling system. Symp Soc Exp Biol *44*, 173-180.

Knop, M., Siegers, K., Pereira, G., Zachariae, W., Winsor, B., Nasmyth, K., and Schiebel, E. (1999). Epitope tagging of yeast genes using a PCR-based strategy: more tags and improved practical routines. Yeast *15*, 963-972.

Kouchi, Z., Shikano, T., Nakamura, Y., Shirakawa, H., Fukami, K., and Miyazaki, S. (2005). The role of EF-hand domains and C2 domain in regulation of enzymatic activity of phospholipase Czeta. J Biol Chem *280*, 21015-21021.

Koyanagi, M., Ono, K., Suga, H., Iwabe, N., and Miyata, T. (1998). Phospholipase C cDNAs from sponge and hydra: antiquity of genes involved in the inositol phospholipid signaling pathway. FEBS Lett *439*, 66-70.

Kudo, N., Wolff, B., Sekimoto, T., Schreiner, E.P., Yoneda, Y., Yanagida, M., Horinouchi, S., and Yoshida, M. (1998). Leptomycin B inhibition of signal-mediated nuclear export by direct binding to CRM1. Exp Cell Res *242*, 540-547.

Kunzler, M., Gerstberger, T., Stutz, F., Bischoff, F.R., and Hurt, E. (2000). Yeast Ran-binding protein 1 (Yrb1) shuttles between the nucleus and cytoplasm and is exported from the nucleus via a CRM1 (XPO1)-dependent pathway. Mol Cell Biol *20*, 4295-4308.

Larman, M.G., Saunders, C.M., Carroll, J., Lai, F.A., and Swann, K. (2004). Cell cycle-dependent Ca2+ oscillations in mouse embryos are regulated by nuclear targeting of PLCzeta. J Cell Sci *117*, 2513-2521.

Larsson, K., Ansell, R., Eriksson, P., and Adler, L. (1993). A gene encoding sn-glycerol 3-phosphate dehydrogenase (NAD+) complements an osmosensitive mutant of Saccharomyces cerevisiae. Mol Microbiol *10*, 1101-1111.

Lassing, I., and Lindberg, U. (1985). Specific interaction between phosphatidylinositol 4,5-bisphosphate and profilactin. Nature *314*, 472-474.

Lea, J.P., Jin, S.G., Roberts, B.R., Shuler, M.S., Marrero, M.B., and Tumlin, J.A. (2002). Angiotensin II stimulates calcineurin activity in proximal tubule epithelia through AT-1 receptor-mediated tyrosine phosphorylation of the PLC-gamma1 isoform. J Am Soc Nephrol *13*, 1750-1756.

Lee, Y.S., Huang, K., Quiocho, F.A., and O'Shea, E.K. (2008). Molecular basis of cyclin-CDK-CKI regulation by reversible binding of an inositol pyrophosphate. Nat Chem Biol *4*, 25-32.
Lee, Y.S., Mulugu, S., York, J.D., and O'Shea, E.K. (2007). Regulation of a cyclin-CDK-CDK inhibitor complex by inositol pyrophosphates. Science *316*, 109-112.

Lee, C.W., Lee, K.H., Lee, S.B., Park, D., and Rhee, S.G. (1994). Regulation of phospholipase C-beta 4 by ribonucleotides and the alpha subunit of Gq. J Biol Chem *269*, 25335-25338.

Lee, K.S., Irie, K., Gotoh, Y., Watanabe, Y., Araki, H., Nishida, E., Matsumoto, K., and Levin, D.E. (1993). A yeast mitogen-activated protein kinase homolog (Mpk1p) mediates signalling by protein kinase C. Mol Cell Biol *13*, 3067-3075.

Lee, C.H., Park, D., Wu, D., Rhee, S.G., and Simon, M.I. (1992). Members of the Gq alpha subunit gene family activate phospholipase C beta isozymes. J Biol Chem *267*, 16044-16047.

Lemmon, M.A. (2003). Phosphoinositide recognition domains. Traffic *4*, 201-213.

Lemmon, M.A., and Ferguson, K.M. (2000). Signal-dependent membrane targeting by pleckstrin homology (PH) domains. Biochem J *350 Pt 1*, 1-18.

Lemmon, M.A., Ferguson, K.M., O'Brien, R., Sigler, P.B., and Schlessinger, J. (1995). Specific and high-affinity binding of inositol phosphates to an isolated pleckstrin homology domain. Proc Natl Acad Sci U S A *92*, 10472-10476.

Leung, S.W., Harreman, M.T., Hodel, M.R., Hodel, A.E., and Corbett, A.H. (2003). Dissection of the karyopherin alpha nuclear localization signal (NLS)-binding groove: functional requirements for NLS binding. J Biol Chem *278*, 41947-41953.

Levin, D.E., Fields, F.O., Kunisawa, R., Bishop, J.M., and Thorner, J. (1990). A candidate protein kinase C gene, PKC1, is required for the S. cerevisiae cell cycle. Cell *62*, 213-224.

Lin, H., Nguyen, P., and Vancura, A. (2002). Phospholipase C interacts with Sgd1p and is required for expression of GPD1 and osmoresistance in Saccharomyces cerevisiae. Mol Genet Genomics *267*, 313-320.

Lin, H., Choi, J.H., Hasek, J., DeLillo, N., Lou, W., and Vancura, A. (2000). Phospholipase C is involved in kinetochore function in Saccharomyces cerevisiae. Mol Cell Biol *20*, 3597-3607.

Liu, N., Fukami, K., Yu, H., and Takenawa, T. (1996). A new phospholipase C delta 4 is induced at S-phase of the cell cycle and appears in the nucleus. J Biol Chem *271*, 355-360.

Llinas, R., Sugimori, M., Lang, E.J., Morita, M., Fukuda, M., Niinobe, M., and Mikoshiba, K. (1994). The inositol high-polyphosphate series blocks synaptic transmission by preventing vesicular fusion: a squid giant synapse study. Proc Natl Acad Sci U S A *91*, 12990-12993.

Lomasney, J.W., Cheng, H.F., Wang, L.P., Kuan, Y., Liu, S., Fesik, S.W., and King, K. (1996). Phosphatidylinositol 4,5-bisphosphate binding to the pleckstrin homology domain of phospholipase C-delta1 enhances enzyme activity. J Biol Chem *271*, 25316-25326.

Longtine, M.S., McKenzie, A., 3rd, Demarini, D.J., Shah, N.G., Wach, A., Brachat, A., Philippsen, P., and Pringle, J.R. (1998). Additional modules for versatile and economical PCR-

based gene deletion and modification in Saccharomyces cerevisiae. Yeast *14*, 953-961.

Lopez, I., Mak, E.C., Ding, J., Hamm, H.E., and Lomasney, J.W. (2001). A novel bifunctional phospholipase c that is regulated by Galpha 12 and stimulates the Ras/mitogen-activated protein kinase pathway. J Biol Chem *276*, 2758-2765.

Lorenz, M.C., and Heitman, J. (1997). Yeast pseudohyphal growth is regulated by GPA2, a G protein alpha homolog. Embo J *16*, 7008-7018.

Lu, A., and Hirsch, J.P. (2005). Cyclic AMP-independent regulation of protein kinase A substrate phosphorylation by Kelch repeat proteins. Eukaryot Cell *4*, 1794-1800.

Luo, H.R., Saiardi, A., Yu, H., Nagata, E., Ye, K., and Snyder, S.H. (2002). Inositol pyrophosphates are required for DNA hyperrecombination in protein kinase c1 mutant yeast. Biochemistry *41*, 2509-2515.

Manzoli, L., Billi, A.M., Rubbini, S., Bavelloni, A., Faenza, I., Gilmour, R.S., Rhee, S.G., and Cocco, L. (1997). Essential role for nuclear phospholipase C beta1 in insulin-like growth factor I-induced mitogenesis. Cancer Res *57*, 2137-2139.

Martelli, A.M., Gilmour, R.S., Bertagnolo, V., Neri, L.M., Manzoli, L., and Cocco, L. (1992). Nuclear localization and signalling activity of phosphoinositidase C beta in Swiss 3T3 cells. Nature *358*, 242-245.

Martelli, A.M., Gilmour, R.S., Neri, L.M., Manzoli, L., Corps, A.N., and Cocco, L. (1991). Mitogen-stimulated events in nuclei of Swiss 3T3 cells. Evidence for a direct link between changes of inositol lipids, protein kinase C requirement and the onset of DNA synthesis. FEBS Lett *283*, 243-246.

Martinez-Pastor, M.T., Marchler, G., Schuller, C., Marchler-Bauer, A., Ruis, H., and Estruch, F. (1996). The Saccharomyces cerevisiae zinc finger proteins Msn2p and Msn4p are required for transcriptional induction through the stress response element (STRE). Embo J *15*, 2227-2235.

Maurer, P., Redd, M., Solsbacher, J., Bischoff, F.R., Greiner, M., Podtelejnikov, A.V., Mann, M., Stade, K., Weis, K., and Schlenstedt, G. (2001). The nuclear export receptor Xpo1p forms distinct complexes with NES transport substrates and the yeast Ran binding protein 1 (Yrb1p). Mol Biol Cell *12*, 539-549.

Mayer, A., Scheglmann, D., Dove, S., Glatz, A., Wickner, W., and Haas, A. (2000). Phosphatidylinositol 4,5-bisphosphate regulates two steps of homotypic vacuole fusion. Mol Biol Cell *11*, 807-817.

Michell, R.H. (2008). Inositol derivatives: evolution and functions. Nat Rev Mol Cell Biol *9*, 151-161.

Michell, R.H. (1997). The multiplying roles of inositol lipids and phosphates in cell control processes. Essays Biochem *32*, 31-47.

Michell, R.H. (1986). Phosphoinositides and Receptor Mechanisms (Putney, Jr, J.W., ed.). Alan R Liss, New York, 1-24.

Michell, R.H. (1982). Is phosphatidylinositol really out of the calcium gate? Nature *296*, 492-493.

Michell, R.H., Kirk, C.J., Jones, L.M., Downes, C.P., and Creba, J.A. (1981). The stimulation of inositol lipid metabolism that accompanies calcium mobilization in stimulated cells: defined

characteristics and unanswered questions. Philos Trans R Soc Lond B Biol Sci *296*, 123-138.

Michell, R.H. (1975). Inositol phospholipids and cell surface receptor function. Biochim Biophys Acta *415*, 81-47.

Michell, R.H., and Hawthorne, J.N. (1965). The site of diphosphoinositide synthesis in rat liver. Biochem Biophys Res Commun *21*, 333-338.

Miller, M.E., and Cross, F.R. (2000). Distinct subcellular localization patterns contribute to functional specificity of the Cln2 and Cln3 cyclins of Saccharomyces cerevisiae. Mol Cell Biol *20*, 542-555.

Morris, J.B., Hinchliffe, K.A., Ciruela, A., Letcher, A.J., and Irvine, R.F. (2000). Thrombin stimulation of platelets causes an increase in phosphatidylinositol 5-phosphate revealed by mass assay. FEBS Lett *475*, 57-60.

Morton, R.K., and Raison, J.K. (1963). A Complete Intracellular Unit for Incorporation of Amino-Acid into Storage Protein Utilizing Adenosine Triphosphate Generated from Phytate. Nature *200*, 429-433.

Mulugu, S., Bai, W., Fridy, P.C., Bastidas, R.J., Otto, J.C., Dollins, D.E., Haystead, T.A., Ribeiro, A.A., and York, J.D. (2007). A conserved family of enzymes that phosphorylate inositol hexakisphosphate. Science *316*, 106-109.

Mumberg, D., Muller, R., and Funk, M. (1994). Regulatable promoters of Saccharomyces cerevisiae: comparison of transcriptional activity and their use for heterologous expression. Nucleic Acids Res *22*, 5767-5768.

Murthy, S.N., Lomasney, J.W., Mak, E.C., and Lorand, L. (1999). Interactions of G(h)/transglutaminase with phospholipase Cdelta1 and with GTP. Proc Natl Acad Sci U S A *96*, 11815-11819.

Murphy, R., and Wente, S.R. (1996). An RNA-export mediator with an essential nuclear export signal. Nature *383*, 357-360.

Nakamura, N., Hirata, A., Ohsumi, Y., and Wada, Y. (1997). Vam2/Vps41p and Vam6/Vps39p are components of a protein complex on the vacuolar membranes and involved in the vacuolar assembly in the yeast Saccharomyces cerevisiae. J Biol Chem *272*, 11344-11349.

Nakaoka, H., Perez, D.M., Baek, K.J., Das, T., Husain, A., Misono, K., Im, M.J., and Graham, R.M. (1994). Gh: a GTP-binding protein with transglutaminase activity and receptor signaling function. Science *264*, 1593-1596.

Narayan, K., and Lemmon, M.A. (2006). Determining selectivity of phosphoinositide-binding domains. Methods *39*, 122-133.

Neumann FT A, G.S. (2005). Tracking individual chromosomes with integrated arrays of Lacop sites and GFP-Laci repressor (PROT15). The EPIGENOME Network of Excellence Epigenome NoE.

Niedenthal, R.K., Riles, L., Johnston, M., and Hegemann, J.H. (1996). Green fluorescent protein as a marker for gene expression and subcellular localization in budding yeast. Yeast *12*, 773-786.

Niinobe, M., Yamaguchi, Y., Fukuda, M., and Mikoshiba, K. (1994). Synaptotagmin is an inositol polyphosphate binding protein: isolation and characterization as an Ins 1,3,4,5-P4 binding protein. Biochem Biophys Res Commun *205*, 1036-1042.

Norris, F.A., Ungewickell, E., and Majerus, P.W. (1995). Inositol hexakisphosphate binds to clathrin assembly protein 3 (AP-3/AP180) and inhibits clathrin cage assembly in vitro. J Biol Chem *270*, 214-217.

Ochocka, A.M., and Pawelczyk, T. (2003). Isozymes delta of phosphoinositide-specific phospholipase C and their role in signal transduction in the cell. Acta Biochim Pol *50*, 1097-1110.

Odom, A.R., Stahlberg, A., Wente, S.R., and York, J.D. (2000). A role for nuclear inositol 1,4,5-trisphosphate kinase in transcriptional control. Science *287*, 2026-2029.

Ogawa, N., Noguchi, K., Sawai, H., Yamashita, Y., Yompakdee, C., and Oshima, Y. (1995). Functional domains of Pho81p, an inhibitor of Pho85p protein kinase, in the transduction pathway of Pi signals in Saccharomyces cerevisiae. Mol Cell Biol *15*, 997-1004.

Okada, M., Ishimoto, T., Naito, Y., Hirata, H., and Yagisawa, H. (2005). Phospholipase Cdelta1 associates with importin beta1 and translocates into the nucleus in a Ca2+-dependent manner. FEBS Lett *579*, 4949-4954.

Okada, M., Fujii, M., Yamaga, M., Sugimoto, H., Sadano, H., Osumi, T., Kamata, H., Hirata, H., and Yagisawa, H. (2002). Carboxyl-terminal basic amino acids in the X domain are essential for the nuclear import of phospholipase C delta1. Genes Cells *7*, 985-996.

Ongusaha, P.P., Hughes, P.J., Davey, J., and Michell, R.H. (1998). Inositol hexakisphosphate in Schizosaccharomyces pombe: synthesis from Ins(1,4,5)P3 and osmotic regulation. Biochem J *335 (Pt 3)*, 671-679.

Overduin, M., Cheever, M.L., and Kutateladze, T.G. (2001). Signaling with phosphoinositides: better than binary. Mol Interv *1*, 150-159.

Palczewski, K., Pulvermuller, A., Buczylko, J., Gutmann, C., and Hofmann, K.P. (1991). Binding of inositol phosphates to arrestin. FEBS Lett *295*, 195-199.

Park, E.S., Won, J.H., Han, K.J., Suh, P.G., Ryu, S.H., Lee, H.S., Yun, H.Y., Kwon, N.S., and Baek, K.J. (1998). Phospholipase C-delta1 and oxytocin receptor signalling: evidence of its role as an effector. Biochem J *331 (Pt 1)*, 283-289.

Park, D., Jhon, D.Y., Lee, C.W., Lee, K.H., and Rhee, S.G. (1993). Activation of phospholipase C isozymes by G protein beta gamma subunits. J Biol Chem *268*, 4573-4576.

Park, D., Jhon, D.Y., Kriz, R., Knopf, J., and Rhee, S.G. (1992). Cloning, sequencing, expression, and Gq-independent activation of phospholipase C-beta 2. J Biol Chem *267*, 16048-16055.

Park, D.J., Min, H.K., and Rhee, S.G. (1991). IgE-induced tyrosine phosphorylation of phospholipase C-gamma 1 in rat basophilic leukemia cells. J Biol Chem *266*, 24237-24240.

Payne, W.E., and Fitzgerald-Hayes, M. (1993). A mutation in PLC1, a candidate phosphoinositide-specific phospholipase C gene from Saccharomyces cerevisiae, causes aberrant mitotic chromosome segregation. Mol Cell Biol *13*, 4351-4364.

Pei, Z.D., and Williamson, J.R. (1998). Mutations at residues Tyr771 and Tyr783 of

phospholipase C-gamma1 have different effects on cell actin-cytoskeleton organization and cell proliferation in CCL-39 cells. FEBS Lett *423*, 53-56.

Perera, N.M., Michell, R.H., and Dove, S.K. (2004). Hypo-osmotic stress activates Plc1p-dependent phosphatidylinositol 4,5-bisphosphate hydrolysis and inositol Hexakisphosphate accumulation in yeast. J Biol Chem *279*, 5216-5226.

Perera, N.M. (2002). '' Phospholipase C activation is implicated in the responses of yeast to several stresses.'' Ph.D. thesis, University of Birmingham, UK.

Proft, M., and Serrano, R. (1999). Repressors and upstream repressing sequences of the stress-regulated ENA1 gene in Saccharomyces cerevisiae: bZIP protein Sko1p confers HOG-dependent osmotic regulation. Mol Cell Biol *19*, 537-546.

Rameh, L.E., and Cantley, L.C. (1999). The role of phosphoinositide 3-kinase lipid products in cell function. J Biol Chem *274*, 8347-8350.

Rameh, L.E., Tolias, K.F., Duckworth, B.C., and Cantley, L.C. (1997). A new pathway for synthesis of phosphatidylinositol-4,5-bisphosphate. Nature *390*, 192-196.

Razzini, G., Brancaccio, A., Lemmon, M.A., Guarnieri, S., and Falasca, M. (2000). The role of the pleckstrin homology domain in membrane targeting and activation of phospholipase Cbeta(1). J Biol Chem *275*, 14873-14881.

Rebecchi, M.J., and Pentyala, S.N. (2000). Structure, function, and control of phosphoinositide-specific phospholipase C. Physiol Rev *80*, 1291-1335.

Rhee, S.G. (2001). Regulation of phosphoinositide-specific phospholipase C. Annu Rev Biochem *70*, 281-312.

Rhee, S.G., and Bae, Y.S. (1997). Regulation of phosphoinositide-specific phospholipase C isozymes. J Biol Chem *272*, 15045-15048.

Rhee, S.G., and Choi, K.D. (1992a). Multiple forms of phospholipase C isozymes and their activation mechanisms. Adv Second Messenger Phosphoprotein Res *26*, 35-61.

Rhee, S.G., and Choi, K.D. (1992b). Regulation of inositol phospholipid-specific phospholipase C isozymes. J Biol Chem *267*, 12393-12396.

Robinson, F.L., and Dixon, J.E. (2006). Myotubularin phosphatases: policing 3-phosphoinositides. Trends Cell Biol *16*, 403-412.

Rodrigues, F., van Hemert, M., Steensma, H.Y., Corte-Real, M., and Leao, C. (2001). Red fluorescent protein (DsRed) as a reporter in Saccharomyces cerevisiae. J Bacteriol *183*, 3791-3794.

Rogers, S., Wells, R., and Rechsteiner, M. (1986). Amino acid sequences common to rapidly degraded proteins: the PEST hypothesis. Science *234*, 364-368.

Rosenwald, I.B., Kaspar, R., Rousseau, D., Gehrke, L., Leboulch, P., Chen, J.J., Schmidt, E.V., Sonenberg, N., and London, I.M. (1995). Eukaryotic translation initiation factor 4E regulates expression of cyclin D1 at transcriptional and post-transcriptional levels. J Biol Chem *270*, 21176-21180.

Rudge, S.A., Anderson, D.M., and Emr, S.D. (2004). Vacuole size control: regulation of PtdIns(3,5)P2 levels by the vacuole-associated Vac14-Fig4 complex, a PtdIns(3,5)P2-specific phosphatase. Mol Biol Cell *15*, 24-36.

Rudolf, M.T., Traynor-Kaplan, A.E., and Schultz, C. (1998). A membrane-permeant, bioactivatable derivative of Ins(1,3,4)P3 and its effect on Cl(-)-secretion from T84 cells. Bioorg Med Chem Lett *8*, 1857-1860.

Rupp, S., Summers, E., Lo, H.J., Madhani, H., and Fink, G. (1999). MAP kinase and cAMP filamentation signaling pathways converge on the unusually large promoter of the yeast FLO11 gene. Embo J *18*, 1257-1269.

Saiardi, A., Resnick, A.C., Snowman, A.M., Wendland, B., and Snyder, S.H. (2005). Inositol pyrophosphates regulate cell death and telomere length through phosphoinositide 3-kinase-related protein kinases. Proc Natl Acad Sci U S A *102*, 1911-1914.

Saiardi, A., Bhandari, R., Resnick, A.C., Snowman, A.M., and Snyder, S.H. (2004). Phosphorylation of proteins by inositol pyrophosphates. Science *306*, 2101-2105.

Saiardi, A., Sciambi, C., McCaffery, J.M., Wendland, B., and Snyder, S.H. (2002). Inositol pyrophosphates regulate endocytic trafficking. Proc Natl Acad Sci U S A *99*, 14206-14211.

Saiardi, A., Caffrey, J.J., Snyder, S.H., and Shears, S.B. (2000a). Inositol polyphosphate multikinase (ArgRIII) determines nuclear mRNA export in Saccharomyces cerevisiae. FEBS Lett *468*, 28-32.

Saiardi, A., Caffrey, J.J., Snyder, S.H., and Shears, S.B. (2000b). The inositol hexakisphosphate kinase family. Catalytic flexibility and function in yeast vacuole biogenesis. J Biol Chem *275*, 24686-24692.

Saiardi, A., Erdjument-Bromage, H., Snowman, A.M., Tempst, P., and Snyder, S.H. (1999). Synthesis of diphosphoinositol pentakisphosphate by a newly identified family of higher inositol polyphosphate kinases. Curr Biol *9*, 1323-1326.

Sambrook, D.R.J. (2001). *Molecular Cloning: A laboratory manual*, Vol Volume 2: 13.36, *third edition* edn (Cold Spring Harbour, New York, USA, Cold Spring Harbour Laboratory Press).

Santarius, M., Lee, C.H., and Anderson, R.A. (2006). Supervised membrane swimming: small G-protein lifeguards regulate PIPK signalling and monitor intracellular PtdIns(4,5)P2 pools. Biochem J *398*, 1-13.

Sarmah, B., Latimer, A.J., Appel, B., and Wente, S.R. (2005). Inositol polyphosphates regulate zebrafish left-right asymmetry. Dev Cell *9*, 133-145.

Sbrissa, D., Ikonomov, O.C., Strakova, J., and Shisheva, A. (2004). Role for a novel signaling intermediate, phosphatidylinositol 5-phosphate, in insulin-regulated F-actin stress fiber breakdown and GLUT4 translocation. Endocrinology *145*, 4853-4865.

Schafer, D.A., Jennings, P.B., and Cooper, J.A. (1996). Dynamics of capping protein and actin assembly in vitro: uncapping barbed ends by polyphosphoinositides. J Cell Biol *135*, 169-179.

Schiavo, G., Gmachl, M.J., Stenbeck, G., Sollner, T.H., and Rothman, J.E. (1995). A possible docking and fusion particle for synaptic transmission. Nature *378*, 733-736.

Schmitt, C., von Kobbe, C., Bachi, A., Pante, N., Rodrigues, J.P., Boscheron, C., Rigaut, G., Wilm, M., Seraphin, B., Carmo-Fonseca, M., *et al.* (1999). Dbp5, a DEAD-box protein required for mRNA export, is recruited to the cytoplasmic fibrils of nuclear pore complex via a conserved interaction with CAN/Nup159p. Embo J *18*, 4332-4347.

Schneider, K.R., Smith, R.L., and O'Shea, E.K. (1994). Phosphate-regulated inactivation of the kinase PHO80-PHO85 by the CDK inhibitor PHO81. Science *266*, 122-126.

Schomerus, C., and Kuntzel, H. (1992). CDC25-dependent induction of inositol 1,4,5-trisphosphate and diacylglycerol in Saccharomyces cerevisiae by nitrogen. FEBS Lett *307*, 249-252.

Schuller, C., Brewster, J.L., Alexander, M.R., Gustin, M.C., and Ruis, H. (1994). The HOG pathway controls osmotic regulation of transcription via the stress response element (STRE) of the Saccharomyces cerevisiae CTT1 gene. Embo J *13*, 4382-4389.

Seeds, A.M., Frederick, J.P., Tsui, M.M., and York, J.D. (2007). Roles for inositol polyphosphate kinases in the regulation of nuclear processes and developmental biology. Adv Enzyme Regul *47*, 10-25.

Seeds, A.M., Bastidas, R.J., and York, J.D. (2005). Molecular definition of a novel inositol polyphosphate metabolic pathway initiated by inositol 1,4,5-trisphosphate 3-kinase activity in Saccharomyces cerevisiae. J Biol Chem *280*, 27654-27661.

Seeds, A.M., Sandquist, J.C., Spana, E.P., and York, J.D. (2004). A molecular basis for inositol polyphosphate synthesis in Drosophila melanogaster. J Biol Chem *279*, 47222-47232.
Seeley, E.S., Kato, M., Margolis, N., Wickner, W., and Eitzen, G. (2002). Genomic analysis of homotypic vacuole fusion. Mol Biol Cell *13*, 782-794.

Shen, H., and Dowhan, W. (1996). Reduction of CDP-diacylglycerol synthase activity results in the excretion of inositol by Saccharomyces cerevisiae. J Biol Chem *271*, 29043-29048.

Shi, J., Wang, H., Hazebroek, J., Ertl, D.S., and Harp, T. (2005). The maize low-phytic acid 3 encodes a myo-inositol kinase that plays a role in phytic acid biosynthesis in developing seeds. Plant J *42*, 708-719.

Shibatohge, M., Kariya, K., Liao, Y., Hu, C.D., Watari, Y., Goshima, M., Shima, F., and Kataoka, T. (1998). Identification of PLC210, a Caenorhabditis elegans phospholipase C, as a putative effector of Ras. J Biol Chem *273*, 6218-6222.

Sidhu, R.S., Clough, R.R., and Bhullar, R.P. (2005). Regulation of phospholipase C-delta1 through direct interactions with the small GTPase Ral and calmodulin. J Biol Chem *280*, 21933-21941.

Sloane-Stanley, G.H. (1953). Anaerobic reactions of phospholipins in brain suspensions. Biochem J *53*, 613-619.

Smith, R.J., Sam, L.M., Justen, J.M., Bundy, G.L., Bala, G.A., and Bleasdale, J.E. (1990). Receptor-coupled signal transduction in human polymorphonuclear neutrophils: effects of a novel inhibitor of phospholipase C-dependent processes on cell responsiveness. J Pharmacol Exp Ther *253*, 688-697.

Smrcka, A.V., and Sternweis, P.C. (1993). Regulation of purified subtypes of phosphatidylinositol-specific phospholipase C beta by G protein alpha and beta gamma subunits. J Biol Chem *268*, 9667-9674.

Song, C., Hu, C.D., Masago, M., Kariyai, K., Yamawaki-Kataoka, Y., Shibatohge, M., Wu, D., Satoh, T., and Kataoka, T. (2001). Regulation of a novel human phospholipase C, PLCepsilon, through membrane targeting by Ras. J Biol Chem *276*, 2752-2757.

Steger, D.J., Haswell, E.S., Miller, A.L., Wente, S.R., and O'Shea, E.K. (2003). Regulation of chromatin remodeling by inositol polyphosphates. Science *299*, 114-116.

Stephens, L.R., and Irvine, R.F. (1990). Stepwise phosphorylation of myo-inositol leading to myo-inositol hexakisphosphate in Dictyostelium. Nature *346*, 580-583.

Strathmann, M., and Simon, M.I. (1990). G protein diversity: a distinct class of alpha subunits is present in vertebrates and invertebrates. Proc Natl Acad Sci U S A *87*, 9113-9117.

Streb, H., Irvine, R.F., Berridge, M.J., and Schulz, I. (1983). Release of Ca2+ from a nonmitochondrial intracellular store in pancreatic acinar cells by inositol-1,4,5-trisphosphate. Nature *306*, 67-69.

Suh, P.G., Park, J.I., Manzoli, L., Cocco, L., Peak, J.C., Katan, M., Fukami, K., Kataoka, T., Yun, S., and Ryu, S.H. (2008). Multiple roles of phosphoinositide-specific phospholipase C isozymes. BMB Rep *41*, 415-434.

Sun, B., Murray, N.R., and Fields, A.P. (1997). A role for nuclear phosphatidylinositol-specific phospholipase C in the G2/M phase transition. J Biol Chem *272*, 26313-26317.

Sutton, R.B., Davletov, B.A., Berghuis, A.M., Sudhof, T.C., and Sprang, S.R. (1995). Structure of the first C2 domain of synaptotagmin I: a novel Ca2+/phospholipid-binding fold. Cell *80*, 929-938.

Tisi, R., Belotti, F., Wera, S., Winderickx, J., Thevelein, J.M., and Martegani, E. (2004). Evidence for inositol triphosphate as a second messenger for glucose-induced calcium signalling in budding yeast. Curr Genet *45*, 83-89.

Toker, A. (2002). Phosphoinositides and signal transduction. Cell Mol Life Sci *59*, 761-779.

Topham, M.K., and Prescott, S.M. (2002). Diacylglycerol kinases: regulation and signaling roles. Thromb Haemost *88*, 912-918.

Traynor-Kaplan, A.E., Harris, A.L., Thompson, B.L., Taylor, P., and Sklar, L.A. (1988). An inositol tetrakisphosphate-containing phospholipid in activated neutrophils. Nature *334*, 353-356.

Trott, A., Shaner, L., and Morano, K.A. (2005). The molecular chaperone Sse1 and the growth control protein kinase Sch9 collaborate to regulate protein kinase A activity in Saccharomyces cerevisiae. Genetics *170*, 1009-1021.

Van der Kaay, J., and Van Haastert, P.J. (1995). Desalting inositolpolyphosphates by dialysis. Anal Biochem *225*, 183-185.

Van Rheenen, J., Achame, E.M., Janssen, H., Calafat, J., and Jalink, K. (2005). PIP2 signaling in lipid domains: a critical re-evaluation. Embo J *24*, 1664-1673.

Vida, T.A., and Emr, S.D. (1995). A new vital stain for visualizing vacuolar membrane dynamics and endocytosis in yeast. J Cell Biol *128*, 779-792.

Voglmaier, S.M., Keen, J.H., Murphy, J.E., Ferris, C.D., Prestwich, G.D., Snyder, S.H., and Theibert, A.B. (1992). Inositol hexakisphosphate receptor identified as the clathrin assembly protein AP-2. Biochem Biophys Res Commun *187*, 158-163.

Wagner, H., Hoerhammer, L., and Wolff, P. (1961). [Thin layer chromatography of phosphatides and glycolipids.]. Biochem Z *334*, 175-184.

Wahl, M.I., Nishibe, S., Kim, J.W., Kim, H., Rhee, S.G., and Carpenter, G. (1990). Identification of two epidermal growth factor-sensitive tyrosine phosphorylation sites of phospholipase C-gamma in intact HSC-1 cells. J Biol Chem *265*, 3944-3948.

Wang, T., Dowal, L., El-Maghrabi, M.R., Rebecchi, M., and Scarlata, S. (2000). The pleckstrin homology domain of phospholipase C-beta(2) links the binding of gbetagamma to activation of the catalytic core. J Biol Chem *275*, 7466-7469.

Watanabe, M., Chen, C.Y., and Levin, D.E. (1994). Saccharomyces cerevisiae PKC1 encodes a protein kinase C (PKC) homolog with a substrate specificity similar to that of mammalian PKC. J Biol Chem *269*, 16829-16836.

Watkins, J.L., Murphy, R., Emtage, J.L., and Wente, S.R. (1998). The human homologue of Saccharomyces cerevisiae Gle1p is required for poly(A)+ RNA export. Proc Natl Acad Sci U S A *95*, 6779-6784.

Weirich, C.S., Erzberger, J.P., Flick, J.S., Berger, J.M., Thorner, J., and Weis, K. (2006). Activation of the DExD/H-box protein Dbp5 by the nuclear-pore protein Gle1 and its coactivator InsP6 is required for mRNA export. Nat Cell Biol *8*, 668-676.

Whitman, M., Downes, C.P., Keeler, M., Keller, T., and Cantley, L. (1988). Type I phosphatidylinositol kinase makes a novel inositol phospholipid, phosphatidylinositol-3-phosphate. Nature *332*, 644-646.

Williams, R.L. (1999). Mammalian phosphoinositide-specific phospholipase C. Biochim Biophys Acta *1441*, 255-267.

Wiradjaja, F., Ooms, L.M., Tahirovic, S., Kuhne, E., Devenish, R.J., Munn, A.L., Piper, R.C., Mayinger, P., and Mitchell, C.A. (2007). Inactivation of the phosphoinositide phosphatases Sac1p and Inp54p leads to accumulation of phosphatidylinositol 4,5-bisphosphate on vacuole membranes and vacuolar fusion defects. J Biol Chem *282*, 16295-16307.

Wong, R., Hadjiyanni, I., Wei, H.C., Polevoy, G., McBride, R., Sem, K.P., and Brill, J.A. (2005). PIP2 hydrolysis and calcium release are required for cytokinesis in Drosophila spermatocytes. Curr Biol *15*, 1401-1406.

Yagisawa, H. (2006). Nucleocytoplasmic shuttling of phospholipase C-delta1: a link to Ca2+. J Cell Biochem *97*, 233-243.

Yagisawa, H., Okada, M., Naito, Y., Sasaki, K., Yamaga, M., and Fujii, M. (2006). Coordinated intracellular translocation of phosphoinositide-specific phospholipase C-delta with the cell cycle. Biochim Biophys Acta *1761*, 522-534.

Yagisawa, H., Yamaga, M., Okada, M., Sasaki, K., and Fujii, M. (2002). Regulation of the intracellular localization of phosphoinositide-specific phospholipase Cdelta(1). Adv Enzyme Regul *42*, 261-284.

Yagisawa, H., Sakuma, K., Paterson, H.F., Cheung, R., Allen, V., Hirata, H., Watanabe, Y., Hirata, M., Williams, R.L., and Katan, M. (1998). Replacements of single basic amino acids in the pleckstrin homology domain of phospholipase C-delta1 alter the ligand binding, phospholipase activity, and interaction with the plasma membrane. J Biol Chem *273*, 417-424.

Yamaga, M., Fujii, M., Kamata, H., Hirata, H., and Yagisawa, H. (1999). Phospholipase C-

delta1 contains a functional nuclear export signal sequence. J Biol Chem *274*, 28537-28541.

Yamaga, M., Kawai, K., Kiyota, M., Homma, Y., and Yagisawa, H. (2008). Recruitment and activation of phospholipase C (PLC)-delta1 in lipid rafts by muscarinic stimulation of PC12 cells: contribution of p122RhoGAP/DLC1, a tumor-suppressing PLCdelta1 binding protein. Adv Enzyme Regul *48*, 41-54.

Yamamoto, T., Takeuchi, H., Kanematsu, T., Allen, V., Yagisawa, H., Kikkawa, U., Watanabe, Y., Nakasima, A., Katan, M., and Hirata, M. (1999). Involvement of EF hand motifs in the Ca(2+)-dependent binding of the pleckstrin homology domain to phosphoinositides. Eur J Biochem *265*, 481-490.

Yang, X., Rudolf, M., Carew, M.A., Yoshida, M., Nerreter, V., Riley, A.M., Chung, S.K., Bruzik, K.S., Potter, B.V., Schultz, C., *et al.* (1999). Inositol 1,3,4-trisphosphate acts in vivo as a specific regulator of cellular signaling by inositol 3,4,5,6-tetrakisphosphate. J Biol Chem *274*, 18973-18980.

Yoko-o, T., Matsui, Y., Yagisawa, H., Nojima, H., Uno, I., and Toh-e, A. (1993). The putative phosphoinositide-specific phospholipase C gene, PLC1, of the yeast Saccharomyces cerevisiae is important for cell growth. Proc Natl Acad Sci U S A *90*, 1804-1808.

Yoneda, Y. (2000). Nucleocytoplasmic protein traffic and its significance to cell function. Genes Cells *5*, 777-787.

York, J.D. (2006). Regulation of nuclear processes by inositol polyphosphates. Biochim Biophys Acta *1761*, 552-559.

York, J.D., Guo, S., Odom, A.R., Spiegelberg, B.D., and Stolz, L.E. (2001). An expanded view of inositol signaling. Adv Enzyme Regul *41*, 57-71.

York, J.D., Odom, A.R., Murphy, R., Ives, E.B., and Wente, S.R. (1999). A phospholipase C-dependent inositol polyphosphate kinase pathway required for efficient messenger RNA export. Science *285*, 96-100.

York, S.J., Armbruster, B.N., Greenwell, P., Petes, T.D., and York, J.D. (2005). Inositol diphosphate signaling regulates telomere length. J Biol Chem *280*, 4264-4269.

Yoshida, M., Nishikawa, M., Nishi, K., Abe, K., Horinouchi, S., and Beppu, T. (1990). Effects of leptomycin B on the cell cycle of fibroblasts and fission yeast cells. Exp Cell Res *187*, 150-156.

Yun, C.W., Tamaki, H., Nakayama, R., Yamamoto, K., and Kumagai, H. (1998). Gpr1p, a putative G-protein coupled receptor, regulates glucose-dependent cellular cAMP level in yeast Saccharomyces cerevisiae. Biochem Biophys Res Commun *252*, 29-33.

Zhao, C., Jung, U.S., Garrett-Engele, P., Roe, T., Cyert, M.S., and Levin, D.E. (1998a). Temperature-induced expression of yeast FKS2 is under the dual control of protein kinase C and calcineurin. Mol Cell Biol *18*, 1013-1022.

Zhao, K., Wang, W., Rando, O.J., Xue, Y., Swiderek, K., Kuo, A., and Crabtree, G.R. (1998b). Rapid and phosphoinositol-dependent binding of the SWI/SNF-like BAF complex to chromatin after T lymphocyte receptor signaling. Cell *95*, 625-636.

Zhang, T., Caffrey, J.J., and Shears, S.B. (2001). The transcriptional regulator, Arg82, is a hybrid kinase with both monophosphoinositol and diphosphoinositol polyphosphate synthase activity. FEBS Lett *494*, 208-212.

Appendix A: Stability of GFP-Plc1p constructs described in this study

It was important control to determine which of the mutant constructs generated in this work were stable to ensure that we are looking at the localisation of GFP-Plc1p constructs rather than of GFP. I examined extracts of these cells subjected to SDS-PAGE, followed by western-blotting of an anti-GFP antibody. The extracts were prepared by brief alkali treatment of yeast cells followed by a standard 3 min boiling in the SDS-PAGE sample buffer (see section 2.13). This method is quick and reduces the potential of construct degradation by released vacuolar proteases as glass bead-mediated disruption of yeast cells.

In wild type cells, as in Fig A. the blot shows: GFP-Plc1p, GFP-Plc1p^{NES}, GFP-Plc1p$^{1-333}$, GFP-Plc1p$^{110-end}$, GFP-Plc1p$^{220-end}$, GFP-Plc1p^{4R}, GFP-Plc1p^{KRLR}, GFP-Plc1p^{CAAX}, GFP-Plc1p^{PKI}, GFP-Plc1p$^{PKI/NES}$, GFP-Plc1p$^{CAAX/NES}$, GFP-Plc1p^{E425G}, GFP-Plc1p^{R1}, GFP-Plc1p$^{R2/3}$, GFP-Plc1p$^{R2/4}$, GFP-Plc1p, GFP-Plc1p$^{4R/E425G}$ and GFP-Plc1p$^{(1-333)+C2}$ appeared to be largely stable under the extraction conditions employed.

GFP-Plc1p$^{220-333}$, GFP-Plc1p$^{1-220}$, and GFP-Plc1p$^{1-110}$ each showed evidence of degradation, with band around the size of GFP (~ 28 kD) in addition to a higher mass band corresponding to the un-degraded construct.

For GFP-Plc1p$^{110-220}$, GFP-Plc1p$^{333-end}$ and GFP-Plc1p^{KKLRK}, only a ~30 kD band that is likely to be liberated GFP is obvious.

For GFP-Plc1p$^{220-333}$, GFP-Plc1p$^{1-220}$ and GFP-Plc1p^{KKLRK}, however, we believe that the degradation is occurring after cell lysis, as these GFP-Plc1p constructs must be at least partially stabile because the expressed fluorescent protein were concentrated in the nucleus: GFP itself does not accumulate in the nucleus (Fig 3.3).

However, the blot did help to explain the diffused fluorescence in GFP-Plc1p$^{1-110}$, GFP-Plc1p$^{110-220}$ and GFP-Plc1p$^{333-end}$. I do not know why these truncations appeared to be more subject to proteolysis.

Thus, these experiments are difficult to interpret and another more efficient method will have to be found to extract these proteins from cells avoiding post-lytic degradation. Experiments carried out as above but in strains deleted for the major vacuolar protease Pep4p, have not yielded better results (data not shown) suggesting that a non-vacuolar protease may be responsible for the observed degradation. Future studies must address this problem, possibly via a combination of protease deficient strains and higher concentrations of protease inhibitors.

Fig A: Stability of GFP-Plc1p mutant constructs by Western-blotting

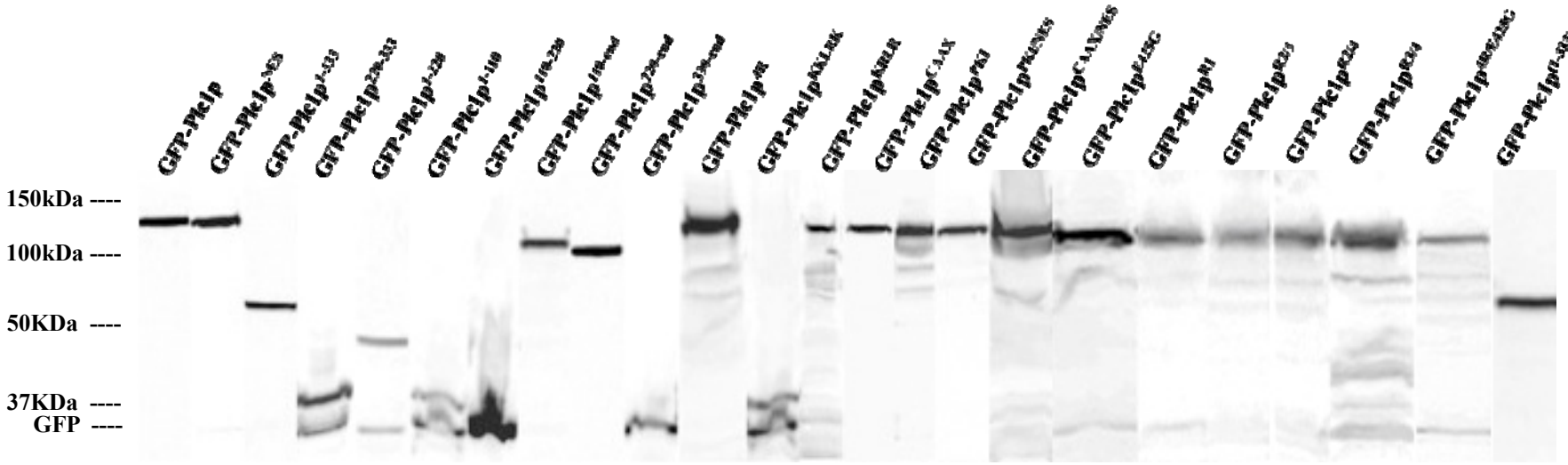

Samples were resolved by SDS-PAGE followed by Western-blotting: 5ml each cell culture (BY4742 cells transformed with each GFP-Plc1p mutant respectively) was grown to $1x10^7$ /ml in SC-Ura-Met media+2% glucose. 32µl(~ 40%) of each total lysate was loaded into each well. Samples were electrophoretically transferred to a nitrocellulose filter followed by incubation with anti-GFP as described in section 2.13.

Appendix B: Fluorescence instensity reading for GFP constructs

B1: Constructs in Chapter 3

[PM: plasma membrane fluorescence intensity; N: nuclear fluorescence intensity; C: cytosolic fluorescence intensity]

Genotype								**Mean**	**SEM**	**Ratio**(N:C)	**Mean**^{Ratio}	**SEM**^{Ratio}
pUG36 in WT											1.191	0.050
1	N	147	149	120	100	103	114	122.167	8.693	0.915		
	C	135	152	130	137	122	125	133.500	4.372			
2	N	179	173	180	168	160	175	172.500	3.063	1.091		
	C	141	171	168	158	158	153	158.167	4.408			
3	N	228	217	227	211	201	217	216.833	4.135	1.178		
	C	195	159	175	185	198	192	184.000	6.022			
4	N	167	175	168	179	182	180	175.167	2.600	1.454		
	C	129	135	114	118	104	123	120.500	4.507			
5	N	200	199	203	202	199	195	199.667	1.145	1.334		
	C	165	140	147	150	146	150	149.667	3.412			
6	N	75	84	83	78	76	78	79.000	1.506	1.056		
	C	79	81	72	77	65	75	74.833	2.344			
7	N	76	66	72	74	77	73	73.000	1.592	1.203		
	C	72	62	46	50	63	71	60.667	4.364			
8	N	212	228	221	206	214	205	214.333	3.621	1.200		
	C	196	179	179	167	172	179	178.667	4.006			
9	N	168	173	164	170	175	150	166.667	3.685	1.133		
	C	157	141	138	155	145	147	147.167	3.081			
10	N	203	213	210	201	224	206	209.500	3.413	1.347		
	C	154	130	173	153	163	160	155.500	5.892			
pUG36 in *plc1Δ*											1.201	0.037
1	N	149	130	132	131	145	134	136.833	3.301	1.039		
	C	132	138	121	138	124	137	131.667	3.062			
2	N	212	196	202	206	213	209	206.333	2.642	1.155		
	C	179	190	191	174	175	163	178.667	4.326			
3	N	179	181	179	181	195	184	183.167	2.482	1.191		
	C	160	165	141	153	157	147	153.833	3.582			
4	N	171	183	165	180	179	176	175.667	2.704	1.346		
	C	126	130	132	132	135	128	130.500	1.310			
5	N	214	218	228	205	217	221	217.167	3.114	1.179		
	C	193	195	171	186	185	175	184.167	3.902			

6	N	196	194	193	202	193	196	195.667	1.382	1.421		
	C	124	153	138	134	146	131	137.667	4.279			
7	N	138	143	148	137	135	142	140.500	1.945	1.074		
	C	122	128	131	139	135	130	130.833	2.386			
8	N	158	162	161	170	154	147	158.667	3.180	1.266		
	C	119	123	130	132	127	121	125.333	2.108			
9	N	171	179	173	160	173	166	170.333	2.679	1.215		
	C	133	137	142	143	146	140	140.167	1.887			
10	N	167	170	168	152	167	169	165.500	2.742	1.121		
	C	136	164	142	149	144	151	147.667	3.921			
pUG36-*PLC1* in WT											1.708	0.043
1	N	174	157	152	164	168	173	164.667	3.593	2.016		
	C	74	80	86	84	79	87	81.667	2.011			
2	N	158	150	157	163	166	165	159.833	2.469	1.806		
	C	97	78	89	86	94	87	88.500	2.717			
3	N	228	220	229	207	235	205	220.667	5.038	1.738		
	C	116	135	111	145	135	120	127.000	5.410			
4	N	213	217	210	218	234	222	219.000	3.445	1.754		
	C	119	123	132	120	125	130	124.833	2.151			
5	N	135	134	137	140	145	139	138.333	1.626	1.660		
	C	88	80	80	82	87	83	83.333	1.406			
6	N	123	131	126	121	119	118	123.000	1.983	1.651		
	C	71	70	75	78	77	76	74.500	1.335			
7	N	142	145	131	136	140	135	138.167	2.088	1.579		
	C	88	92	91	73	87	94	87.500	3.085			
8	N	150	149	144	148	142	152	147.500	1.544	1.715		
	C	79	77	89	84	95	92	86.000	2.944			
9	N	91	88	109	96	89	99	95.333	3.232	1.521		
	C	59	53	77	66	61	60	62.667	3.333			
10	N	109	111	104	117	108	108	109.500	1.765	1.634		
	C	62	64	67	68	71	70	67.000	1.414			
pUG36-*PLC1* in *plc1Δ*											1.654	0.042
1	N	100	109	99	98	101	104	101.833	1.662	1.571		
	C	63	67	60	66	63	70	64.833	1.447			
2	N	81	84	83	81	80	76	80.833	1.138	1.492		
	C	57	54	56	50	50	58	54.167	1.424			

3	N	176	173	171	178	174	188	176.667	2.472	1.584		
	C	124	113	114	97	115	106	111.500	3.731			
4	N	181	185	190	208	186	209	193.167	4.989	1.941		
	C	106	114	85	97	92	103	99.500	4.233			
5	N	106	105	103	97	102	104	102.833	1.302	1.615		
	C	66	73	60	72	54	57	63.667	3.232			
6	N	176	179	174	180	181	178	178.000	1.065	1.661		
	C	104	90	104	120	115	110	107.167	4.277			
7	N	196	175	186	197	182	200	189.333	4.030	1.618		
	C	113	123	121	106	110	129	117.000	3.568			
8	N	190	176	172	186	183	179	181.000	2.708	1.588		
	C	109	116	117	123	105	114	114.000	2.582			
9	N	197	190	201	196	202	196	197.000	1.751	1.830		
	C	119	110	108	101	107	101	107.667	2.728			
10	N	171	179	176	174	186	183	178.167	2.301	1.635		
	C	108	111	105	117	108	105	109.000	1.844			
pUG36-*PLC1*^{NES} in WT											2.273	0.049
1	N	95	98	100	98	96	102	98.167	1.046	2.464		
	C	35	33	37	45	41	48	39.833	2.400			
2	N	96	86	91	92	87	94	91.000	1.592	2.505		
	C	40	36	34	40	32	36	36.333	1.308			
3	N	87	91	84	81	91	86	86.667	1.606	2.464		
	C	32	39	37	31	32	40	35.167	1.621			
4	N	77	83	82	86	85	81	82.333	1.308	2.157		
	C	40	41	35	36	37	40	38.167	1.014			
5	N	186	192	190	180	176	180	184.000	2.582	2.300		
	C	84	69	75	88	86	78	80.000	2.978			
6	N	91	86	97	94	92	88	91.333	1.626	2.157		
	C	46	52	32	38	41	45	42.333	2.836			
7	N	86	84	82	78	73	81	80.667	1.892	2.180		
	C	39	37	41	37	36	32	37.000	1.238			
8	N	75	78	74	74	73	77	75.167	0.792	2.098		
	C	42	40	32	38	30	33	35.833	1.973			
9	N	81	84	76	83	76	72	78.667	1.926	2.117		
	C	33	44	41	35	32	38	37.167	1.922			
10	N	86	77	80	85	78	85	81.833	1.621	2.284		

	C	35	40	37	38	34	31	35.833	1.302			
pUG36-*PLC1*$^{1\text{-}999nt}$ in WT											1.718	0.055
1	N	196	215	212	213	204	194	205.667	3.712	1.700		
	C	103	116	107	132	137	131	121.000	5.837			
2	N	215	212	216	228	227	223	220.167	2.750	1.543		
	C	135	136	165	127	149	144	142.667	5.445			
3	N	173	167	181	176	177	183	176.167	2.344	1.816		
	C	93	96	97	99	95	102	97.000	1.291			
4	N	94	86	88	96	91	87	90.333	1.647	1.477		
	C	67	65	64	59	54	58	61.167	2.023			
5	N	179	188	178	174	171	177	177.833	2.358	2.068		
	C	77	83	76	90	94	96	86.000	3.512			
6	N	117	119	116	115	120	110	116.167	1.447	1.864		
	C	55	62	65	67	60	65	62.333	1.783			
7	N	153	141	138	148	146	154	146.667	2.603	1.689		
	C	84	87	86	88	87	89	86.833	0.703			
8	N	156	158	173	170	155	160	162.000	3.109	1.591		
	C	102	107	103	105	96	98	101.833	1.701			
9	N	104	105	106	99	100	108	103.667	1.430	1.798		
	C	56	61	57	58	55	59	57.667	0.882			
10	N	89	96	82	85	87	99	89.667	2.679	1.635		
	C	52	51	52	53	58	63	54.833	1.922			
pUG36-*PLC1*$^{660\text{-}999nt}$ in WT											1.318	0.022
1	N	164	169	173	174	166	165	168.500	1.727	1.231		
	C	134	114	136	132	157	148	136.833	6.013			
2	N	183	171	174	195	186	185	182.333	3.556	1.362		
	C	125	131	127	138	135	147	133.833	3.291			
3	N	158	154	155	157	158	150	155.333	1.256	1.324		
	C	116	112	119	121	124	112	117.333	1.994			
4	N	150	148	140	145	137	140	143.333	2.092	1.311		
	C	120	116	104	104	107	105	109.333	2.824			
5	N	131	126	138	137	136	128	132.667	2.060	1.266		
	C	94	119	113	111	101	91	104.833	4.578			
6	N	119	120	115	110	107	111	113.667	2.124	1.194		
	C	100	96	88	89	97	101	95.167	2.242			
7	N	145	146	141	149	156	150	147.833	2.088	1.386		

	C	101	110	119	98	102	110	106.667	3.180			
8	N	140	139	134	147	138	131	138.167	2.242	1.370		
	C	105	104	93	94	109	100	100.833	2.600			
9	N	123	131	133	128	129	124	128.000	1.592	1.322		
	C	91	112	97	94	92	95	96.833	3.156			
10	N	146	151	148	158	146	156	150.833	2.104	1.416		
	C	104	108	97	116	109	105	106.500	2.566			
pUG36-*PLC1*$^{1\text{-}660nt}$ in WT											1.383	0.035
1	N	77	80	77	84	80	83	80.167	1.195	1.212		
	C	64	64	67	69	65	68	66.167	0.872			
2	N	83	84	81	85	90	82	84.167	1.302	1.358		
	C	56	64	65	64	57	66	62.000	1.770			
3	N	125	144	129	144	136	147	137.500	3.677	1.401		
	C	100	101	97	101	100	90	98.167	1.740			
4	N	125	128	124	129	135	142	130.500	2.790	1.362		
	C	103	96	94	100	90	92	95.833	2.007			
5	N	70	71	68	63	64	68	67.333	1.308	1.274		
	C	50	51	54	55	56	51	52.833	1.014			
6	N	67	68	63	68	71	68	67.500	1.057	1.387		
	C	49	51	54	47	44	47	48.667	1.430			
7	N	120	111	109	102	118	109	111.500	2.693	1.574		
	C	73	70	68	70	75	69	70.833	1.078			
8	N	129	130	114	127	129	123	125.333	2.486	1.301		
	C	104	86	91	105	97	95	96.333	3.007			
9	N	106	115	113	108	118	110	111.667	1.838	1.526		
	C	79	70	71	72	73	74	73.167	1.302			
10	N	112	107	118	110	109	111	111.167	1.537	1.441		
	C	74	71	77	84	73	84	77.167	2.301			
pUG36-*PLC1*$^{1\text{-}330nt}$ in WT											1.195	0.025
1	N	198	187	203	189	188	192	192.833	2.600	1.243		
	C	152	145	166	162	149	157	155.167	3.260			
2	N	137	138	132	131	133	136	134.500	1.176	1.180		
	C	118	120	108	115	107	116	114.000	2.176			
3	N	123	124	120	135	125	126	125.500	2.078	1.102		
	C	117	110	121	112	110	113	113.833	1.778			
4	N	116	128	133	123	130	129	126.500	2.487	1.159		

	C	122	114	101	107	108	103	109.167	3.156			
5	N	151	148	155	150	146	152	150.333	1.282	1.116		
	C	126	145	138	131	135	133	134.667	2.642			
6	N	146	138	144	149	136	145	143.000	2.033	1.192		
	C	124	119	124	129	108	116	120.000	3.022			
7	N	118	125	123	121	116	118	120.167	1.400	1.214		
	C	99	98	94	104	100	99	99.000	1.317			
8	N	104	94	100	97	91	93	96.500	1.979	1.133		
	C	89	91	79	86	82	84	85.167	1.815			
9	N	174	167	172	173	172	178	172.667	1.453	1.244		
	C	148	155	125	131	132	142	138.833	4.672			
10	N	229	246	235	246	220	229	234.167	4.222	1.368		
	C	161	172	176	185	158	175	171.167	4.110			
pUG36-*PLC1*$^{330\text{-}660nt}$ in WT											1.190	0.019
1	N	232	221	230	236	231	232	230.333	2.044	1.194		
	C	184	183	199	208	191	192	192.833	3.859			
2	N	225	224	212	224	221	223	221.500	1.979	1.154		
	C	189	182	196	199	209	177	192.000	4.789			
3	N	230	230	233	239	231	234	232.833	1.400	1.323		
	C	191	180	188	177	162	158	176.000	5.495			
4	N	111	119	122	111	115	112	115.000	1.880	1.150		
	C	103	101	93	100	106	97	100.000	1.862			
5	N	92	99	95	100	99	96	96.833	1.249	1.107		
	C	84	86	92	90	94	79	87.500	2.277			
6	N	84	92	79	84	87	93	86.500	2.172	1.215		
	C	65	68	79	74	75	66	71.167	2.301			
7	N	214	222	212	211	220	219	216.333	1.874	1.240		
	C	171	161	180	192	176	167	174.500	4.433			
8	N	141	140	134	136	135	138	137.333	1.145	1.208		
	C	105	103	118	114	124	118	113.667	3.333			
9	N	124	122	122	126	125	128	124.500	0.957	1.144		
	C	111	116	97	107	111	111	108.833	2.638			
10	N	130	127	120	124	133	128	127.000	1.862	1.169		
	C	105	105	101	110	117	114	108.667	2.486			
pUG36-*PLC1*$^{330nt\text{-}end}$ in WT											2.061	0.042
1	N	122	130	122	119	132	116	123.500	2.553	2.099		

	C	50	65	63	55	62	58	58.833	2.301			
2	N	76	75	72	79	78	78	76.333	1.054	1.775		
	C	43	43	46	41	47	38	43.000	1.342			
3	N	78	75	83	79	81	80	79.333	1.116	2.183		
	C	33	38	34	37	41	35	36.333	1.202			
4	N	97	103	101	103	99	101	100.667	0.955	2.083		
	C	43	45	58	51	48	45	48.333	2.246			
5	N	119	111	109	114	113	115	113.500	1.408	2.233		
	C	58	43	52	59	47	46	50.833	2.701			
6	N	118	127	87	111	107	126	112.667	6.070	2.146		
	C	56	53	50	53	54	49	52.500	1.057			
7	N	71	72	67	71	72	66	69.833	1.078	1.913		
	C	41	37	30	43	31	37	36.500	2.125			
8	N	124	118	114	111	123	121	118.500	2.110	2.079		
	C	60	54	55	56	55	62	57.000	1.317			
9	N	83	82	83	84	81	79	82.000	0.730	2.076		
	C	40	44	39	41	37	36	39.500	1.176			
10	N	67	67	69	73	68	70	69.000	0.931	2.020		
	C	35	32	34	35	34	35	34.167	0.477			
pUG36-*PLC1*$^{660nt\text{-}end}$ in WT											2.103	0.038
1	N	213	212	211	195	219	212	210.333	3.283	1.927		
	C	122	93	99	123	108	110	109.167	4.909			
2	N	214	204	209	210	209	199	207.500	2.141	2.072		
	C	99	100	95	102	105	100	100.167	1.352			
3	N	198	189	188	202	194	200	195.167	2.372	2.209		
	C	85	87	93	88	97	80	88.333	2.445			
4	N	195	191	183	182	199	200	191.667	3.180	2.118		
	C	91	93	92	88	98	81	90.500	2.320			
5	N	110	103	106	100	116	108	107.167	2.286	2.248		
	C	46	56	43	40	48	53	47.667	2.459			
6	N	140	138	144	150	149	155	146.000	2.646	2.131		
	C	72	57	64	71	68	79	68.500	3.063			
7	N	185	188	189	190	176	178	184.333	2.431	2.127		
	C	85	82	88	90	95	80	86.667	2.246			
8	N	178	177	175	159	162	165	169.333	3.393	1.946		
	C	92	94	82	85	81	88	87.000	2.160			

9	N	224	201	207	197	221	201	208.500	4.631	2.270		
	C	91	95	106	94	83	82	91.833	3.609			
10	N	111	106	101	109	110	111	108.000	1.592	1.982		
	C	54	54	57	58	50	54	54.500	1.147			
pUG36-*PLC1*^{4R} in WT											1.514	0.035
1	N	211	218	212	214	222	220	216.167	1.833	1.595		
	C	139	141	129	126	142	136	135.500	2.693			
2	N	181	178	171	172	175	181	176.333	1.783	1.451		
	C	120	118	115	126	126	124	121.500	1.857			
3	N	205	199	207	209	202	213	205.833	2.040	1.542		
	C	131	122	131	139	140	138	133.500	2.814			
4	N	204	197	212	205	207	211	206.000	2.221	1.559		
	C	135	129	120	132	141	136	132.167	2.937			
5	N	104	97	97	90	89	94	95.167	2.242	1.366		
	C	68	63	73	72	74	68	69.667	1.687			
6	N	90	87	82	85	92	94	88.333	1.838	1.377		
	C	58	61	67	67	65	67	64.167	1.558			
7	N	152	154	148	153	158	146	151.833	1.759	1.393		
	C	114	111	116	108	106	99	109.000	2.503			
8	N	171	172	191	183	183	186	181.000	3.235	1.694		
	C	99	114	108	104	106	110	106.833	2.104			
9	N	190	183	197	191	187	196	190.667	2.171	1.591		
	C	133	120	112	120	113	121	119.833	3.070			
10	N	124	133	136	151	142	130	136.000	3.873	1.575		
	C	94	77	86	84	97	80	86.333	3.190			
pUG36-*PLC1*^{KKLRK} in WT											1.468	0.030
1	N	176	178	168	173	162	156	168.833	3.487	1.425		
	C	112	108	128	118	121	124	118.500	3.052			
2	N	181	171	165	164	179	185	174.167	3.582	1.401		
	C	111	128	118	122	128	139	124.333	3.938			
3	N	162	165	158	163	165	160	162.167	1.138	1.329		
	C	122	139	125	117	114	115	122.000	3.812			
4	N	151	155	144	151	153	156	151.667	1.745	1.550		
	C	108	96	104	104	81	94	97.833	4.003			
5	N	131	141	139	133	140	138	137.000	1.653	1.476		
	C	102	90	88	93	89	95	92.833	2.120			

6	N	175	158	158	152	157	159	159.833	3.198	1.596		
	C	87	95	101	107	98	113	100.167	3.728			
7	N	125	115	121	119	125	125	121.667	1.687	1.440		
	C	82	81	82	81	93	88	84.500	2.012			
8	N	141	144	147	138	140	143	142.167	1.302	1.619		
	C	92	83	89	89	93	81	87.833	1.973			
9	N	147	138	140	151	145	146	144.500	1.945	1.474		
	C	92	99	95	96	104	102	98.000	1.844			
10	N	144	141	149	139	141	147	143.500	1.586	1.373		
	C	99	102	109	106	107	104	104.500	1.478			
pUG36-*PLC1*^{KRLR} in WT											1.571	0.046
1	N	201	196	190	195	200	207	198.167	2.386	1.556		
	C	123	119	125	138	128	131	127.333	2.716			
2	N	153	140	142	162	155	145	149.500	3.490	1.341		
	C	103	117	112	108	118	111	111.500	2.291			
3	N	202	192	197	194	202	205	198.667	2.092	1.624		
	C	121	119	114	124	126	130	122.333	2.290			
4	N	183	167	180	180	180	179	178.167	2.301	1.579		
	C	111	118	116	121	104	107	112.833	2.701			
5	N	133	122	128	122	122	126	125.500	1.821	1.543		
	C	77	80	74	86	85	86	81.333	2.092			
6	N	163	165	170	168	172	167	167.500	1.335	1.637		
	C	92	102	94	111	116	99	102.333	3.870			
7	N	180	175	176	184	185	188	181.333	2.124	1.835		
	C	96	87	106	97	108	99	98.833	3.092			
8	N	172	170	181	175	175	185	176.333	2.305	1.726		
	C	100	103	102	96	102	110	102.167	1.869			
9	N	215	204	202	210	211	208	208.333	1.944	1.450		
	C	142	159	141	141	145	134	143.667	3.403			
10	N	179	183	186	179	171	187	180.833	2.400	1.416		
	C	129	130	120	119	137	131	127.667	2.824			
pUG36-*PLC1*^{PKI} in WT											0.710	0.017
1	N	102	109	117	110	101	108	107.833	2.386	0.639		
	C	166	162	168	174	178	164	168.667	2.512			
2	N	151	158	162	149	158	153	155.167	2.023	0.655		
	C	249	230	223	238	240	242	237.000	3.759			

3	N	153	153	154	161	163	144	154.667	2.765	0.762		
	C	215	202	200	205	195	201	203.000	2.745			
4	N	121	118	128	112	119	120	119.667	2.108	0.750		
	C	159	166	164	156	167	145	159.500	3.374			
5	N	115	111	123	118	114	110	115.167	1.956	0.757		
	C	154	150	158	148	155	148	152.167	1.682			
6	N	176	170	171	187	170	184	176.333	3.062	0.729		
	C	230	243	250	244	246	238	241.833	2.857			
7	N	188	185	182	180	195	188	186.333	2.171	0.769		
	C	239	237	240	250	240	248	242.333	2.171			
8	N	80	83	82	80	82	79	81.000	0.632	0.632		
	C	128	124	130	127	129	131	128.167	1.014			
9	N	164	171	166	168	162	169	166.667	1.358	0.699		
	C	250	242	211	243	245	240	238.500	5.673			
10	N	160	149	151	159	156	145	153.333	2.431	0.704		
	C	219	213	224	214	220	216	217.667	1.687			
pUG36-*PLC1*$^{NES/PKI}$ in WT											0.830	0.015
1	N	150	158	160	152	159	166	157.500	2.363	0.773		
	C	203	201	196	201	211	210	203.667	2.362			
2	N	183	179	191	184	183	178	183.000	1.880	0.799		
	C	234	238	220	212	223	248	229.167	5.394			
3	N	175	180	188	169	179	171	177.000	2.817	0.837		
	C	201	214	212	208	211	223	211.500	2.952			
4	N	118	107	111	108	115	111	111.667	1.706	0.772		
	C	156	142	150	137	132	151	144.667	3.756			
5	N	139	133	145	135	143	144	139.833	2.040	0.850		
	C	165	163	174	170	148	167	164.500	3.658			
6	N	133	122	128	138	141	139	133.500	2.997	0.880		
	C	157	159	144	152	148	150	151.667	2.290			
7	N	132	124	135	138	140	131	133.333	2.333	0.901		
	C	142	140	137	166	154	149	148.000	4.405			
8	N	124	130	136	124	133	136	130.500	2.247	0.804		
	C	163	168	161	158	166	158	162.333	1.687			
9	N	104	95	90	88	92	101	95.000	2.582	0.793		
	C	120	114	126	118	123	118	119.833	1.721			
10	N	188	179	184	190	189	192	187.000	1.932	0.890		

	C	202	214	201	212	210	222	210.167	3.208			
pUG36-*PLC1*$^{NES/CAAX}$ in WT											1.725	0.098
1	N	80	81	75	79	80	84	79.833	1.195	1.497		
	C	50	58	52	46	59	55	53.333	2.028			
2	N	94	98	92	94	98	94	95.000	1.000	1.672		
	C	62	51	58	53	51	66	56.833	2.548			
3	N	73	70	71	73	73	80	73.333	1.430	1.447		
	C	51	52	49	54	44	54	50.667	1.542			
4	N	120	126	103	117	128	112	117.667	3.783	1.646		
	C	60	75	73	71	78	72	71.500	2.513			
5	N	120	114	118	110	121	118	116.833	1.682	1.565		
	C	77	66	74	77	71	83	74.667	2.376			
6	N	94	100	95	92	97	92	95.000	1.265	1.913		
	C	52	49	48	51	52	46	49.667	0.989			
7	N	86	89	87	94	86	92	89.000	1.366	1.723		
	C	54	51	48	55	53	49	51.667	1.145			
8	N	78	72	74	73	76	75	74.667	0.882	1.459		
	C	44	49	61	54	50	49	51.167	2.358			
9	N	187	179	187	181	179	182	182.500	1.500	2.483		
	C	71	67	69	73	71	90	73.500	3.403			
10	N	79	85	88	86	89	77	84.000	2.000	1.846		
	C	46	40	43	48	50	46	45.500	1.455			
pUG36-*PLC1* in *xpo1-1*												
23'C											1.517	0.031
1	N	93	86	87	88	86	96	89.333	1.706	1.501		
	C	60	62	55	60	61	59	59.500	0.992			
2	N	92	98	94	98	82	100	94.000	2.683	1.435		
	C	64	68	69	66	61	65	65.500	1.176			
3	N	80	77	76	83	75	81	78.667	1.282	1.489		
	C	55	53	46	52	53	58	52.833	1.621			
4	N	101	103	108	110	107	100	104.833	1.662	1.682		
	C	63	65	60	61	66	59	62.333	1.145			
5	N	101	106	105	99	107	93	101.833	2.167	1.579		
	C	60	72	69	62	59	65	64.500	2.110			
6	N	72	84	82	84	76	74	78.667	2.171	1.532		
	C	50	58	55	53	48	44	51.333	2.060			

7	N	116	111	110	106	118	107	111.333	1.961	1.617		
	C	66	65	74	70	67	71	68.833	1.400			
8	N	88	83	87	82	80	79	83.167	1.493	1.324		
	C	57	66	60	67	65	62	62.833	1.579			
9	N	86	87	80	82	86	83	84.000	1.125	1.478		
	C	56	53	68	62	52	50	56.833	2.810			
10	N	81	84	77	76	75	72	77.500	1.765	1.530		
	C	53	51	49	53	50	48	50.667	0.843			
37'C											1.649	0.050
1	N	107	114	130	118	120	108	116.167	3.487	1.602		
	C	74	70	74	71	69	77	72.500	1.232			
2	N	130	122	125	131	114	121	123.833	2.574	1.492		
	C	80	85	81	88	86	78	83.000	1.592			
3	N	105	112	114	105	109	101	107.667	1.994	1.780		
	C	63	71	59	61	52	57	60.500	2.604			
4	N	154	141	147	157	150	153	150.333	2.333	2.022		
	C	69	76	78	65	75	83	74.333	2.629			
5	N	101	96	94	98	90	97	96.000	1.528	1.582		
	C	65	61	60	55	64	59	60.667	1.476			
6	N	106	117	108	112	101	98	107.000	2.852	1.625		
	C	72	63	58	63	71	68	65.833	2.212			
7	N	141	133	130	122	138	135	133.167	2.725	1.627		
	C	86	79	76	86	84	80	81.833	1.682			
8	N	98	102	89	85	95	101	95.000	2.769	1.615		
	C	57	64	66	55	59	52	58.833	2.182			
9	N	99	85	92	90	88	89	90.500	1.945	1.686		
	C	49	64	57	50	47	55	53.667	2.578			
10	N	80	84	82	78	84	79	81.167	1.046	1.462		
	C	59	58	50	53	57	56	55.500	1.384			
pUG36-*PLC1* in *XPO1*												
23'C											1.616	0.046
1	N	72	67	71	69	73	70	70.333	0.882	1.695		
	C	38	40	43	49	39	40	41.500	1.648			
2	N	74	66	63	65	70	66	67.333	1.626	1.469		
	C	45	43	49	45	43	50	45.833	1.222			
3	N	83	79	74	76	77	76	77.500	1.285	1.609		

	C	50	55	49	48	45	42	48.167	1.815			
4	N	126	131	127	123	125	119	125.167	1.641	1.873		
	C	66	63	76	63	66	67	66.833	1.956			
5	N	98	99	100	106	101	95	99.833	1.493	1.707		
	C	62	53	58	60	61	57	58.500	1.335			
6	N	81	86	85	82	78	87	83.167	1.400	1.631		
	C	50	43	53	48	54	58	51.000	2.129			
7	N	99	111	106	103	107	109	105.833	1.759	1.453		
	C	73	79	71	75	67	72	72.833	1.641			
8	N	90	97	94	84	93	79	89.500	2.766	1.384		
	C	65	70	58	64	62	69	64.667	1.820			
9	N	83	85	89	79	84	89	84.833	1.558	1.714		
	C	54	52	56	43	41	51	49.500	2.487			
10	N	89	87	96	101	103	95	95.167	2.587	1.627		
	C	60	57	59	54	58	63	58.500	1.232			
37'C											1.669	0.063
1	N	109	106	100	105	96	102	103.000	1.897	1.666		
	C	66	58	57	54	70	66	61.833	2.587			
2	N	82	70	75	70	72	73	73.667	1.838	1.464		
	C	50	44	52	58	48	50	50.333	1.892			
3	N	90	86	91	82	92	84	87.500	1.668	1.683		
	C	60	61	49	45	50	47	52.000	2.781			
4	N	131	127	133	139	145	142	136.167	2.833	2.161		
	C	45	70	65	58	67	73	63.000	4.155			
5	N	113	123	126	118	120	117	119.500	1.875	1.719		
	C	70	81	74	62	61	69	69.500	3.063			
6	N	112	107	113	104	100	108	107.333	1.994	1.699		
	C	66	61	56	71	57	68	63.167	2.496			
7	N	83	85	81	91	89	85	85.667	1.520	1.440		
	C	53	58	52	68	65	61	59.500	2.617			
8	N	97	94	99	109	101	95	99.167	2.227	1.545		
	C	71	55	66	59	66	68	64.167	2.442			
9	N	82	86	83	89	78	80	83.000	1.633	1.633		
	C	51	45	50	56	54	49	50.833	1.579			
10	N	151	124	134	140	148	131	138.000	4.219	1.676		
	C	76	84	88	77	83	86	82.333	1.978			

pUG36-*PLC1* in WT												
37'C											1.637	0.072
1	N	108	103	100	109	101	106	104.500	1.522	1.435		
	C	68	62	69	78	84	76	72.833	3.250			
2	N	91	89	83	89	91	88	88.500	1.204	1.553		
	C	53	57	58	60	53	61	57.000	1.390			
3	N	85	80	86	91	92	88	87.000	1.789	1.695		
	C	50	56	52	50	48	52	51.333	1.116			
4	N	161	146	161	171	170	152	160.167	4.012	1.945		
	C	85	78	78	89	86	78	82.333	2.011			
5	N	156	125	140	151	138	145	142.500	4.448	1.647		
	C	92	85	82	88	90	82	86.500	1.708			
6	N	79	75	72	80	73	75	75.667	1.308	1.549		
	C	51	46	52	52	45	47	48.833	1.302			
23'C (shifted from 37'C)											1.737	0.080
1	N	156	166	151	160	153	166	158.667	2.629	2.021		
	C	76	76	79	82	78	80	78.500	0.957			
2	N	234	220	230	244	240	239	234.500	3.519	1.790		
	C	140	123	117	141	132	133	131.000	3.856			
3	N	249	240	249	235	224	250	241.167	4.222	1.762		
	C	136	145	123	130	144	143	136.833	3.628			
4	N	187	174	176	183	179	174	178.833	2.151	1.720		
	C	101	92	112	116	103	100	104.000	3.550			
5	N	94	96	95	97	91	96	94.833	0.872	1.714		
	C	54	58	52	47	57	64	55.333	2.362			
6	N	72	77	74	75	78	82	76.333	1.430	1.414		
	C	55	56	52	55	56	50	54.000	1.000			
pUG36-*PLC1* in WT Hypo-osmotic shock												
2min											1.543	0.051
1	N	124	111	117	119	115	125	118.500	2.187	1.431		
	C	78	81	76	85	87	90	82.833	2.212			
2	N	169	165	159	162	161	155	161.833	1.973	1.671		
	C	87	92	110	105	92	95	96.833	3.591			
3	N	70	71	63	67	68	65	67.333	1.229	1.597		
	C	39	40	46	47	43	38	42.167	1.537			
4	N	81	86	92	94	92	91	89.333	1.994	1.901		

	C	48	41	48	44	48	53	47.000	1.673			
5	N	176	170	160	161	166	159	165.333	2.728	1.565		
	C	104	101	110	102	109	108	105.667	1.563			
6	N	217	203	203	216	198	211	208.000	3.183	1.361		
	C	161	153	151	159	145	148	152.833	2.535			
7	N	68	63	70	72	67	70	68.333	1.282	1.530		
	C	45	44	43	39	51	46	44.667	1.606			
8	N	62	65	59	65	61	66	63.000	1.125	1.562		
	C	42	39	38	38	43	42	40.333	0.919			
9	N	65	56	57	59	61	66	60.667	1.687	1.411		
	C	43	39	41	45	46	44	43.000	1.065			
10	N	254	240	252	254	250	239	248.167	2.810	1.405		
	C	167	163	194	176	169	191	176.667	5.308			
15min											1.592	0.026
1	N	175	186	180	185	187	192	184.167	2.414	1.563		
	C	126	116	122	119	111	113	117.833	2.301			
2	N	167	165	169	163	156	164	164.000	1.826	1.509		
	C	109	101	104	110	115	113	108.667	2.171			
3	N	83	77	74	72	83	77	77.667	1.856	1.612		
	C	49	52	51	44	45	48	48.167	1.302			
4	N	72	77	75	73	71	75	73.833	0.910	1.629		
	C	42	45	49	54	44	38	45.333	2.275			
5	N	244	250	236	251	241	248	245.000	2.366	1.771		
	C	133	140	143	140	136	138	138.333	1.430			
6	N	221	212	218	232	225	227	222.500	2.884	1.524		
	C	140	143	150	141	152	150	146.000	2.145			
7	N	191	193	200	198	188	196	194.333	1.838	1.548		
	C	131	120	135	112	122	133	125.500	3.658			
8	N	171	168	164	173	166	167	168.167	1.352	1.651		
	C	98	110	104	101	92	106	101.833	2.587			
9	N	221	229	216	223	215	216	220.000	2.221	1.495		
	C	141	121	159	158	148	156	147.167	5.941			
10	N	83	77	74	72	83	77	77.667	1.856	1.612		
	C	49	52	51	44	45	48	48.167	1.302			
2hrs											1.612	0.041
1	N	92	86	82	87	86	88	86.833	1.327	1.644		

	C	57	56	51	47	54	52	52.833	1.493			
2	N	240	249	233	247	250	232	241.833	3.280	1.539		
	C	152	148	156	168	178	141	157.167	5.552			
3	N	134	118	123	129	131	116	125.167	2.982	1.784		
	C	70	69	66	84	61	71	70.167	3.135			
4	N	124	121	112	115	109	110	115.167	2.496	1.592		
	C	81	73	65	74	70	71	72.333	2.155			
5	N	129	116	127	118	124	115	121.500	2.432	1.841		
	C	71	64	61	66	60	74	66.000	2.266			
6	N	181	180	188	186	177	168	180.000	2.910	1.581		
	C	108	104	114	117	123	117	113.833	2.798			
7	N	191	196	189	196	192	195	193.167	1.195	1.547		
	C	112	129	126	135	128	119	124.833	3.321			
8	N	113	115	108	116	119	107	113.000	1.915	1.455		
	C	77	74	68	88	84	75	77.667	2.951			
9	N	104	106	110	119	101	115	109.167	2.798	1.688		
	C	60	78	67	58	61	64	64.667	2.963			
10	N	124	117	121	118	123	118	120.167	1.195	1.451		
	C	90	84	75	82	76	90	82.833	2.664			
pUG36-*PLC1* in WT Hyper-osmotic shock												
2min											1.589	0.044
1	N	199	195	200	198	199	211	200.333	2.246	1.565		
	C	128	126	132	130	132	120	128.000	1.862			
2	N	182	186	183	169	182	175	179.500	2.566	1.440		
	C	139	130	122	115	119	123	124.667	3.509			
3	N	161	168	165	176	169	163	167.000	2.176	1.556		
	C	106	100	113	118	96	111	107.333	3.383			
4	N	168	163	157	159	167	168	163.667	1.961	1.945		
	C	84	83	84	89	78	87	84.167	1.537			
5	N	210	199	200	193	195	202	199.833	2.442	1.543		
	C	130	139	134	127	123	124	129.500	2.513			
6	N	211	217	206	212	211	203	210.000	2.000	1.607		
	C	124	127	136	127	137	133	130.667	2.201			
7	N	58	64	63	59	57	65	61.000	1.390	1.612		
	C	41	40	37	39	32	38	37.833	1.302			
8	N	67	61	65	56	62	66	62.833	1.662	1.467		

	C	42	40	43	41	44	47	42.833	1.014			
9	N	60	59	58	59	63	60	59.833	0.703	1.617		
	C	41	30	35	36	38	42	37.000	1.789			
10	N	120	101	111	102	122	112	111.333	3.575	1.536		
	C	73	74	70	69	76	73	72.500	1.057			
15min											1.638	0.036
1	N	113	123	132	123	119	128	123.000	2.720	1.732		
	C	66	75	72	67	74	72	71.000	1.506			
2	N	90	105	106	93	100	103	99.500	2.693	1.668		
	C	57	63	52	61	59	66	59.667	1.994			
3	N	115	121	121	130	114	124	120.833	2.414	1.510		
	C	75	78	86	82	82	77	80.000	1.653			
4	N	130	134	132	135	143	130	134.000	1.983	1.564		
	C	73	86	90	85	88	92	85.667	2.741			
5	N	62	56	61	69	69	65	63.667	2.060	1.744		
	C	41	37	38	35	36	32	36.500	1.232			
6	N	70	78	76	74	75	78	75.167	1.222	1.469		
	C	46	52	54	50	54	51	51.167	1.222			
7	N	136	133	131	126	128	126	130.000	1.653	1.848		
	C	74	65	72	69	72	70	70.333	1.282			
8	N	100	96	98	84	93	99	95.000	2.422	1.624		
	C	54	57	55	59	66	60	58.500	1.765			
9	N	142	126	133	128	130	122	130.167	2.810	1.624		
	C	78	76	75	87	86	79	80.167	2.088			
10	N	116	106	101	110	109	107	108.167	2.023	1.595		
	C	78	73	53	65	67	71	67.833	3.506			
2hrs											1.626	0.067
1	N	104	95	103	96	115	99	102.000	2.989	1.360		
	C	72	75	74	73	79	77	75.000	1.065			
2	N	104	102	103	106	107	102	104.000	0.856	1.526		
	C	65	66	61	71	72	74	68.167	2.023			
3	N	242	237	235	209	240	234	232.833	4.922	2.013		
	C	115	116	115	111	120	117	115.667	1.202			
4	N	204	180	193	185	176	191	188.167	4.110	1.470		
	C	135	131	139	117	113	133	128.000	4.282			
5	N	141	132	124	131	137	135	133.333	2.376	1.646		
	C	80	84	78	85	81	78	81.000	1.211			

6	N	145	134	150	146	140	131	141.000	3.011	1.963		
	C	68	80	75	69	67	72	71.833	2.023			
7	N	116	111	106	107	118	114	112.000	1.983	1.680		
	C	63	64	71	72	64	66	66.667	1.585			
8	N	115	111	113	104	108	111	110.333	1.585	1.505		
	C	71	79	73	78	69	70	73.333	1.726			
9	N	60	63	57	68	62	58	61.333	1.626	1.540		
	C	40	44	39	42	41	33	39.833	1.537			
10	N	76	70	71	74	75	70	72.667	1.085	1.557		
	C	49	47	46	43	45	50	46.667	1.054			
pUG36-*PLC1* in WT Rapamycine treated											1.787	0.060
1	N	115	110	101	107	110	106	108.167	1.922	2.003		
	C	50	49	55	53	56	61	54.000	1.789			
2	N	73	66	68	63	68	66	67.333	1.358	1.629		
	C	43	46	37	37	40	45	41.333	1.606			
3	N	165	151	154	161	158	161	158.333	2.092	1.915		
	C	81	78	83	87	83	84	82.667	1.229			
4	N	114	110	124	119	122	115	117.333	2.155	1.626		
	C	74	77	69	70	68	75	72.167	1.493			
5	N	212	206	205	210	207	204	207.333	1.256	2.126		
	C	99	95	92	101	93	105	97.500	2.062			
6	N	130	129	141	137	136	138	135.167	1.922	1.886		
	C	71	67	73	72	72	75	71.667	1.085			
7	N	127	126	121	123	129	121	124.500	1.360	1.653		
	C	78	67	68	76	84	79	75.333	2.704			
8	N	113	107	110	108	111	107	109.333	0.989	1.526		
	C	71	78	74	69	64	74	71.667	1.978			
9	N	134	142	136	141	140	135	138.000	1.390	1.747		
	C	75	83	82	77	80	77	79.000	1.291			
10	N	143	151	146	136	145	150	145.167	2.212	1.763		
	C	83	92	79	80	76	84	82.333	2.261			
pUG36-*PLC1* in WT Nocodazole treated											1.622	0.066
1	N	225	228	240	219	223	215	225.000	3.531	1.767		
	C	126	119	127	129	139	124	127.333	2.716			
2	N	208	204	206	214	208	202	207.000	1.693	2.013		
	C	105	107	114	92	103	96	102.833	3.219			

3	N	145	147	142	140	142	150	144.333	1.520	1.485		
	C	92	104	101	91	91	104	97.167	2.651			
4	N	113	115	110	115	119	121	115.500	1.628	1.843		
	C	69	61	57	60	61	68	62.667	1.944			
5	N	156	150	152	155	149	160	153.667	1.687	1.532		
	C	97	96	93	123	102	91	100.333	4.787			
6	N	134	136	123	137	127	134	131.833	2.272	1.548		
	C	78	90	87	88	85	83	85.167	1.740			
7	N	155	136	140	144	131	139	140.833	3.341	1.749		
	C	79	84	74	83	81	82	80.500	1.478			
8	N	116	122	107	118	114	118	115.833	2.072	1.460		
	C	84	81	84	77	74	76	79.333	1.745			
9	N	107	120	116	109	110	117	113.167	2.120	1.439		
	C	80	76	72	81	77	86	78.667	1.961			
10	N	80	79	82	88	84	86	83.167	1.424	1.382		
	C	62	60	55	63	61	60	60.167	1.138			
pUG36-*PLC1* in WT Hydroxyurea treated											1.537	0.013
1	N	88	82	95	96	90	94	90.833	2.167	1.531		
	C	60	62	57	55	57	65	59.333	1.520			
2	N	95	90	85	80	83	87	86.667	2.171	1.490		
	C	57	60	62	55	54	61	58.167	1.352			
3	N	180	188	184	187	184	195	186.333	2.076	1.544		
	C	118	118	119	126	120	123	120.667	1.308			
4	N	182	195	188	193	192	185	189.167	2.056	1.563		
	C	122	127	119	125	120	113	121.000	2.017			
5	N	122	124	112	121	126	119	120.667	1.994	1.557		
	C	78	71	86	81	71	78	77.500	2.377			
6	N	122	120	121	117	125	128	122.167	1.579	1.566		
	C	83	80	78	70	84	73	78.000	2.266			
7	N	110	106	107	105	108	116	108.667	1.626	1.452		
	C	73	78	70	73	78	77	74.833	1.352			
8	N	211	220	209	223	215	210	214.667	2.348	1.567		
	C	135	143	136	138	140	130	137.000	1.826			
9	N	174	183	179	193	190	184	183.833	2.845	1.587		
	C	125	123	121	116	110	100	115.833	3.859			
10	N	95	97	87	96	90	105	95.000	2.543	1.508		

	C	65	60	68	62	53	70	63.000	2.503			
pUG36-*PLC1* DMSO treated(control)											1.649	0.026
1	N	249	236	250	245	251	245	246.000	2.251	1.689		
	C	145	155	142	146	140	146	145.667	2.108			
2	N	126	122	126	132	125	130	126.833	1.470	1.605		
	C	72	82	89	81	73	77	79.000	2.595			
3	N	169	163	166	158	161	159	162.667	1.726	1.814		
	C	87	94	83	86	96	92	89.667	2.076			
4	N	133	128	130	132	136	131	131.667	1.116	1.583		
	C	75	83	85	77	84	95	83.167	2.880			
5	N	254	242	240	246	243	244	244.833	2.007	1.563		
	C	159	146	148	158	163	166	156.667	3.283			
6	N	75	70	75	74	78	69	73.500	1.384	1.683		
	C	43	37	44	42	47	49	43.667	1.706			
7	N	76	80	73	78	69	78	75.667	1.647	1.566		
	C	51	48	51	42	55	43	48.333	2.060			
8	N	63	60	65	66	62	69	64.167	1.302	1.704		
	C	41	39	32	38	36	40	37.667	1.333			
9	N	55	62	56	57	58	60	58.000	1.065	1.575		
	C	37	38	35	39	37	35	36.833	0.654			
10	N	74	70	71	79	75	78	74.500	1.478	1.706		
	C	48	43	44	40	42	45	43.667	1.116			
Genotype								**Mean**	**SEM**	**Ratio**(PM:N:C)	**Mean**^{Ratio}	**SEM**^{Ratio}
pUG36-*PLC1*^{CAAX} in WT											1.139	0.031
1	PM	205	211	214	205	207	213	209.167	1.641	1.153	1.144	0.043
	N	194	189	183	184	194	198	190.333	2.459	1.050	1.000	0.000
	C	190	175	188	171	180	184	181.333	3.029	1.000		
2	PM	198	184	171	199	211	168	188.500	6.961	1.281		
	N	170	162	160	171	154	164	163.500	2.604	1.111		
	C	143	141	140	150	158	151	147.167	2.868	1.000		
3	PM	66	65	71	66	70	66	67.333	1.022	1.251		
	N	61	62	57	60	61	64	60.833	0.946	1.130		
	C	60	54	50	48	52	59	53.833	1.973	1.000		
4	PM	112	123	131	113	116	132	121.167	3.628	1.247		
	N	126	128	122	137	128	125	127.667	2.076	1.314		
	C	93	100	97	96	96	101	97.167	1.195	1.000		

5	PM	138	143	129	126	120	133	131.500	3.394	1.075		
	N	168	176	172	159	183	175	172.167	3.321	1.407		
	C	125	121	126	120	116	126	122.333	1.647	1.000		
6	PM	125	127	118	112	121	126	121.500	2.349	1.070		
	N	133	134	127	136	150	149	138.167	3.790	1.217		
	C	119	110	113	115	118	106	113.500	2.012	1.000		
7	PM	127	125	131	125	148	135	131.833	3.600	1.106		
	N	136	132	134	137	124	143	134.333	2.565	1.127		
	C	122	119	115	114	125	120	119.167	1.701	1.000		
8	PM	113	114	125	131	125	130	123.000	3.173	1.010		
	N	122	121	121	116	118	121	119.833	0.946	0.984		
	C	121	132	117	118	126	117	121.833	2.469	1.000		
9	PM	108	111	102	109	104	118	108.667	2.305	1.028		
	N	103	99	106	103	103	108	103.667	1.256	0.981		
	C	111	105	104	105	112	97	105.667	2.216	1.000		
10	PM	88	89	90	86	91	93	89.500	0.992	1.167		
	N	85	86	84	87	85	87	85.667	0.494	1.117		
	C	75	78	80	77	73	77	76.667	0.989	1.000		
pUG36-*CAAX* in WT											1.396	0.022
1	PM	119	113	120	117	130	124	120.500	2.405	1.351	1.079	0.043
	N	90	97	97	86	95	91	92.667	1.801	1.039	1.000	0.000
	C	95	90	89	88	92	81	89.167	1.922	1.000		
2	PM	131	119	120	122	120	134	124.333	2.642	1.429		
	N	88	87	86	83	81	82	84.500	1.176	0.971		
	C	91	93	84	83	85	86	87.000	1.653	1.000		
3	PM	137	139	135	141	147	136	139.167	1.797	1.535		
	N	83	81	85	87	85	90	85.167	1.276	0.939		
	C	81	86	94	98	103	82	90.667	3.685	1.000		
4	PM	153	143	138	142	144	137	142.833	2.330	1.382		
	N	112	107	99	102	103	101	104.000	1.932	1.006		
	C	100	103	101	108	100	108	103.333	1.542	1.000		
5	PM	171	157	152	166	149	160	159.167	3.400	1.404		
	N	120	118	115	117	123	118	118.500	1.118	1.046		
	C	110	111	119	109	115	116	113.333	1.606	1.000		
6	PM	180	174	185	178	187	181	180.833	1.922	1.405		
	N	127	125	127	119	134	130	127.000	2.049	0.987		

	C	131	124	125	132	128	132	128.667	1.453	1.000
7	PM	237	234	246	230	237	234	236.333	2.201	1.418
	N	231	235	223	220	226	231	227.667	2.305	1.366
	C	154	158	167	174	170	177	166.667	3.685	1.000
8	PM	136	134	124	135	133	161	137.167	5.082	1.434
	N	108	123	132	128	110	123	120.667	3.947	1.261
	C	97	98	104	88	95	92	95.667	2.231	1.000
9	PM	106	109	132	115	113	108	113.833	3.877	1.331
	N	86	90	98	93	102	97	94.333	2.376	1.103
	C	86	90	82	85	79	91	85.500	1.875	1.000
10	PM	133	130	137	127	134	138	133.167	1.701	1.270
	N	122	115	111	108	112	105	112.167	2.414	1.070
	C	106	101	105	110	107	100	104.833	1.537	1.000

Vacuole morphology under salt stress:

WT		**1-2/cell**	**3-4/cell**	**5-8/cell**	**≥9/cell**
Untreated	Exp I	4	6	4	0
	%	0.286	0.429	0.286	0.000
	Exp II	7	6	1	0
	%	0.500	0.429	0.071	0.000
	Exp III	8	4	1	0
	%	0.615	0.308	0.077	0.000
	Mean(%)	0.467	0.388	0.145	0.000
	SEM	0.097	0.040	0.071	0.000
hyper-osmotic shock	Exp I	3	7	3	10
(0.6M NaCl 10min)	%	0.130	0.304	0.130	0.435
	Exp II	2	3	5	6
	%	0.125	0.188	0.313	0.375
	Exp III	2	3	5	10
	%	0.100	0.150	0.250	0.500
	Mean(%)	0.118	0.214	0.231	0.437
	SEM	0.009	0.046	0.053	0.036
hyper-osmotic shock	Exp I	8	11	3	0
(0.06M NaCl 60min)	%	0.364	0.500	0.136	0.000
	Exp II	8	5	1	0
	%	0.571	0.357	0.071	0.000
	Exp III	12	4	1	0
	%	0.706	0.235	0.059	0.000
	Mean(%)	0.547	0.364	0.089	0.000
	SEM	0.100	0.076	0.024	0.000
plc1Δ		**1-2/cell**	**3-4/cell**	**5-8/cell**	**≥9/cell**
Untreated	Exp I	2	1	3	6
	%	0.167	0.083	0.250	0.500
	Exp II	1	1	3	7
	%	0.083	0.083	0.250	0.583
	Exp III	1	2	2	4
	%	0.111	0.222	0.222	0.444
	Mean(%)	0.120	0.130	0.241	0.509
	SEM	0.025	0.046	0.009	0.040
hyper-osmotic shock	Exp I	1	1	2	8
(0.6M NaCl 10min)	%	0.083	0.083	0.167	0.667
	Exp II	3	4	3	14
	%	0.125	0.167	0.125	0.583
	Exp III	3	3	2	10
	%	0.167	0.167	0.111	0.556
	Mean(%)	0.125	0.139	0.134	0.602
	SEM	0.024	0.028	0.017	0.033
hyper-osmotic shock	Exp I	1	1	2	8
(0.06M NaCl 60min)	%	0.083	0.083	0.167	0.667
	Exp II	2	2	3	12
	%	0.105	0.105	0.158	0.632
	Exp III	1	3	3	9
	%	0.063	0.188	0.188	0.563
	Mean(%)	0.084	0.125	0.171	0.620
	SEM	0.012	0.032	0.009	0.031
PLC1^{NES}		**1-2/cell**	**3-4/cell**	**5-8/cell**	**≥9/cell**
Untreated	Exp I	0	0	1	11
	%	0.000	0.000	0.083	0.917
	Exp II	0	1	1	8

	%	0.000	0.100	0.100	0.800
	Exp III	0	0	2	12
	%	0.000	0.000	0.143	0.857
	Mean(%)	0.000	0.033	0.109	0.858
	SEM	0.000	0.033	0.018	0.034
hyper-osmotic shock	Exp I	0	0	0	10
(0.6M NaCl 10min)	%	0.000	0.000	0.000	1.000
	Exp II	0	0	2	15
	%	0.000	0.000	0.118	0.882
	Exp III	0	0	0	9
	%	0.000	0.000	0.000	1.000
	Mean(%)	0.000	0.000	0.039	0.961
	SEM	0.000	0.000	0.039	0.039
hyper-osmotic shock	Exp I	0	2	3	10
(0.06M NaCl 60min)	%	0.000	0.133	0.200	0.667
	Exp II	0	1	3	11
	%	0.000	0.067	0.200	0.733
	Exp III	0	1	2	10
	%	0.000	0.077	0.154	0.769
	Mean(%)	0.000	0.092	0.185	0.723
	SEM	0.000	0.021	0.015	0.030
PLC1^{CAAX}		**1-2/cell**	**3-4/cell**	**5-8/cell**	**≥9/cell**
Untreated	Exp I	5	3	1	0
	%	0.556	0.333	0.111	0.000
	Exp II	11	5	1	0
	%	0.647	0.294	0.059	0.000
	Exp III	13	9	1	0
	%	0.565	0.391	0.044	0.000
	Mean(%)	0.589	0.340	0.071	0.000
	SEM	0.029	0.028	0.020	0.000
hyper-osmotic shock	Exp I	0	1	1	9
(0.6M NaCl 10min)	%	0.000	0.091	0.091	0.818
	Exp II	0	1	2	11
	%	0.000	0.071	0.143	0.786
	Exp III	0	2	1	15
	%	0.000	0.111	0.056	0.833
	Mean(%)	0.000	0.091	0.096	0.812
	SEM	0.000	0.011	0.025	0.014
hyper-osmotic shock	Exp I	18	3	0	0
(0.06M NaCl 60min)	%	0.857	0.143	0.000	0.000
	Exp II	11	1	0	0
	%	0.917	0.083	0.000	0.000
	Exp III	17	0	0	0
	%	1.000	0.000	0.000	0.000
	Mean(%)	0.925	0.075	0.000	0.000
	SEM	0.041	0.041	0.000	0.000
PLC1^{PKI}		**1-2/cell**	**3-4/cell**	**5-8/cell**	**≥9/cell**
Untreated	Exp I	2	1	2	7
	%	0.167	0.083	0.167	0.583
	Exp II	2	1	2	8
	%	0.154	0.077	0.154	0.615
	Exp III	0	1	1	9
	%	0.000	0.091	0.091	0.818
	Mean(%)	0.107	0.084	0.137	0.672
	SEM	0.054	0.004	0.023	0.074

hyper-osmotic shock (0.6M NaCl 10min)	Exp I	0	0	0	7
	%	0.000	0.000	0.000	1.000
	Exp II	0	1	1	5
	%	0.000	0.143	0.143	0.714
	Exp III	0	0	0	9
	%	0.000	0.000	0.000	1.000
	Mean(%)	0.000	0.048	0.048	0.905
	SEM	0.000	0.048	0.048	0.095
hyper-osmotic shock (0.06M NaCl 60min)	Exp I	2	0	0	7
	%	0.222	0.000	0.000	0.778
	Exp II	0	0	1	3
	%	0.000	0.000	0.250	0.750
	Exp III	0	1	2	9
	%	0.000	0.083	0.167	0.750
	Mean(%)	0.074	0.028	0.139	0.759
	SEM	0.074	0.028	0.073	0.009

B2: Constructs in Chapter 4

[PM: plasma membrane fluorescence intensity; N: nuclear fluorescence intensity; C: cytosolic fluorescence intensity]

Genotype								**Mean**	**SEM**	**Ratio**(PM:C)	**Ratio**(N:C)	**Ratio**(PM:N)	**Mean**$^{Ratio(PM:C)}$ **SEM**$^{Ratio(PM:C)}$	**Mean**$^{Ratio(N:C)}$ **SEM**$^{Ratio(N:C)}$	**Mean**$^{Ratio(PM:N)}$ **SEM**$^{Ratio(PM:N)}$
pUG36-*PLC1* in WT															
1	PM	35	35	37	38	41	39	37.500	0.957	0.843	1.491	0.565	0.742	1.703	0.444
	N	64	68	65	67	64	70	66.333	0.989				0.013	0.078	0.021
	C	47	48	41	44	39	48	44.500	1.565						
2	PM	63	57	62	56	50	52	56.667	2.124	0.759	2.270	0.334			
	N	169	174	168	168	178	160	169.500	2.500						
	C	75	69	63	78	82	81	74.667	3.018						
3	PM	66	58	70	64	63	75	66.000	2.408	0.719	1.800	0.399			
	N	158	162	167	162	174	169	165.333	2.362						
	C	98	90	95	88	86	94	91.833	1.869						
4	PM	48	44	58	51	55	60	52.667	2.499	0.744	1.565	0.475			
	N	100	99	126	106	124	110	110.833	4.778						
	C	72	75	70	71	69	68	70.833	1.014						
5	PM	48	52	49	51	48	51	49.833	0.703	0.757	1.458	0.519			
	N	95	93	93	96	98	101	96.000	1.265						
	C	71	68	65	60	62	69	65.833	1.740						
6	PM	102	114	87	104	88	90	97.500	4.440	0.687	1.629	0.422			
	N	227	229	236	232	234	228	231.000	1.461						
	C	132	137	140	150	148	144	141.833	2.786						
7	PM	89	101	88	94	90	96	93.000	2.033	0.738	1.772	0.416			
	N	208	227	234	218	228	225	223.333	3.721						
	C	137	133	120	117	123	126	126.000	3.141						
8	PM	62	56	60	53	64	69	60.667	2.333	0.751	1.967	0.382			
	N	148	164	159	169	165	149	159.000	3.568						
	C	79	82	76	75	84	89	80.833	2.151						
9	PM	56	60	54	56	71	65	60.333	2.667	0.708	1.648	0.430			
	N	136	151	147	129	139	140	140.333	3.201						
	C	96	88	86	74	83	84	85.167	2.926						
10	PM	52	58	51	40	52	43	49.333	2.704	0.715	1.425	0.502			
	N	96	101	99	103	97	94	98.333	1.358						
	C	67	66	71	67	69	74	69.000	1.238						
pUG36-*PLC1* in *plc1Δ*															
1	PM	76	62	75	72	60	73	69.667	2.813	0.771	1.708	0.451	0.770	1.649	0.468
	N	156	157	162	153	148	150	154.333	2.076				0.014	0.025	0.011
	C	89	88	80	90	92	103	90.333	3.040						

2	PM	46	48	38	45	36	44	42.833	1.939	0.714	1.736	0.411		
	N	101	110	93	99	120	102	104.167	3.877					
	C	67	65	62	55	52	59	60.000	2.366					
3	PM	57	55	62	59	63	63	59.833	1.376	0.827	1.717	0.482		
	N	128	112	120	125	133	127	124.167	2.982					
	C	68	71	70	78	75	72	72.333	1.476					
4	PM	61	64	62	58	60	59	60.667	0.882	0.751	1.592	0.472		
	N	135	120	121	133	124	139	128.667	3.273					
	C	81	80	74	83	77	90	80.833	2.242					
5	PM	90	89	88	94	102	91	92.333	2.108	0.778	1.642	0.474		
	N	196	187	189	202	200	195	194.833	2.414					
	C	119	114	115	121	127	116	118.667	1.978					
6	PM	63	73	83	74	70	79	73.667	2.848	0.747	1.454	0.513		
	N	142	149	145	141	139	145	143.500	1.455					
	C	97	102	108	86	101	98	98.667	2.985					
7	PM	40	41	44	46	40	43	42.333	0.989	0.833	1.616	0.515		
	N	75	78	82	78	92	88	82.167	2.688					
	C	52	50	53	51	50	49	50.833	0.601					
8	PM	36	35	37	32	39	38	36.167	1.014	0.702	1.693	0.415		
	N	88	92	89	87	80	87	87.167	1.621					
	C	54	58	52	49	45	51	51.500	1.803					
9	PM	86	92	93	84	83	90	88.000	1.732	0.760	1.650	0.460		
	N	185	207	192	204	172	187	191.167	5.288					
	C	111	119	122	108	112	123	115.833	2.574					
10	PM	61	65	66	64	63	62	63.500	0.764	0.818	1.680	0.487		
	N	130	131	137	125	127	133	130.500	1.746					
	C	73	81	70	87	71	84	77.667	2.963					
pUG36-*ARG82* in WT														
1	PM	62	62	72	70	68	72	67.667	1.892	0.712	1.742	0.409	0.728	1.642	0.446
	N	158	165	164	169	171	166	165.500	1.839				0.022	0.037	0.018
	C	94	92	90	102	95	97	95.000	1.713						
2	PM	29	28	31	33	27	31	29.833	0.910	0.886	1.535	0.577			
	N	50	55	48	54	50	53	51.667	1.116						
	C	34	35	30	35	38	30	33.667	1.282						
3	PM	51	58	52	42	54	56	52.167	2.286	0.647	1.676	0.386			
	N	137	135	143	129	134	133	135.167	1.905						
	C	85	84	80	78	77	80	80.667	1.308						
4	PM	65	78	69	63	54	65	65.667	3.201	0.722	1.498	0.482			
	N	139	140	134	129	135	141	136.333	1.856						
	C	94	83	98	94	85	92	91.000	2.366						

5	PM	65	52	60	60	56	61	59.000	1.826	0.664	1.657	0.401			
	N	148	144	152	156	138	145	147.167	2.587						
	C	89	84	96	81	93	90	88.833	2.272						
6	PM	75	71	59	60	62	63	65.000	2.646	0.649	1.624	0.400			
	N	161	161	159	162	167	166	162.667	1.282						
	C	108	90	102	108	92	101	100.167	3.146						
7	PM	95	105	98	82	87	90	92.833	3.361	0.737	1.837	0.401			
	N	210	234	242	237	231	235	231.500	4.552						
	C	131	127	122	126	130	120	126.000	1.770						
8	PM	100	108	99	80	82	89	93.000	4.531	0.785	1.633	0.481			
	N	187	192	197	203	197	185	193.500	2.778						
	C	110	126	122	117	111	125	118.500	2.837						
9	PM	85	84	79	76	72	89	80.833	2.574	0.700	1.450	0.483			
	N	167	169	159	172	168	170	167.500	1.839						
	C	110	116	114	123	121	109	115.500	2.320						
10	PM	32	35	30	34	33	47	35.167	2.469	0.779	1.771	0.440			
	N	76	82	83	87	79	73	80.000	2.066						
	C	45	47	45	43	48	43	45.167	0.833						
pUG36-*ARG82* in *arg82Δ*															
1	PM	78	73	74	74	75	77	75.167	0.792	0.708	1.637	0.432	0.725	1.623	0.447
	N	177	169	179	173	167	178	173.833	2.040				0.006	0.027	0.004
	C	110	111	105	102	101	108	106.167	1.701						
2	PM	90	83	75	74	85	84	81.833	2.522	0.739	1.631	0.453			
	N	217	22	197	208	211	228	180.500	31.974						
	C	120	121	118	119	111	112	116.833	1.740						
3	PM	45	42	40	39	44	42	42.000	0.931	0.733	1.672	0.438			
	N	98	93	96	92	96	100	95.833	1.222						
	C	55	53	50	58	63	65	57.333	2.376						
4	PM	96	98	106	103	97	101	100.167	1.579	0.764	1.817	0.420			
	N	241	240	236	242	233	238	238.333	1.382						
	C	130	133	129	134	133	128	131.167	1.014						
5	PM	109	112	107	110	101	105	107.333	1.606	0.751	1.669	0.450			
	N	229	250	238	243	231	239	238.333	3.159						
	C	140	141	134	153	154	135	142.833	3.554						
6	PM	82	95	93	91	91	96	91.333	2.044	0.718	1.567	0.458			
	N	199	207	195	201	195	199	199.333	1.820						
	C	137	118	112	123	139	134	127.167	4.527						
7	PM	77	76	82	71	80	83	78.167	1.815	0.710	1.566	0.453			
	N	168	177	170	168	174	178	172.500	1.821						
	C	99	111	126	100	109	116	110.167	4.143						

8	PM	79	80	70	78	75	78	76.667	1.498	0.715	1.616	0.443			
	N	167	176	171	169	177	179	173.167	1.973						
	C	106	120	101	100	110	106	107.167	2.971						
9	PM	101	95	94	98	89	90	94.500	1.875	0.707	1.571	0.450			
	N	210	215	208	212	211	204	210.000	1.528						
	C	133	120	145	126	138	140	133.667	3.801						
10	PM	100	91	89	94	95	91	93.333	1.606	0.703	1.483	0.474			
	N	199	198	191	194	201	199	197.000	1.528						
	C	131	132	127	133	141	133	132.833	1.869						
pUG36-*ARG82* in *plc1Δ*															
1	PM	97	91	89	78	99	94	91.333	3.062	0.744	1.811	0.410	0.771	1.640	0.471
	N	219	216	235	222	225	218	222.500	2.814				0.027	0.028	0.015
	C	115	127	120	132	110	133	122.833	3.825						
2	PM	91	103	106	88	87	80	92.500	4.089	0.823	1.604	0.513			
	N	188	180	189	173	171	180	180.167	3.027						
	C	109	105	126	111	122	101	112.333	3.981						
3	PM	105	98	102	92	95	88	96.667	2.578	0.801	1.546	0.518			
	N	186	199	180	193	170	191	186.500	4.217						
	C	123	133	116	119	126	107	120.667	3.639						
4	PM	83	87	90	75	70	75	80.000	3.204	0.889	1.733	0.513			
	N	155	160	152	162	158	149	156.000	2.017						
	C	85	95	90	90	92	88	90.000	1.390						
5	PM	118	95	115	111	97	90	104.333	4.800	0.696	1.630	0.427			
	N	250	253	243	238	250	233	244.500	3.212						
	C	145	153	131	145	159	167	150.000	5.132						
6	PM	86	91	94	81	92	96	90.000	2.266	0.610	1.554	0.393			
	N	236	221	214	242	217	245	229.167	5.498						
	C	150	153	129	144	161	148	147.500	4.372						
7	PM	103	102	91	88	99	98	96.833	2.469	0.702	1.656	0.424			
	N	217	220	237	228	233	236	228.500	3.433						
	C	143	145	137	122	138	143	138.000	3.445						
8	PM	98	83	90	86	84	79	86.667	2.704	0.837	1.663	0.503			
	N	164	176	169	175	170	179	172.167	2.242						
	C	109	105	99	101	107	100	103.500	1.668						
9	PM	90	98	92	88	72	80	86.667	3.783	0.726	1.499	0.485			
	N	193	187	181	164	168	180	178.833	4.512						
	C	121	123	128	115	121	108	119.333	2.836						
10	PM	50	53	54	61	63	51	55.333	2.201	0.885	1.704	0.520			
	N	108	101	113	105	110	102	106.500	1.910						
	C	60	61	72	62	64	56	62.500	2.187						

pUG36-*PLC1* in *arg82Δ*

1	PM	116	125	122	102	115	123	117.167	3.439	1.182	1.461	0.809	1.128	1.736	0.662
	N	140	136	145	141	159	148	144.833	3.301				0.017	0.078	0.030
	C	92	100	92	104	111	96	99.167	3.038						
2	PM	122	135	145	120	114	117	125.500	4.890	1.162	1.662	0.699			
	N	177	182	186	184	178	170	179.500	2.363						
	C	106	115	111	102	114	100	108.000	2.569						
3	PM	115	116	103	120	111	117	113.667	2.445	1.021	1.554	0.657			
	N	184	171	179	160	178	166	173.000	3.670						
	C	112	111	115	107	109	114	111.333	1.229						
4	PM	125	127	140	124	130	137	130.500	2.693	1.135	1.909	0.595			
	N	219	221	207	237	215	218	219.500	4.031						
	C	113	108	116	121	107	125	115.000	2.910						
5	PM	102	97	110	94	102	112	102.833	2.880	1.062	2.088	0.509			
	N	201	208	200	215	197	192	202.167	3.341						
	C	99	93	88	108	95	98	96.833	2.750						
6	PM	101	93	85	89	88	87	90.500	2.363	1.170	2.216	0.528			
	N	176	171	175	165	174	167	171.333	1.838						
	C	87	77	78	67	75	80	77.333	2.667						
7	PM	95	76	78	99	92	97	89.500	4.072	1.126	1.444	0.779			
	N	112	119	115	120	114	109	114.833	1.701						
	C	86	81	74	83	76	77	79.500	1.875						
8	PM	183	180	167	153	169	148	166.667	5.731	1.135	1.672	0.679			
	N	239	242	252	250	241	249	245.500	2.232						
	C	141	140	160	152	155	133	146.833	4.238						
9	PM	172	156	143	139	152	153	152.500	4.710	1.092	1.758	0.621			
	N	250	247	248	254	244	230	245.500	3.384						
	C	134	135	139	141	149	140	139.667	2.186						
10	PM	101	91	95	82	98	107	95.667	3.518	1.193	1.599	0.746			
	N	121	126	136	124	132	130	128.167	2.257						
	C	74	87	82	76	77	85	80.167	2.151						

pUG36-*PLC1* + pYCplac111-*ARG82* in *arg82Δ*

1	PM	65	71	70	74	61	67	68.000	1.897	0.824	1.479	0.557	0.755	1.563	0.487
	N	120	125	121	136	114	116	122.000	3.215				0.037	0.043	0.027
	C	88	83	77	92	77	78	82.500	2.592						
2	PM	66	74	89	87	74	63	75.500	4.342	0.983	1.646	0.597			
	N	121	126	131	122	124	135	126.500	2.232						
	C	75	66	63	70	93	94	76.833	5.522						
3	PM	38	57	42	51	46	52	47.667	2.860	0.765	1.693	0.452			
	N	112	108	119	102	91	101	105.500	3.973						

	C	58	59	59	62	69	67	62.333	1.892					
4	PM	42	35	52	43	38	39	41.500	2.405	0.856	1.550	0.552		
	N	77	79	73	69	75	78	75.167	1.515					
	C	45	42	56	61	41	46	48.500	3.314					
5	PM	81	88	69	80	75	74	77.833	2.701	0.663	1.825	0.363		
	N	221	230	218	211	197	208	214.167	4.672					
	C	126	114	123	119	103	119	117.333	3.313					
6	PM	77	67	63	81	84	79	75.167	3.390	0.727	1.487	0.489		
	N	160	158	151	147	155	151	153.667	1.994					
	C	114	112	77	93	113	111	103.333	6.168					
7	PM	59	49	52	53	46	45	50.667	2.108	0.788	1.609	0.490		
	N	98	105	101	109	108	100	103.500	1.839					
	C	70	61	68	59	58	70	64.333	2.290					
8	PM	86	91	92	90	76	82	86.167	2.535	0.593	1.475	0.402		
	N	217	209	218	219	211	212	214.333	1.706					
	C	128	149	144	152	148	151	145.333	3.648					
9	PM	76	94	80	77	71	72	78.333	3.412	0.574	1.565	0.367		
	N	214	225	204	202	230	207	213.667	4.723					
	C	134	143	127	149	136	130	136.500	3.354					
10	PM	63	59	62	59	61	67	61.833	1.222	0.779	1.296	0.601		
	N	106	110	98	99	104	100	102.833	1.905					
	C	81	80	79	76	83	77	79.333	1.054					
pUG36-*PLC1* + pYCplac111 in *arg82Δ*														
1	PM	59	60	69	63	54	61	61.000	2.017	1.137	1.798	0.632	1.152	1.674	0.699
	N	99	102	86	95	97	100	96.500	2.320				0.007	0.063	0.028
	C	56	55	54	56	48	53	53.667	1.229						
2	PM	198	212	188	190	219	198	200.833	5.009	1.170	1.454	0.804			
	N	240	250	252	253	249	254	249.667	2.076						
	C	163	170	179	180	169	169	171.667	2.679						
3	PM	100	117	94	103	99	95	101.333	3.412	1.128	2.052	0.550			
	N	187	192	183	178	184	182	184.333	1.944						
	C	98	78	93	97	85	88	89.833	3.135						
4	PM	114	104	105	108	122	111	110.667	2.728	1.155	1.910	0.605			
	N	181	180	179	188	184	186	183.000	1.461						
	C	107	89	89	91	97	102	95.833	3.060						
5	PM	116	127	128	121	110	128	121.667	3.040	1.157	1.550	0.746			
	N	164	167	161	170	165	151	163.000	2.696						
	C	115	109	102	99	101	105	105.167	2.428						
6	PM	169	162	155	150	166	160	160.333	2.860	1.163	1.543	0.754			
	N	214	217	211	206	210	218	212.667	1.856						

	C	145	141	139	138	134	130	137.833	2.151						
7	PM	110	115	101	113	116	104	109.833	2.496	1.119	1.720	0.651			
	N	164	168	172	162	175	172	168.833	2.072						
	C	102	107	101	93	89	97	98.167	2.664						
8	PM	98	107	104	99	95	94	99.500	2.078	1.159	1.711	0.678			
	N	148	154	155	136	146	142	146.833	2.949						
	C	89	98	70	92	88	78	85.833	4.135						
9	PM	83	86	88	88	96	104	90.833	3.167	1.140	1.354	0.842			
	N	108	105	109	110	107	108	107.833	0.703						
	C	86	78	82	79	73	80	79.667	1.764						
10	PM	200	180	182	170	179	178	181.500	4.064	1.194	1.645	0.726			
	N	245	250	252	249	254	250	250.000	1.238						
	C	158	155	157	150	148	144	152.000	2.266						
pUG36-*PLC1* + pUG34-*ARG82*^{D131A} in *arg82*Δ															
1	PM	101	105	99	107	104	96	102.000	1.673	1.032	1.653	0.624	1.163	1.862	0.634
	N	165	172	168	166	150	159	163.333	3.180				0.044	0.092	0.028
	C	92	100	93	99	100	109	98.833	2.496						
2	PM	118	113	123	114	100	119	114.500	3.253	1.130	1.849	0.611			
	N	196	179	188	195	186	180	187.333	2.940						
	C	101	98	99	106	103	101	101.333	1.174						
3	PM	84	90	98	111	96	97	96.000	3.697	1.095	1.546	0.708			
	N	134	145	142	133	129	130	135.500	2.668						
	C	83	97	85	90	89	82	87.667	2.275						
4	PM	112	106	111	107	109	116	110.167	1.493	1.168	2.366	0.494			
	N	235	237	209	234	210	214	223.167	5.498						
	C	91	86	82	98	105	104	94.333	3.887						
5	PM	159	172	163	172	139	155	160.000	5.046	1.529	1.984	0.770			
	N	215	206	208	219	197	201	207.667	3.383						
	C	108	108	102	100	109	101	104.667	1.667						
6	PM	171	170	194	193	200	189	186.167	5.160	1.183	1.555	0.761			
	N	240	244	250	234	246	254	244.667	2.906						
	C	153	170	172	159	147	143	157.333	4.863						
7	PM	92	89	97	95	83	98	92.333	2.305	1.099	1.599	0.687			
	N	136	133	136	132	125	144	134.333	2.539						
	C	83	80	88	84	82	87	84.000	1.238						
8	PM	98	81	77	73	92	100	86.833	4.643	1.271	2.388	0.532			
	N	162	157	163	181	153	163	163.167	3.919						
	C	65	68	65	58	70	84	68.333	3.547						
9	PM	81	79	77	75	87	79	79.667	1.687	1.072	1.812	0.592			
	N	133	134	127	134	136	144	134.667	2.246						

	C	77	74	69	69	77	80	74.333	1.856						
10	PM	109	103	101	110	108	122	108.833	3.005	1.050	1.873	0.561			
	N	188	198	195	201	193	190	194.167	1.990						
	C	103	106	106	107	101	99	103.667	1.308						
pUG36-*PLC1* + pUG34-*ARG82*$^{\Delta asp}$ in *arg82*Δ															
1	PM	91	94	90	96	102	104	96.167	2.344	0.733	1.559	0.470	0.723	1.608	0.451
	N	211	205	188	213	211	199	204.500	3.914				0.022	0.027	0.016
	C	122	129	137	130	145	124	131.167	3.497						
2	PM	72	98	103	82	101	90	91.000	4.953	0.677	1.551	0.436			
	N	194	207	216	214	205	216	208.667	3.499						
	C	139	131	129	124	140	144	134.500	3.128						
3	PM	44	37	33	45	42	43	40.667	1.909	0.850	1.568	0.542			
	N	80	75	74	76	72	73	75.000	1.155						
	C	51	48	47	50	47	44	47.833	1.014						
4	PM	73	68	87	77	88	82	79.167	3.240	0.749	1.711	0.438			
	N	183	182	177	186	173	184	180.833	1.990						
	C	101	98	112	101	109	113	105.667	2.629						
5	PM	83	94	75	77	79	85	82.167	2.810	0.700	1.753	0.400			
	N	214	202	205	197	207	209	205.667	2.390						
	C	136	126	117	103	109	113	117.333	4.890						
6	PM	102	98	85	87	93	112	96.167	4.110	0.745	1.601	0.465			
	N	202	208	210	208	210	203	206.833	1.424						
	C	116	121	117	126	153	142	129.167	6.140						
7	PM	103	121	107	88	95	88	100.333	5.200	0.694	1.433	0.485			
	N	203	205	212	209	194	219	207.000	3.474						
	C	141	139	132	149	161	145	144.500	4.048						
8	PM	92	80	83	88	93	96	88.667	2.525	0.734	1.657	0.443			
	N	209	201	182	210	200	199	200.167	4.110						
	C	112	114	112	136	130	121	120.833	4.151						
9	PM	116	124	101	108	99	120	111.333	4.193	0.782	1.607	0.487			
	N	226	231	218	227	237	233	228.667	2.692						
	C	141	134	131	141	157	150	142.333	3.981						
10	PM	91	83	70	82	85	90	83.500	3.085	0.568	1.639	0.346			
	N	251	234	245	248	232	236	241.000	3.266						
	C	138	146	150	132	141	175	147.000	6.154						
pUG36-*PLC1* in WT															
U73122 1h															
1	PM	51	58	55	54	50	52	53.333	1.202	0.691	1.585	0.436	0.762	1.627	0.483
	N	118	127	126	124	123	116	122.333	1.801				0.011	0.110	0.023
	C	88	79	75	80	65	76	77.167	3.070						

2	PM	54	66	72	60	72	66	65.000	2.864	0.791	1.584	0.499			
	N	129	140	121	133	122	136	130.167	3.114						
	C	77	80	81	81	89	85	82.167	1.721						
3	PM	42	46	43	41	40	46	43.000	1.033	0.766	1.513	0.506			
	N	81	89	86	84	82	88	85.000	1.317						
	C	57	53	63	54	54	56	56.167	1.493						
4	PM	45	47	43	40	41	44	43.333	1.054	0.747	1.351	0.553			
	N	78	74	81	78	82	77	78.333	1.174						
	C	63	55	57	59	54	60	58.000	1.366						
5	PM	33	31	32	33	30	34	32.167	0.601	0.751	1.650	0.455			
	N	68	66	79	74	69	68	70.667	1.994						
	C	41	42	40	38	49	47	42.833	1.740						
6	PM	40	42	43	39	44	41	41.500	0.764	0.761	1.428	0.533			
	N	78	81	74	75	79	80	77.833	1.138						
	C	52	58	54	53	51	59	54.500	1.335						
7	PM	50	49	48	51	49	51	49.667	0.494	0.786	1.612	0.488			
	N	102	105	97	100	105	102	101.833	1.249						
	C	61	66	64	68	61	59	63.167	1.400						
8	PM	53	42	55	47	51	53	50.167	1.973	0.816	1.618	0.504			
	N	94	93	103	97	104	106	99.500	2.262						
	C	54	66	63	65	60	61	61.500	1.765						
9	PM	52	48	49	50	51	50	50.000	0.577	0.726	1.312	0.554			
	N	94	88	90	88	92	90	90.333	0.955						
	C	70	72	67	71	66	67	68.833	1.014						
10	PM	72	66	58	57	60	61	62.333	2.319	0.781	2.618	0.298			
	N	203	213	210	207	214	207	209.000	1.693						
	C	82	76	99	71	76	75	79.833	4.094						
DMSO 1h															
1	PM	65	59	60	78	65	66	65.500	2.766	0.756	1.790	0.422	0.778	1.634	0.481
	N	155	159	159	154	151	153	155.167	1.327				0.019	0.041	0.020
	C	85	98	81	84	89	83	86.667	2.512						
2	PM	66	59	61	55	56	62	59.833	1.662	0.708	1.562	0.453			
	N	129	130	132	132	134	135	132.000	0.931						
	C	85	89	82	88	81	82	84.500	1.384						
3	PM	66	61	66	56	55	50	59.000	2.633	0.761	1.548	0.492			
	N	124	128	112	123	118	115	120.000	2.463						
	C	74	79	81	72	76	83	77.500	1.727						
4	PM	50	53	51	57	54	50	52.500	1.118	0.765	1.563	0.489			
	N	105	108	111	106	105	109	107.333	0.989						
	C	71	66	74	65	70	66	68.667	1.453						

5	PM	51	45	46	53	52	50	49.500	1.335	0.712	1.722	0.414			
	N	120	118	116	119	120	125	119.667	1.229						
	C	71	68	74	63	71	70	69.500	1.522						
6	PM	48	47	42	47	49	45	46.333	1.022	0.869	1.681	0.517			
	N	88	92	97	87	94	80	89.667	2.459						
	C	52	51	49	56	54	58	53.333	1.358						
7	PM	47	50	50	51	57	50	50.833	1.352	0.843	1.591	0.530			
	N	100	90	101	93	98	94	96.000	1.770						
	C	56	70	64	61	51	60	60.333	2.667						
8	PM	68	63	69	55	56	69	63.333	2.642	0.705	1.887	0.374			
	N	175	163	173	169	169	168	169.500	1.708						
	C	100	85	86	78	96	94	89.833	3.351						
9	PM	58	62	62	57	61	55	59.167	1.195	0.803	1.579	0.509			
	N	110	123	120	118	113	114	116.333	1.978						
	C	71	72	70	78	77	74	73.667	1.333						
10	PM	56	59	60	52	63	61	58.500	1.607	0.862	1.418	0.608			
	N	99	89	98	100	97	94	96.167	1.662						
	C	71	69	72	61	68	66	67.833	1.621						
pUG36-*PLC1* in *arg82Δ*															
U73122 1h															
1	PM	46	57	63	56	62	55	56.500	2.487	0.706	1.760	0.401	0.819	1.658	0.499
	N	146	132	143	145	128	151	140.833	3.628				0.020	0.047	0.021
	C	75	85	69	90	82	79	80.000	3.033						
2	PM	54	55	52	51	49	45	51.000	1.483	0.725	1.571	0.462			
	N	114	107	113	104	107	118	110.500	2.172						
	C	72	76	58	74	74	68	70.333	2.704						
3	PM	46	49	50	50	55	52	50.333	1.229	0.795	1.708	0.465			
	N	101	123	100	122	109	94	108.167	4.936						
	C	60	62	75	63	59	61	63.333	2.404						
4	PM	55	50	46	49	46	53	49.833	1.493	0.923	1.775	0.520			
	N	94	95	106	97	90	93	95.833	2.242						
	C	59	49	57	49	56	54	54.000	1.713						
5	PM	53	56	51	50	41	43	49.000	2.380	0.776	1.916	0.405			
	N	133	112	108	131	116	126	121.000	4.258						
	C	62	61	67	59	58	72	63.167	2.182						
6	PM	37	43	48	43	40	38	41.500	1.648	0.838	1.545	0.542			
	N	78	72	76	79	75	79	76.500	1.118						
	C	47	52	50	48	48	52	49.500	0.885						
7	PM	46	40	46	47	51	47	46.167	1.447	0.871	1.538	0.566			
	N	89	78	80	82	83	77	81.500	1.765						

	C	53	59	58	54	48	46	53.000	2.129					
8	PM	60	55	54	53	51	54	54.500	1.232	0.847	1.531	0.553		
	N	104	98	97	104	95	93	98.500	1.875					
	C	56	71	70	60	62	67	64.333	2.431					
9	PM	56	55	56	55	52	62	56.000	1.342	0.866	1.423	0.609		
	N	96	93	88	87	90	98	92.000	1.807					
	C	74	63	65	57	58	71	64.667	2.789					
10	PM	47	54	50	42	45	44	47.000	1.789	0.847	1.814	0.467		
	N	106	94	98	103	101	102	100.667	1.706					
	C	55	58	52	59	58	51	55.500	1.384					
DMSO 1h														
1	PM	60	56	60	66	66	54	60.333	2.028	1.191	1.658	0.718	1.161	1.610	0.734
	N	85	84	77	88	81	89	84.000	1.826				0.016	0.071	0.032
	C	50	54	55	54	44	47	50.667	1.820						
2	PM	66	67	64	71	65	71	67.333	1.229	1.232	1.500	0.821			
	N	78	85	76	82	83	88	82.000	1.807						
	C	53	58	57	52	50	58	54.667	1.406						
3	PM	121	107	111	118	113	106	112.667	2.431	1.045	1.856	0.563			
	N	199	203	190	200	211	198	200.167	2.798						
	C	101	111	112	111	100	112	107.833	2.330						
4	PM	108	110	105	112	111	102	108.000	1.571	1.178	1.465	0.804			
	N	138	139	135	129	130	135	134.333	1.667						
	C	99	94	88	90	85	94	91.667	2.044						
5	PM	118	137	145	115	110	121	124.333	5.572	1.166	2.163	0.539			
	N	230	221	230	238	240	225	230.667	2.985						
	C	94	93	116	121	98	118	106.667	5.302						
6	PM	168	185	181	182	160	164	173.333	4.333	1.149	1.475	0.779			
	N	230	225	218	225	217	220	222.500	2.045						
	C	141	139	151	145	171	158	150.833	4.929						
7	PM	191	183	201	189	208	194	194.333	3.648	1.181	1.378	0.857			
	N	240	228	212	229	227	224	226.667	3.685						
	C	170	168	161	159	171	158	164.500	2.377						
8	PM	170	182	167	171	184	179	175.500	2.884	1.174	1.501	0.782			
	N	221	225	220	230	222	228	224.333	1.647						
	C	146	155	157	145	142	152	149.500	2.460						
9	PM	79	85	81	87	88	80	83.333	1.563	1.104	1.459	0.756			
	N	109	115	105	104	117	111	110.167	2.136						
	C	77	75	64	82	75	80	75.500	2.566						
10	PM	83	71	86	78	84	81	80.500	2.202	1.187	1.644	0.722			
	N	108	115	107	110	113	116	111.500	1.522						

	C	65	68	78	72	61	63	67.833	2.574						
U73244 1h															
1	PM	139	144	142	126	132	148	138.500	3.324	1.118	1.977	0.566	1.145	1.599	0.727
	N	229	250	238	254	252	246	244.833	3.919				0.017	0.063	0.029
	C	130	124	128	113	125	123	123.833	2.414						
2	PM	136	128	133	138	132	139	134.333	1.687	1.065	1.976	0.539			
	N	255	242	247	248	254	250	249.333	1.961						
	C	117	127	126	129	123	135	126.167	2.455						
3	PM	183	142	139	128	156	162	151.667	8.003	1.110	1.563	0.710			
	N	202	210	218	205	229	218	213.667	4.072						
	C	130	150	129	139	135	137	136.667	3.106						
4	PM	113	117	129	116	110	114	116.500	2.693	1.097	1.507	0.728			
	N	153	160	159	166	158	164	160.000	1.880						
	C	117	110	108	101	98	103	106.167	2.822						
5	PM	132	139	124	120	132	121	128.000	3.066	1.157	1.437	0.805			
	N	153	166	156	162	157	160	159.000	1.897						
	C	106	120	113	111	109	105	110.667	2.231						
6	PM	142	109	112	125	123	117	121.333	4.835	1.178	1.521	0.774			
	N	160	157	152	155	153	163	156.667	1.726						
	C	106	101	110	108	103	90	103.000	2.921						
7	PM	123	116	113	117	112	115	116.000	1.592	1.184	1.524	0.777			
	N	145	158	138	147	149	159	149.333	3.273						
	C	112	97	90	100	96	93	98.000	3.130						
8	PM	115	102	101	112	110	105	107.500	2.320	1.267	1.627	0.779			
	N	129	140	146	142	131	140	138.000	2.696						
	C	71	81	85	95	93	84	84.833	3.544						
9	PM	109	107	104	102	101	98	103.500	1.648	1.167	1.455	0.802			
	N	117	137	125	136	134	125	129.000	3.235						
	C	75	82	71	99	100	105	88.667	5.903						
10	PM	89	84	92	89	95	90	89.833	1.493	1.105	1.406	0.786			
	N	112	111	121	117	115	110	114.333	1.706						
	C	78	91	75	82	76	86	81.333	2.552						
pUG36-*PLC1*^{H439L} in *arg82Δ*															
1	PM	57	54	51	49	47	52	51.667	1.453	0.787	2.193	0.359	0.870	1.925	0.459
	N	129	157	138	144	136	160	144.000	5.000				0.025	0.077	0.022
	C	73	66	65	67	61	62	65.667	1.745						
2	PM	45	55	52	60	53	59	54.000	2.221	0.905	2.106	0.430			
	N	126	130	131	109	136	122	125.667	3.853						
	C	64	66	56	59	57	56	59.667	1.764						
3	PM	58	53	73	66	59	50	59.833	3.458	0.913	2.369	0.386			

	N	150	160	183	144	142	152	155.167	6.145						
	C	69	58	73	64	64	65	65.500	2.078						
4	PM	48	56	58	60	50	51	53.833	1.973	0.852	1.850	0.461			
	N	124	107	120	118	121	111	116.833	2.651						
	C	55	63	69	70	58	64	63.167	2.414						
5	PM	50	45	57	55	49	50	51.000	1.770	0.781	1.811	0.431			
	N	110	122	115	118	121	124	118.333	2.108						
	C	62	65	65	73	58	69	65.333	2.140						
6	PM	60	55	52	51	58	59	55.833	1.537	0.786	1.725	0.456			
	N	117	115	129	122	124	128	122.500	2.320						
	C	71	80	66	68	72	69	71.000	2.000						
7	PM	98	100	106	104	108	111	104.500	1.996	0.858	1.947	0.441			
	N	242	249	250	238	230	214	237.167	5.528						
	C	123	113	135	119	123	118	121.833	3.038						
8	PM	120	121	105	99	121	115	113.500	3.828	0.915	1.996	0.459			
	N	250	246	231	255	253	250	247.500	3.528						
	C	120	123	112	118	143	128	124.000	4.374						
9	PM	124	148	151	134	137	176	145.000	7.376	1.051	1.791	0.587			
	N	250	242	237	254	252	248	247.167	2.638						
	C	130	142	150	124	131	151	138.000	4.612						
10	PM	113	97	95	98	122	113	106.333	4.544	0.852	1.459	0.584			
	N	180	183	180	173	195	182	182.167	2.937						
	C	114	125	134	123	116	137	124.833	3.790						
pUG36-*PLC1*^{E425G} in *arg82*Δ															
1	PM	181	175	164	174	173	169	172.667	2.348	1.223	1.129	1.084	1.159	1.696	0.707
	N	162	150	170	154	165	155	159.333	3.095				0.013	0.093	0.047
	C	140	138	143	144	137	145	141.167	1.352						
2	PM	124	144	134	173	142	151	144.667	6.810	1.097	1.702	0.645			
	N	234	220	231	233	209	219	224.333	4.063						
	C	124	142	133	132	129	131	131.833	2.414						
3	PM	152	152	141	143	155	140	147.167	2.676	1.153	1.742	0.662			
	N	240	235	219	220	209	211	222.333	5.149						
	C	125	127	125	129	126	134	127.667	1.406						
4	PM	131	143	130	135	139	133	135.167	2.040	1.174	1.821	0.645			
	N	201	211	202	218	217	209	209.667	2.940						
	C	112	108	130	108	115	118	115.167	3.371						
5	PM	150	140	148	130	138	170	146.000	5.633	1.086	1.644	0.660			
	N	230	210	224	229	231	203	221.167	4.826						
	C	133	159	120	115	154	126	134.500	7.406						
6	PM	125	118	111	113	134	108	118.167	3.995	1.164	2.294	0.508			

	N	240	237	211	252	240	217	232.833	6.364						
	C	101	107	110	104	95	92	101.500	2.837						
7	PM	107	97	124	119	109	114	111.667	3.896	1.149	1.942	0.592			
	N	190	193	186	182	196	185	188.667	2.155						
	C	92	101	98	95	94	103	97.167	1.740						
8	PM	115	106	104	95	112	116	108.000	3.256	1.137	1.474	0.771			
	N	141	139	136	142	139	143	140.000	1.033						
	C	95	105	98	100	85	87	95.000	3.152						
9	PM	105	98	97	102	102	100	100.667	1.202	1.194	1.466	0.814			
	N	115	120	144	124	122	117	123.667	4.279						
	C	84	86	90	79	85	82	84.333	1.520						
10	PM	141	128	121	127	109	120	124.333	4.333	1.209	1.749	0.691			
	N	184	172	182	179	180	182	179.833	1.721						
	C	100	101	104	102	104	106	102.833	0.910						
pUG36-*PLC1*^{E425G} in *plc1*Δ															
1	PM	110	105	85	90	93	110	98.833	4.438	1.392	1.763	0.790	1.388	1.741	0.808
	N	132	124	119	127	122	127	125.167	1.851				0.046	0.091	0.027
	C	65	75	65	74	68	79	71.000	2.380						
2	PM	111	113	117	132	120	110	117.167	3.341	1.535	1.583	0.970			
	N	108	126	118	124	120	129	120.833	3.038						
	C	74	84	71	72	74	83	76.333	2.319						
3	PM	95	89	84	79	95	90	88.667	2.565	1.337	1.814	0.737			
	N	113	124	122	117	125	121	120.333	1.856						
	C	72	66	70	58	67	65	66.333	1.978						
4	PM	88	85	83	87	79	83	84.167	1.327	1.238	1.517	0.816			
	N	89	117	115	101	105	92	103.167	4.708						
	C	63	69	68	66	70	72	68.000	1.291						
5	PM	87	75	110	96	82	90	90.000	4.946	1.406	1.917	0.734			
	N	116	129	123	121	117	130	122.667	2.404						
	C	66	60	73	64	60	61	64.000	2.049						
6	PM	82	103	123	80	105	101	99.000	6.537	1.588	1.963	0.809			
	N	118	115	123	124	130	124	122.333	2.140						
	C	66	61	59	65	64	59	62.333	1.256						
7	PM	61	59	80	67	72	71	68.333	3.159	1.344	1.826	0.736			
	N	90	93	99	98	92	85	92.833	2.120						
	C	52	50	46	55	53	49	50.833	1.302						
8	PM	56	54	59	48	51	56	54.000	1.612	1.174	1.380	0.850			
	N	60	65	63	65	67	61	63.500	1.088						
	C	51	50	42	47	45	41	46.000	1.673						
9	PM	119	121	108	115	110	120	115.500	2.232	1.240	1.322	0.938			

	N	121	123	116	137	125	117	123.167	3.103					
	C	93	99	90	94	87	96	93.167	1.740					
10	PM	145	131	108	81	82	91	106.333	10.917	1.628	2.329	0.699		
	N	163	130	165	151	150	154	152.167	5.108					
	C	66	62	63	66	65	70	65.333	1.145					
pUG36-*PLC1* in *ipk1Δ*														
1	PM	76	82	80	57	60	58	68.833	4.778	0.677	1.456	0.465	0.772	1.585	0.495
	N	155	148	150	142	152	141	148.000	2.266				0.021	0.060	0.024
	C	94	108	99	98	93	118	101.667	3.921						
2	PM	63	70	67	65	70	67	67.000	1.125	0.773	1.462	0.529			
	N	127	123	126	125	130	129	126.667	1.054						
	C	84	81	91	82	87	95	86.667	2.231						
3	PM	60	65	71	61	64	60	63.500	1.727	0.819	1.667	0.492			
	N	126	122	128	131	133	135	129.167	1.956						
	C	76	72	86	74	72	85	77.500	2.604						
4	PM	65	76	61	72	80	78	72.000	3.088	0.780	1.599	0.488			
	N	153	149	140	146	148	150	147.667	1.801						
	C	95	89	82	98	93	97	92.333	2.445						
5	PM	60	65	61	44	53	50	55.500	3.212	0.742	1.312	0.565			
	N	91	96	98	100	103	101	98.167	1.740						
	C	75	72	67	77	78	80	74.833	1.922						
6	PM	55	58	63	76	60	53	60.833	3.361	0.787	1.573	0.500			
	N	123	116	121	124	126	120	121.667	1.430						
	C	82	80	79	69	87	67	77.333	3.169						
7	PM	75	72	60	50	49	52	59.667	4.667	0.923	1.415	0.652			
	N	99	94	98	90	87	81	91.500	2.814						
	C	59	62	70	60	66	71	64.667	2.092						
8	PM	49	53	51	50	50	57	51.667	1.202	0.728	1.620	0.449			
	N	105	109	120	115	124	117	115.000	2.864						
	C	74	73	70	67	68	74	71.000	1.265						
9	PM	73	68	58	62	67	75	67.167	2.626	0.694	2.031	0.342			
	N	195	188	192	200	198	207	196.667	2.704						
	C	96	100	102	99	94	90	96.833	1.797						
10	PM	59	64	80	71	78	66	69.667	3.353	0.798	1.719	0.464			
	N	139	154	149	159	143	157	150.167	3.250						
	C	87	90	96	86	82	83	87.333	2.092						
pUG36-*PLC1* in *kcs1Δ*														
1	PM	44	42	40	37	43	45	41.833	1.195	0.721	1.443	0.500	0.712	1.464	0.493
	N	86	90	81	85	82	78	83.667	1.726				0.013	0.050	0.020
	C	61	55	56	56	58	62	58.000	1.183						

2	PM	61	56	60	51	52	55	55.833	1.662	0.756	1.415	0.534			
	N	106	96	99	105	107	114	104.500	2.592						
	C	82	74	65	84	68	70	73.833	3.146						
3	PM	56	65	62	54	63	62	60.333	1.764	0.713	1.305	0.546			
	N	110	107	114	112	107	113	110.500	1.232						
	C	80	94	85	84	90	75	84.667	2.777						
4	PM	66	69	64	59	56	61	62.500	1.945	0.724	1.297	0.558			
	N	119	112	111	109	108	113	112.000	1.592						
	C	82	90	85	91	76	94	86.333	2.716						
5	PM	60	72	73	76	75	63	69.833	2.725	0.727	1.542	0.472			
	N	139	154	146	143	158	148	148.000	2.864						
	C	102	96	104	99	85	90	96.000	2.978						
6	PM	77	74	68	60	70	85	72.333	3.471	0.628	1.742	0.360			
	N	205	179	225	187	213	195	200.667	6.955						
	C	106	117	118	112	120	118	115.167	2.136						
7	PM	51	43	47	40	50	37	44.667	2.290	0.759	1.453	0.522			
	N	94	78	85	82	90	84	85.500	2.335						
	C	62	60	58	62	56	55	58.833	1.222						
8	PM	99	88	80	77	86	92	87.000	3.266	0.708	1.746	0.406			
	N	221	203	218	212	218	215	214.500	2.617						
	C	123	128	120	130	116	120	122.833	2.167						
9	PM	67	67	61	73	79	79	71.000	2.966	0.743	1.351	0.550			
	N	133	136	112	122	134	137	129.000	4.050						
	C	83	99	97	101	99	94	95.500	2.680						
10	PM	65	59	62	66	68	74	65.667	2.108	0.641	1.341	0.478			
	N	132	135	141	133	145	139	137.500	2.062						
	C	110	102	99	89	98	117	102.500	4.006						
pUG36-*PLC1* in *kcs1Δvip1Δ*															
1	PM	78	71	56	69	78	77	71.500	3.471	0.668	1.396	0.479	0.722	1.503	0.481
	N	142	149	155	158	144	148	149.333	2.525				0.016	0.037	0.009
	C	100	104	102	111	115	110	107.000	2.394						
2	PM	76	81	77	84	52	65	72.500	4.877	0.721	1.454	0.496			
	N	147	146	143	148	144	149	146.167	0.946						
	C	113	103	118	88	96	85	100.500	5.433						
3	PM	56	54	63	51	72	71	61.167	3.646	0.681	1.434	0.475			
	N	133	138	122	118	128	134	128.833	3.124						
	C	90	86	90	96	89	88	89.833	1.376						
4	PM	73	76	70	68	65	57	68.167	2.725	0.740	1.770	0.418			
	N	153	148	158	184	154	182	163.167	6.410						
	C	106	101	91	80	92	83	92.167	4.094						

5	PM	72	62	77	60	48	66	64.167	4.135	0.635	1.389	0.457			
	N	146	137	140	136	152	131	140.333	3.084						
	C	100	96	112	106	105	87	101.000	3.578						
6	PM	60	57	52	77	73	70	64.833	4.045	0.828	1.647	0.503			
	N	132	124	118	139	133	128	129.000	3.011						
	C	74	84	90	68	84	70	78.333	3.630						
7	PM	133	127	140	140	142	113	132.500	4.522	0.773	1.434	0.539			
	N	247	252	250	238	246	241	245.667	2.171						
	C	173	185	162	169	158	181	171.333	4.295						
8	PM	123	134	106	117	102	126	118.000	4.987	0.722	1.473	0.490			
	N	241	239	244	250	232	238	240.667	2.472						
	C	159	169	166	170	162	154	163.333	2.525						
9	PM	73	75	84	80	81	82	79.167	1.740	0.745	1.569	0.475			
	N	169	163	166	161	172	170	166.833	1.740						
	C	109	112	99	100	111	107	106.333	2.275						
10	PM	80	87	102	73	89	94	87.500	4.169	0.707	1.466	0.482			
	N	188	186	178	175	177	185	181.500	2.232						
	C	126	133	121	125	117	121	123.833	2.257						
pUG36-*PLC1* in *vip1*Δ															
1	PM	102	99	90	86	84	72	88.833	4.445	0.756	1.450	0.522	0.731	1.495	0.490
	N	176	166	165	177	167	171	170.333	2.124				0.019	0.037	0.014
	C	118	120	124	126	121	96	117.500	4.455						
2	PM	72	74	64	69	59	74	68.667	2.472	0.659	1.406	0.469			
	N	148	144	149	142	146	150	146.500	1.258						
	C	104	97	107	104	112	101	104.167	2.088						
3	PM	82	78	71	73	78	68	75.000	2.129	0.743	1.611	0.461			
	N	166	170	155	156	168	161	162.667	2.578						
	C	103	97	108	97	101	100	101.000	1.693						
4	PM	76	79	72	76	76	87	77.667	2.076	0.805	1.428	0.563			
	N	133	140	135	137	144	138	137.833	1.579						
	C	86	90	96	106	101	100	96.500	3.030						
5	PM	97	97	99	107	100	96	99.333	1.647	0.601	1.359	0.442			
	N	230	227	232	224	225	209	224.500	3.334						
	C	161	150	184	164	158	174	165.167	4.942						
6	PM	78	84	74	77	83	91	81.167	2.496	0.802	1.502	0.534			
	N	155	158	159	147	142	151	152.000	2.708						
	C	108	90	105	99	101	104	101.167	2.574						
7	PM	66	84	72	78	83	77	76.667	2.777	0.741	1.491	0.497			
	N	159	143	148	164	154	158	154.333	3.148						
	C	97	92	101	104	115	112	103.500	3.585						

8	PM	73	79	74	88	80	77	78.500	2.202	0.700	1.584	0.442			
	N	168	171	183	186	182	176	177.667	2.929						
	C	113	109	116	130	97	108	112.167	4.438						
9	PM	83	86	106	83	78	72	84.667	4.716	0.732	1.372	0.534			
	N	160	167	149	159	161	156	158.667	2.431						
	C	120	115	129	110	120	100	115.667	4.055						
10	PM	45	38	39	46	44	52	44.000	2.082	0.772	1.751	0.441			
	N	100	104	92	98	110	95	99.833	2.638						
	C	47	60	52	61	59	63	57.000	2.517						
pUG36-*PLC1* + pUG34-*ARG82*^{G344R} in *arg82*Δ															
1	PM	187	155	146	134	121	118	143.500	10.452	1.255	1.988	0.631	1.154	1.770	0.665
	N	250	236	210	225	222	221	227.333	5.667				0.026	0.075	0.035
	C	108	109	120	113	128	108	114.333	3.313						
2	PM	171	125	159	151	145	144	149.167	6.337	1.206	1.788	0.674			
	N	226	214	223	229	211	224	221.167	2.892						
	C	115	129	127	132	123	116	123.667	2.848						
3	PM	128	126	125	122	146	164	135.167	6.735	1.157	1.679	0.689			
	N	188	191	202	211	196	189	196.167	3.646						
	C	106	113	119	120	119	124	116.833	2.600						
4	PM	175	163	183	162	148	194	170.833	6.740	1.281	1.503	0.853			
	N	219	198	195	201	213	176	200.333	6.152						
	C	129	133	140	128	136	134	133.333	1.820						
5	PM	109	103	123	120	115	106	112.667	3.252	1.050	1.635	0.642			
	N	206	205	21	212	200	209	175.500	30.944						
	C	101	96	112	113	110	112	107.333	2.894						
6	PM	150	107	143	123	120	112	125.833	6.992	1.075	2.130	0.505			
	N	249	250	254	242	249	251	249.167	1.621						
	C	98	119	112	124	120	129	117.000	4.442						
7	PM	140	139	149	155	133	129	140.833	3.970	1.199	1.949	0.615			
	N	225	223	232	230	237	227	229.000	2.082						
	C	126	121	114	112	109	123	117.500	2.766						
8	PM	119	121	123	116	123	145	124.500	4.241	1.184	1.868	0.634			
	N	205	185	218	187	175	209	196.500	6.771						
	C	108	101	98	103	109	112	105.167	2.182						
9	PM	114	124	111	137	119	134	123.167	4.316	1.025	1.872	0.547			
	N	218	228	231	223	232	218	225.000	2.556						
	C	120	121	114	123	124	119	120.167	1.447						
10	PM	173	162	165	170	143	150	160.500	4.780	1.109	1.287	0.862			
	N	196	189	180	179	190	183	186.167	2.701						
	C	151	134	145	138	153	147	144.667	3.018						

pUG36-*PLC1* + pUG34-*ARG82* in *arg82Δ*

1	PM	86	97	109	94	93	99	96.333	3.116	0.666	1.403	0.475	0.705	1.564	0.456
	N	196	210	206	204	208	194	203.000	2.671				0.023	0.065	0.019
	C	147	152	150	149	141	129	144.667	3.490						
2	PM	89	88	77	71	96	85	84.333	3.667	0.597	1.495	0.399			
	N	213	204	222	225	207	197	211.333	4.402						
	C	154	152	137	150	124	131	141.333	5.084						
3	PM	91	84	86	78	74	76	81.500	2.680	0.679	2.031	0.334			
	N	240	248	245	249	253	227	243.667	3.774						
	C	120	110	126	108	106	150	120.000	6.772						
4	PM	114	96	101	113	122	119	110.833	4.175	0.591	1.234	0.479			
	N	245	150	247	245	254	247	231.333	16.323						
	C	205	197	166	183	197	177	187.500	5.999						
5	PM	97	93	95	81	92	95	92.167	2.344	0.720	1.539	0.468			
	N	190	188	199	198	200	207	197.000	2.852						
	C	113	141	139	118	127	130	128.000	4.546						
6	PM	87	96	85	91	78	89	87.667	2.472	0.755	1.636	0.461			
	N	192	196	187	192	185	188	190.000	1.653						
	C	114	125	112	112	116	118	116.167	2.007						
7	PM	100	86	89	78	82	81	86.000	3.215	0.747	1.443	0.518			
	N	166	159	166	151	182	173	166.167	4.393						
	C	122	118	125	110	107	109	115.167	3.070						
8	PM	73	81	84	93	81	82	82.333	2.629	0.847	1.532	0.553			
	N	157	148	155	149	154	130	148.833	4.028						
	C	105	102	84	90	97	105	97.167	3.516						
9	PM	87	81	90	84	88	90	86.667	1.453	0.723	1.769	0.409			
	N	216	209	204	201	217	225	212.000	3.670						
	C	123	125	121	117	112	121	119.833	1.905						
10	PM	106	105	91	92	102	92	98.000	2.887	0.730	1.557	0.469			
	N	206	218	209	204	219	199	209.167	3.240						
	C	136	139	136	151	124	120	134.333	4.536						

pUG36-*PLC1* + pUG34 in *arg82Δ*

1	PM	135	153	140	136	125	134	137.167	3.754	1.288	2.352	0.548	1.160	1.837	0.642
	N	249	250	255	247	252	250	250.500	1.118				0.023	0.087	0.025
	C	101	103	102	107	114	112	106.500	2.232						
2	PM	160	118	108	109	111	149	125.833	9.286	1.154	1.856	0.622			
	N	196	211	217	211	192	187	202.333	4.991						
	C	96	114	111	112	107	114	109.000	2.805						
3	PM	119	110	105	105	108	116	110.500	2.377	1.017	1.561	0.651			
	N	162	160	173	180	172	171	169.667	3.040						

	C	110	101	95	116	112	118	108.667	3.648						
4	PM	111	109	106	100	114	105	107.500	2.012	1.215	2.164	0.561			
	N	201	193	184	186	189	196	191.500	2.617						
	C	111	98	75	84	80	83	88.500	5.482						
5	PM	83	91	84	100	96	105	93.167	3.591	1.090	2.101	0.519			
	N	175	182	176	188	177	180	179.667	1.978						
	C	85	88	78	83	89	90	85.500	1.839						
6	PM	112	109	99	110	116	123	111.500	3.253	1.182	1.733	0.682			
	N	163	167	162	167	168	154	163.500	2.141						
	C	104	98	87	89	91	97	94.333	2.629						
7	PM	170	180	176	159	148	154	164.500	5.214	1.191	1.685	0.707			
	N	233	244	230	230	216	244	232.833	4.277						
	C	133	147	142	129	135	143	138.167	2.810						
8	PM	159	123	150	157	159	122	145.000	7.243	1.155	1.817	0.636			
	N	220	225	229	231	229	234	228.000	2.000						
	C	140	128	116	125	121	123	125.500	3.334						
9	PM	120	115	109	122	119	111	116.000	2.129	1.206	1.685	0.716			
	N	160	157	158	166	163	168	162.000	1.807						
	C	99	97	100	88	98	95	96.167	1.778						
10	PM	86	95	88	94	92	87	90.333	1.563	1.099	1.418	0.775			
	N	118	120	124	114	113	110	116.500	2.094						
	C	78	88	80	83	86	78	82.167	1.721						
pUG36-*PLC1* in *arg82Δ*															
DMSO 2hrs															
1	PM	66	59	69	67	68	60	64.833	1.740	1.063	1.992	0.534	1.166	1.654	0.719
	N	127	115	123	119	128	117	121.500	2.187				0.021	0.073	0.035
	C	57	61	63	63	60	62	61.000	0.931						
2	PM	98	80	89	78	77	79	83.500	3.394	1.222	1.359	0.899			
	N	91	96	96	88	91	95	92.833	1.352						
	C	67	75	73	65	66	64	68.333	1.856						
3	PM	100	85	90	105	100	104	97.333	3.283	1.180	1.691	0.698			
	N	135	142	140	141	136	143	139.500	1.335						
	C	80	81	78	84	90	82	82.500	1.708						
4	PM	92	88	98	90	96	89	92.167	1.641	1.229	2.118	0.580			
	N	165	168	161	150	161	148	158.833	3.301						
	C	80	72	68	70	83	77	75.000	2.422						
5	PM	90	86	89	89	85	81	86.667	1.382	1.169	1.409	0.829			
	N	110	104	98	108	104	103	104.500	1.708						
	C	74	72	70	70	81	78	74.167	1.833						
6	PM	124	120	111	116	105	114	115.000	2.733	1.065	1.590	0.670			

	N	175	187	168	171	170	159	171.667	3.756						
	C	119	111	102	97	110	109	108.000	3.120						
7	PM	135	132	117	126	118	129	126.167	3.005	1.188	1.449	0.820			
	N	163	160	157	140	147	156	153.833	3.535						
	C	109	101	106	102	112	107	106.167	1.701						
8	PM	74	70	73	74	70	76	72.833	0.980	1.278	1.596	0.800			
	N	91	90	100	92	87	86	91.000	2.033						
	C	57	55	62	50	64	54	57.000	2.129						
9	PM	73	75	67	76	76	69	72.667	1.563	1.141	1.599	0.714			
	N	104	109	98	95	101	104	101.833	2.023						
	C	64	61	59	66	70	62	63.667	1.606						
10	PM	82	79	78	82	84	85	81.667	1.116	1.124	1.741	0.646			
	N	129	122	131	125	129	123	126.500	1.500						
	C	76	66	75	79	78	62	72.667	2.848						
InsP_5 15min															
1	PM	130	162	160	135	117	106	135.000	9.209	1.500	1.609	0.932	1.357	1.820	0.761
	N	147	144	139	149	148	142	144.833	1.579				0.048	0.087	0.039
	C	88	95	85	87	92	93	90.000	1.592						
2	PM	93	100	142	88	121	131	112.500	8.984	1.403	1.603	0.875			
	N	132	127	129	122	134	127	128.500	1.727						
	C	77	90	78	81	80	75	80.167	2.151						
3	PM	164	180	153	147	150	188	163.667	6.922	1.409	1.884	0.748			
	N	218	230	229	204	215	217	218.833	3.945						
	C	110	99	114	126	132	116	116.167	4.778						
4	PM	119	124	110	102	139	115	118.167	5.186	1.393	1.737	0.802			
	N	143	140	152	143	157	149	147.333	2.642						
	C	90	83	81	85	78	92	84.833	2.182						
5	PM	159	145	152	150	149	153	151.333	1.909	1.417	1.847	0.767			
	N	199	195	201	192	199	198	197.333	1.333						
	C	95	118	105	108	99	116	106.833	3.719						
6	PM	70	88	81	79	82	74	79.000	2.582	1.148	2.535	0.453			
	N	180	182	179	176	161	169	174.500	3.274						
	C	67	64	71	78	70	63	68.833	2.242						
7	PM	112	116	103	101	110	109	108.500	2.291	1.247	1.632	0.764			
	N	142	146	136	152	144	132	142.000	2.921						
	C	84	82	90	89	85	92	87.000	1.592						
8	PM	65	68	59	63	69	61	64.167	1.600	1.271	1.888	0.673			
	N	100	93	98	89	91	101	95.333	2.044						
	C	51	45	49	53	54	51	50.500	1.310						
9	PM	91	87	90	94	96	100	93.000	1.897	1.646	1.947	0.845			

	N	112	107	110	106	118	107	110.000	1.844					
	C	59	56	51	54	60	59	56.500	1.432					
10	PM	83	80	78	86	91	77	82.500	2.172	1.135	1.523	0.745		
	N	109	104	110	115	114	112	110.667	1.626					
	C	74	68	75	69	72	78	72.667	1.542					
InsP_5 2hrs														
1	PM	52	57	54	56	57	57	55.500	0.847	1.189	1.500	0.793	1.294	1.799	0.721
	N	75	65	65	71	69	75	70.000	1.844				0.036	0.048	0.016
	C	41	47	47	52	47	46	46.667	1.430						
2	PM	64	67	62	49	56	53	58.500	2.837	1.258	1.896	0.664			
	N	92	90	84	88	86	89	88.167	1.167						
	C	43	50	45	46	47	48	46.500	0.992						
3	PM	61	56	53	60	56	55	56.833	1.249	1.348	1.921	0.702			
	N	76	85	87	81	77	80	81.000	1.770						
	C	38	40	41	45	37	52	42.167	2.272						
4	PM	65	57	53	55	52	58	56.667	1.909	1.232	1.822	0.676			
	N	83	80	89	88	73	90	83.833	2.676						
	C	52	42	44	43	45	50	46.000	1.653						
5	PM	98	73	77	80	116	110	92.333	7.451	1.556	1.947	0.799			
	N	118	112	120	122	112	109	115.500	2.125						
	C	64	62	61	60	55	54	59.333	1.626						
6	PM	96	94	88	107	89	109	97.167	3.646	1.207	1.718	0.702			
	N	144	125	142	130	139	150	138.333	3.783						
	C	90	81	85	71	79	77	80.500	2.680						
7	PM	52	56	57	55	60	59	56.500	1.176	1.246	1.577	0.790			
	N	77	74	65	70	69	74	71.500	1.765						
	C	45	47	56	41	43	40	45.333	2.376						
8	PM	77	59	58	52	66	60	62.000	3.512	1.174	1.744	0.673			
	N	90	87	98	99	84	95	92.167	2.496						
	C	51	58	55	51	50	52	52.833	1.249						
9	PM	65	77	74	57	60	68	66.833	3.177	1.298	1.900	0.683			
	N	92	90	100	104	100	101	97.833	2.257						
	C	51	53	56	54	47	48	51.500	1.432						
10	PM	88	87	89	88	91	83	87.667	1.085	1.433	1.965	0.730			
	N	122	110	119	124	121	125	120.167	2.212						
	C	61	59	63	65	63	56	61.167	1.327						
pUG36-*PLC1*^{E425G} in *plc1*Δ														
DMSO 2hrs														
1	PM	75	65	68	66	69	71	69.000	1.483	1.423	2.292	0.621	1.392	1.668	0.851
	N	108	112	113	111	105	118	111.167	1.815				0.018	0.084	0.034

	C	53	50	49	48	46	45	48.500	1.176					
2	PM	119	111	108	114	110	118	113.333	1.820	1.456	1.925	0.756		
	N	147	146	160	153	145	148	149.833	2.330					
	C	92	80	74	75	78	68	77.833	3.291					
3	PM	101	100	98	96	97	102	99.000	0.966	1.338	1.649	0.811		
	N	114	112	119	132	137	118	122.000	4.139					
	C	71	76	69	78	79	71	74.000	1.713					
4	PM	115	97	94	100	101	104	101.833	2.982	1.462	1.624	0.900		
	N	116	114	118	112	110	109	113.167	1.424					
	C	70	68	68	63	72	77	69.667	1.909					
5	PM	60	48	55	61	57	51	55.333	2.076	1.425	1.494	0.954		
	N	55	57	62	54	58	62	58.000	1.390					
	C	37	36	39	39	42	40	38.833	0.872					
6	PM	55	58	49	45	55	52	52.333	1.926	1.276	1.350	0.946		
	N	56	52	59	60	52	53	55.333	1.453					
	C	45	39	43	40	41	38	41.000	1.065					
7	PM	101	107	98	105	102	99	102.000	1.414	1.360	1.818	0.748		
	N	142	138	133	132	130	143	136.333	2.231					
	C	73	68	77	76	74	82	75.000	1.897					
8	PM	123	124	122	130	120	133	125.333	2.060	1.340	1.483	0.904		
	N	139	133	144	142	138	136	138.667	1.626					
	C	98	92	88	92	93	98	93.500	1.586					
9	PM	112	128	137	132	129	149	131.167	4.949	1.388	1.444	0.961		
	N	132	130	138	142	136	141	136.500	1.962					
	C	88	90	92	99	101	97	94.500	2.141					
10	PM	129	135	128	121	131	123	127.833	2.104	1.447	1.600	0.904		
	N	139	142	146	142	141	138	141.333	1.145					
	C	96	81	84	97	89	83	88.333	2.801					
InsP_5 15min														
1	PM	209	156	149	189	170	182	175.833	9.053	1.509	1.784	0.846	1.382	1.566	0.885
	N	209	215	204	185	219	215	207.833	5.049				0.037	0.054	0.013
	C	120	105	108	118	121	127	116.500	3.413						
2	PM	160	155	163	159	162	162	160.167	1.195	1.255	1.441	0.870			
	N	219	166	191	172	186	170	184.000	8.046						
	C	129	113	128	131	126	139	127.667	3.461						
3	PM	141	123	171	112	113	126	131.000	9.081	1.406	1.555	0.904			
	N	153	140	143	144	148	141	144.833	1.990						
	C	109	94	88	91	90	87	93.167	3.321						
4	PM	120	122	127	126	130	121	124.333	1.606	1.463	1.606	0.911			
	N	126	135	140	139	137	142	136.500	2.320						

	C	94	87	81	77	84	87	85.000	2.380					
5	PM	48	49	50	43	44	44	46.333	1.229	1.343	1.488	0.903		
	N	53	47	48	56	50	54	51.333	1.453					
	C	32	30	32	35	40	38	34.500	1.586					
6	PM	45	41	48	46	42	45	44.500	1.057	1.296	1.471	0.881		
	N	53	45	48	52	56	49	50.500	1.607					
	C	33	35	28	37	33	40	34.333	1.667					
7	PM	202	199	195	204	198	200	199.667	1.282	1.383	1.415	0.978		
	N	196	204	199	229	194	203	204.167	5.212					
	C	132	166	148	144	140	136	144.333	4.910					
8	PM	197	170	154	173	194	196	180.667	7.219	1.604	1.942	0.826		
	N	206	197	202	234	235	239	218.833	7.795					
	C	113	112	118	120	102	111	112.667	2.578					
9	PM	95	90	87	94	88	93	91.167	1.352	1.181	1.359	0.870		
	N	98	97	118	107	99	110	104.833	3.400					
	C	72	73	76	82	83	77	77.167	1.851					
10	PM	86	91	105	107	99	94	97.000	3.337	1.379	1.600	0.862		
	N	113	111	109	114	110	118	112.500	1.335					
	C	69	67	68	72	74	72	70.333	1.116					
InsP_5 2hrs														
1	PM	149	155	137	142	139	145	144.500	2.729	1.412	2.254	0.626	1.441	1.569	0.933
	N	234	222	199	237	248	244	230.667	7.320				0.041	0.076	0.037
	C	100	108	97	103	101	105	102.333	1.585						
2	PM	72	78	71	65	71	66	70.500	1.910	1.391	1.520	0.916			
	N	70	72	78	75	84	83	77.000	2.338						
	C	51	52	49	50	54	48	50.667	0.882						
3	PM	67	68	72	63	129	114	85.500	11.607	1.618	1.562	1.036			
	N	85	87	85	76	80	82	82.500	1.648						
	C	47	59	49	52	56	54	52.833	1.815						
4	PM	70	74	75	68	74	69	71.667	1.229	1.433	1.573	0.911			
	N	75	80	65	83	84	85	78.667	3.106						
	C	49	50	51	49	47	54	50.000	0.966						
5	PM	95	92	97	82	87	91	90.667	2.231	1.451	1.533	0.946			
	N	101	88	100	99	89	98	95.833	2.358						
	C	61	62	67	61	66	58	62.500	1.384						
6	PM	61	69	67	78	71	70	69.333	2.261	1.224	1.376	0.889			
	N	80	76	81	78	75	78	78.000	0.931						
	C	56	55	60	52	56	61	56.667	1.358						
7	PM	181	158	168	157	153	160	162.833	4.159	1.494	1.479	1.010			
	N	175	158	161	159	154	160	161.167	2.937						

	C	106	112	107	109	114	106	109.000	1.366						
8	PM	78	82	74	69	68	70	73.500	2.277	1.441	1.386	1.040			
	N	75	78	66	71	70	64	70.667	2.155						
	C	57	52	51	50	53	43	51.000	1.880						
9	PM	75	63	76	69	74	67	70.667	2.108	1.676	1.601	1.047			
	N	62	65	69	69	68	72	67.500	1.432						
	C	44	45	39	40	42	43	42.167	0.946						
10	PM	64	63	65	82	70	72	69.333	2.917	1.272	1.404	0.906			
	N	84	78	66	70	83	78	76.500	2.918						
	C	53	54	54	53	60	53	54.500	1.118						
pUG36-*PLC1*^{KRLR} in *arg82Δ*															
1	PM	177	175	169	170	186	192	178.167	3.719	1.118	1.542	0.725	1.162	1.492	0.784
	N	238	250	239	243	254	250	245.667	2.692				0.015	0.040	0.021
	C	160	162	160	155	162	157	159.333	1.145						
2	PM	149	135	182	189	177	180	168.667	8.774	1.212	1.744	0.695			
	N	239	241	245	242	239	250	242.667	1.726						
	C	142	137	160	134	134	128	139.167	4.564						
3	PM	98	107	102	100	105	110	103.667	1.838	1.187	1.410	0.842			
	N	122	117	128	125	128	119	123.167	1.887						
	C	81	72	78	100	88	105	87.333	5.277						
4	PM	87	72	75	79	88	85	81.000	2.720	1.133	1.305	0.868			
	N	95	87	98	100	96	84	93.333	2.603						
	C	67	71	69	66	75	81	71.500	2.306						
5	PM	108	110	114	111	110	104	109.500	1.360	1.237	1.429	0.866			
	N	128	118	132	122	130	129	126.500	2.187						
	C	92	84	94	96	84	81	88.500	2.553						
6	PM	150	146	159	161	174	201	165.167	8.195	1.089	1.531	0.711			
	N	228	227	234	250	222	232	232.167	3.953						
	C	146	150	148	154	151	161	151.667	2.171						
7	PM	157	159	150	161	148	166	156.833	2.774	1.200	1.611	0.745			
	N	202	215	213	218	202	213	210.500	2.790						
	C	111	117	138	142	143	133	130.667	5.518						
8	PM	119	118	124	127	130	122	123.333	1.892	1.121	1.364	0.822			
	N	145	154	146	153	158	144	150.000	2.352						
	C	109	110	115	107	113	106	110.000	1.414						
9	PM	74	71	69	70	72	73	71.500	0.764	1.195	1.407	0.850			
	N	76	83	85	82	90	89	84.167	2.088						
	C	60	62	65	59	56	57	59.833	1.352						
10	PM	119	129	118	128	120	125	123.167	1.956	1.125	1.574	0.715			
	N	181	162	171	168	177	175	172.333	2.777						

	C	112	102	108	114	104	117	109.500	2.391						
pUG36-*PLC1*^{4R} in *arg82Δ*															
1	PM	68	79	78	78	68	74	74.167	2.072	0.689	1.650	0.417	0.697	1.804	0.389
	N	177	178	168	179	179	185	177.667	2.246				0.022	0.053	0.015
	C	115	88	96	108	120	119	107.667	5.346						
2	PM	69	70	65	73	66	70	68.833	1.195	0.678	2.039	0.333			
	N	200	215	212	203	211	201	207.000	2.620						
	C	105	108	98	94	104	100	101.500	2.094						
3	PM	73	85	84	74	65	64	74.167	3.664	0.705	1.623	0.435			
	N	167	180	171	163	170	173	170.667	2.348						
	C	119	105	100	95	104	108	105.167	3.321						
4	PM	85	74	62	66	93	80	76.667	4.773	0.667	1.809	0.369			
	N	211	203	216	205	207	206	208.000	1.932						
	C	123	122	120	110	109	106	115.000	3.055						
5	PM	48	50	47	51	56	60	52.000	2.049	0.774	2.010	0.385			
	N	125	138	136	140	131	140	135.000	2.422						
	C	68	73	65	66	70	61	67.167	1.701						
6	PM	61	60	65	60	56	55	59.500	1.478	0.687	1.671	0.411			
	N	150	142	144	130	147	156	144.833	3.582						
	C	90	93	85	90	75	87	86.667	2.591						
7	PM	48	44	40	46	40	36	42.333	1.820	0.767	1.861	0.412			
	N	104	101	93	104	109	105	102.667	2.201						
	C	50	57	56	53	59	56	55.167	1.302						
8	PM	38	40	37	32	41	37	37.500	1.285	0.771	1.637	0.471			
	N	78	82	78	79	77	84	79.667	1.116						
	C	45	49	51	52	50	45	48.667	1.229						
9	PM	45	46	41	38	47	50	44.500	1.765	0.527	1.679	0.314			
	N	144	139	145	130	148	145	141.833	2.651						
	C	91	87	78	89	86	76	84.500	2.487						
10	PM	74	58	60	57	58	66	62.167	2.713	0.706	2.057	0.343			
	N	175	180	192	182	174	183	181.000	2.658						
	C	81	80	90	86	99	92	88.000	2.933						
pUG36-*PLC1*$^{R2/3}$ in *arg82Δ*															
1	PM	176	166	174	158	170	164	168.000	2.733	1.069	1.165	0.917	1.023	1.451	0.713
	N	177	184	181	189	182	186	183.167	1.701				0.028	0.056	0.029
	C	172	150	149	171	159	142	157.167	5.043						
2	PM	156	131	156	129	182	166	153.333	8.341	0.973	1.496	0.650			
	N	242	238	241	230	218	246	235.833	4.183						
	C	158	159	168	154	147	160	157.667	2.836						
3	PM	63	65	77	61	91	93	75.000	5.842	1.175	1.661	0.708			

	N	101	104	107	116	105	103	106.000	2.160						
	C	58	59	63	66	72	65	63.833	2.088						
4	PM	91	101	98	93	108	114	100.833	3.609	0.904	1.356	0.667			
	N	146	152	158	152	151	148	151.167	1.682						
	C	106	114	116	108	121	104	111.500	2.680						
5	PM	79	101	103	90	77	81	88.500	4.646	0.894	1.305	0.685			
	N	136	127	119	130	131	132	129.167	2.358						
	C	102	105	100	92	95	100	99.000	1.932						
6	PM	94	74	86	83	80	82	83.167	2.713	1.102	1.296	0.850			
	N	111	97	86	96	98	99	97.833	3.260						
	C	70	76	72	85	77	73	75.500	2.172						
7	PM	143	158	166	98	106	99	128.333	12.640	1.108	1.666	0.665			
	N	190	198	189	194	192	195	193.000	1.366						
	C	118	107	126	103	109	132	115.833	4.686						
8	PM	120	117	107	113	118	152	121.167	6.447	0.997	1.342	0.743			
	N	166	173	159	151	162	167	163.000	3.088						
	C	111	118	117	129	130	124	121.500	3.041						
9	PM	58	61	70	74	71	75	68.167	2.868	1.062	1.701	0.624			
	N	116	104	108	115	104	108	109.167	2.136						
	C	65	63	61	70	62	64	64.167	1.302						
10	PM	73	72	65	72	69	74	70.833	1.352	0.951	1.526	0.623			
	N	119	116	106	107	118	116	113.667	2.319						
	C	72	68	80	75	78	74	74.500	1.746						
pUG36-*PLC1*$^{R2/4}$ in *arg82Δ*															
1	PM	106	100	101	99	112	111	104.833	2.330	1.111	1.412	0.787	1.127	1.396	0.819
	N	131	140	143	133	125	127	133.167	2.903				0.015	0.054	0.032
	C	90	91	96	94	98	97	94.333	1.333						
2	PM	104	97	92	100	102	107	100.333	2.171	1.144	1.622	0.706			
	N	142	136	144	146	145	140	142.167	1.515						
	C	87	84	86	92	95	82	87.667	2.011						
3	PM	105	108	140	114	146	141	125.667	7.592	1.144	1.754	0.652			
	N	198	193	181	195	185	204	192.667	3.451						
	C	118	113	116	101	104	107	109.833	2.798						
4	PM	208	135	122	146	129	201	156.833	15.439	1.160	1.432	0.811			
	N	179	197	187	195	204	199	193.500	3.686						
	C	148	142	125	129	134	133	135.167	3.458						
5	PM	176	179	158	140	166	168	164.500	5.772	1.053	1.439	0.732			
	N	218	223	234	227	230	216	224.667	2.848						
	C	160	163	149	146	153	166	156.167	3.280						
6	PM	208	199	189	207	166	152	186.833	9.407	1.128	1.251	0.902			

	N	201	210	207	203	206	216	207.167	2.182						
	C	156	168	174	179	154	163	165.667	4.039						
7	PM	152	146	149	156	165	171	156.500	3.956	1.078	1.217	0.886			
	N	182	173	182	183	165	175	176.667	2.883						
	C	140	139	144	146	152	150	145.167	2.136						
8	PM	147	138	143	128	130	134	136.667	3.029	1.105	1.388	0.796			
	N	164	168	179	176	171	172	171.667	2.201						
	C	111	124	132	127	118	130	123.667	3.232						
9	PM	157	187	168	165	162	153	165.333	4.863	1.107	1.213	0.913			
	N	183	182	172	191	182	177	181.167	2.600						
	C	145	141	153	149	156	152	149.333	2.261						
10	PM	166	179	213	185	215	188	191.000	7.904	1.238	1.233	1.004			
	N	193	188	183	191	195	192	190.333	1.745						
	C	145	152	153	158	151	167	154.333	3.051						
pUG36-*PLC1*$^{R3/4}$ in *arg82Δ*															
1	PM	89	93	103	90	91	96	93.667	2.124	1.029	1.443	0.713	0.845	1.467	0.586
	N	131	128	132	130	137	130	131.333	1.256				0.044	0.064	0.040
	C	91	87	81	100	94	93	91.000	2.646						
2	PM	88	111	110	105	148	112	112.333	8.011	1.017	1.195	0.851			
	N	138	128	131	134	127	134	132.000	1.693						
	C	113	107	115	110	106	112	110.500	1.432						
3	PM	88	79	75	82	89	93	84.333	2.777	0.932	1.455	0.641			
	N	122	129	130	134	142	133	131.667	2.692						
	C	87	93	95	88	97	83	90.500	2.187						
4	PM	89	78	90	91	110	133	98.500	8.086	0.793	1.478	0.537			
	N	174	183	193	180	183	188	183.500	2.668						
	C	103	118	112	138	141	133	124.167	6.290						
5	PM	81	75	77	83	102	92	85.000	4.171	0.651	1.310	0.497			
	N	178	174	168	164	168	175	171.167	2.167						
	C	137	134	132	128	133	120	130.667	2.445						
6	PM	127	121	118	102	126	115	118.167	3.736	0.859	1.497	0.574			
	N	209	201	200	220	213	192	205.833	4.126						
	C	132	134	142	150	135	132	137.500	2.918						
7	PM	73	67	69	70	65	68	68.667	1.116	0.843	1.716	0.491			
	N	143	142	137	136	147	134	139.833	2.023						
	C	82	77	85	90	77	78	81.500	2.141						
8	PM	100	93	87	78	70	77	84.167	4.571	0.737	1.899	0.388			
	N	210	212	231	224	219	205	216.833	3.945						
	C	101	118	107	122	113	124	114.167	3.646						
9	PM	71	67	73	68	66	68	68.833	1.078	0.616	1.218	0.506			

	N	142	138	138	134	129	135	136.000	1.807					
	C	115	124	120	112	100	99	111.667	4.201					
10	PM	100	86	89	77	96	114	93.667	5.220	0.971	1.463	0.664		
	N	148	132	139	144	142	142	141.167	2.197					
	C	94	99	102	104	84	96	96.500	2.918					
pUG36-*PLC1*^{R1} in *arg82Δ*														
1	PM	67	63	67	73	57	51	63.000	3.225	0.758	2.098	0.361	0.831	1.987	0.431
	N	163	159	176	179	187	183	174.500	4.559				0.035	0.110	0.029
	C	91	83	84	80	87	74	83.167	2.386						
2	PM	56	52	61	60	71	69	61.500	2.997	0.913	2.312	0.395			
	N	157	151	152	157	155	162	155.667	1.626						
	C	76	62	67	70	63	66	67.333	2.092						
3	PM	51	46	45	44	45	50	46.833	1.195	0.719	2.765	0.260			
	N	176	172	179	178	186	190	180.167	2.713						
	C	75	71	72	67	60	46	65.167	4.377						
4	PM	57	65	64	61	66	73	64.333	2.186	0.744	1.832	0.406			
	N	163	165	169	142	170	142	158.500	5.321						
	C	81	93	86	94	78	87	86.500	2.592						
5	PM	77	82	88	87	115	88	89.500	5.396	0.901	2.059	0.438			
	N	198	219	201	205	195	209	204.500	3.538						
	C	105	101	95	100	94	101	99.333	1.687						
6	PM	50	54	69	56	64	58	58.500	2.825	1.104	1.871	0.590			
	N	97	95	92	95	103	113	99.167	3.146						
	C	46	47	52	50	61	62	53.000	2.828						
7	PM	41	43	39	40	38	42	40.500	0.764	0.781	1.582	0.494			
	N	83	86	72	88	79	84	82.000	2.352						
	C	57	49	51	48	53	53	51.833	1.327						
8	PM	41	42	38	42	40	40	40.500	0.619	0.815	1.470	0.555			
	N	75	74	73	76	73	67	73.000	1.291						
	C	54	57	45	43	52	47	49.667	2.246						
9	PM	48	44	39	32	36	43	40.333	2.376	0.747	1.938	0.385			
	N	108	109	96	107	103	105	104.667	1.944						
	C	60	53	55	51	49	56	54.000	1.592						
10	PM	42	42	40	41	42	47	42.333	0.989	0.825	1.942	0.425			
	N	99	95	101	95	106	102	99.667	1.745						
	C	53	50	49	51	48	57	51.333	1.333						
pUG36-*PLC1*$^{4R/E425G}$ in *arg82Δ*														
1	PM	59	61	62	61	58	65	61.000	1.000	0.799	1.168	0.684	0.794	1.160	0.687
	N	98	82	89	88	86	92	89.167	2.227				0.017	0.025	0.017
	C	74	79	70	82	77	76	76.333	1.687						

2	PM	65	57	62	57	61	53	59.167	1.759	0.814	1.128	0.722		
	N	82	87	85	77	79	82	82.000	1.506					
	C	79	68	74	75	69	71	72.667	1.687					
3	PM	62	69	62	63	67	59	63.667	1.498	0.736	1.183	0.622		
	N	95	113	102	101	103	100	102.333	2.418					
	C	85	80	91	83	88	92	86.500	1.910					
4	PM	68	78	69	71	55	65	67.667	3.095	0.717	1.067	0.672		
	N	100	107	105	94	98	100	100.667	1.926					
	C	91	92	94	100	96	93	94.333	1.333					
5	PM	42	41	42	37	44	40	41.000	0.966	0.879	1.300	0.676		
	N	54	55	68	63	65	59	60.667	2.290					
	C	44	43	46	50	44	53	46.667	1.626					
6	PM	32	40	37	35	31	38	35.500	1.432	0.822	1.278	0.644		
	N	60	54	53	50	58	56	55.167	1.470					
	C	44	44	43	45	42	41	43.167	0.601					
7	PM	78	67	67	64	81	72	71.500	2.766	0.737	1.129	0.653		
	N	112	106	100	111	116	112	109.500	2.306					
	C	102	92	90	104	96	98	97.000	2.236					
8	PM	88	89	85	78	82	73	82.500	2.513	0.843	1.027	0.821		
	N	102	110	95	96	105	95	100.500	2.540					
	C	99	93	105	101	94	95	97.833	1.905					
9	PM	62	64	61	77	52	71	64.500	3.528	0.740	1.128	0.656		
	N	101	103	93	102	97	94	98.333	1.745					
	C	87	86	85	87	91	87	87.167	0.833					
10	PM	65	52	51	61	52	58	56.500	2.349	0.856	1.192	0.718		
	N	76	79	80	81	79	77	78.667	0.760					
	C	65	70	68	64	61	68	66.000	1.342					
pUG36-*PLC1*$^{4R/E425G}$ in *plc1*Δ														
1	PM	65	70	64	57	50	60	61.000	2.852	0.812	1.047	0.775	0.775	1.169	0.666
	N	70	75	78	84	80	85	78.667	2.305				0.016	0.025	0.021
	C	75	76	80	75	74	71	75.167	1.195						
2	PM	58	62	55	48	53	50	54.333	2.108	0.731	1.175	0.622			
	N	88	87	86	90	88	85	87.333	0.715						
	C	79	73	70	71	74	79	74.333	1.585						
3	PM	51	50	45	57	52	50	50.833	1.579	0.792	1.291	0.614			
	N	80	83	87	78	85	84	82.833	1.352						
	C	63	65	65	69	59	64	64.167	1.327						
4	PM	48	44	41	45	49	45	45.333	1.174	0.834	1.160	0.720			
	N	61	65	67	57	66	62	63.000	1.528						
	C	57	54	55	53	55	52	54.333	0.715						

5	PM	115	129	123	114	110	116	117.833	2.822	0.758	1.137	0.666			
	N	177	174	181	171	176	182	176.833	1.701						
	C	145	160	149	157	166	156	155.500	3.085						
6	PM	111	88	93	98	97	127	102.333	5.840	0.754	1.189	0.634			
	N	160	163	159	160	169	157	161.333	1.726						
	C	143	131	128	138	132	142	135.667	2.539						
7	PM	114	105	111	101	116	114	110.167	2.414	0.676	1.130	0.598			
	N	180	178	189	196	177	185	184.167	3.005						
	C	153	172	172	167	155	159	163.000	3.454						
8	PM	78	84	80	78	81	66	77.833	2.535	0.767	1.110	0.691			
	N	109	108	116	109	122	112	112.667	2.216						
	C	93	102	108	103	104	99	101.500	2.078						
9	PM	70	87	85	82	77	88	81.500	2.814	0.864	1.129	0.765			
	N	105	104	103	111	112	104	106.500	1.607						
	C	92	93	101	94	95	91	94.333	1.453						
10	PM	49	60	48	55	53	43	51.333	2.431	0.760	1.321	0.576			
	N	94	81	87	97	93	83	89.167	2.638						
	C	68	71	65	68	62	71	67.500	1.432						
pUG36-*PLC1*^{4R} in *plc1*Δ															
1	PM	90	96	105	104	105	107	101.167	2.725	0.706	1.422	0.496	0.798	1.477	0.540
	N	205	210	197	199	207	205	203.833	2.007				0.022	0.025	0.010
	C	152	141	145	135	142	145	143.333	2.290						
2	PM	110	109	110	106	111	105	108.500	0.992	0.787	1.522	0.517			
	N	210	204	211	208	212	214	209.833	1.424						
	C	130	132	140	142	144	139	137.833	2.286						
3	PM	122	112	130	128	115	133	123.333	3.461	0.777	1.492	0.521			
	N	240	225	235	245	230	245	236.667	3.333						
	C	162	157	154	163	164	152	158.667	2.060						
4	PM	117	128	130	129	110	122	122.667	3.242	0.735	1.344	0.547			
	N	224	229	219	229	218	226	224.167	1.956						
	C	181	172	156	168	158	166	166.833	3.763						
5	PM	110	109	84	93	89	105	98.333	4.529	0.774	1.430	0.541			
	N	175	189	174	188	179	185	181.667	2.679						
	C	122	130	121	128	131	130	127.000	1.789						
6	PM	74	71	75	67	68	76	71.833	1.537	0.860	1.461	0.589			
	N	118	115	119	128	127	125	122.000	2.191						
	C	88	86	87	82	78	80	83.500	1.668						
7	PM	67	57	54	52	58	70	59.667	2.951	0.856	1.593	0.538			
	N	108	110	112	113	107	116	111.000	1.366						
	C	74	65	62	75	70	72	69.667	2.108						

8	PM	63	69	62	55	49	56	59.000	2.887	0.715	1.446	0.494		
	N	121	128	115	114	118	120	119.333	2.060					
	C	90	82	81	76	78	88	82.500	2.247					
9	PM	77	74	72	70	56	67	69.333	3.007	0.827	1.435	0.576		
	N	120	122	119	121	123	117	120.333	0.882					
	C	78	85	87	83	80	90	83.833	1.815					
10	PM	50	43	46	51	53	48	48.500	1.478	0.942	1.628	0.579		
	N	85	89	88	81	78	82	83.833	1.740					
	C	49	50	51	55	54	50	51.500	0.992					
pUG36-*PLC1*$^{1\text{-}999nt}$ in *arg82Δ*														
1	PM	71	70	74	72	75	67	71.500	1.176	0.800	2.011	0.398	0.818	1.439	0.580
	N	181	183	179	182	178	175	179.667	1.202				0.020	0.065	0.030
	C	88	89	87	91	89	92	89.333	0.760						
2	PM	53	54	57	60	52	54	55.000	1.211	0.838	1.282	0.653			
	N	85	89	79	84	82	86	84.167	1.400						
	C	62	66	70	65	67	64	65.667	1.116						
3	PM	50	49	52	48	52	50	50.167	0.654	0.858	1.336	0.642			
	N	78	79	78	79	75	80	78.167	0.703						
	C	58	61	55	56	58	63	58.500	1.232						
4	PM	57	45	55	47	50	55	51.500	1.996	0.925	1.243	0.745			
	N	69	70	71	66	72	67	69.167	0.946						
	C	59	52	58	60	51	54	55.667	1.563						
5	PM	58	54	58	52	57	56	55.833	0.980	0.838	1.458	0.575			
	N	101	99	96	95	100	92	97.167	1.400						
	C	70	65	62	64	73	66	66.667	1.667						
6	PM	56	55	60	45	54	47	52.833	2.330	0.832	1.360	0.612			
	N	91	88	81	87	83	88	86.333	1.498						
	C	70	58	68	62	63	60	63.500	1.893						
7	PM	40	47	48	43	49	46	45.500	1.384	0.667	1.501	0.445			
	N	101	95	97	110	106	105	102.333	2.333						
	C	68	65	63	75	73	65	68.167	1.973						
8	PM	42	44	35	39	44	37	40.167	1.537	0.806	1.408	0.572			
	N	70	75	69	73	65	69	70.167	1.424						
	C	53	49	54	45	48	50	49.833	1.352						
9	PM	46	36	41	42	38	37	40.000	1.528	0.825	1.443	0.571			
	N	71	70	74	66	71	68	70.000	1.125						
	C	42	49	48	51	49	52	48.500	1.432						
10	PM	31	32	40	33	34	38	34.667	1.453	0.788	1.348	0.584			
	N	60	58	65	56	58	59	59.333	1.256						
	C	44	48	45	44	42	41	44.000	1.000						

pUG36-*PLC1*$^{660nt\text{-}end}$ in *arg82Δ*

1	PM	24	25	29	23	32	30	27.167	1.493	0.787	2.826	0.279	0.786	2.832	0.326
	N	99	93	100	103	92	98	97.500	1.727				0.021	0.295	0.048
	C	30	31	39	36	38	33	34.500	1.522						
2	PM	32	30	31	29	29	25	29.333	0.989	0.834	2.697	0.309			
	N	103	91	95	99	93	88	94.833	2.227						
	C	42	32	36	29	35	37	35.167	1.815						
3	PM	37	37	39	41	33	35	37.000	1.155	0.716	3.123	0.229			
	N	157	164	168	164	161	154	161.333	2.092						
	C	48	49	52	54	55	52	51.667	1.116						
4	PM	35	36	40	39	33	34	36.167	1.138	0.751	3.578	0.210			
	N	157	164	174	175	180	184	172.333	4.120						
	C	47	53	44	53	50	42	48.167	1.887						
5	PM	27	24	26	25	27	20	24.833	1.078	0.756	3.178	0.238			
	N	107	111	103	100	99	106	104.333	1.856						
	C	33	34	30	30	35	35	32.833	0.946						
6	PM	38	38	35	34	36	39	36.667	0.803	0.685	4.343	0.158			
	N	231	226	216	240	233	248	232.333	4.522						
	C	55	44	54	65	46	57	53.500	3.128						
7	PM	40	33	35	37	36	37	36.333	0.955	0.739	3.807	0.194			
	N	176	190	179	199	196	183	187.167	3.807						
	C	49	58	52	42	49	45	49.167	2.272						
8	PM	47	48	50	45	47	48	47.500	0.671	0.893	1.505	0.594			
	N	77	82	79	81	80	81	80.000	0.730						
	C	50	49	55	50	61	54	53.167	1.851						
9	PM	49	44	42	43	40	41	43.167	1.302	0.814	1.440	0.566			
	N	77	80	79	75	74	73	76.333	1.145						
	C	54	53	52	54	50	55	53.000	0.730						
10	PM	52	46	52	49	55	49	50.500	1.285	0.881	1.828	0.482			
	N	104	105	98	110	104	108	104.833	1.682						
	C	59	56	55	57	58	59	57.333	0.667						

pUG36-*PLC1*$^{1\text{-}999nt+C2}$ in *arg82Δ*

1	PM	43	37	36	35	40	35	37.667	1.308	0.846	3.404	0.249	0.777	2.166	0.371
	N	156	144	149	150	148	162	151.500	2.630				0.010	0.145	0.020
	C	44	43	42	47	46	45	44.500	0.764						
2	PM	32	38	30	40	31	36	34.500	1.668	0.772	1.944	0.397			
	N	87	89	91	84	86	84	86.833	1.138						
	C	45	46	40	49	43	45	44.667	1.229						
3	PM	30	36	34	38	33	36	34.500	1.147	0.796	1.696	0.469			
	N	72	75	74	73	76	71	73.500	0.764						

	C	48	45	36	42	48	41	43.333	1.892						
4	PM	35	39	29	30	32	36	33.500	1.565	0.814	1.781	0.457			
	N	76	67	70	70	77	80	73.333	2.060						
	C	38	37	39	44	47	42	41.167	1.579						
5	PM	28	23	27	30	36	26	28.333	1.801	0.766	1.896	0.404			
	N	67	66	68	70	78	72	70.167	1.797						
	C	38	37	33	35	39	40	37.000	1.065						
6	PM	41	50	50	51	44	46	47.000	1.633	0.766	2.043	0.375			
	N	117	129	131	124	121	130	125.333	2.290						
	C	65	57	59	64	61	62	61.333	1.229						
7	PM	44	56	46	41	45	41	45.500	2.262	0.780	2.111	0.369			
	N	117	121	119	132	127	123	123.167	2.257						
	C	59	55	53	61	63	59	58.333	1.520						
8	PM	40	48	40	50	45	39	43.667	1.909	0.724	2.365	0.306			
	N	150	145	131	139	153	138	142.667	3.353						
	C	67	62	58	59	56	60	60.333	1.563						
9	PM	40	39	41	38	44	42	40.667	0.882	0.748	2.160	0.347			
	N	110	122	119	118	113	122	117.333	1.994						
	C	48	56	51	64	50	57	54.333	2.404						
10	PM	36	34	40	38	43	42	38.833	1.424	0.759	2.254	0.337			
	N	118	119	113	126	101	115	115.333	3.393						
	C	56	47	54	45	52	53	51.167	1.740						
pUG36-*PLC1* in *arg82Δvps41Δ*															
1	PM	158	160	161	179	159	155	162.000	3.502	0.991	1.488	0.666	1.140	1.681	0.679
	N	238	233	254	245	250	240	243.333	3.201				0.025	0.032	0.011
	C	167	156	160	155	168	175	163.500	3.191						
2	PM	161	180	183	178	170	173	174.167	3.260	1.114	1.575	0.708			
	N	244	250	245	238	252	248	246.167	2.040						
	C	145	148	155	160	167	163	156.333	3.518						
3	PM	65	57	60	55	70	66	62.167	2.358	1.215	1.674	0.726			
	N	80	84	92	90	80	88	85.667	2.092						
	C	53	50	48	48	52	56	51.167	1.276						
4	PM	78	90	88	95	96	87	89.000	2.658	1.203	1.631	0.738			
	N	123	120	118	118	123	122	120.667	0.955						
	C	83	70	72	72	70	77	74.000	2.082						
5	PM	86	72	78	87	74	71	78.000	2.864	1.164	1.744	0.668			
	N	113	120	124	109	120	115	116.833	2.242						
	C	70	59	64	71	68	70	67.000	1.897						
6	PM	76	73	77	88	84	99	82.833	3.945	1.206	1.859	0.649			
	N	131	128	124	133	122	128	127.667	1.687						

	C	69	75	74	63	70	61	68.667	2.319					
7	PM	89	100	92	102	101	99	97.167	2.182	1.187	1.692	0.702		
	N	134	150	143	139	125	140	138.500	3.452					
	C	86	87	81	78	80	79	81.833	1.537					
8	PM	125	143	108	124	120	114	122.333	4.890	1.154	1.748	0.660		
	N	193	196	172	183	178	190	185.333	3.792					
	C	100	105	112	101	110	108	106.000	1.983					
9	PM	84	78	76	78	82	89	81.167	1.973	1.171	1.776	0.659		
	N	120	127	120	126	118	128	123.167	1.759					
	C	73	78	72	64	62	67	69.333	2.472					
10	PM	67	64	80	85	81	75	75.333	3.393	0.993	1.618	0.614		
	N	118	117	126	119	133	123	122.667	2.486					
	C	88	78	72	77	80	60	75.833	3.816					
pUG36-*PLC1* in *arg82Δ*														
0.9M NaCl														
1	PM	193	182	194	177	188	193	187.833	2.845	1.345	1.150	1.169	1.296	1.281	1.026
	N	157	156	148	151	155	197	160.667	7.397				0.030	0.043	0.047
	C	143	145	138	133	144	135	139.667	2.060						
2	PM	135	123	128	142	140	160	138.000	5.285	1.202	1.380	0.871			
	N	160	163	156	150	160	162	158.500	1.962						
	C	107	112	109	126	122	113	114.833	3.070						
3	PM	93	97	92	88	73	89	88.667	3.393	1.415	1.465	0.966			
	N	92	87	88	99	95	90	91.833	1.851						
	C	65	67	62	61	64	57	62.667	1.430						
4	PM	110	102	109	115	112	109	109.500	1.765	1.341	1.096	1.223			
	N	85	95	88	90	92	87	89.500	1.478						
	C	83	80	78	86	80	83	81.667	1.174						
5	PM	94	87	84	88	83	87	87.167	1.579	1.144	1.407	0.813			
	N	110	117	98	101	110	107	107.167	2.798						
	C	77	79	76	73	78	74	76.167	0.946						
6	PM	91	95	92	105	118	104	100.833	4.206	1.375	1.323	1.040			
	N	95	93	92	105	95	102	97.000	2.145						
	C	76	75	70	74	72	73	73.333	0.882						
7	PM	154	145	143	130	144	109	137.500	6.505	1.329	1.296	1.025			
	N	129	136	130	139	138	133	134.167	1.701						
	C	97	99	107	102	104	112	103.500	2.232						
8	PM	118	119	102	112	106	97	109.000	3.615	1.164	1.429	0.814			
	N	138	127	129	133	136	140	133.833	2.088						
	C	94	93	98	96	97	84	93.667	2.076						
9	PM	120	119	108	133	124	118	120.333	3.333	1.407	1.201	1.172			

	N	99	107	112	104	101	93	102.667	2.692					
	C	84	85	90	92	85	77	85.500	2.141					
10	PM	107	94	96	135	105	122	109.833	6.467	1.239	1.066	1.162		
	N	102	99	87	91	90	98	94.500	2.432					
	C	92	84	87	94	85	90	88.667	1.626					
hypo-osmotic shock (0.09M NaCl) 2min														
1	PM	84	95	86	101	92	91	91.500	2.513	1.207	1.662	0.726	1.255	1.445	0.882
	N	128	125	123	131	121	128	126.000	1.506				0.040	0.056	0.044
	C	71	74	80	76	73	81	75.833	1.621						
2	PM	99	104	98	97	102	112	102.000	2.266	1.163	1.333	0.873			
	N	122	111	118	109	121	120	116.833	2.242						
	C	90	83	85	87	93	88	87.667	1.453						
3	PM	98	88	90	100	91	95	93.667	1.944	1.322	1.198	1.104			
	N	86	91	82	83	80	87	84.833	1.621						
	C	74	77	71	67	66	70	70.833	1.701						
4	PM	136	128	137	133	132	134	133.333	1.308	1.325	1.276	1.038			
	N	127	134	122	128	125	135	128.500	2.078						
	C	101	105	100	96	100	102	100.667	1.202						
5	PM	109	110	114	108	123	113	112.833	2.242	1.073	1.418	0.756			
	N	146	152	150	157	144	146	149.167	1.973						
	C	104	101	106	110	109	101	105.167	1.579						
6	PM	117	108	104	98	117	106	108.333	3.062	1.069	1.541	0.694			
	N	150	159	156	154	158	160	156.167	1.515						
	C	105	94	96	107	104	102	101.333	2.124						
7	PM	79	86	101	104	124	124	103.000	7.642	1.290	1.743	0.740			
	N	139	131	142	148	135	140	139.167	2.386						
	C	72	71	78	84	83	91	79.833	3.135						
8	PM	142	135	81	134	89	140	120.167	11.235	1.484	1.562	0.950			
	N	133	126	116	133	132	119	126.500	3.063						
	C	89	84	78	82	77	76	81.000	2.033						
9	PM	122	128	113	85	122	89	109.833	7.499	1.227	1.225	1.002			
	N	106	111	112	104	115	110	109.667	1.647						
	C	88	96	86	99	93	75	89.500	3.510						
10	PM	85	81	82	78	76	77	79.833	1.400	1.392	1.488	0.936			
	N	82	81	76	89	91	93	85.333	2.716						
	C	54	62	57	53	58	60	57.333	1.406						
hypo-osmotic shock (0.09M NaCl) 30min														
1	PM	97	98	110	180	185	141	135.167	16.329	0.930	1.635	0.569	1.205	1.658	0.766
	N	231	232	244	250	240	229	237.667	3.412				0.053	0.106	0.069
	C	141	156	139	144	152	140	145.333	2.871						

2	PM	180	152	108	121	112	140	135.500	11.242	1.120	1.928	0.581		
	N	233	232	224	236	228	247	233.333	3.221					
	C	121	118	113	108	148	118	121.000	5.715					
3	PM	85	114	93	90	140	131	108.833	9.421	1.223	2.185	0.560		
	N	197	196	202	195	193	184	194.500	2.432					
	C	80	87	82	95	93	97	89.000	2.887					
4	PM	125	113	124	110	120	123	119.167	2.548	1.058	2.071	0.511		
	N	227	243	238	234	216	242	233.333	4.208					
	C	122	98	107	120	116	113	112.667	3.648					
5	PM	93	98	97	86	100	96	95.000	2.033	1.140	1.936	0.589		
	N	167	160	158	153	167	163	161.333	2.231					
	C	92	84	80	81	81	82	83.333	1.820					
6	PM	89	90	86	84	92	96	89.500	1.746	1.370	1.625	0.843		
	N	107	108	102	112	105	103	106.167	1.493					
	C	61	67	65	71	70	58	65.333	2.076					
7	PM	154	167	158	165	154	160	159.667	2.231	1.219	1.249	0.976		
	N	170	153	158	168	163	170	163.667	2.860					
	C	134	133	127	134	128	130	131.000	1.265					
8	PM	132	133	158	161	145	146	145.833	4.949	1.173	1.340	0.875		
	N	158	166	168	170	171	167	166.667	1.892					
	C	136	131	121	118	126	114	124.333	3.373					
9	PM	62	66	52	54	64	59	59.500	2.277	1.240	1.222	1.014		
	N	58	59	55	60	62	58	58.667	0.955					
	C	47	49	48	50	45	49	48.000	0.730					
10	PM	58	57	52	57	49	52	54.167	1.493	1.578	1.383	1.140		
	N	48	47	46	50	45	49	47.500	0.764					
	C	33	36	32	29	37	39	34.333	1.498					
pUG36-*ARG82*^{D131A} in *arg82*Δ														
1	PM	63	66	53	52	45	51	55.000	3.235	0.721	1.592	0.453	0.738	1.581	0.467
	N	118	123	124	128	117	119	121.500	1.727				0.006	0.008	0.005
	C	72	74	75	79	78	80	76.333	1.282						
2	PM	48	46	63	59	64	61	56.833	3.198	0.751	1.632	0.460			
	N	132	129	122	124	116	118	123.500	2.527						
	C	82	80	75	75	64	78	75.667	2.591						
3	PM	40	42	41	44	39	42	41.333	0.715	0.754	1.541	0.489			
	N	80	89	82	85	84	87	84.500	1.335						
	C	54	50	53	58	50	64	54.833	2.197						
4	PM	53	49	53	40	44	42	46.833	2.301	0.749	1.603	0.468			
	N	102	101	110	95	98	95	100.167	2.301						
	C	59	63	68	65	62	58	62.500	1.522						

5	PM	80	88	81	63	62	58	72.000	5.092	0.702	1.571	0.447			
	N	161	157	159	164	160	165	161.000	1.238						
	C	110	108	105	92	98	102	102.500	2.729						
6	PM	78	72	70	81	78	75	75.667	1.687	0.760	1.554	0.489			
	N	160	153	150	158	152	155	154.667	1.542						
	C	105	107	100	93	97	95	99.500	2.277						
7	PM	85	90	78	79	64	68	77.333	4.030	0.746	1.580	0.472			
	N	160	161	169	162	168	163	163.833	1.537						
	C	108	103	100	114	96	101	103.667	2.616						
8	PM	62	70	56	52	75	67	63.667	3.547	0.706	1.560	0.453			
	N	137	140	142	148	142	135	140.667	1.856						
	C	95	78	80	87	104	97	90.167	4.175						
9	PM	71	72	70	61	59	67	66.667	2.231	0.750	1.570	0.478			
	N	148	147	140	127	136	139	139.500	3.149						
	C	88	92	91	80	93	89	88.833	1.922						
10	PM	60	54	63	59	68	64	61.333	1.961	0.740	1.610	0.460			
	N	133	135	129	138	130	135	133.333	1.382						
	C	83	72	90	75	89	88	82.833	3.135						
pUG36-*PLC1* in *gpr1Δ*															
1	PM	59	55	49	52	51	54	53.333	1.430	0.764	1.473	0.519	0.715	1.641	0.442
	N	108	104	106	96	100	103	102.833	1.759				0.019	0.062	0.021
	C	64	70	79	66	69	71	69.833	2.120						
2	PM	37	48	41	49	42	45	43.667	1.856	0.749	1.683	0.445			
	N	100	96	106	98	96	93	98.167	1.833						
	C	56	58	60	57	58	61	58.333	0.760						
3	PM	55	48	47	44	42	49	47.500	1.839	0.652	1.403	0.465			
	N	105	97	104	100	102	105	102.167	1.302						
	C	74	77	79	65	74	68	72.833	2.182						
4	PM	49	47	44	45	48	49	47.000	0.856	0.801	1.690	0.474			
	N	96	105	98	94	100	102	99.167	1.641						
	C	62	60	55	60	57	58	58.667	1.022						
5	PM	33	29	36	30	34	37	33.167	1.302	0.819	1.494	0.548			
	N	65	59	63	57	58	61	60.500	1.258						
	C	40	42	41	40	39	41	40.500	0.428						
6	PM	99	97	70	77	81	73	82.833	5.036	0.680	1.933	0.352			
	N	234	241	226	230	238	244	235.500	2.778						
	C	104	111	118	133	128	137	121.833	5.300						
7	PM	81	88	84	79	74	80	81.000	1.932	0.669	1.985	0.337			
	N	223	232	252	250	238	248	240.500	4.703						
	C	128	117	120	115	125	122	121.167	1.990						

8	PM	83	89	105	90	92	86	90.833	3.114	0.660	1.729	0.382		
	N	241	233	230	244	241	239	238.000	2.191					
	C	154	138	132	130	129	143	137.667	3.921					
9	PM	85	90	81	88	89	83	86.000	1.461	0.695	1.637	0.425		
	N	202	216	198	206	195	198	202.500	3.117					
	C	122	111	141	130	108	130	123.667	5.129					
10	PM	77	97	102	97	89	85	91.167	3.781	0.659	1.386	0.476		
	N	197	200	179	184	195	195	191.667	3.363					
	C	156	138	126	127	150	133	138.333	5.024					
pUG36-*PLC1* in *arg82Δgpr1Δ*														
1	PM	143	154	146	147	134	122	141.000	4.633	0.980	1.696	0.578	1.173	1.769	0.681
	N	254	248	230	234	250	248	244.000	3.933				0.057	0.083	0.050
	C	148	147	141	132	144	151	143.833	2.750						
2	PM	108	161	89	125	117	111	118.500	9.811	1.207	1.691	0.714			
	N	172	151	159	163	172	179	166.000	4.179						
	C	108	94	97	118	87	85	98.167	5.186						
3	PM	108	113	99	95	102	113	105.000	3.066	1.079	1.909	0.565			
	N	170	173	192	197	195	188	185.833	4.715						
	C	99	101	90	94	98	102	97.333	1.856						
4	PM	75	67	78	82	99	101	83.667	5.548	1.290	2.249	0.574			
	N	110	153	136	160	156	160	145.833	8.035						
	C	71	58	60	61	66	73	64.833	2.522						
5	PM	147	137	139	134	121	143	136.833	3.673	0.962	1.748	0.551			
	N	250	246	252	238	251	254	248.500	2.363						
	C	149	138	141	139	134	152	142.167	2.822						
6	PM	117	112	106	94	93	121	107.167	4.785	0.946	2.124	0.445			
	N	234	242	245	252	243	228	240.667	3.461						
	C	116	108	97	101	124	134	113.333	5.760						
7	PM	57	59	52	56	54	59	56.167	1.138	1.387	1.819	0.762			
	N	72	73	79	74	66	78	73.667	1.909						
	C	39	41	40	38	43	42	40.500	0.764						
8	PM	41	39	35	39	40	36	38.333	0.955	1.100	1.464	0.752			
	N	53	56	52	47	49	49	51.000	1.342						
	C	36	38	34	30	32	39	34.833	1.424						
9	PM	150	149	146	142	153	153	148.833	1.740	1.287	1.326	0.971			
	N	153	149	143	155	160	160	153.333	2.692						
	C	119	117	114	112	114	118	115.667	1.116						
10	PM	102	97	96	89	107	111	100.333	3.263	1.494	1.660	0.900			
	N	114	107	104	107	118	119	111.500	2.592						
	C	64	73	64	66	74	62	67.167	2.072						

Appendix C: *P*-value tables

[$^{***}P < 0.001$; $0.001 < ^{**}P < 0.01$; $0.01 < ^{*}P < 0.05$; n.s.: not significant]

C1: for Chapter 3

P-value (Nuclear/Cytosolic)	GFP-Plc1p in WT
GFP-Plc1p in *plc1Δ*	n.s.

P-value (Nuclear/Cytosolic)	GFP-Plc1p in WT
GFP in WT	***

P-value (Nuclear/Cytosolic)	GFP-Plc1p in XPO1 23°C	GFP-Plc1p in *xpo1-1* 37°C
GFP-Plc1p in XPO1 37°C	n.s.	n.s.
GFP-Plc1p in *xpo1-1* 23°C	*	**

P-value (Nuclear/Cytosolic)	WT untreat
DMSO	n.s.
rapamycin	n.s.
nocodazle	n.s.
hydroxyurea	**

P-value (Nuclear/Cytosolic)	23°C (untreat)	23°C (shifted from 37°C)
37°C	n.s.	n.s.
23°C (shifted from 37°C)	n.s.	

P-value (Nuclear/Cytosolic)	hyper 2 min	hyper 15 min	hyper 2 h
untreated	*	n.s.	n.s.

P-value (Nuclear/Cytosolic)	hypo 2 min	hypo 15 min	hypo 2 h
untreated	*	*	n.s.

P-value (Nuclear/Cytosolic)	hypo 2 min	hypo 15 min	hypo 2 h
hyper 2 h	n.s.	n.s.	n.s.

P-value (Nuclear/Cytosolic)	GFP-Plc1p
GFP-Plc1p^{NES}	***

P-value (Nuclear/Cytosolic)	GFP-Plc1p
GFP-Plc1p$^{1-333}$	n.s.

P-value (Nuclear/Cytosolic)	GFP-Plc1p	GFP
GFP-Plc1p$^{1-333}$	***	*
GFP-Plc1p $^{1-220}$	***	**
GFP-Plc1p $^{1-110}$	***	n.s.
GFP-Plc1p $^{110-220}$	***	n.s.

P-value (Nuclear/Cytosolic)	GFP-Plc1p	GFP-Plc1p^{NES}	GFP-Plc1p$^{220-end}$
GFP-Plc1p$^{110-end}$	***	**	n.s.
GFP-Plc1p$^{220-end}$	***	**	

P-value (Nuclear/Cytosolic)	GFP-Plc1p
GFP-Plc1p^{4R} in WT	**
GFP-Plc1p^{KKLRK} in WT	***
GFP-Plc1p^{KRLR} in WT	**

P-value (Nuclear/Cytosolic)	GFP-Plc1p
GFP-Plc1p^{CAAX}	***

P-value	GFP-CAAX		
	PM/Cytosolic	Nuclear/Cytosolic	PM/Nuclear
GFP-Plc1p^{CAAX}	***	***	*

P-value (Nuclear/Cytosolic)	GFP-Plc1p
GFP-Plc1p^{PKI}	***

P-value (Nuclear/Cytosolic)	GFP-Plc1p	GFP-Plc1p^{NES}	GFP-Plc1p^{CAAX}
GFP-Plc1p$^{NES/CAAX}$	n.s.	***	***

P-value (Nuclear/Cytosolic)	GFP-Plc1p	GFP-Plc1p^{NES}	GFP-Plc1p^{PKI}

GFP-Plc1p$^{NES/PKI}$	***	***	***

Vacuole morphology under salt stress:

WT vs. *plc1Δ*	1-2/cells	3-4/cells	5-8/cells	≥ 9/cells
untreated	*	**	n.s.	**
Hyper-osmotic shocked	n.s.	n.s.	n.s.	*
Hypo-osmotic shocked	*	*	*	**

WT vs. *PLC1*^{CAAX}	1-2/cells	3-4/cells	5-8/cells	≥ 9/cells
untreated	n.s.	n.s.	n.s.	n.s.
Hyper-osmotic shocked	**	n.s.	n.s.	**
Hypo-osmotic shocked	*	*	*	n.s.

plc1Δ vs. *PLC1*^{CAAX}	1-2/cells	3-4/cells	5-8/cells	≥ 9/cells
untreated	***	*	**	**
Hyper-osmotic shocked	*	n.s.	n.s.	**
Hypo-osmotic shocked	***	n.s.	**	**

plc1Δ vs. *PLC1*^{NES}	1-2/cells	3-4/cells	5-8/cells	≥ 9/cells
untreated	*	n.s.	**	**
Hyper-osmotic shocked	*	*	n.s.	**
Hypo-osmotic shocked	*	n.s.	n.s.	*

plc1Δ vs. *PLC1*^{PKI}	1-2/cells	3-4/cells	5-8/cells	≥ 9/cells
untreated	n.s.	n.s.	*	*
Hyper-osmotic shocked	*	n.s.	n.s.	*
Hypo-osmotic shocked	n.s.	*	n.s.	*

PLC1^{NES} vs. *PLC1*^{PKI}	1-2/cells	3-4/cells	5-8/cells	≥ 9/cells
untreated	n.s.	n.s.	n.s.	n.s.

Hyper-osmotic shocked	/	n.s.	n.s.	n.s.
Hypo-osmotic shocked	n.s.	n.s.	n.s.	n.s.

C2: for Chapter 4

P-value	Nuclear/Cytosolic
GFP-Arg82p in WT vs. GFP-Arg82p in *arg82Δ*	n.s.
GFP-Arg82p in WT vs. GFP-Plc1p in WT	n.s.

P-value	PM/Cytosolic	Nuclear/Cytosolic	PM/Nuclear
GFP-Plc1p in *arg82Δ* vs. GFP-Plc1p in WT	***	n.s.	***
GFP-Plc1p in WT vs. GFP-Plc1p in *arg82Δ* + pYCplac111-*ARG82*	n.s.	n.s.	n.s.
GFP-Plc1p in *arg82Δ* + pYCplac111 vs. GFP-Plc1p in *arg82Δ*	n.s.	n.s.	n.s.

P-value	PM/Cytosolic	Nuclear/Cytosolic	PM/Nuclear
GPF-Arg82p in *plc1Δ* vs. GPF-Arg82p in WT	n.s.	n.s.	n.s.

P-value	PM/Cytosolic	Nuclear/Cytosolic	PM/Nuclear
GFP-Plc1p in *arg82Δ*+ pYCplac111-*ARG82*^{D131A} vs. GFP-Plc1p in *arg82Δ*	n.s.	n.s.	n.s.
GFP-Plc1p in *arg82Δ*+ pYCplac111-*ARG82*^{D131A} vs. GFP-Plc1p in *arg82Δ*+ pYCplac111-*ARG82*	***	*	**
GFP-Plc1p in *arg82Δ*+ pYCplac111-*ARG82*$^{\Delta asp}$ vs. GFP-Plc1p in *arg82Δ*	***	n.s.	***
GFP-Plc1p in *arg82Δ*+ pYCplac111-*ARG82*$^{\Delta asp}$ vs. GFP-Plc1p in *arg82Δ*+ pYCplac111-*ARG82*	n.s.	n.s.	n.s.

P-value	PM/Cytosolic	Nuclear/Cytosolic	PM/Nuclear
GFP-ARG82p^{D131A} in *arg82Δ* vs. GFP-ARG82p in *arg82Δ*	n.s.	n.s.	n.s.

P-value	PM/Cytosolic	Nuclear/Cytosolic	PM/Nuclear
GFP-Plc1p in WT 5 μM U73122 1h vs.	n.s.	n.s.	n.s.

GFP-Plc1p in WT			
GFP-Plc1p in WT 0.26% DMSO 1h vs. GFP-Plc1p in WT	n.s.	n.s.	n.s.

P-value	PM/Cytosolic	Nuclear/Cytosolic	PM/Nuclear
GFP-Plc1p in *arg82Δ* 5 μM U73122 1h vs. GFP-Plc1p in *arg82Δ*	***	n.s.	***
GFP-Plc1p in *arg82Δ* 0.26% DMSO 1h vs. GFP-Plc1p in *arg82Δ*	n.s.	n.s.	n.s.
GFP-Plc1p in *arg82Δ* 5 μM U73433 1h vs. GFP-Plc1p in *arg82Δ*	n.s.	n.s.	n.s.

P-value	PM/Cytosolic	Nuclear/Cytosolic	PM/Nuclear
GFP-Plc1p^{H439L} in *arg82Δ* vs. GFP-Plc1p in *arg82Δ*	***	n.s.	***
GFP-Plc1p^{E425G} in *arg82 Δ* vs. GFP-Plc1p in *arg82Δ*	n.s.	n.s.	n.s.

P-value	PM/Cytosolic	Nuclear/Cytosolic	PM/Nuclear
GFP-Plc1p^{E425G} in *plc1Δ* vs. GFP-Plc1p in *plc1Δ*	***	n.s.	***
GFP-Plc1p^{E425G} in *plc1Δ* vs. GFP-Plc1p^{E425G} in *arg82Δ*	***	n.s.	n.s.

P-value	PM/Cytosolic	Nuclear/Cytosolic	PM/Nuclear
GFP-Plc1p in *ipk1Δ* vs. GFP-Plc1p in WT	n.s.	n.s.	n.s.
GFP-Plc1p in *ipk1Δ* vs. GFP-Plc1p in *arg82Δ*	***	n.s.	***
GFP-Plc1p in *kcs1Δ* vs. GFP-Plc1p in WT	n.s.	*	n.s.
GFP-Plc1p in *kcs1Δ* vs. GFP-Plc1p in *arg8 2 Δ*	***	**	***
GFP-Plc1p in *vip1Δ* vs. GFP-Plc1p in WT	n.s.	*	n.s.
GFP-Plc1p in *vip1Δ* vs. GFP-Plc1p in *arg82Δ*	***	*	***
GFP-Plc1p in *vip1Δkcs1Δ* vs. GFP-Plc1p in WT	n.s.	*	n.s.
GFP-Plc1p in *vip1Δkcs1Δ* vs. GFP-Plc1p in *arg82 Δ*	***	*	***

P-value	PM/Cytosolic	Nuclear/Cytosolic	PM/Nuclear
GFP-Plc1p in *arg82Δ* + pUG34-*ARG82*^{G344R} vs. GFP-Plc1p in *arg82Δ*	n.s.	n.s.	n.s.
GFP-Plc1p in *arg82Δ* + pUG34-*ARG82* vs. GFP-Plc1p in WT	n.s.	n.s.	n.s.
GFP-Plc1p in *arg82Δ* + pUG34 vs. GFP-Plc1p in *arg82Δ*	n.s.	n.s.	n.s.

P-value	PM/Cytosolic	Nuclear/Cytosolic	PM/Nuclear
GFP-Plc1p in *arg82Δ* 0.1% (v:v) DMSO vs. GFP-Plc1p in *arg82Δ*	n.s.	n.s.	n.s.
GFP-Plc1p in *arg82Δ* 100mM InsP_5 15min vs. GFP-Plc1p in *arg82Δ*	***	n.s.	*
GFP-Plc1p in *arg82Δ* 100mM InsP_5 2hrs vs. GFP-Plc1p in *arg82Δ*	***	n.s.	n.s.
GFP-Plc1p in *arg82Δ* 100mM InsP_5 15min vs. GFP-Plc1p in *arg82Δ* 100mM InsP_5 2hrs	n.s.	n.s.	n.s.

P-value	PM/Cytosolic	Nuclear/Cytosolic	PM/Nuclear
GFP-Plc1p^{E425G} in *plc1Δ* 0.1% (v:v) DMSO vs. GFP-Plc1p^{E425G} in *plc1Δ*	n.s.	n.s.	n.s.
GFP-Plc1p^{E425G} in *plc1Δ* 100μM InsP_5 15min vs. GFP-Plc1p^{E425G} in *plc1Δ*	n.s.	n.s.	*
GFP-Plc1p^{E425G} in *plc1Δ* 100μM InsP_5 2hrs vs. GFP-Plc1p^{E425G} in *plc1Δ*	n.s.	n.s.	**
GFP-Plc1p^{E425G} in *plc1Δ* 100μM InsP_5 15min vs. GFP-Plc1p^{E425G} in *plc1Δ* 100μM InsP_5 2hrs	n.s.	n.s.	n.s.

P-value	PM/Cytosolic	Nuclear/Cytosolic	PM/Nuclear
GFP-Plc1p^{KRLR} in *arg82Δ* vs. GFP-Plc1p in *arg82Δ*	n.s.	**	**
GFP-Plc1p^{4R} in *arg82Δ* vs. GFP-Plc1p in *arg82Δ*	***	n.s.	***

P-value	PM/Cytosolic	Nuclear/Cytosolic	PM/Nuclear
GFP-Plc1p$^{R2/3}$ in *arg82Δ* vs. GFP-Plc1p in *arg82Δ*	**	**	n.s.
GFP-Plc1p$^{R2/3}$ in *arg82Δ* vs. GFP-Plc1p^{4R} in *arg82Δ*	***	***	***
GFP-Plc1p$^{R2/4}$ in *arg82Δ* vs. pUG36-PLC1 in *arg82Δ*	n.s.	**	**
GFP-Plc1p$^{R2/4}$ in *arg82Δ* vs. GFP-Plc1p^{4R} in *arg82Δ*	***	***	***
GFP-Plc1p$^{R3/4}$ in *arg82Δ* vs. pUG36-PLC1 in *arg82Δ*	***	*	n.s.

GFP-Plc1p$^{R3/4}$ in *arg82Δ* vs. GFP-Plc1p^{4R} in *arg82Δ*	**	***	***
GFP-Plc1p^{R1} in *arg82Δ* vs. GFP-Plc1p in *arg82Δ*	***	*	***
GFP-Plc1p^{R1} in *arg82Δ* vs. GFP-Plc1p^{4R} in *arg82Δ*	**	n.s.	n.s.

P-value	PM/Cytosolic	Nuclear/Cytosolic	PM/Nuclear
GFP-Plc1p$^{4R/E425G}$ in *plc1Δ* vs. GFP-Plc1p in *plc1Δ*	n.s.	***	***
GFP-Plc1p$^{4R/E425G}$ in *plc1Δ* vs. GFP-Plc1p^{4R} in *plc1Δ*	n.s.	***	***
GFP-Plc1p$^{4R/E425G}$ in *plc1Δ* vs. GFP-Plc1p^{E425G} in *plc1Δ*	***	***	***
GFP-Plc1p$^{4R/E425G}$ in *arg82Δ* vs. GFP-Plc1p in *arg82Δ*	***	***	n.s.
GFP-Plc1p$^{4R/E425G}$ in *arg82Δ* vs. GFP-Plc1p^{4R} in *arg82Δ*	***	***	***
GFP-Plc1p$^{4R/E425G}$ in *arg82Δ* vs. GFP-Plc1p^{E425G} in *arg82Δ*	***	***	n.s.

P-value	PM/Cytosolic	Nuclear/Cytosolic	PM/Nuclear
GFP-Plc1p$^{1-333}$ in *arg82Δ* vs. GFP-Plc1p in *arg82Δ*	***	**	*
GFP-Plc1p$^{220-end}$ in *arg82Δ* vs. GFP-Plc1p in *arg82Δ*	***	**	***
GFP-Plc1p$^{(1-333)+C2}$ in *arg82Δ* vs. GFP-Plc1p in *arg82Δ*	***	*	***

P-value	PM/Cytosolic	Nuclear/Cytosolic	PM/Nuclear
GFP-Plc1p in *arg82Δ vps41Δ* vs. GFP-Plc1p in *arg82Δ*	n.s.	n.s.	n.s.

P-value	PM/Cytosolic	Nuclear/Cytosolic	PM/Nuclear
GFP-Plc1p in *arg82Δ* 0.9M NaCl vs. GFP-Plc1p in *arg82Δ*	***	***	***
GFP-Plc1p in *arg82Δ* 0.9M NaCl vs.	n.s.	*	*

GFP-Plc1p in *arg82Δ* 10 × 0.9M NaCl 2 min			
GFP-Plc1p in *arg82Δ* 10 × 0.9M NaCl 2 min vs. GFP-Plc1p in *arg82Δ*	**	**	***
GFP-Plc1p in *arg82Δ* 10 × 0.9M NaCl 30 min vs. GFP-Plc1p in *arg82Δ*	n.s.	n.s.	n.s.
GFP-Plc1p in *arg82Δ* 10 × 0.9M NaCl 2 min vs. GFP-Plc1p in *arg82Δ* 10 × 0.9M NaCl 30 min	n.s.	n.s.	n.s.

P-value	PM/Cytosolic	Nuclear/Cytosolic	PM/Nuclear
GFP-Plc1p in *gpr1Δ* vs. GFP-Plc1p in WT	n.s.	n.s.	n.s.
GFP-Plc1p in *gpr1Δ* vs. GFP-Plc1p in *gpr1Δ arg82Δ*	***	n.s.	***
GFP-Plc1p in *gpr1Δ arg82Δ* vs. GFP-Plc1p in *arg82Δ*	n.s.	n.s.	n.s.